Contributions to the problems of classification, regression and study of an inverse problem in finance

Jean-Baptiste Monnier

Université Paris Diderot - Paris VII
UFR de Mathématiques

Thèse de Doctorat

présentée pour obtenir le titre de

Docteur en Sciences de l'Université Paris VII

Spécialité: Mathématiques Appliquées

soutenue par

Jean-Baptiste MONNIER

Quelques contributions en classification, régression et étude d'un problème inverse en finance

Directrice de thèse: **Dominique PICARD**

Soutenue publiquement le **6 décembre 2011**, devant le jury composé de:

M. Jean-Yves Audibert,	*Capital Fund Management*
M. Francis Bach,	*I.N.R.I.A., École Normale Supérieure*
M. Arnaud Gloter,	*Université d'Évry Val d'Essonne*
M. Oleg Lepski,	*Université de Provence*
Mme Dominique Picard,	*Université Paris Diderot*
M. Peter Tankov,	*Université Paris Diderot*

au vu des rapports de:

M. Arnaud Gloter,	*Université d'Évry Val d'Essonne*
M. Michael Kohler,	*Technische Universität Darmstadt*

Acknowledgments. I owe my deepest gratitude to my PhD adviser, Dominique Picard. Dominique, I would like to thank you for the kindness you have shown toward my work and myself over the past two and a half years. Thank you for sharing with me your scientific knowledge and rigor; they both permeate throughout my PhD thesis today. More importantly, I would like to thank you for your constant encouragements, especially when times were tougher, and for the enjoyable times spent in your office or around a cup of tea; I hope there will be many more.
I would also like to thank Gérard Kerkyacharian for being such a great professor (as his MSc student) and scientific interlocutor (as a PhD student). Gérard, thank you for your enlightening scientific advices, for being so welcoming and for your great sense of humor. All of our conversations have given me plenty of food for thought.
I am very grateful to Arnaud Gloter and Michael Kohler for having taken the time to read and review my PhD manuscript. I am deeply honored by the presence of Jean-Yves Audibert, Francis Bach, Arnaud Gloter, Oleg Lepski and Peter Tankov in my PhD defense panel. Their own works have been the seeds of the humble results described in this manuscript.
In particular, I would like to show my gratitude to Peter Tankov for his careful reading of a first draft of Chapter 7. The present version of this Chapter has benefited from many of his insightful comments.
It is a pleasure to thank Pierre Alquier, Stéphane Boucheron and Karine Tribouley, who have shared with me their teaching experience throughout my teacher assistant duties. A special thanks to Erwan Le Pennec for his kindness, availability and for setting me up with late Isidore.
This thesis would not have been possible without the efficient help of Pascal Chiettini, Régine Guittard, Agathe Nguyen and Jacques Portès to whom I address my most sincere thanks.
On an other note, I would also like to thank all the (former) PhD students on the fifth floor at Chevaleret for being such good company. A very special thanks to Marc Roger de Campagnolle and Raquel Barrera for being so kind, to Nini for being so sweet, to my "little brother" Thomas Vareschi for his wicked sense of humor, to Avenilde Romo for her friendship, to Dimitrios Vlitas for the many good times spent together, to Thomas Lim for the good laughs, to Idris Kharroubi for his wisdom, to Simone Scotti for his original jokes and to Raphaël Lachièze-Rey for the (too few) good beers.
This thesis would not have been possible without the support of my friends from ECP, LSE, P7 and the CIUP. It is not possible to quote every single one of you in such a limited amount of space, but be sure that you are all in my heart and memories. I would like to thank more particularly Pierre Gireau, Vincent Loreau, Nicolas Guillemont, Augustin Guillemont, Xavier Larmurier, Alexis de Fontenay, Virginie Vinson, Cécile Varin, Marie Duthilleul, Mathieu Guerchoux, Sébastien Uzel, Laurent Gautier, Carl de Vergie, Hugues and Sanaa Le Gendre, Yara Chakhtoura and Fabien Delahaye; Aron Balas, Dennis van Berkel, Joseph Gay, Scott Bremer, Dale Park, Praveen Joseph and Bernhard Rzymelka; Rodolphe Katz, Alizée Hutin and Jérémie Dayan; Edwina Caffa, Aurore Vaïtinadapoulé, Tim Geelhaar, Ninon Thiem, Caroline Haddad, Simon Keo, Viviane Oliveira, Anna Shapovalova, Antonio Bozza, Enrica De Sario, Lucinda Deurveilher and Benjamin Lan Sun Luk; and Thibaut de Rincquesen. A very special thanks to my very dear friend Marie-Chan Tamari, thank you for your wonderful friendship.
Closest to my heart are my three sisters Axelle Gueugnier (and her husband Thibault Gueugnier), Céline Monnier and Sarah George Thengungal. A very special thanks to Sarah, thank you for having stood on my side for so many years, you have been to me like the lighthouse of Pharos, always shining and unwavering in the midst of great oceans and mile-high waves.
My last thoughts are to Elena Réan, thank you for everything, well beyond what my words can express.

Contents overview

Contents

1

Introduction

Cette thèse est constituée de trois contributions à la statistique non paramétrique. Deux d'entre elles touchent au problème de régression non paramétrique. Elles ont pour but de généraliser les méthodes d'estimation en ondelettes à (i) la régression en design aléatoire inconnu (voir Chapter 5) ainsi qu'à (ii) la régression sur un design qui prend ses valeurs sur une sous-variété de l'espace euclidien ambiant $\mathbb{R}^d$ (voir Chapter 6). De manière intéressante, les nouvelles méthodes d'estimation que nous présentons dans le cadre de la régression en design aléatoire inconnu trouvent des applications directes en classification (voir Chapter 5). Enfin, notre dernière contribution traite d'un problème inverse bien connu des universitaires et des professionnels de la finance, lequel consiste à estimer la densité risque neutre (RND) à partir des prix d'options cotés sur le marché (voir Chapter 7). Chapter 5, Chapter 6 et Chapter 7 sont en intégralité constitués d'articles publiés ou soumis à des revues scientifiques et nous profitons de cette introduction pour détailler leurs contenus. Notons au passage que les Chapter 5, Chapter 6 et Chapter 7 redéfinissent leurs propres notations et peuvent donc se lire indépendamment du reste du manuscrit.

Trois chapitres supplémentaires sont mis à la disposition du lecteur. Ils contiennent certains détails plus techniques ou des résultats mieux connus. Chapter 2 contient un rappel détaillé des résultats d'optimalité relatifs aux procédures d'estimation linéaires et non linéaires en ondelettes. Chapter 3 contient une présentation détaillée des espaces de fonctions utilisés dans cette introduction ainsi que quelques résultats fondamentaux sur les analyses multi-résolutions (MRA) et bases d'ondelettes associées. Finalement Chapter 4 contient quelques rappels utiles sur les frames. Nous renvoyons explicitement à ces chapitres dans le corps du texte à certains endroits judicieusement choisis. Toutefois, le lecteur est prié de se référer à ces chapitres pour plus d'informations sur les thèmes concernés.

Contents

1.1 Quelques problèmes de statistique non paramétrique. On commence par décrire quelques problèmes classiques en statistique auxquels nous nous intéresserons par la suite. Il est bien connu que les problèmes d'estimation de densité et de régression non paramétrique sont intimement liés et nous commençons donc par présenter ces deux problèmes. Nous introduisons ensuite le problème de classification binaire supervisée. Tout au long de ce chapitre, et à moins qu'il en soit indiqué autrement, Ω désignera un sous-ensemble de $\mathbb{R}^d$. Pour fixer les idées, disons qu' Ω désigne le cube unité $[0,1]^d$ de $\mathbb{R}^d$.

1.1.1 Le problème d'estimation de densité. Soient $X_1, \dots, X_n$ n réalisations indépendantes d'une même variable aléatoire X qui prend ses valeurs dans Ω et dont la loi de probabilité est inconnue. Faisons l'hypothèse que la loi de X admet une densité $f : \Omega \mapsto \mathbb{R}^+$ par rapport à la mesure de Lebesgue λ sur Ω. L'objectif ici consiste à estimer f à partir des n observations $X_1, \dots, X_n$.

1.1.2 Le problème de régression non paramétrique. Soient $(X_1, Y_1), \dots, (X_n, Y_n)$ n réalisations indépendantes d'un même vecteur aléatoire (X, Y) de loi inconnue mais tel que $X \in \Omega$ et $Y \in \mathbb{R}$. On écrit $f(.) = \mathbb{E}(Y|X = .)$ l'espérance conditionnelle de Y sachant X. Avec ces notations, on peut écrire

$$Y_i = f(X_i) + \xi_i, \qquad i = 1, \dots, n, \tag{1.1}$$

où la variable aléatoire ξ vérifie $\mathbb{E}(\xi|X) = 0$ et la fonction de régression $f : \Omega \mapsto \mathbb{R}$ est inconnue. Par souci de simplicité, nous ferons l'hypothèse que la variable aléatoire ξ est gaussienne centrée, de variance σ^2 et indépendante de X. L'objectif consiste ici à estimer f à partir des n observations $(X_1, Y_1), \dots, (X_n, Y_n)$. Dans ce qui suit, nous noterons μ la densité du design X par rapport à la mesure de Lebesgue λ sur Ω et $\mathcal{A} = \{\tau \in \Omega : \mu(\tau) > 0\}$ le support de μ dans Ω.

1.1.3 Quelques hypothèses standards en régression non paramétrique. Dans ce qui suit, nous allons faire un usage fréquent des hypothèses suivantes.
(**D1**) Il existe $0 < \mu_{\min} \leq \mu_{\max} < \infty$ telles que $\mu_{\min} \leq \mu(\tau) \leq \mu_{\max}$ pour tout $\tau \in \mathcal{A}$.
(**S1**) $\mathcal{A} = \Omega = [0,1]^d$.
De manière à alléger les notations, nous ferons référence à la conjonction de ces deux hypothèses par (**CS1**). On note par $\mathcal{D}_b(\mathcal{A})$ l'ensemble des densités dont le support est $\mathcal{A}$ et qui sont uniformément bornées inférieurement par $\mu_{\min}$ et supérieurement par $\mu_{\max}$ sur $\mathcal{A}$.

1.1.4 Relation entre régression et estimation de densité. Dans le cas particulier où le design est uniformément distribué sur Ω, c'est à dire $\mu = \mu^* = \lambda/|\Omega|$, où $|\Omega|$ désigne le volume euclidien de Ω, les deux problèmes de régression et d'estimation de densité sont intimement connectés. En fait, si l'on considère les estimateurs en ondelettes de f, les résultats obtenus dans le cadre de l'estimation de densité peuvent être transposés, moyennant certains ajustements, au cadre de l'estimation de la fonction de régression, à la condition que $\mu = \mu^*$ et sous des hypothèses adéquates sur le bruit de régression ξ. Les preuves reposent d'ailleurs sur des arguments similaires dans les deux cas. Nous donnons une rapide rétrospective de ces résultats au Chapter 2.
Cependant, dès que $\mu \neq \mu^*$, les deux problèmes nécessitent des traitements différents et les résultats connus en estimation de densité ne sont plus valides en régression. Nous proposons une

solution originale destinée à remédier à ce problème au Chapter 5. Dans cette thèse, nous nous intéressons aussi au problème de classification.

1.1.5 Le problème de classification. Le problème de classification consiste à prédire "au mieux" (voir Section 1.4) le label $Y \in \{0,1\}$ associé à un nouvelle observation $X \in \Omega$, étant données les observations $\mathcal{D}_n = \{(X_i, Y_i), 1 \leq i \leq n\}$. La meilleure stratégie de classification envisageable est connue sous le nom de méthode de Bayes (voir [1]) et consiste à choisir $Y = 1$ si $\mathbb{P}(Y = 1|X) \geq 1/2$ et $Y = 0$ sinon. Le classifieur de Bayes associé $h^* : \Omega \mapsto \{0,1\}$ s'écrit $h^*(X) = \mathbb{1}_{\{f(X) \geq 1/2\}}$ où l'on a écrit $f(.) = \mathbb{P}(Y = 1|X = .)$. Il existe de nombreuses façons d'élaborer une stratégie de classification à partir des données $\mathcal{D}_n$. L'une d'entre elles, appelée méthode "plug-in", consiste à reproduire la stratégie du classifieur de Bayes à l'aide d'un estimateur f_n de la fonction de régression $f(.) = \mathbb{P}(Y = 1|X = .)$. Par analogie avec le problème de régression, on peut écrire $Y = f(X) + \xi$ avec $\mathbb{E}(\xi|X) = 0$, sauf que la variable aléatoire ξ est désormais bornée et telle que $|\xi| \leq 1$. En fait, comme nous le verrons plus tard, le problème de classification est, à proprement parler, plus facile que le problème de régression correspondant associé à la méthode plug-in.

Quelques notations. Par la suite, on notera λ la mesure de Lebesgue sur un sous-ensemble $\mathcal{X}$ de Ω. De manière à alléger les notations, nous écrirons $\|.\|_{\mathbb{L}_p(\mathcal{X})}$ en lieu et place de $\|.\|_{\mathbb{L}_p(\mathcal{X},\lambda)}$ (voir Chapter 3), ou même $\|.\|_{\mathbb{L}_p}$ quand il sera clair d'après le contexte que l'espace sous-jacent est $\mathcal{X}$. De plus, étant données deux fonctions positives $a(z)$ et $b(z)$ d'une variable $z \in \mathbb{R}$, on écrira $a(z) \asymp b(z)$ pour signifier qu'il existe deux constantes $c, C > 0$ indépendantes de z telles que $ca(z) \leq b(z) \leq Ca(z)$ pour tout z. On dira de ces constantes qu'elles sont universelles ou absolues. D'autre part, la variable qui jouera le rôle de z sera soit spécifiée, soit identifiable sans équivoques d'après le contexte.

1.2 Présentation du cadre théorique minimax. Présentons maintenant le cadre minimax dans lequel nous analyserons les procédures d'estimation. On se place dans le contexte du problème de régression décrit ci-dessus. Notons f_n un estimateur de f construit sur les n observations $(X_1, Y_1), \ldots, (X_n, Y_n)$. Supposons que f appartienne à un boule $\mathcal{B}(\mathcal{F}, M)$ de rayon M d'une large classe de fonctions $\mathcal{F}$. Typiquement, $\mathcal{F}$ sera un espace de Besov $B^s_{\tau,q}(\Omega)$ dont la construction détaillée est donnée en Section 3.1. Nous mesurons la performance d'un estimateur f_n de f par l'intermédiaire de la fonction de perte $\ell(.,.) : \mathcal{F} \times \mathcal{F} \mapsto \mathbb{R}^+$. En régression, il est standard de choisir la distance $\mathbb{L}_p$ comme fonction de perte. C'est à dire $\ell(f_n, f) = \|f_n - f\|^p_{\mathbb{L}_p}$ pour $p \in [1, \infty)$ et $\ell(f_n, f) = \|f_n - f\|_{\mathbb{L}_\infty}$ lorsque $p = \infty$. En classification binaire supervisée et avec un léger abus de notations, on mesure la perte d'un classifieur $h_n : \Omega \mapsto \{0,1\}$ par rapport au classifieur de Bayes h^* à l'aide de la fonction de perte $\ell(h_n, h^*) = \mathbb{E}(\mathbb{1}_{\{Y \neq h_n(X)\}} - \mathbb{1}_{\{Y \neq h^*(X)\}}|\mathcal{D}_n)$ (voir Section 1.4). Dans le cadre théorique minimax, la qualité d'un estimateur f_n de f est mesurée par sa pire performance moyenne sur la boule $\mathcal{B}(\mathcal{F}, M)$, c'est à dire,

$$\sup_{f \in \mathcal{B}(\mathcal{F},M)} \mathbb{E}\ell(f, f_n).$$

Dans ce contexte, la meilleure performance $R_n(\mathcal{F})$ qui peut être atteinte par un estimateur donné f_n de f est appelée la vitesse minimax et s'écrit comme

$$R_n(\mathcal{F}) = \inf_{\theta_n} \sup_{f \in \mathcal{B}(\mathcal{F},M)} \mathbb{E}\ell(f, \theta_n),$$

où l'infinimum est pris sur toutes les fonctions mesurables de l'échantillon de points $(X_1, Y_1), \ldots, (X_n, Y_n)$. En particulier, un estimateur f_n de f sera dit "minimax optimal" si sa performance est de l'ordre de la meilleure performance possible, c'est à dire,

$$\sup_{f \in \mathcal{B}(\mathcal{F},M)} \mathbb{E}\ell(f, f_n) \leq C R_n(\mathcal{F}), \qquad \forall n \in \mathbb{N},$$

pour une constante universelle C. Nous écrirons aussi que f_n est "quasi minimax optimal" si sa performance est, à un facteur $\log n$ près, de l'ordre de la performance optimale, c'est à dire,

$$\sup_{f \in \mathcal{B}(\mathcal{F},M)} \mathbb{E}\ell(f, f_n) \leq C (\log n)^{\delta} R_n(\mathcal{F}), \qquad \forall n \in \mathbb{N},$$

pour une constante universelle $\delta > 0$. Dans la suite, nous nous efforcerons de construire un estimateur f_n de f qui soit (quasi) minimax optimal pour une large classe de fonctions $\mathcal{F}$ et une grande variété de pertes ℓ. Tournons nous maintenant vers la première contribution de cette thèse.

1.3 Régression linéaire localisée en ondelettes sur un design aléatoire. Dans cette Section, nous expliquons dans un premier temps pourquoi les méthodes classiques d'estimation en ondelettes ne fonctionnent plus dès que $\mu \neq \mu^* = \lambda/|\Omega|$. Nous discutons ensuite brièvement les travaux scientifiques passés relatifs à la transposition des méthodes d'ondelettes au cas de la régression en design aléatoire de densité inconnue. Parmi les nombreux estimateurs envisageables en design aléatoire, l'estimateur par polynômes locaux (LPE) est bien connu pour sa flexibilité et ses performances théoriques remarquables (voir [2, 3]). Or il s'avère que la procédure d'estimation locale en ondelettes que nous proposons au Chapter 5 présente une certaine similarité avec la procédure d'estimation par polynômes locaux. C'est pourquoi nous prenons le temps de faire quelques rappels relatifs au LPE. Finalement, nous présentons la procédure de régression locale en ondelettes, telle qu'elle est décrite au Chapter 5. Nous clôturons cette Section par quelques pistes de recherche.

1.3.1 L'échec des procédures conventionnelles d'estimation en ondelettes lorsque $\mu \neq \mu^*$. Le lecteur intéressé pourra trouver un rappel détaillé des procédures d'estimation traditionnelles en ondelettes et des résultats théoriques associés au Chapter 2. On rappelle brièvement ici la construction des estimateurs classiques en ondelettes. Supposons que l'on dispose d'une analyse multi-résolution (MRA) de Ω élaborée à partir des fonctions d'échelle à support compact de Daubechies $(\varphi_{j,k})$, $j \geq 0$, $k \in \mathcal{Z}_j^d \subset \mathbb{Z}^d$ où $\#\mathcal{Z}_j^d = 2^{jd}$. Elle est constituée d'espaces d'approximation emboîtés $(V_j)_{j \geq 0}$ qui reproduisent les polynômes dont le degré est au plus égal à $r-1$, pour un $r \in \mathbb{N}$ fixé. On suppose dorénavant que l'on travaille avec ce type de MRA, que l'on désignera par r-MRA (voir Section 3.2.2). La projection orthogonale de f sur V_j peut s'écrire

de deux manière différentes $\mathscr{P}_j f$ et $\mathscr{W}_j f$, en terme de fonctions d'échelles $(\varphi_{j,k})$ ou d'ondelettes $(\psi_{j,k})$, respectivement. On rappelle en effet qu'on a,

$$\mathscr{P}_j f = \sum_{k \in \mathcal{Z}_j^d} \alpha_{j,k} \varphi_{j,k}, \qquad \alpha_{j,k} = \langle f, \varphi_{j,k} \rangle,$$
$$\mathscr{W}_j f = \sum_{t=-1}^{j-1} \sum_{k \in \Lambda_t} \beta_{t,k} \psi_{t,k}, \qquad \beta_{t,k} = \langle f, \psi_{t,k} \rangle,$$

où, pour tout $t \geq 0$, $\Lambda_t \subset \mathbb{Z}^d$ et $\#\Lambda_t \asymp 2^{td}$. Traditionnellement, la première représentation donne lieu aux procédures d'estimation linéaire $\mathscr{P}_j f_n$ de f alors que la deuxième donne lieu aux procédures d'estimation non-linéaires $\mathscr{W}_J f_n$ par seuillage de coefficients d'ondelettes (voir Chapter 2 pour plus de détails). On retiendra ici que les coefficients $\alpha_{j,k}$ et $\beta_{j,k}$ correspondant sont respectivement estimés par,

$$\alpha_{j,k}^{(n)} = \frac{|\Omega|}{n} \sum_{i=1}^{n} Y_i \varphi_{j,k}(X_i), \qquad \beta_{j,k}^{(n)} = \frac{|\Omega|}{n} \sum_{i=1}^{n} Y_i \psi_{j,k}(X_i). \tag{1.2}$$

En design aléatoire et lorsque $\mu \neq \mu^*$, les estimateurs standards $\alpha_{j,k}^{(n)}$ et $\beta_{j,k}^{(n)}$ sont perturbés par la mesure du design μ et ne convergent plus vers les vrais coefficients $\alpha_{j,k} = \langle f, \varphi_{j,k} \rangle$ et $\beta_{j,k} = \langle f, \psi_{j,k} \rangle$. De telle sorte que $\mathscr{P}_j f_n$ et $\mathscr{W}_J f_n$ ne convergent plus vers leurs vraies contreparties. Comme en témoignent les travaux précédents en ce domaine, le problème de l'estimation des coefficients $\alpha_{j,k}$ et $\beta_{j,k}$ lorsque le design est aléatoire et de loi μ inconnue est délicat.

1.3.2 Revue des travaux scientifiques antérieurs. De nombreux auteurs ont tenté de transposer les résultats d'optimalité des procédures d'estimation en ondelettes au cas de la régression en design aléatoire inconnu, de manière à bénéficier des avantages propres aux analyses multi-résolutions (MRA) et bases d'ondelettes associées. Nous n'avons pas ici pour objectif de présenter une revue exhaustive des travaux antérieurs, mais nous nous contentons de faire référence aux travaux qui présentent un lien avec les développements présentés dans cette thèse.
La littérature relative à l'étude des estimateurs par ondelettes en design aléatoire inconnu se divise en deux grands courants. (i) Le premier courant regroupe les travaux dont l'objectif est d'élaborer des algorithmes de construction de bases d'ondelettes qui "s'adaptent" à la mesure (empirique) du design (voir [4, 5, 6, 7]). (ii) Le second est constitué des travaux qui utilisent les bases d'ondelettes traditionnelles, comme dans le cas où $\mu = \mu^*$, mais modifient la façon d'estimer les coefficients du développement en série de f correspondant (voir [8, 9, 10, 11, 12]). Notre travail s'inscrit dans cette deuxième ligne de recherche.
Comme indiqué dans [9], le succès du LPE en design aléatoire vient du fait qu'il est implicitement construit comme un "ratio", lequel élimine en grande partie l'influence du design. Dans un contexte d'estimation en ondelettes, une première suggestion fut donc de considérer "l'estimateur ratio" de f (voir [13, 14, 15] par exemple), bien connu de la littérature sur l'estimation par décomposition sur une base orthonormée de fonctions (voir [16, 17] et [1, Chap. 17] ainsi que les références qui y sont incluses). En gros, l'estimateur ratio est l'équivalent en ondelettes de l'estimateur de Nadaraya-Watson (voir [18, 19]). L'estimateur ratio est élaboré sur l'observation que $f(x) = f(x)\mu(x)/\mu(x)$ (là où $\mu(x) \neq 0$) où les fonctions $g(x) = f(x)\mu(x)$ et $\mu(x)$ sont

toutes les deux facilement estimables via les estimateurs en ondelettes traditionnels. Si bien que f est estimée par le ratio des deux estimateurs correspondant. L'estimateur ratio repose donc malheureusement sur l'estimation de la densité du design μ elle-même et c'est pourquoi cette méthode nécessite d'imposer autant de régularité sur μ que sur f.
De manière à contourner ce problème, une autre approche a été proposée par [20, 21]. Ils travaillent dans le cas $d = 1$ et prennent $\Omega = [0, 1]$. Notons G la fonction de répartition du design et par G^{-1} son inverse généralisé. Leur approche consiste à estimer $f \circ G^{-1}$ en utilisant des procédures conventionnelles d'estimation en ondelettes. C'est pourquoi leurs résultats sont exprimés en fonction de la régularité de $f \circ G^{-1}$. Malheureusement, cette méthode ne se généralise pas directement au cas multivarié, puisque G n'admet plus d'inverse dès que $d \geq 2$.
Dans un autre registre, [22] obtient un estimateur en ondelettes adaptatif quasi minimax optimal pour une large classe d'espaces de Besov sous l'hypothèse (**CS1**) par le biais de méthodes de sélection de modèles. Ces résultats ne sont donc valides que pour la perte correspondant à la distance de $\mathbb{L}_2(\Omega)$.
D'autres résultats connexes peuvent être trouvés dans [23, 24, 25, 26].

1.3.3 L'estimateur par polynômes locaux. Laissons pour un moment les estimateurs en ondelettes de coté et concentrons nous sur l'estimateur par polynômes locaux (LPE). Le LPE est bien connu pour sa flexibilité et ses performances remarquables en régression sur un design aléatoire dont la loi est inconnue. Il est en effet prouvé dans [2, 3] que le LPE est minimax optimal sur des boules de Hölder $\mathcal{B}(\mathscr{C}^s(\Omega), M)$ et pour une large classe de pertes correspondant à la distance de $\mathbb{L}_p(\Omega)$, $p \in (0, \infty]$. À l'époque, les résultats publiés par Stone amélioraient ceux des travaux antérieurs puisqu'ils n'imposaient aucune hypothèse de régularité sur μ au-delà de (**D1**) et étaient valides en toutes dimensions d. Bien que ces résultats soient non-adaptatifs, le problème de l'adaptation du LPE a depuis lors été résolu (voir [27, 28, 29] par exemple). La construction du LPE et ses performances théoriques sont rappelées dans l'appendice de ce chapitre.
Naturellement, nous aimerions donc construire une procédure linéaire d'estimation en ondelettes qui présente des performances théoriques au moins comparables à celles du LPE et bénéficie des avantages calculatoires propres aux estimateurs en ondelettes.

1.3.4 Notre contribution. Au Chapter 5, nous étendons les résultats d'optimalité des procédures linéaires d'estimation en ondelettes au cas où le design est aléatoire de densité inconnue. La contribution du Chapter 5 se décompose en trois parties. (i) Nous supposons initialement que le support $\mathcal{A}$ de la densité du design est connu et montrons que, contrairement à une idée répandue, il est possible de construire un estimateur $f^{@}$ de f sur une analyse multi-résolution, qui vérifie des résultats d'optimalité semblables à ceux du LPE. Nous montrons de plus que $f^{@}$ exploite avantageusement la structure de treillis de la MRA sur laquelle il est construit, ce qui lui permet d'être plus performant d'un point de vue calculatoire que le LPE. Nous illustrons cette propriété à travers une série de simulations. (ii) Dans un second temps, nous montrons comment cette procédure d'estimation locale peut être modifiée pour être encore valide dans le cas où $\mathcal{A}$ est inconnu et nous notons $f^{✠}$ l'estimateur correspondant de f. De manière intéressante $f^{✠}$ présente des performances théoriques similaires à celles du LPE. De plus $f^{✠}$ exploite toujours, d'une certaine manière, la structure de treillis de la MRA sur laquelle il est construit et conserve donc un avantage calculatoire sur les estimateurs à noyau tels que le LPE. (iii) Finalement nous

nous tournons vers le problème de classification binaire supervisée et montrons que $f^{\maltese}$ peut servir à la construction de règles de classifications adaptatives et minimax, qui peuvent en outre atteindre des vitesses de convergence "super rapides" sous une hypothèse de marge. Cette dernière application à la classification n'est pas détaillée dans cette section mais plutôt traitée un peu plus tard en Section 1.4.

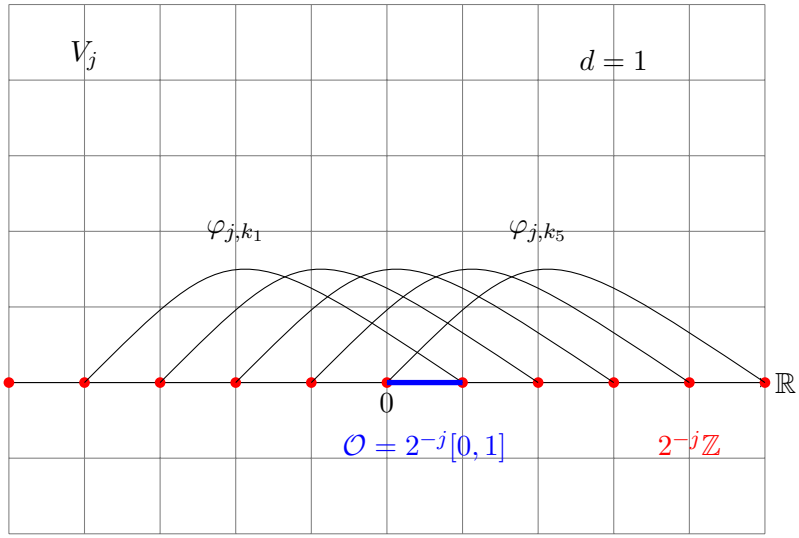

FIGURE *1.1 – Description des cellules de localisation $\mathcal{O}$ et de leurs relations aux Supp$\varphi_{j,k}$.*

1.3.4.1 La procédure d'estimation locale en ondelettes. Dans le Chapter 5, nous introduisons une nouvelle procédure linéaire d'estimation en ondelettes obtenue par projections localisées sur les espaces d'approximation (V_j). En gros, la procédure repose sur les observations suivantes. Remarquons d'abord que tout point $x \in \mathcal{A}$ appartient à une cellule $\mathcal{O}$ du treillis $2^{-j}\mathbb{Z}^d \cap \Omega$ sous-jacent à V_j (voir Chapter 3 pour plus de détails). Par ailleurs, et puisque les V_j sont construits sur des fonctions d'échelle à support compact, la valeur d'un élément quelconque g de V_j sur cette cellule $\mathcal{O}$ n'est influencée que par un nombre fini m_φ et indépendant de j de fonctions d'échelles : celles dont le support est d'intersection non vide avec la cellule (voir Figure 5.1). De telle manière qu'un estimateur de f en tout point de cette cellule peut être obtenu par régression "locale" contre les m_φ fonctions d'échelle correspondantes. En particulier, on note (φ_{j,k_i}), $1 \le i \le m_\varphi$ les m_φ fonctions d'échelle dont le support est d'intersection non vide avec la cellule $\mathcal{O}$ du treillis $2^{-j}\mathbb{Z}^d \cap \Omega$. Alors, pour tout $x \in \mathcal{O}$, l'évaluation de l'estimateur $f_j^{@}(x) = \alpha_{j,k_1}^{@}\varphi_{j,k_1}(x) + \ldots + \alpha_{j,k_{m_\varphi}}^{@}\varphi_{j,k_{m_\varphi}}(x)$ est réduite à l'estimation des coefficients $(\alpha_{j,k_i}^{@})$, $1 \le i \le m_\varphi$. Ces derniers sont obtenus par moindres-carrés sur $\mathcal{O}$ comme l'unique minimiseur en $a = (a_1, \ldots, a_{m_\varphi}) \in \mathbb{R}^{m_\varphi}$ de la somme suivante,

$$\sum_{i=1}^{n} \left(Y_i - \sum_{t=1}^{m_\varphi} a_t \varphi_{j,k_t}(X_i) \right)^2 \mathbb{1}_{\mathcal{O}}(X_i). \tag{1.3}$$

Si cette somme admet plusieurs minimiseurs, alors on prend $(\alpha_{j,k_i}^{@}) = 0$, $1 \le i \le m_\varphi$, c'est à dire $f_j^{@}(x) = 0$ pour tout $x \in \mathcal{O}$. L'estimateur $f_j^{@}$ de f obtenu en suivant cette procédure est ajusté

par un seuillage spectral de la matrice de régression "locale" associée, dans le même esprit que pour le LPE (voir appendice). Plus précisément, on prend $f_j^{@}(x) = 0$ pour tout $x \in \mathcal{O}$ si le plus petite valeur propre de la matrice de régression locale associée à la cellule $\mathcal{O}$ est inférieure à un seuil π_n^{-1}, choisit typiquement tel que $\pi_n = \log n$.

1.3.4.2 Inversion de la matrice de Gram sous (**CS1**). Le problème décrit en eq. (1.3) admet une unique solution si et seulement si la matrice de Gram empirique G associée aux (φ_{j,k_i}), $1 \leq i \leq m_\varphi$ est inversible. Rappelons au passage que la matrice de Gram en question est de taille $m_\varphi \times m_\varphi$ et de terme général

$$G_{i,\ell} = \frac{1}{n} \sum_{t=1}^{n} \varphi_{j,k_i}(X_t)\varphi_{j,k_\ell}(X_t)\mathbb{1}_{\mathcal{O}}(X_t).$$

Bien entendu, cette matrice est aléatoire. Puisqu'elle contient un nombre fini m_φ^2 de termes, le contrôle de la plus petite valeur propre de G devient aisé dès que $\mathbb{E}G$ est elle-même inversible. Évidemment, le contrôle de la plus petite valeur propre de $\mathbb{E}G$ se réduit au contrôle de l'infinimum sur $u = (u_1, \ldots, u_{m_\varphi}) \in \mathbb{S}^{m_\varphi - 1}$ de

$$\mathbb{E}(u_1\varphi_{j,k_1}(X) + \ldots + u_{m_\varphi}\varphi_{j,k_{m_\varphi}}(X))^2\mathbb{1}_{\mathcal{O}}(X),$$

lequel est borné inférieurement par une constante strictement positive $g_{\min}$ sous (**S1**), qui ne dépend ni de j, ni de $\mathcal{O}$ et donc ni de x. Ce dernier résultat repose sur un argument de compacité joint à la "propriété d'indépendance linéaire locale" des fonctions d'échelle (φ_k) que nous détaillerons plus bas en Section 1.3.4.4. Nous verrons plus tard que, si l'on relaxe l'hypothèse (**S1**), alors une analyse plus fine est requise.

1.3.4.3 Résultats d'optimalité sous (**CS1**). Notons $f_j^{@}$ l'estimateur linéaire en ondelettes de f obtenu par projections localisées sur V_j, avec un seuillage spectral de la matrice de régression locale G de niveau $\pi_n^{-1} = (\log n)^{-1}$.

Quelques résultats théoriques. On définit par ailleurs les variables j_r, j_s, J et $t(n)$ de telle manière que,

$$2^{j_r} = \lfloor n^{\frac{1}{2r+d}} \rfloor, \qquad 2^{j_s} = \lfloor n^{\frac{1}{2s+d}} \rfloor,$$
$$2^{Jd} = \lfloor nt(n)^{-2} \rfloor, \qquad t(n)^2 = \kappa\pi_n^2 \log n,$$

où κ est un nombre réel positif que nous choisirons ultérieurement. De plus, on pose $\mathcal{J}_n = \{j_r, j_r + 1, \ldots, J-1, J\}$. Nous obtenons au Chapter 5 le résultat de concentration exponentiel suivant.

Theorem 1.3.1. *Soit $r \in \mathbb{N}$. Supposons que l'hypothèse* (**CS1**) *soit vérifiée et que l'erreur ξ en eq. (1.1) soit gaussienne centrée, de variance σ^2 et indépendante de X. Supposons de plus que f appartienne à une boule $\mathcal{B}(Lip^s(\Omega), M)$ de rayon M de l'espace de Lipschitz $Lip^s(\Omega)$ pour un $s \in (0, r)$. Alors, pour tout $j \in \mathcal{J}_n$, tout $\delta > 2M2^{-js}\max(1, 3\pi_n R^d \mu_{\max})$ et tout $x \in \mathcal{A}$, on*

obtient le résultat suivant

$$\sup_{\mu\in\mathcal{D}_b(\mathcal{A})}\sup_{f\in\mathcal{B}(Lip^s(\Omega),M)}\mathbb{P}_f^{\otimes n}(|f(x)-f_j^{@}(x)|\geq\delta)$$
$$\leq 2R^{2d}\exp\left(-n2^{-jd}\frac{\pi_n^{-2}}{2\mu_{\max}R^{4d}+\frac{4}{3}R^{2d}\pi_n^{-1}}\right)\mathbb{1}_{\{\delta\leq M\}}+R^d\Lambda\left(\frac{\delta 2^{-j\frac{d}{2}}}{2\pi_n R^d}\right), \tag{1.4}$$

où $R=2r-1$, $\mathcal{D}_b(\mathcal{A})$ a été définit en Section 1.1.3 et Λ est tel que,

$$\Lambda(\delta)=1\wedge\left\{\frac{2\sigma(\mu_{\max}+2^{j\frac{d}{2}}\delta)^{\frac{1}{2}}}{\delta\sqrt{2\pi n}}\exp\left(-\frac{n\delta^2\sigma^{-2}}{\mu_{\max}+2^{j\frac{d}{2}}\delta}\right)\right\}$$
$$+2\exp\left(-\frac{n\delta^2}{2\mu_{\max}+\frac{4}{3}2^{j\frac{d}{2}}\delta}\right).$$

Ce résultat est très similaire à celui obtenu sous (**CS2′**) pour le LPE (voir appendice). En particulier, il permet de dériver l'optimalité de l'estimateur par projections locales $f^{@}$ lorsque f appartient à des boules de Lipschitz et pour une vaste classe de pertes correspondant aux distances de $\mathbb{L}_p(\mathcal{A},\mu)$, $p\in[1,\infty)$.

Corollary 1.3.1. *Soit $r\in\mathbb{N}$ et supposons que* (**CS1**) *soit vérifiée. Supposons de plus que f appartienne à la boule $\mathcal{B}(Lip^s(\Omega),M)$ de l'espace de Lipschitz $Lip^s(\Omega)$ pour un $s\in(0,r)$. On définit j_s tel que $2^{j_s}=\lfloor n^{\frac{1}{2s+d}}\rfloor$. Alors, pour tout $p\in[1,\infty)$, nous obtenons,*

$$\sup_{\mu\in\mathcal{D}_b(\mathcal{A})}\sup_{f\in\mathcal{B}(Lip^s(\Omega),M)}\mathbb{E}^{\otimes n}\|f-f_{j_s}^{@}\|^p_{\mathbb{L}_p(\mathcal{A},\mu)}\leq C(p)\pi_n^p n^{-\frac{sp}{2s+d}},$$

où $\mathcal{D}_b(\mathcal{A})$ a été définit en Section 1.1.3. Ce résultat et la borne inférieure associée (voir Theorem 5.7.3), prouvent que $f_{j_s}^{@}$ est quasi minimax optimal sur les boules de $Lip^s(\Omega)$.

En particulier, cela prouve qu'il est possible d'utiliser une MRA pour élaborer un estimateur $f^{@}$ de f qui soit minimax optimal sous le seul jeu d'hypothèses (**CS1**).

Résumé des performances théoriques de la procédure locale. Plus précisément, nos résultats sont valides (i) en toutes dimensions d ; (ii) pour une large classe de pertes $\mathbb{L}_p(\mathcal{A},\mu), p\in[1,\infty)$; (iii) et une vaste échelle d'espaces de Lipschitz $Lip^s(\Omega)$, $s\in(0,r)$; (iv) et ne requièrent aucune hypothèse sur μ au-delà de (**D1**). En particulier, et contrairement à la plupart des autres méthodes d'estimation en ondelettes, aucune hypothèse de régularité sur μ n'est nécessaire.

Performances calculatoires. D'un point de vue calculatoire, $f^{@}$ surclasse les autres estimateurs de f sous l'hypothèse (**D1**) puisque il exploite la structure de treillis de la MRA sur laquelle il est bâtit. En particulier, le calcul de $f_j^{@}$ ne requiert au plus que 2^{jd} régressions pour pouvoir être évalué en tous points de $\mathcal{A}$, alors que n'importe quel autre estimateur à noyau doit être recalculé à chaque nouvelle évaluation.

Commentaires. En fait $f^{@}$ présente un caractère hybride entre les estimateurs en ondelettes et les estimateurs à noyau, tels que le LPE. D'une part, $f^{@}$ possède l'efficacité calculatoire des

estimateurs en ondelettes et d'autre part il présente les mêmes performances théoriques que le LPE. En particulier $f^{@}$ reste un estimateur linéaire de f (modulo le seuillage spectral de la matrice de régression locale), et ne peut rendre compte de régularités plus fines que celles décrites par les espaces de Lipschitz. On donne le résultat d'une simulation avec la version adaptative de $f^{@}$ (voir plus bas) en design aléatoire non uniforme en Figure 1.2.

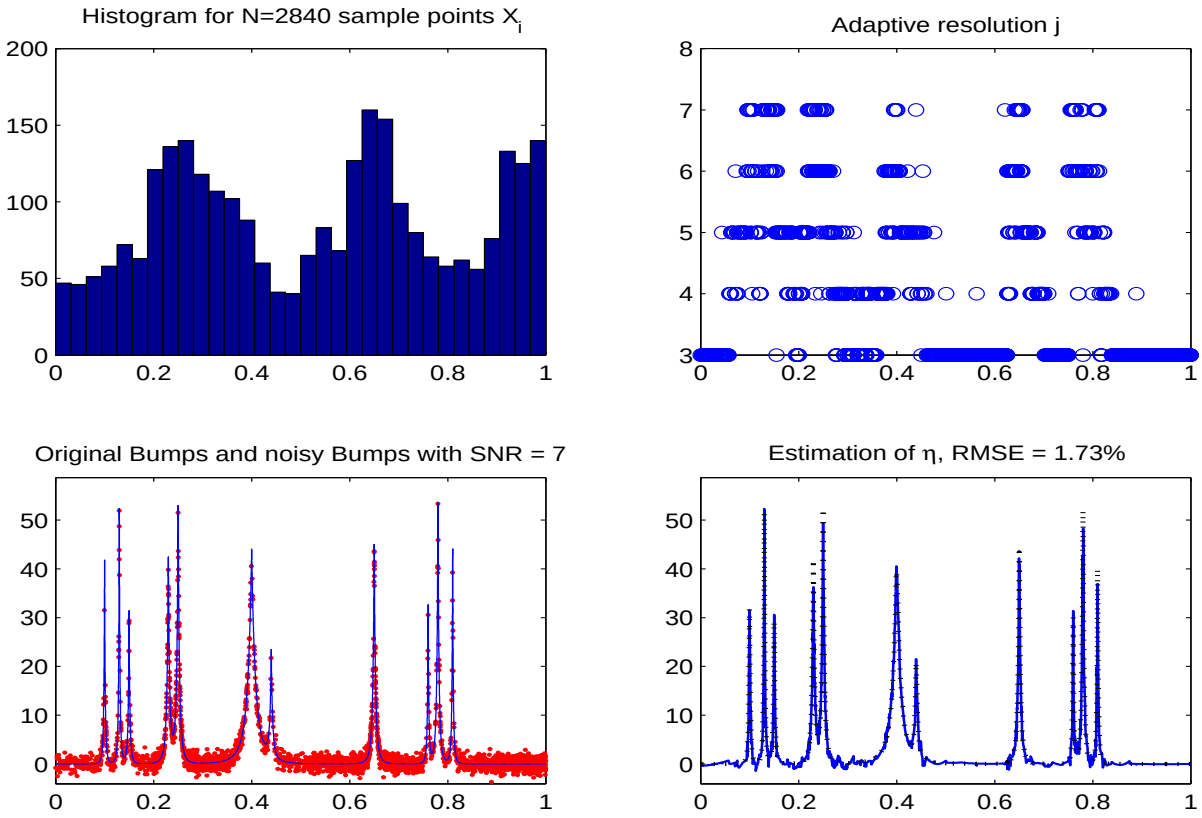

FIGURE *1.2 – Dans le sens des aiguilles d'une montre à partir de la figure en haut à gauche, on représente : un histogramme des points X_i qui constituent le design ; le niveau de résolution choisit de manière adaptative par la méthode de Lepski en chaque point X_i du design ; le vrai signal f (points noirs) ainsi que l'estimateur $f^{@}$ (ligne bleue continue) en chaque point X_i ; et finalement le signal original f (ligne bleue continue) accompagné de sa version bruitée Y_i aux points X_i (points rouges).*

1.3.4.4 Relaxation de l'hypothèse (**S1**). De manière intéressante, la nature **locale** de $f^{@}$ permet de relaxer l'hypothèse (**S1**) selon laquelle $\mathcal{A}$ est connu pour considérer le cas où $\mathcal{A}$ est lui-même inconnu bien que vérifiant une hypothèse de régularité (**S2**) décrite plus bas. Cette dernière configuration permet de traiter le cas où la densité μ s'annule sur Ω tout en restant bornée sur son support $\mathcal{A}$, une configuration particulièrement adaptée au problème de classification supervisée sous hypothèse de marge. En fait, tous les résultats d'optimalité obtenus pour $f^{@}$ peuvent être transposés au cas où $\mathcal{A}$ est inconnu, à la seule condition que $\mathcal{A}$ soit suffisamment régulier et que la procédure d'estimation soit modifiée de manière adéquate. Par la suite, on

note (**CS2**) la conjonction des deux hypothèses (**D1**) et (**S2**).

Modification de la procédure d'estimation localisée lorsque $\mathcal{A}$ est inconnu. Commençons par quelques remarques élémentaires. Sous (**CS1**) toutes les cellules du treillis de la MRA sont strictement incluses dans le support $\mathcal{A}$ de μ, puisque, la frontière de $\mathcal{A}$ coïncide exactement avec certaines branches du treillis $2^{-j}\mathbb{Z}^d$. De telle sorte que le problème de régression locale est le même sur chacune des cellules du treillis. Sous (**CS2**), en revanche, $\mathcal{A}$ est inconnu et il est fort possible que la frontière de $\mathcal{A}$ ne coïncide plus avec les branches du treillis $2^{-j}\mathbb{Z}^d$ sous-jacent. Il faut donc traiter l'effet de bord qui correspond aux cellules du treillis qui chevauchent la frontière de $\mathcal{A}$. Si toutes les configurations de chevauchement sont possibles, alors il n'y a aucun espoir d'obtenir un contrôle uniforme en x et en j sur la plus petite valeur propre de l'espérance de la matrice de régression locale.
Une façon de remédier à ce problème lorsque $\mathcal{A}$ n'est pas connu consiste à imposer une contrainte de régularité (**S2**) sur la frontière de $\mathcal{A}$ et à permettre aux cellules de régression locale de glisser de manière à ce que leur centre appartienne toujours au support $\mathcal{A}$. C'est le caractère locale de la calibration de notre procédure d'estimation qui nous autorise à faire glisser les cellules de régression locale. Avec des cellules glissantes et sous (**CS2**), nous obtenons de nouveau un contrôle uniforme en x et en j sur la plus petite valeur propre de l'espérance de la matrice de régression locale.
Plus précisément, on se donne une cellule $\mathcal{O}$ du treillis $2^{-j}\mathbb{Z}^d$. On peut considérer la cellule $\mathcal{O} = 2^{-j}[0,1]^d$, par exemple. On note $\mathcal{O}(x) = x - 2^{-j-1} + \mathcal{O}$ la version de la cellule $\mathcal{O}$ centrée en x. Supposons maintenant que l'on veuille estimer f en un point $x \in \mathcal{A}$. Une première stratégie d'estimation consisterait à effectuer un régression locale sur $\mathcal{O}(x)$ avec les fonctions d'échelle associées à cette cellule. Cependant, en déplaçant la cellule $\mathcal{O}$ avec le point $x \in \mathcal{A}$ auquel on veut estimer f, on perd tous les avantages calculatoires offerts par la structure de treillis de la MRA sous-jacente. En fait, si l'on s'arrêtait ici, on obtiendrait un estimateur $f^{\maltese}(x)$ de $f(x)$ qui ressemblerait étrangement à un estimateur à noyau, mis à part le fait que le noyau serait remplacé par un jeu fini de fonctions d'échelles.
Même si le support $\mathcal{A}$ est inconnu sous (**S2**), il peut être partiellement identifié puisque les points du design X_i appartiennent à $\mathcal{A}$. C'est cette information qui va nous permettre d'exploiter à nouveau les avantages calculatoires offerts par la structure de treillis de la MRA sous-jacente. Dans un soucis de simplicité, supposons que nous disposons d'un jeu de données de taille $2n$ et divisons le en deux jeux de données de taille n que l'on note $\mathcal{D}_n = \{(X_i, Y_i), i = 1, \dots, n\}$ et $\mathcal{D}'_n = \{(X'_i, Y'_i), i = 1, \dots, n\}$ (bien entendu, des développements similaires sont valides avec un échantillon initial de taille $2n+1$). Alors, on peut d'une part utiliser les points du design X'_i de $\mathcal{D}'_n$ pour identifier $\mathcal{A}$ et d'autre part se servir de $\mathcal{D}_n$ pour calibrer notre estimateur. Plus précisément, la procédure d'estimation $f^{\maltese}$ peut s'écrire comme suit. On se donne un point $x \in \mathcal{A}$ auquel on veut estimer f. Alors deux cas possibles se présentent. (i) Soit la cellule $\mathcal{O}(x)$ centrée en x ne contient aucun point du design X'_i de $\mathcal{D}'_n$ et on prend alors $f^{\maltese}(x) = 0$. (ii) Soit la cellule $\mathcal{O}(x)$ centrée en x contient au moins un point du design X'_i de $\mathcal{D}'_n$. On sélectionne l'un des X'_i dans $\mathcal{O}(x)$ que l'on note X'_{i_x} (la procédure de sélection n'a aucune importance au-delà de considérations purement calculatoires). Par construction, x est contenu dans la cellule $\mathcal{O}(X'_{i_x})$ centrée en X'_{i_x}. On calcule alors $f^{\maltese}(x)$ à partir du jeu de données $\mathcal{D}_n$ par régression locale sur les fonctions d'échelle associées à la cellule $\mathcal{O}(X'_{i_x})$ centrée en X'_{i_x}. Remarquons ici que, par construction, X'_{i_x} est indépendant des points de $\mathcal{D}_n$. C'est une propriété cruciale de la procédure

d'estimation sous (**CS2**) qui permet de mener les calculs à leur terme sans plus de difficultés que pour la procédure d'estimation décrite plus haut sous (**CS1**). Et cela explique au passage pourquoi il était nécessaire de scinder en deux l'échantillon initial.
Discutons brièvement la construction de $f^{\maltese}$. On sait qu'un point du design X'_i de $\mathcal{D}'_n$ appartient au support $\mathcal{A}$. On peut donc effectuer une régression locale sur $\mathcal{O}(X'_i)$. Ce faisant, on obtient un estimateur $f^{\maltese}$ de f en tous points x appartenant à $\mathcal{O}(X'_i) \cap \mathcal{A}$. Remarquons par ailleurs que, sous (**D1**), les points du design X'_i peuplent le support $\mathcal{A}$ de manière assez dense, de telle sorte que l'union des cellules $\mathcal{O}(X'_i)$ centrées aux points du design X'_i de $\mathcal{D}'_n$ recouvre entièrement $\mathcal{A}$, à un ensemble de mesure (quasi) exponentiellement décroissante en n près. Si bien que le calcul de $f^{\maltese}$ en tous points $x \in \mathcal{A}$ nécessite au plus une régression locale par point X'_i du design, c'est à dire au plus n régressions. Notons finalement que cet avantage calculatoire de $f^{\maltese}$ sur les estimateurs à noyau peut être optimisé. En effet, la régression locale en un point du design X'_i de $\mathcal{D}'_n$ peut être omise si la cellule $\mathcal{O}(X'_i)$ centrée en X'_i est elle-même incluse dans l'union de plusieurs autres cellules centrées en d'autres points du design de $\mathcal{D}'_n$. De manière à optimiser les performances calculatoires de $f^{\maltese}$, on choisira si possible X'_{i_x} comme l'un des X'_i dans $\mathcal{O}(x)$ pour lequel une régression locale a déjà été calculée ou n'importe lequel des X'_i dans $\mathcal{O}(x)$ autrement.

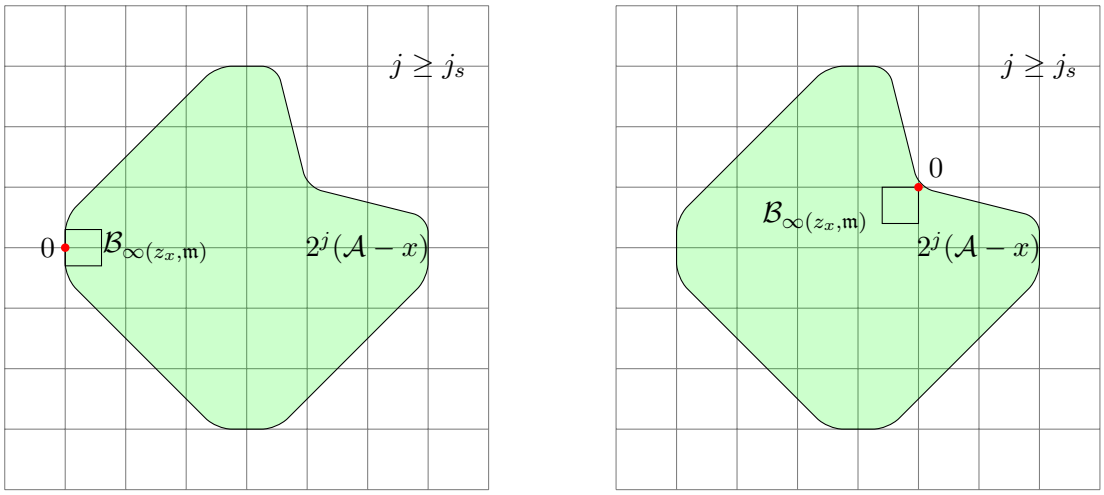

FIGURE *1.3* – (**S2**) *permet au support $\mathcal{A}$ d'être non-convexe et éventuellement à plusieurs composantes.*

Description de l'hypothèse (**S2**). Dans un premier temps, rappelons en quoi consiste l'hypothèse de régularité (**S2**). On note $\mathfrak{m}_0$ une constante universelle telle que $\mathfrak{m}_0 \in (0,1)$ et on rappelle que $2^{j_s} = \lfloor n^{\frac{1}{2s+d}} \rfloor$. (**S2**) peut alors s'écrire,
(**S2**) $\Omega = \mathbb{R}^d$ et $\mathcal{A}$ appartient à $\mathscr{A}_{j_s}$, où

$$\mathscr{A}_{j_s} := \{\mathcal{A} \subset \mathbb{R}^d : \exists \mathfrak{m} \geq \mathfrak{m}_0, \forall x \in \mathcal{A}, \\ \exists z_x \in \mathbb{R}^d, 0 \in \mathcal{B}_\infty(z_x, \mathfrak{m}) \subset 2^{j_s}(\mathcal{A}-x)\}.$$

En d'autres termes, cela veut dire que le support $\mathcal{A}$ de μ est constitué de petits hyper-cubes, et se prête donc aisément à une procédure d'estimation construite sur le treillis d'une MRA

(voir Figure 5.2). En fait, cette hypothèse de régularité a été conçue pour permettre d'exploiter directement la "propriété d'indépendance linéaire locale" des fonctions d'échelle. Mais avant de décrire cette propriété, attardons nous un instant sur le comportement de la matrice de Gram empirique sous (**CS2**), où (**CS2**) désigne l'occurrence conjointe de (**D1**) et (**S2**).

Inversion de la matrice de Gram sous (**CS2**). Rappelons que puisque $\mathcal{A}$ est désormais inconnu, nous faisons bouger le treillis avec le point x auquel nous souhaitons estimer f. On considère la cellule $\mathcal{O} = 2^{-j}[0,1]^d$ du treillis $2^{-j}\mathbb{Z}^d$ au niveau de résolution j. Par construction, x appartient à la cellule $\mathcal{O}(X'_{i_x})$ centrée en X'_{i_x}. Centrer $\mathcal{O}$ en X'_{i_x} revient, de manière équivalente, à translater tous les points de $\mathbb{R}^d$ de manière à ce que X'_{i_x} soit au centre de la cellule $\mathcal{O}$, c'est à dire au point $2^{-j-1} \in \mathbb{R}^d$ (dont toutes les coordonnées sont égales à $2^{-j-1} \in \mathbb{R}$). Posons à cet effet $\widetilde{X}_i = X_i - X'_{i_x} + 2^{-j-1}$. Notons par (φ_{j,k_i}), $1 \le i \le m_\varphi$ les fonctions d'échelle dont le support est d'intersection non vide avec $\mathcal{O}$. L'estimateur de f au point x s'écrit alors comme $f_j^{\maltese}(x)$ où l'on définit $f_j^{\maltese}(x) = \alpha_{j,k_1}^{\maltese}\varphi_{j,k_1}(x - X'_{i_x} + 2^{-j-1}) + \ldots + \alpha_{j,k_{m_\varphi}}^{\maltese}\varphi_{j,k_{m_\varphi}}(x - X'_{i_x} + 2^{-j-1})$. Comme lors de la construction de $f^{@}$ les $(\alpha_{j,k_i}^{\maltese})$, $1 \le i \le m_\varphi$ sont obtenus par moindres-carrés comme l'unique minimiseur en $a = (a_1, \ldots, a_{m_\varphi}) \in \mathbb{R}^{m_\varphi}$ de la somme suivante,

$$\begin{aligned}
&\sum_{i=1}^{n}\left(Y_i - \sum_{t=1}^{m_\varphi} a_t\varphi_{j,k_t}(X_i - X'_{i_x} + 2^{-j-1})\right)^2 \mathbb{1}_{\mathcal{O}}(X_i - X'_{i_x} + 2^{-j-1}) \\
=&\sum_{i=1}^{n}\left(Y_i - \sum_{t=1}^{m_\varphi} a_t\varphi_{j,k_t}(\widetilde{X}_i)\right)^2 \mathbb{1}_{\mathcal{O}}(\widetilde{X}_i). \qquad (1.5)
\end{aligned}$$

Si cette somme admet plusieurs minimiseurs, alors on prend $f^{\maltese}(x) = 0$. La matrice de Gram empirique correspondante G a pour terme général

$$G_{i,\ell} = \frac{1}{n}\sum_{t=1}^{n}\varphi_{j,k_i}(\widetilde{X}_t)\varphi_{j,k_\ell}(\widetilde{X}_t)\mathbb{1}_{\mathcal{O}}(\widetilde{X}_t). \qquad (1.6)$$

Désormais, on raisonne conditionnellement à X'_{i_x}. Puisque la matrice de Gram G contient un nombre fini m_φ^2 de termes, le contrôle de la plus petite valeur propre de G devient aisé dès que $\mathbb{E}[G|X'_{i_x}]$ est elle-même inversible. Évidemment, le contrôle de la plus petite valeur propre de $\mathbb{E}[G|X'_{i_x}]$ se réduit au contrôle de l'infinimum sur $u = (u_1, \ldots, u_{m_\varphi}) \in \mathbb{S}^{m_\varphi - 1}$ de

$$\begin{aligned}
&\mathbb{E}\left[\left(\sum_{t=1}^{m_\varphi} u_t\varphi_{j,k_t}(X - X'_{i_x} + 2^{-j-1})\right)^2 \mathbb{1}_{\mathcal{O}}(X - X'_{i_x} + 2^{-1})\middle| X'_{i_x}\right] \\
&= \int_{2^j(\mathcal{A} - X'_{i_x}) \cap [-2^{-1}, 2^{-1}]^d} dw\mu(w)(u_1\varphi_{k_1}(w + 2^{-1}) + \ldots + u_{m_\varphi}\varphi_{k_{m_\varphi}}(w + 2^{-1}))^2 \\
&\ge \mu_{\min} \inf_{\mathfrak{m} \ge \mathfrak{m}_0} \inf_{z \in \mathcal{B}_\infty(2^{-1}, \mathfrak{m})} \int_{\mathcal{B}_\infty(z, \mathfrak{m}) \cap [0,1]^d} dw(u_1\varphi_{k_1}(w) + \ldots u_{m_\varphi}\varphi_{k_{m_\varphi}}(w))^2, \qquad (1.7)
\end{aligned}$$

où la première égalité résulte de l'indépendance de X'_{i_x} par rapport aux points de $\mathcal{D}_n$ et la dernière inégalité résulte d'une application directe de (**S2**), puisque l'argument sous l'intégrale est positif et que l'on suppose $j \ge j_s$. Notons que la borne inférieure ne dépend ni de j, ni de X'_{i_x}

et donc ni de x. Si bien qu'on obtient un contrôle de la plus petite valeur propre de $\mathbb{E}[G|X'_{i_x}]$, et donc de G, uniforme en x et en j.
L'inversibilité de l'espérance conditionnelle de la matrice de Gram $\mathbb{E}[G|X'_{i_x}]$ sous l'hypothèse (**S2**) repose en fait sur la borne inférieure décrite en eq. (1.7) et la "propriété d'indépendance linéaire locale" des fonctions d'échelle (φ_k), que nous rappelons plus bas.
Au passage, remarquons ici que dans (**S2**), $\mathscr{A}_{j_s}$ depend de la régularité s de f. Ceci résulte du fait que pour construire une version adaptative de $f^{\maltese}$ via la méthode de Lepski, il n'est nécessaire de contrôler la déviation de $f_j^{\maltese}(x)$ par rapport à $f(x)$, et donc l'inversibilité de $\mathbb{E}[G|X'_{i_x}]$, que pour $j \geq j_s$.

La propriété d'indépendance linéaire locale. L'hypothèse (**S2**) a été pensée de manière à pouvoir utiliser la propriété d'indépendance linéaire locale des fonctions d'échelle. Cette dernière a été initialement décrite dans [30] et peut s'exprimer de la manière suivante. Soit $\mathfrak{m}$ une constante telle que $\mathfrak{m} > 0$ et $z \in \mathcal{B}_\infty(2^{-1}, \mathfrak{m})$. Les fonctions d'échelle (φ_{k_i}) $1 \leq i \leq m_\varphi$ dont le support est d'intersection non vide avec la cellule $[0,1]^d$ du treillis $\mathbb{Z}^d$ vérifient la propriété d'indépendance linéaire locale en ce sens que $\sum_{1\leq i\leq m_\varphi} \alpha_{k_i}\varphi_{k_i} = 0$ sur le domaine $\mathcal{B}_\infty(z,\mathfrak{m})$ si et seulement si $\alpha_{k_i} = 0$ pour tout $1 \leq i \leq m_\varphi$.

Argument de compacité et conclusion. Un argument de compacité, joint à la propriété d'indépendance linéaire locale des fonctions d'échelle, permet alors de montrer que le membre de droite de l'eq. (1.7) est borné inférieurement par une constante strictement positive, uniformément pour tout $u \in \mathbb{S}^{m_\varphi - 1}$. Si bien que la matrice $\mathbb{E}[G|X'_{i_x}]$ est inversible sous (**CS2**) et à nouveau, $f^{\maltese}$ est obtenu par seuillage spectral de la matrice de régression locale G, dans le même esprit que pour $f^{@}$ et le LPE.

Résultats d'optimalité sous (**CS2**). On montre donc que, sous (**CS2**) et avec un échantillon de taille $2n$, $f_j^{\maltese}$ vérifie des résultats de concentration exponentielle et d'optimalité minimax équivalents à ceux vérifiés par $f_j^{@}$, et ce pour tout $j \in \mathcal{J}_n$ où $\mathcal{J}_n = \{j_s, j_s+1, \dots, J\}$. En particulier, on obtient le résultat de concentration ponctuelle suivant pour $f^{\maltese}$.

Theorem 1.3.2. *Soit $r \in \mathbb{N}$. Supposons que l'hypothèse* (**CS2**) *soit vérifiée et que l'erreur ξ en eq. (1.1) soit gaussienne centrée, de variance σ^2 et indépendante de X. Supposons de plus que f appartienne à une boule $\mathcal{B}(Lip^s(\Omega), M)$ de rayon M de l'espace de Lipschitz $Lip^s(\Omega)$ pour un $s \in (0,r)$. Alors, pour tout $j \in \mathcal{J}_n$, tout $\delta > 2M2^{-js}\max(1, 3\pi_n R^d \mu_{\max})$, tout $x \in \mathcal{A}$, on obtient le résultat suivant,*

$$\sup_{\mathcal{A}\in\mathscr{A}_{j_s}} \sup_{\mu\in\mathcal{D}_b(\mathcal{A})} \sup_{f\in\mathcal{B}(Lip^s(\Omega),M)} \mathbb{P}_f^{\otimes n}(|f(x) - f_j^{\maltese}(x)| \geq \delta)$$
$$\leq 3R^{2d}\exp\left(-\frac{n2^{-jd}\pi_n^{-2}}{2\mu_{\max}R^{4d} + \frac{4}{3}R^{2d}\pi_n^{-1}}\right)\mathbb{1}_{\{\delta\leq M\}} + R^d\Lambda\left(\frac{\delta 2^{-j\frac{d}{2}}}{2\pi_n R^d}\right), \tag{1.8}$$

où $R = 2r-1$, $\mathcal{D}_b(\mathcal{A})$ a été définit en Section 1.1.3 et $\mathscr{A}_{j_s}$ dans (**S2**) *et Λ est la fonction définit en Théorème 1.3.1.*

Remarquons que ce résultat de concentration pour $f^{\maltese}$ est exactement le même que celui obtenu pour $f^{@}$ en Théorème 1.3.1, mis à part le fait que la première constante devant l'exponentielle

dans la borne supérieure vaut désormais $3R^{2d}$ et que l'on travaille avec un échantillon de taille $2n$.

1.3.4.5 Commentaires. Il est important de remarquer que le support $\mathcal{A}$ de μ joue un rôle crucial dans les résultats exposés ci-dessus. En fait, le support $\mathcal{A}$ de μ doit être connu pour pouvoir profiter pleinement de l'avantage calculatoire offert par les bases d'ondelettes. En effet, la structure de treillis sous-jacente à la MRA doit être exactement adaptée au support $\mathcal{A}$ pour une performance optimale.
Lorsque le support $\mathcal{A}$ est inconnu, il est toujours possible exploiter les avantages calculatoires offerts par le treillis de la MRA sous-jacente sous (**CS2**). Bien que la procédure d'estimation $f^{✠}$ correspondante soit plus performante d'un point de vue calculatoire que les estimateurs à noyau, elle demeure plus complexe que la procédure $f^{@}$ sous (**CS1**), c'est à dire lorsque $\mathcal{A}$ est connu.
Il est à noter que les procédures locales d'estimation en ondelettes peuvent être rendues adaptatives en utilisant la méthode de Lepski (voir Chapter 5). Le recours à la méthode de Lepski dans un contexte d'ondelettes peut dans un premier temps paraître surprenant. On peut toutefois en trouver des antécédents dans certains travaux scientifiques passés tels que [31].

1.3.4.6 Perspectives. Comme détaillé dans la rétrospective du Chapter 2, les estimateurs linéaires en ondelettes sont potentiellement optimaux sur une classe de régularité constituée par les espaces de Besov $B^s_{\tau,q}(\Omega)$, $1/\tau \leq 1/p$, lorsque la perte est mesurée en distance $\mathbb{L}_p(\Omega)$. Ces derniers espaces de Besov sont bien plus gros que l'espace de Lipschitz $Lip^s(\Omega)$. Il serait donc intéressant de savoir si il est possible de généraliser les résultats d'optimalité minimax obtenus pour $f^{@}$ et $f^{✠}$ à ces espaces de Besov.

1.4 Application des procédures localisées d'estimation en ondelettes à la classification.

Les procédures d'estimation locale en ondelettes décrites dans la Section précédente sont particulièrement adaptées au problème de classification binaire. Mais rappelons dans un premier temps la nature de ce problème.

1.4.1 Classifieurs de type plug-in et régression.

Dans ce qui suit, nous nous intéressons exclusivement aux méthodes d'estimation de type plug-in. Mais avant de définir ces méthodes, faisons quelques rappels sur le classifieur de Bayes.

Le problème de classification. On rappelle que $f(.) = \mathbb{P}(Y = 1|X = .)$. Il est bien connu que le classifieur de Bayes h^* définit par

$$h^*(\tau) = \mathbb{1}_{\{\tau \in \mathcal{Q}^*\}}, \qquad \mathcal{Q}^* = \{\tau \in \mathcal{A} : 2f(\tau) - 1 \geq 0\}, \tag{1.9}$$

admet la meilleure performance parmi tous les classifieurs possibles dans le sens où il minimise la probabilité d'erreur $\mathbb{P}(Y \neq h^*(X))$ (voir [1]). Bien entendu, il est inconnu en pratique puisque la loi du couple (X, Y) est elle-même inconnue.

Difficulté du problème de classification. Il est clair que si le classifieur de Bayes doit retourner un label erroné, ce sera vraisemblablement pour un X qui tombe dans un bande $\{\tau \in \mathcal{A} : |f(\tau) - 1/2| \leq t\}$ pour un t positif mais petit. C'est dans cette bande que le problème de classification est le plus difficile, puisqu'un label Y associé à un point X localisé dans cette zone a quasiment autant de chances de valoir 1 que 0. L'hypothèse de marge que nous présenterons plus bas est donc toute naturelle dans le sens où elle vient contrôler l'impact de cette bande sur les résultats minimax finaux.

Estimation plug-in du classifieur de Bayes. Tout estimateur h_n de la règle de Bayes admet la représentation de type $h_n(\tau) = \mathbb{1}_{\{\tau \in \mathcal{Q}_n\}}$ pour un sous-ensemble Borélien $\mathcal{Q}_n$ de Ω. Si bien qu'estimer le classifieur de Bayes revient à estimer $\mathcal{Q}^*$ par un ensemble $\mathcal{Q}_n$. Étant donné un estimateur non paramétrique f_n de f, l'approche de type plug-in consiste à estimer $\mathcal{Q}^*$ par $\mathcal{Q}_n = \{\tau \in \Omega : 2f_n(\tau) - 1 \geq 0\}$ et donc h^* par $h_n(\tau) = \mathbb{1}_{\{\tau \in \mathcal{Q}_n\}}$. À partir de maintenant h_n désignera exclusivement l'estimateur plug-in associé à un estimateur f_n de f. Remarquons que $\mathcal{Q}_n$ est définit comme un sous-ensemble de Ω et non du support $\mathcal{A}$, puisque ce dernier est éventuellement inconnu. Toutefois, cela n'a aucune importance puisque X prend ses valeurs dans $\mathcal{A}$, si bien que $\mathcal{Q}_n \cap \mathcal{A}^c$ n'a aucun impact sur la règle d'estimation h_n.

Mesure de la performance d'un classifieur de type plug-in. Comme décrit ci-dessus, un classifieur de type plug-in h_n est en fait un estimateur du classifieur de Bayes h^*, construit sur un estimateur f_n de f. On mesure la performance de h_n dans le cadre théorique minimax avec la fonction de perte $\ell(h_n, h^*) = \mathbb{P}(Y \neq h_n(X)|\mathcal{D}_n) - \mathbb{P}(Y \neq h^*(X)|\mathcal{D}_n)$. Elle mesure le surplus de taux d'erreur engendré par l'utilisation du classifieur h_n plutôt que le classifieur de Bayes h^*.

Lien entre classification et régression. En fait, une inégalité permet de lier directement la performance du classifieur plug-in h_n à la performance de l'estimateur f_n de f en régression non paramétrique sur un design aléatoire de loi inconnue. Nous avons en effet

$$\mathbb{E}^{\otimes n}\ell(h_n, h^*) \leq 2\mathbb{E}^{\otimes n}\|f_n - f\|_{\mathbb{L}_1(\Omega,\mu)}. \tag{1.10}$$

Avec des classifieurs de type plug-in, il est donc possible d'obtenir des vitesses de convergence sur le risque minimax $\mathbb{E}\ell(h_n, h^*)$ directement à partir de vitesses de convergences obtenues en régression sur un design aléatoire. Pour cette raison, il est souvent dit que le problème de classification est plus facile que le problème de régression.

1.4.2 Revue des travaux scientifiques antérieurs. Maintenant, nous procédons à une brève revue des résultats connus en classification avec des classifieurs de type plug-in. Un des résultats les plus anciens à ce sujet se trouve dans [32], où il est prouvé qu'il est possible de construire des classifieurs plug-in qui sont asymptotiquement optimaux. Plus tard, il a été signalé dans [33] que le problème de classification n'est en fait sensible au comportement de la loi jointe du vecteur (X, Y) qu'à la frontière $\partial\mathcal{Q}^*$ de $\mathcal{Q}^*$. [34] prouve par ailleurs que des combinaisons convexes de classifieurs de type plug-in peuvent atteindre, dans des circonstances appropriées, des vitesses de convergence "rapides" (c'est à dire plus rapide que la vitesse de convergence paramétrique $n^{-1/2}$). Puis [35] prouve que les classifieurs plug-in peuvent même atteindre des vitesses "super rapides" (c'est à dire plus rapide que n^{-1}). Tous ces résultats nécessitent bien

entendu une hypothèse de régularité sur f (voir [36]), mais aussi une hypothèse de marge (**MA**), que l'on détaille plus bas. Finalement, [35] prouve que, sous des hypothèses de régularité et de marge, les classifieurs de type plug-in sont minimax optimaux lorsque f appartient à une boule de l'espace de Hölder $\mathscr{C}^s(\Omega)$. Voir aussi [37] à cet effet.

L'hypothèse de marge. Cette hypothèse permet de contrôler le comportement de la loi jointe de (X, Y) à la frontière de $\mathcal{Q}^*$. En suivant les notations de [35], on peut l'écrire comme suit.
(**MA**) Il existe deux constantes C_0 et ϑ telles que

$$\mathbb{P}(0 < |2f(X) - 1| < t) \leq c_0 t^{\vartheta}, \quad \forall t > 0.$$

L'hypothèse de marge permet donc de contrôler le comportement de la loi jointe du couple (X, Y) dans la zone où le problème de classification est le plus difficile et contribue à le simplifier. Elle apparaît de plus naturellement dans les calculs à travers la décomposition suivante,

$$\mathbb{E}^{\otimes n}\ell(h_n, h^*) \leq \delta\mathbb{P}(0 < |2f(X) - 1| \leq \delta) + \mathbb{E}|f_n(X) - f(X)|\mathbb{1}_{\{|f_n(X)-f(X)|\geq\delta\}},$$

où δ peut être choisi de manière à équilibrer les deux termes dans la borne supérieure.

1.4.3 Quelques résultats théoriques. Il arrive souvent en classification que l'on n'ait aucune information sur la loi jointe du vecteur (X, Y). En particulier le support $\mathcal{A}$ de μ est éventuellement inconnu. L'hypothèse (**S2**) est bien adaptée à ce cadre théorique puisqu'elle ne fait rien de plus qu'une hypothèse de régularité sur $\mathcal{A}$. On peut donc envisager d'estimer f par l'estimateur de projections localisées en ondelettes $f^{\maltese}$ sous (**CS2**). Les résultats de concentration exponentielle (en probabilité conditionnelle) de $f^{\maltese}(x)$ vers $f(x)$ en tout point $x \in \mathcal{A}$ permettent d'obtenir des résultats d'optimalité sur le classifieur plug-in associé $h^{\maltese}$ semblables à ceux énoncés dans [35, Lemma 3.1], lesquels sont dérivés à l'aide d'un classifieur plug-in construit sur un estimateur par polynômes locaux de f. Rappelons que, sous (**CS2**), on travaille avec un échantillon de taille $2n$ divisé en deux sous-échantillons $\mathcal{D}_n$ et $\mathcal{D}'_n$ de tailles n, où $\mathcal{D}'_n$ sert à identifier le support $\mathcal{A}$ de μ et $\mathcal{D}_n$ à calibrer l'estimateur $f^{\maltese}$ de f. On obtient alors le résultat suivant.

Corollary 1.4.1. *Soit $r \in \mathbb{N}$. Supposons que* (**MA**) *et* (**CS2**) *soient vérifiées et que f appartienne à la boule $\mathcal{B}(Lip^s(\Omega), M)$ de rayon M de l'espace de Lipschitz $Lip^s(\Omega)$ pour un $s \in (0, r)$. On note $h^{\maltese}_{j_s}$ le classifieur de type plug-in construit sur l'estimateur $f^{\maltese}_{j_s}$ de f où j_s est tel que $2^{j_s} = \lfloor n^{\frac{1}{2s+d}} \rfloor$. Alors on obtient*

$$\sup_{f\in\mathcal{B}(Lip^s(\Omega),M)} \mathbb{E}\ell(h^{\maltese}_{j_s}, h^*) \leq C_{15} n^{-\frac{s}{2s+d}(1+\vartheta)}$$

pour une constante universelle C_{15} définit au Chapter 5 et une perte $\ell(h, h^*) = \mathbb{P}(Y \neq h(X)|\mathcal{D}_n) - \mathbb{P}(Y \neq h^*(X)|\mathcal{D}_n)$. Ce résultat peut être rendu adaptatif en utilisant la version adaptative de l'estimateur par projection localisée en ondelettes. Par ailleurs, on prouve aussi au Chapter 5 que cette vitesse est minimax optimale.

1.4.4 Perspectives. De manière intéressante, ces résultats pourraient certainement être généralisés à la sphère en utilisant les needlets à support "compact" décrites dans [38].

1.5 Régression sur la sphère avec des needlets. Le Chapter 6 s'attache à généraliser les méthodes de régression en ondelettes au cas où le design X prend ses valeurs sur la sphère $\mathbb{S}^d$ de $\mathbb{R}^{d+1}$. Il est clair que l'hypersphère $\mathbb{S}^d$, vue comme un partie de l'espace ambiant $\mathbb{R}^{d+1}$, n'est pas stable par translation ou dilatation le long des coordonnées euclidiennes de $\mathbb{R}^{d+1}$. De sorte que la structure de treillis euclidienne sous-jacente aux MRAs de $\mathbb{R}^{d+1}$ n'est pas adaptée à cette variété, ce qui rend les procédures d'estimation traditionnelles en ondelettes a priori inutilisables. Dans ce qui suit, nous rappelons brièvement pourquoi les idées les plus simples ne permettent pas de restaurer l'optimalité des méthodes d'estimation en ondelettes classiques sur $\mathbb{R}^{d+1}$. Nous rappelons ensuite qu'il est possible de construire un tight frame sur la sphère, qui présente des propriétés voisines de celles des ondelettes euclidiennes et dont les éléments sont appelés needlets. Finalement, nous détaillons les résultats du Chapter 6 où nous prouvons qu'il est possible d'élaborer des procédures d'estimation par seuillage de coefficients de needlets qui son minimax optimales pour une large classe d'espaces de Besov sur la sphère.

1.5.1 L'échec des procédures d'estimation en ondelettes lorsque $\Omega = \mathbb{S}^d$**.** Ici nous décrivons pourquoi les idées les plus naïves ne permettent pas de transposer les MRA euclidiennes à la sphère et expliquons les sources de difficulté dans la conception d'une MRA intrinsèque à la sphère.

L'échec des solutions les plus naïves. Une proposition immédiate consisterait à abandonner le système de coordonnées euclidiennes pour se concentrer sur le système de coordonnées sphériques. Il est bien connu que $\mathbb{S}^d$ peut être paramétrée par d angles $(\theta, \rho_1, \dots, \rho_{d-1})$ tels que $\theta \in [0, 2\pi)$ et $\rho_i \in [0, \pi]$ pour $i = 1, \dots, d-1$. De telle sorte que la sphère $\mathbb{S}^d$ est l'image d'un hyper-rectangle de $\mathbb{R}^d$ par un difféomorphisme. Une solution évidente consisterait donc à analyser les phénomènes sur la sphère à partir d'une MRA euclidienne de ce dernier hyper-rectangle. Cette construction admet cependant plusieurs limitations intrinsèques. En premier lieu, elle donne une importance prépondérante aux deux pôles de la sphère (qui correspondent à certaines arrêtes de l'hyper-rectangle). D'autre part, cela donne lieu à un maillage qui n'est pas uniforme à la surface de la sphère, mais plutôt très fin au niveau des pôles et très lâche au niveau de l'équateur. Ces deux limitations contribuent à déformer toute procédure d'estimation construite sur ce type de MRA.

Les needlets comme solution. Par ailleurs, élaborer une MRA intrinsèque à la sphère semble bien plus difficile que dans $\mathbb{R}^d$, puisque il n'existe pas d'opérateur de dilatation sur la sphère et le groupe des rotations de $\mathbb{S}^d$ est bien plus complexe que celui des translations euclidiennes. Malgré tout, [39, 40] parviennent à élaborer un tight frame de needlets, qui semble en fait être un outil parfaitement adapté à la sphère. Ces frames sont construits de manière très générique à partir d'une base orthonormée d'harmoniques sphériques de $\mathbb{L}_2(\mathbb{S}^d)$, présentent des propriétés similaires à celles des ondelettes euclidiennes et peuvent donc donner lieu à des analyse multi-résolution sur la sphère.

1.5.2 Revue des travaux scientifiques antérieurs. Le problème de l'élaboration d'une MRA intrinsèque à la sphère a été abordé par de nombreux articles scientifiques qui ont donné lieu à la création de nombreux frames intrinsèques à la sphère (voir [41, 42] par exemple). Commençons par rappeler quelques propriétés bien connues de $\mathbb{L}_2(\mathbb{S}^d)$.

Les harmoniques sphériques. On rappelle que l'ensemble des harmoniques sphériques de degré ν, noté $\mathcal{H}_\nu$, est constitué de la restriction à $\mathbb{S}^d$ de l'ensemble des polynômes g de $\mathbb{R}^{d+1}$ de degré ν qui sont homogènes ($g = \sum_{|\alpha|=\nu} a_\alpha x^\alpha$ où $\alpha = (\alpha_1, \ldots, \alpha_{d+1})$ et $|\alpha| = \sum \alpha_i$) et harmoniques ($\Delta g = \sum \partial g / \partial x_i^2 = 0$). Comme détaillé dans [43, Chap. 4], l'ensemble $\mathbb{L}_2(\mathbb{S}^d)$ des fonctions de carré intégrable sur $\mathbb{S}^d$ se décompose en somme directe de sous-espaces d'harmoniques sphériques $\mathcal{H}_\nu$ de degré ν, pour $\nu \in \mathbb{N}$, et il existe une base orthonormée d'harmoniques sphériques de $\mathbb{L}_2(\mathbb{S}^d)$. Cependant, les éléments de cette base ne sont pas localisés, ce qui les rend inadéquates pour représenter des fonctions à support "compact" ou à comportement muti-échelle sur la sphère (voir [42, p. 32]). En fait, cette base d'harmoniques sphériques est à la sphère $\mathbb{S}^d$ ce que la base de Fourier est à $\mathbb{R}^d$ (voir [43]).
Pour être plus précis, notons $P_\nu(\tau, \xi)$, $\tau, \xi \in \mathbb{S}^d$, le noyau du projecteur orthogonal de $\mathbb{L}_2(\mathbb{S}^d)$ dans $\mathcal{H}_\nu$, et remarquons que P_ν est zonal, c'est à dire $P_\nu(\tau, \xi) = P_\nu(\langle \tau, \xi \rangle)$ où $\langle ., . \rangle$ désigne le produit scalaire de $\mathbb{R}^{d+1}$. Comme décrit au Chapter 6, P_ν est en fait, à une constante multiplicative près, le polynôme de Legendre L_ν de degré ν, $P_\nu(x) \propto L_\nu(x)$, $x \in [-1, 1]$. Les mauvaises propriétés de localisation des L_ν (et donc des P_ν) témoignent des mauvaises propriétés de localisation des éléments de la base d'harmoniques sphériques de $\mathbb{L}_2(\mathbb{S}^d)$ (voir Figure 1.4).

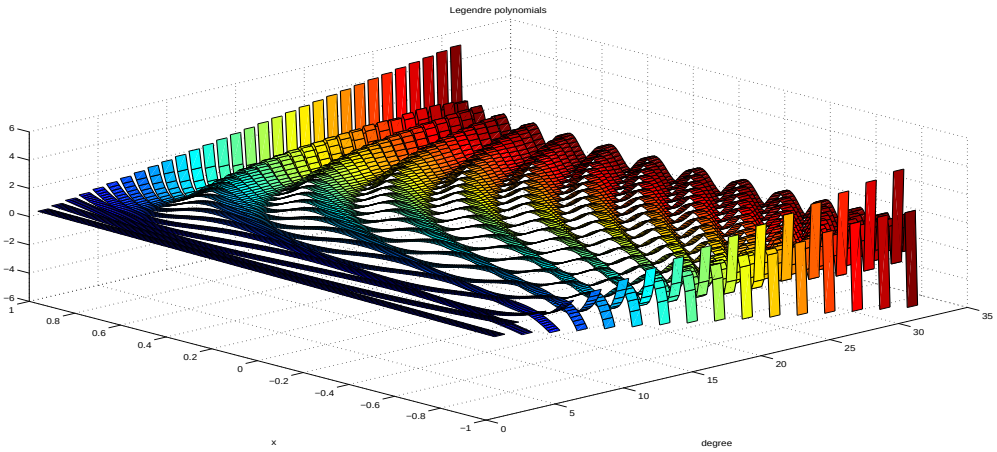

FIGURE *1.4 – Illustration des mauvaises propriétés de localisation des polynômes de Legendre* $L_\nu(x)$, $x \in [-1, 1]$ *pour* $1 \leq \nu \leq 30$.

Localisation des noyaux de projection. Il est remarquable que ces harmoniques sphériques peuvent toutefois servir d'éléments de base dans la construction de frames bien concentrés sur la sphère appelés needlet frames, qui sont bien supérieurs aux frames qui les ont précédés (voir [40, 39]). Comme initialement décrit dans [39], il est possible de construire des noyaux de projection localisés Λ_j à partir de combinaisons linéaires bien choisies des P_ν, ce qui est rappelé dans [40, Theorem 2.2] et détaillé ci-dessous.

Theorem 1.5.1. *Soit a une fonction de $\mathscr{C}^\infty[0, \infty)$ qui satisfasse l'une des deux conditions suivantes,*

- *$Supp(a) \subset [0, 2]$, $a(t) = 1$ sur $[0, 1]$ et $0 \leq a(t) \leq 1$ sur $[1, 2]$; ou bien,*
- *$Supp(a) \subset [1/2, 2]$.*

On a alors le résultat suivant. Pour tout $j \geq 0$, on pose

$$\Lambda_j(x) = \sum_{\nu=0}^{\infty} a(\nu/2^j) P_\nu(x), \qquad x \in [-1,1].$$

Pour tout $k > 0$ et $r \geq 0$, il existe une constante $c_{k,r} > 0$ qui dépend uniquement de k, r, d et a telle que

$$|\frac{d^r}{dx^r}\Lambda_j(\cos\theta)| \leq c_{k,r}\frac{2^{j(d+2r)}}{(1+2^j\theta)^k}, \qquad \theta \in [0,\pi].$$

Les needlets sont ensuite directement obtenues via une formule de cubature comme sous-produits des noyaux Λ_j, dont elles héritent les propriétés de localisation. Dans ce qui suit, on écrit $(\psi_{j,\eta})_{j\geq -1,\eta\in\mathcal{Z}_j}$ le frame de needlets associé aux noyaux $(\Lambda_j)_{j\geq -1}$, où les $(\mathcal{Z}_j)_{j\geq -1}$ sont des sous-ensembles discrets de $\mathbb{S}^d$ tels que $\#\mathcal{Z}_j \asymp 2^{jd}$. On peut alors rappeler le résultat suivant décrit dans [40, Theorem 3.1].

Theorem 1.5.2. *Pour tout $f \in \mathbb{L}_p(\mathbb{S}_d)$ et $p \in [1,\infty)$, ou $p = \infty$ et f continue, on obtient*

$$\lim_{J\to\infty} \|f - \sum_{j\geq -1}^{J}\sum_{\eta\in\mathcal{Z}_j} \beta_{j,\eta}\psi_{j,\eta}\|_{\mathbb{L}_p(\mathbb{S}^d)} = 0,$$

où on a noté $\beta_{j,\eta} = \langle f, \psi_{j,\eta}\rangle = \int_{\mathbb{S}^d} f(x)\psi_{j,\eta}(x)\mathfrak{M}(dx)$ et $\mathfrak{M}$ désigne la mesure de Haar sur $\mathbb{S}^d$.

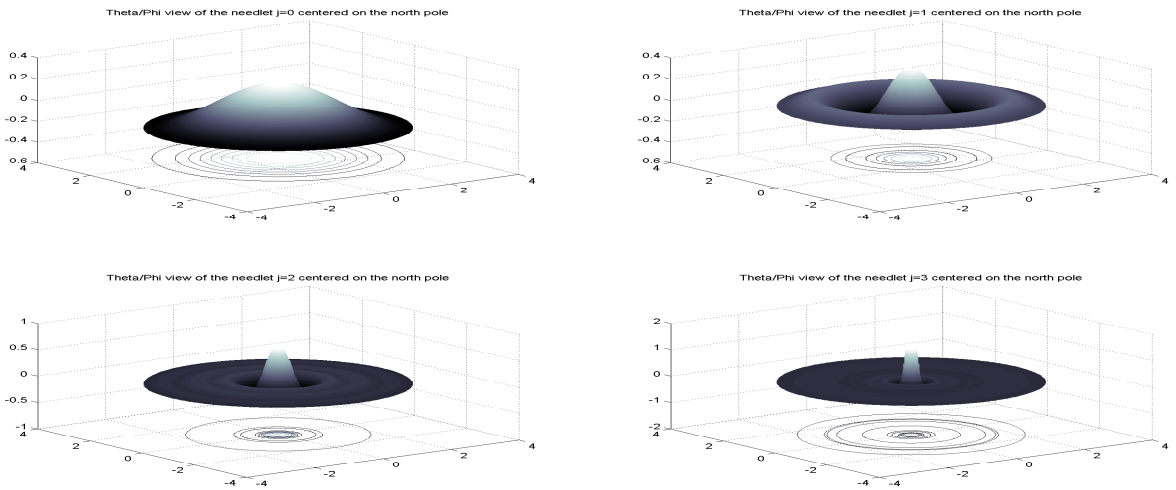

FIGURE *1.5 – Ces graphiques représentent les needlets $\psi_{j,\eta}$ pour $\eta = \eta_0 := (0,0,1)$ (coordonnées cartésiennes), et $j \in \{0,1,2,3\}$. Nous montrons une vue polaire des needlets, c'est à dire $\psi_{j,\eta_0} = \psi_{j,\eta_0}(\varphi,\theta)$, où φ et θ réfèrent respectivement à la colatitude et à la longitude en coordonnées sphériques. Dans cette représentation polaire, on laisse φ jouer le rôle de la longueur r du vecteur radial alors que θ représente l'angle entre ce vecteur radial et l'axe des abscisses (Ox).*

Le tight frame de needlets. Bien que les needlets $(\psi_{j,\eta})_{j\geq -1,\eta\in\mathcal{Z}_j}$ ne constituent pas une base orthonormée sur la sphère, elles forment un tight frame de $\mathbb{L}_2(\mathbb{S}^d)$ et peuvent donc être utilisées comme si elles étaient une base orthonormée, ce qui fait d'elles des éléments de base très naturels sur la sphère (voir [39]). Pour un rappel sur les frames, le lecteur est renvoyé au Chapter 4.
Les needlets bénéficient d'un large spectre de propriétés intéressantes. (i) Elles sont en fait semi-orthogonales en ce sens que deux needlets quelconques appartenant à des niveaux de résolution $j_1, j_2 \in \mathbb{N}$ et distantes d'au moins deux niveaux, c'est à dire telles que $|j_1 - j_2| \geq 2$, sont orthogonales. (ii) D'autre part, chaque needlet est localisée autour d'un centre appartenant à $\mathbb{S}^d$ et décroît à vitesse quasi-exponentielle en s'éloignant de ce point (voir Figure 1.5). (iii) Ces propriétés de localisation leur confèrent un caractère universel qui leur permet de caractériser les espaces de Besov sur la sphère (voir [39, Th. 6.2]). (iv) Finalement, les needlets sont véritablement multi-échelles puisque elles se concentrent de plus en plus autour de leur centre quand le niveau de résolution augmente (voir Figure 6.1). Pour toutes ces raisons, les needlet frames sont déjà utilisés dans le cadre d'applications en astrophysique (voir [44, 45, 46]).

1.5.3 Notre contribution. Au Chapter 6, nous considérons le problème de régression non paramétrique avec design uniformément distribué sur $\Omega = \mathbb{S}^d$. Nous introduisons une procédure d'estimation sur $\Omega = \mathbb{S}^d$ élaborée à partir de needlets, qui est multi-échelle, robuste et facile à mettre en oeuvre puisqu'elle ne nécessite en pratique que la calibration d'un unique paramètre (voir Section 6.7). L'utilisation des needlets dans un contexte statistique sur la sphère n'est pas nouvelle, mais a fait l'objet d'un effort intense de recherche au cours de dernières années. Comme indiqué plus haut, les ondelettes euclidiennes et les needlets partagent de nombreux points communs, de telle sorte que les procédures d'estimation par seuillage d'ondelettes peuvent être directement transposées aux needlets. Rappelons que la quasi-optimalité des procédures d'estimation par seuillage de coefficients de needlets a été prouvée dans un contexte d'estimation de densité avec $\Omega = \mathbb{S}^d$ dans [47].
Notre contribution est en fait une sorte de complément naturel à cette dernière référence puisque nous transposons les résultats d'optimalité minimax des procédures d'estimation par seuillage de coefficients de needlets décrits dans [47] au problème de régression sur un design uniformément distribué à la surface de $\mathbb{S}^d$. Nous saisissons cette opportunité pour réaliser un vaste éventail de simulations numériques avec ces nouvelles procédures d'estimation et nous étudions un raffinement de la procédure qui consiste à utiliser un seuil aléatoire pour le seuillage des coefficients de needlets.

Seuillage stochastique contre seuillage déterministe. Nous étudions deux estimateurs $f^{\circledast}$ et $f^{\bigstar}$ de f construits par seuillage de coefficients de needlets, avec des seuils respectivement stochastiques et déterministes. Ces deux estimateurs sont de la forme suivante,

$$f_J^{\diamond} = \sum_{j=-1}^{J} \sum_{\eta\in\mathcal{Z}_j} T_{j,\eta}^{\diamond}(\beta_{j,\eta}^{(n)})\psi_{j,\eta}, \qquad \beta_{j,\eta}^{(n)} = \frac{|\mathbb{S}^d|}{n}\sum_{i=1}^{n} Y_i\psi_{j,\eta}(X_i),$$

où $T_{j,\eta}^{\diamond}(x) = \mathbb{1}_{\{x\geq\varepsilon_{j,\eta}^{\diamond}\}}$ et $\diamond$ peut être remplacé indifféremment par $\bigstar$ ou $\circledast$. Nous prouvons que ces deux estimateurs sont quasi optimaux au sens minimax, expliquons en quoi le seuillage stochastique est supérieur au seuillage déterministe et effectuons des simulations afin de familiariser le lecteur avec la procédure, montrer qu'elle fonctionne correctement et qu'elle se met en oeuvre

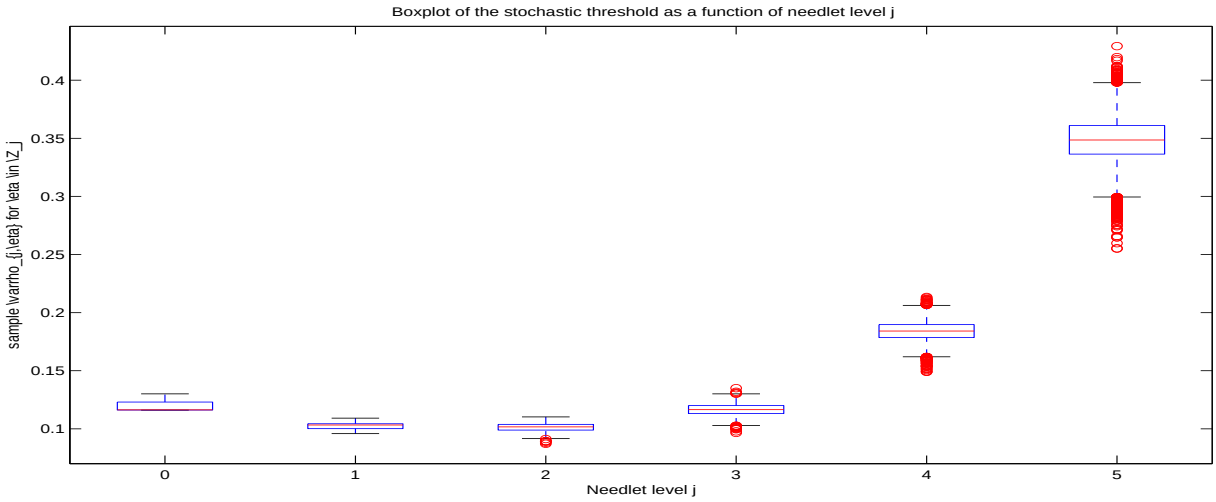

FIGURE *1.6 – Ce graphique représente un "box-plot" des échantillons* $\{\varrho_{j,\eta}\}$ *regroupés par niveaux de résolution* j*, pour* $j \in \{0,1,2,3,4,5\}$*. Il est clair que la moyenne et la variance de* ϱ *augmente de manière importante aux niveaux de résolution* $j = 4$ *et* $j = 5$*.*

rapidement et simplement.
Plus précisément, $f^\star$ est construit sur un seuillage dur déterministe de la forme $\varepsilon^\star_{j,\eta} = \varepsilon^\star = \kappa\sqrt{\log n/n}$ pour une constante $\kappa > 0$ à calibrer. Alors que $f^\circledast$ est construit sur un seuillage stochastique $\varepsilon^\circledast_{j,\eta} = \kappa\varrho_{j,\eta}\sqrt{\log n/n}$ du coefficient de needlet $\beta^{(n)}_{j,k}$, pour un facteur stochastique $\varrho_{j,\eta}$ choisit tout naturellement comme $\varrho^2_{j,\eta} = \mathbb{V}\mathrm{ar}(\beta^{(n)}_{j,\eta}|X_1,\dots,X_n)$.

Quelques résultats théoriques. Pour être plus précis, on considère ici un problème de régression sur la sphère, c'est à dire avec $\Omega = \mathbb{S}^d$. On cherche donc à recouvrer la fonction de régression f à partir de l'observation d'un jeux de n réalisations indépendantes (X_i, Y_i) de la variable aléatoire (X, Y) telle que,

$$Y = f(X) + \sigma\xi, \tag{1.11}$$

où X est uniformément distribué à la surface de la sphère, ξ est gaussienne centrée réduite, σ quantifie l'ordre de grandeur du bruit ξ et f est supposée appartenir à une large classe d'espaces de Besov. On obtient au Chapter 6 le résultat suivant.

Theorem 1.5.3. *Soit* $\Omega = \mathbb{S}^d$ *et* $f \in \mathbb{L}_\infty(\Omega)$*. Considérons l'estimateur* $f^\diamond$ *de* f *construit sur* n *observations indépendantes et identiquement distribuées* (X_i, Y_i) *tirées du modèle décrit en eq. (1.11), où* $f^\diamond$ *désigne de manière indifférente* $f^\circledast$ *ou* $f^\star$*. On prend* $J = Cn/\log n$ *pour une constante* C *bien choisit (voir Theorem 6.6.1). Alors, pour* $d \geq 1$*,* $s > \frac{d}{\tau}$*,* $\tau \in (0,\infty]$*, et* $p \in [1,\infty)$*, il existe une constante* c_p *telle que, sous des conditions adéquates sur* κ *(voir*

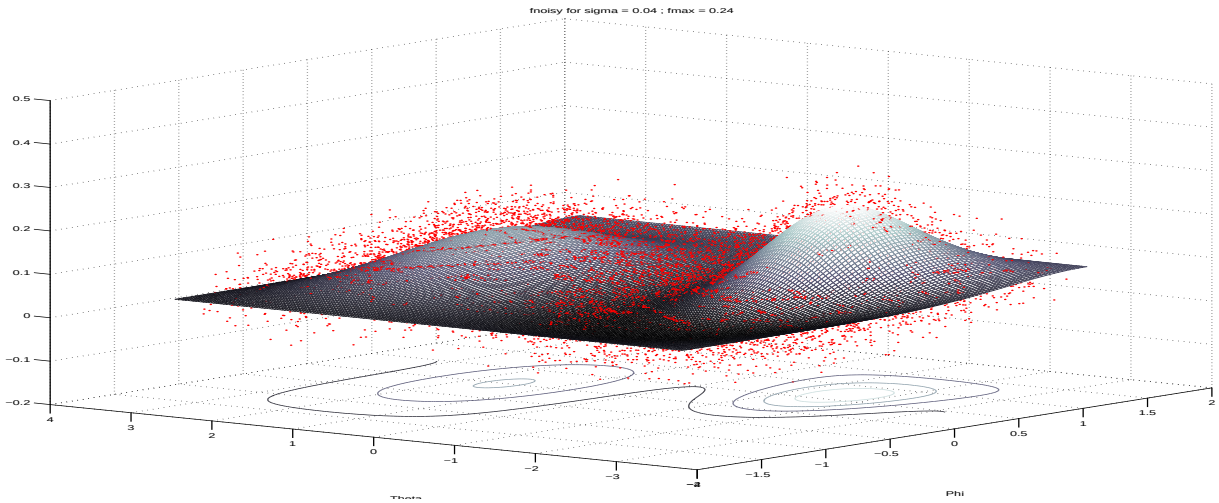

FIGURE *1.7 – Cette figure représente la fonction* $f : x \in \mathbb{S}^2 \mapsto 0.65\exp(-k_1\|x-x_1\|_2)/b_1 + 0.35\exp(-k_2\|x-x_2\|_2)/b_2$ *sur une grille de points de la sphère unité de* $\mathbb{R}^3$ *paramétrés par leur colatitude* φ *et longitude* θ *(en coordonnées sphériques). On choisit* $x_1 = (0,1,0)$, $x_2 = (0,-0.8,0.6)$, $k_1 = 0.7$, $k_2 = 2$ *et* $b_i = \int_{\mathbb{S}^2}\exp(k_i\|x-x_i\|_2)\mathfrak{M}(dx)$, $i = 1,2$, *où* $\mathfrak{M}$ *désigne la mesure de Haar sur la sphère. On prend* $\sigma = 0.04$ *et représente* $N = 10,000$ *observations bruitées* Y_i *aux points* X_i *uniformément distribués sur la sphère et simulés en utilisant les transformations* $\theta = 2\pi(\text{rand}() - .5)$ *et* $\varphi = \sin^{-1}(2\text{rand}() - 1)$.

Theorem 6.6.1),

$$\sup_{f\in\mathcal{B}(B^s_{\tau,q}(\Omega),M)} \mathbb{E}\|f^\diamond - f\|^p_{\mathbb{L}_p(\Omega)} \le c_p\{\log n\}^p \left(\frac{n}{\log n}\right)^{-\frac{ps}{2s+d}}, \qquad si\ s > \frac{dp}{2}\left(\frac{1}{\tau}-\frac{1}{p}\right)^+, \tag{1.12}$$

$$\sup_{f\in\mathcal{B}(B^s_{\tau,q}(\Omega),M)} \mathbb{E}\|f^\diamond - f\|^p_{\mathbb{L}_p(\Omega)} \le c_p\{\log n\}^p \left(\frac{n}{\log n}\right)^{-p\frac{s-d(\frac{1}{\tau}-\frac{1}{p})}{2(s-d[\frac{1}{\tau}-\frac{1}{2}])}}, \qquad si\ s \le \frac{dp}{2}\left(\frac{1}{\tau}-\frac{1}{p}\right)^+. \tag{1.13}$$

Un résultat similaire est obtenu pour $p = \infty$ *(voir Theorem 6.6.1). On prouve par ailleurs que ces vitesses sont quasi minimax optimales au Chapter 6.*

Quelques résultats pratiques. La procédure d'estimation par seuillage de coefficients de needlets est relativement simple à implémenter et à prendre en main puisqu'elle repose sur le choix du seul paramètre κ. On observe sans surprises via nos simulations que le seuillage stochastique améliore de manière non négligeable les performances de l'estimateur en needlets par rapport au seuillage déterministe. Comme indiqué en Figure 1.6, l'influence du seuillage stochastique se fait d'autant plus sentir que J est grand. Enfin, on présente les résultats d'une simulation menée avec $f^\circledast$ en Figure 1.7 et Figure 1.8.

1.5.4 Perspectives. Tous les résultats décrits ci-dessus sont valides sous l'hypothèse que le design est réparti de manière uniforme sur la sphère. Cependant, on pourrait envisager généraliser

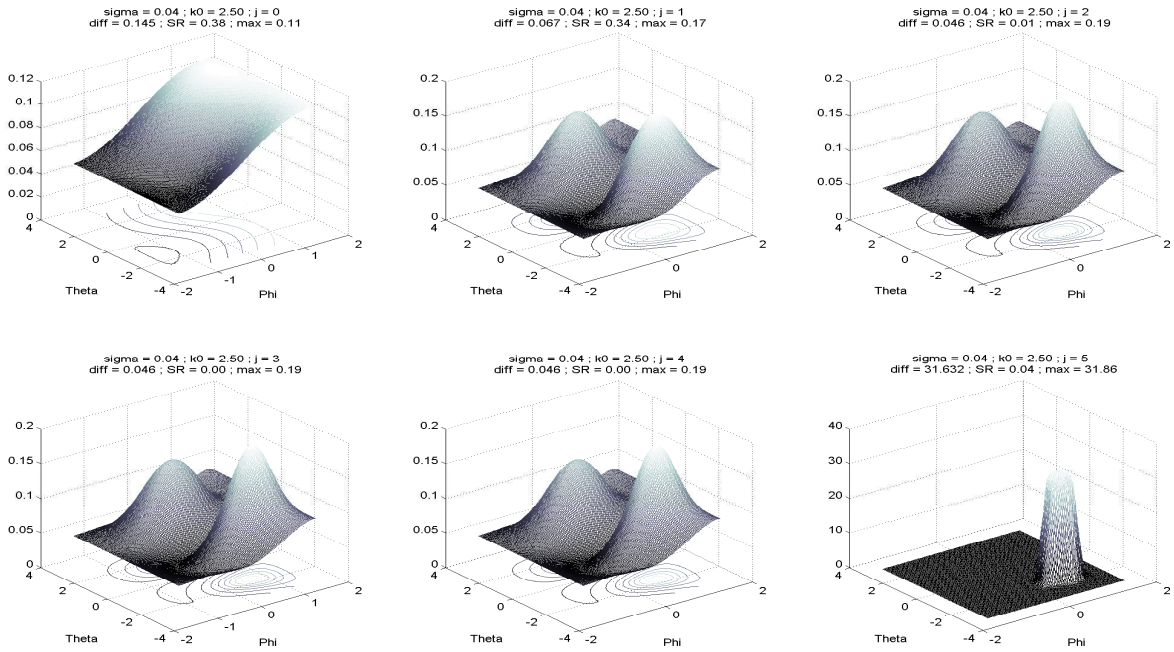

FIGURE *1.8 – Cette figure représente $f^{\circledast}$ calculé à partir de* $20,000$ *vecteurs* (X_i, Y_i). *De manière à pouvoir clairement observer la contribution de chaque niveau* j *à la valeur de l'estimateur en chaque point, on représente* $f_J^{\circledast}$ *pour* $J = 0, 1, 2, 3$ *sur une grille. Le titre de chacune des sous-figures indique en particulier le pourcentage de coefficients de needlets qui survivent au seuillage au niveau* J, *sous le label SR. Dans ce cas particulier, on constate qu'aucun coefficient ne survit au seuillage aux niveaux* $J = 3$ *et* $J = 4$.

ces résultats au cas où la densité du design n'est plus uniforme via une procédure de calibration locale, comme décrit plus haut avec des ondelettes à support compact. Ceci est rendu possible par l'existence de needlet frames dont le support est "compact" sur la sphère (voir [38]).
De plus, les needlet frames sont construits par le biais d'une méthode très générique. C'est pourquoi nous pourrions envisager des procédures d'estimation similaires sur des variétés plus générales. Ceci fait l'objet de recherches menées par Gérard Kerkyacharian, George Kyriazis, Francis Narcowich, Pencho Petrushev, Dominique Picard, Joseph D. Ward et leurs collaborateurs.

1.6 Contribution à un problème inverse en mathématiques financières. La dernière contribution de ce manuscrit est d'une nature légèrement différente et a pour objet un problème inverse bien connu en finance. Plus précisément, nous proposons au Chapter 7 un nouvel algorithme de programmation quadratique simple et rapide qui permet de retrouver la densité risque neutre (RND) à partir des prix d'options cotés sur les marchés. De manière intéressante, ce résultat est construit à partir d'un calcul explicite de la décomposition en valeurs singulières d'opérateurs de prix "restreints". Dans cette Section, nous commençons par introduire le problème inverse en question et expliquons en quoi il diffère des problèmes inverses habituellement rencontrés en statistique. Nous décrivons ensuite les résultats obtenus au Chapter 7 et donnons des perspectives de recherche.

1.6.1 Problèmes et objectifs. Commençons par introduire le problème d'estimation de la densité risque neutre.

1.6.1.1 Présentation. Au cours des quatre dernières décennies, l'hypothèse d'absence d'opportunités d'arbitrage s'est avérée être un point de départ fructueux qui a donné naissance à un riche cadre théorique pour le pricing de produits dérivés connu aujourd'hui sous le nom de "théorie du pricing par absence d'opportunités d'arbitrage". Cette théorie repose sur deux théorèmes fondamentaux. Le "Premier Théorème Fondamental du Pricing d'Actif" (voir [48, p. 72]) prouve qu'un marché est dépourvu d'opportunités d'arbitrage si et seulement il existe une mesure $\mathbb{Q}$ équivalente à la mesure historique (ou statistique) $\mathbb{P}$ sous laquelle le processus de prix sous-jacent est une martingale. C'est pourquoi $\mathbb{Q}$ est souvent connue sous le nom de "mesure martingale". Le "Second Théorème Fondamental du Pricing d'Actif" (voir [48, p. 73]) prouve à son tour que cette mesure martingale est unique si et seulement si le marché est "complet" (voir [48, p. 300] pour une définition de ce terme). Notons $S_\tau \in \mathbb{R}^+$ le prix du sous-jacent à une date future fixée τ et par $\pi(S_\tau)$ le payoff d'une option maturant à la date τ. En supposant qu'elle existe, on note q la densité marginale de S_τ sous la mesure $\mathbb{Q}$ par rapport à la mesure de Lebesgue sur l'axe des réels positifs. Le prix de cette option obtenu sous l'hypothèse d'absence d'opportunités d'arbitrage s'écrit comme l'espérance réactualisée de son payoff sous $\mathbb{Q}$ (voir [49]),

$$e^{-r\tau}\mathbb{E}_{\mathbb{Q}}\pi(S_\tau) = e^{-r\tau}\int_{x\geq 0}\pi(x)\mathbb{Q}(S_\tau \in dx) = e^{-r\tau}\int_{x\geq 0}\pi(x)q(x)dx,$$

où r représente le taux d'intérêt sans risque instantané (ou continu). Il est de notoriété commune que les marchés financiers sont en fait incomplet, ne serait-ce que du fait de la présence de sauts dans les processus de prix. Dans un tel contexte, et comme décrit plus haut, il existe éventuellement de nombreuses densités q, et donc, autant de systèmes de prix cohérents. Notons $\mathscr{Q}$ l'ensemble correspondant des densités q potentiellement valides. Les éléments q de $\mathscr{Q}$ sont le plus souvent appelés densités risque neutre (RNDs) et nous utiliserons donc ce terme dans ce qui suit.

De l'intérêt de la RND. Les RNDs sont d'un intérêt crucial pour les Banques Centrales et, en fait, toutes les institutions et les individus qui portent un intérêt aux marchés financiers, puisqu'elles décrivent le sentiment du marché relatif au prix d'un sous-jacent à un date future (voir [50]). Elles présentent aussi un intérêt non négligeable pour les professionnels de l'industrie des dérivés financiers puisque la connaissance de q permet de donner un prix aux nouveaux produits dérivés de telle sorte qu'il n'existe pas d'opportunité d'arbitrage statique avec les produits dérivés déjà cotés sur le marché. Pour ces raisons, les travaux relatifs à l'estimation de la RND sont très nombreux. Ils ont été écrits pour l'essentiel dans les années 1990 et 2000. Nous n'avons pas pour objectif de présenter une revue détaillée de ces travaux ici. En fait, d'excellentes revues à jour peuvent être trouvées dans [51, 52]. Des revues plus anciennes mais toujours intéressantes peuvent être trouvées dans [53, 50].

Les options d'achat (call) et de vente (put). Parmi tous les produits dérivés, les options d'achat et de vente jouent un rôle très particulier puisqu'elles sont les plus liquides sur le marché, et à ce titre, il semble naturel de penser qu'elles sont échangées au juste prix. Rappelons qu'un call de strike ξ et de maturité τ donne à son détenteur le droit d'acheter le sous-jacent à maturité τ

au prix ξ. C'est donc une assurance contre une hausse du prix du sous-jacent au-delà de ξ. Son payoff s'écrit $\theta(S_\tau, \xi) = (S_\tau - \xi)^+$, où on a noté $(x)^+ = \max(x, 0)$ pour $x \in \mathbb{R}$. Par opposition, une option put donne à son détenteur le droit de vendre le sous-jacent au prix ξ à maturité τ. C'est donc une assurance contre une baisse du prix du sous-jacent S_τ en dessous de ξ et son payoff s'écrit $\theta^*(S_\tau, \xi) = (\xi - S_\tau)^+$.

1.6.1.2 Le problème. D'après la fameuse formule de Breeden-Litzenberger, la dérivée seconde des prix de call et de put par rapport à leur strike sont toutes deux égales à la valeur réactualisée de la RND $e^{-r\tau}q$ (voir [54]). De fait, il serait possible de calculer la RND directement à partir des prix de call ou de put, si nous disposions d'un continuum de prix d'options cotés sur le marché. Cependant, ce n'est pas le cas, et seulement un très petit nombre d'options sont cotées à chaque maturité à des strikes voisins du prix forward du sous-jacent pour cette maturité. Selon le sous-jacent, on compte de l'ordre de 5 à 50 prix pour un maturité donnée τ. Pour compliquer encore plus les choses, les cotes n'apparaissent pas sous la forme d'un prix unique. Les marchands d'option donnent en fait un prix à l'offre ("bid price") auquel ils proposent d'acheter l'option et un prix à l'achat ("ask price") auquel ils proposent de vendre l'option. La différence entre ces deux prix est connue sous le nom de "bid-ask spread". Pour une introduction intéressante à la nature des prix d'options et aux potentielles sources d'erreurs qu'ils contiennent, le lecteur est renvoyé à [55, p.786].

1.6.1.3 Objectifs. Idéalement, nous souhaiterions retrouver q à partir des prix d'options cotés sur le marché par une méthode non paramétrique de manière à n'imposer aucune contrainte de modélisation sur q. Cependant, étant donné le peu de prix d'options disponibles sur le marché et la présence d'un spread bid-ask, il est clair que l'utilisation de méthodes conventionnelles d'estimation non paramétrique n'aurait que peu de sens. En fait, de nombreuses RND sont potentiellement compatibles avec les prix tels qu'ils sont cotés sur le marché. C'est pourquoi, le défi principal du problème d'estimation de la RND consiste à identifier, par des méthodes non paramétriques, une RND compatible avec les prix de marché selon un critère typiquement d'entropie ou de régularité. De plus, il est crucial que l'algorithme d'estimation soit rapide et simple à implémenter de manière à pouvoir être utilisé par les professionnels du domaine. Étant données ces considérations pratiques, il est clair que le contrôle du biais d'estimation est, dans un premier temps, d'un intérêt secondaire. C'est en ce sens que ce problème diffère des problèmes inverses classiquement rencontrés en statistique.

1.6.1.4 Revue des travaux scientifiques antérieurs. Historiquement, trois approches principales ont été étudiées pour retrouver une RND à partir des prix d'options cotés : les méthodes paramétriques, les méthodes non paramétriques et les modèles du processus de prix du sous-jacent. Chacune d'elles a ses points forts et ses points faibles. Les méthodes paramétriques sont bien adaptées aux échantillons de données de petite taille et garantissent que l'estimateur de q est bien une densité en toutes circonstances. Toutefois, elles contraignent la RND à appartenir à une famille paramétrique de densités. D'autre part, les modèles du processus de prix du sous-jacent sont à l'origine du premier grand succès de la théorie du pricing par non-arbitrage avec le fameux mouvement Brownien géométrique (voir [56, 57]). Cependant, les limites de la distribution log-normale sont maintenant bien connues et, à ce jour, aucun autre processus de prix

n'a été proposé qui reproduise avec fidélité la dynamique réelle des processus de prix et soit suffisamment simple pour donner lieu à des développements analytiques explicites. Les méthodes non paramétriques permettent d'éviter ces problèmes dans le sens où elles ne nécessitent pas de faire des hypothèses hasardeuses sur le processus de prix (elles sont dites modèle-indépendantes) et permettent de retrouver toutes les densités possibles et imaginables. Le principal défaut des méthodes non paramétriques est qu'elles sont généralement très gourmandes en données et en puissance de calcul. Revenons dans un premier temps brièvement sur quelques travaux scientifiques antérieurs ayant trait aux méthodes d'estimation non paramétriques de la RND. Nous pouvons classifier ces contributions de la façon suivante.

Les méthodes de type développement en série. Elles incluent les développements de type Edgeworth (voir [58]) ou cumulant (voir [59]), qui permettent d'estimer un nombre fini de cumulants de la RND. Elles incluent aussi les méthodes de développement sur une base orthonormée comme celle des polynômes de Hermite (voir [60]), lesquelles font appel à des techniques Hilbertiennes bien connues et permettent d'obtenir le milieu de la RND.

Les méthodes de régression à noyau. Un récent exemple en est donné dans [61] où les auteurs introduisent un estimateur par polynômes locaux de la RND qui vérifie des contraintes de forme. Remarquons que leur procédure d'estimation est élaborée à partir des prix moyens d'option (la moyenne du prix d'achat et du prix de vente) et nécessite donc un pré-traitement des données de manière à les rendre sans arbitrages. De plus, la RND obtenue via cette procédure dépend du noyau choisi pour l'évaluation de l'estimateur par polynômes locaux et il n'est donc pas clair de quelle manière cette RND peut être comparée à d'autres RND potentiellement valides en terme d'entropie ou de régularité.

La méthode du maximum d'entropie. Elle est présentée dans [62, 63] où la RND q est obtenue par maximisation d'un critère d'entropie. D'après [53, p. 19], cette méthode mène souvent à des estimateurs multi-modaux puisqu'elle n'impose aucune contrainte de régularité sur la densité estimée. Par ailleurs il est écrit dans [64, p.1620] que cette méthode présente des problèmes de convergence.

Autres méthodes. Elles n'appartiennent à aucune des trois catégories précédentes. Parmi elles, on peut citer la méthode d'approximation par convolution positive (PCA) de [65]. En pratique, cette méthode estime une combinaison linéaire convexe finie (mais large) de densités gaussiennes à partir des prix de put moyens et les poids de la combinaison linéaire servent d'approximation discrète de la RND. Cette méthode présente donc une certaine similarité avec celle présentée dans [64] puisqu'elle calibre une loi de probabilité discrète aux prix d'options moyens.
On peut aussi faire référence à la méthode de volatilité implicite régularisée (SML) décrite dans [51]. Cette méthode utilise la formule de Black-Scholes comme transformée non-linéaire. Elle consiste à faire passer un polynôme à travers les volatilités implicites obtenues à partir des prix d'options moyens cotés sur le marché, et à utiliser le continuum de prix d'options obtenu de cette manière pour en déduire la RND à partir de la formule de Breeden-Litzenberger. [51] raffine cette méthode en prenant les prix bid-ask en considération au niveau de la calibration aux volatilités implicites. La méthode SML donne accès à la partie centrale de la RND autour du prix forward. [51] propose de plus une méthode pour accrocher des queues de distribution de type "valeurs

extrêmes généralisées" (GEV) à l'estimateur de la RND ainsi obtenu. La méthode SML est peu commode et peut paraître étrange puisqu'elle nécessite de passer constamment de l'espace des prix à l'espace des volatilités implicites et vice-versa. Il est par ailleurs écrit dans [66] que la méthode SML est moins stable et moins précise que certaines méthodes paramétriques bien plus simples.

1.6.2 Estimation stable de la RND par une méthode spectrale. Au Chapter 7, nous proposons une méthode originale capable de retrouver la RND à partir des prix d'options cotés sur les marchés en s'appuyant sur les propriétés spectrales de certains opérateurs de prix.

1.6.2.1 Notre contribution. Au Chapter 7, nous proposons une nouvelle méthode pour estimer la RND directement à partir des prix cotés, à l'offre et à la vente, des options de put. Plus précisément, nous proposons de voir le problème d'estimation de la RND comme un problème inverse. Nous montrons d'abord qu'il est possible de définir des opérateurs de prix d'option d'achat et de vente "restreints" qui admettent une décomposition en valeurs singulières (SVD) qu'il est possible de calculer explicitement. Nous montrons ensuite que ce nouveau cadre théorique permet de mettre au point un algorithme de programmation quadratique simple et rapide qui permet de recouvrer la RND la plus régulière telle que les prix d'option de vente associés se trouvent entre les prix à la achat et à la vente cotés sur le marché. On désigne cette méthode par le nom de "méthode d'estimation spectrale" (SRM). De manière intéressante, la SVD des opérateurs de prix restreints offre un autre point de vue sur le problème d'estimation de la RND à partir des prix de marché. La SRM présente de nombreux avantages sur les méthodes existantes d'estimation de la RND en ce sens que, (1) bien que totalement non paramétrique, elle est simple à implémenter et donne lieu à un algorithme rapide puisqu'il s'agit de résoudre un unique programme quadratique ; (2) elle prend les prix à l'achat et à la vente d'options de put comme seuls paramètres d'entrée et ne requiert donc aucun pré-traitement des données de marché ; (3) elle est robuste en ce sens qu'elle fonctionne très bien avec seulement quelques prix de marché ; (4) elle retourne la densité la plus régulière donnant lieu à des prix d'option de vente situés entre les prix à l'achat et à la vente correspondant cotés sur les marchés. La RND estimée est donc aussi régulière que possible ; (5) elle retourne un formule fermée pour la RND sur l'intervalle $[0, B]$ de $\mathbb{R}^+$ où B est une constante positive qui peut être choisie de manière arbitraire. Nous obtenons donc l'intégralité de la queue gauche de la RND ainsi que sa partie centrale et une partie de sa queue droite. Nous confrontons cet algorithme à des données réelles et simulées et obtenons des résultats intéressant en pratique. La SRM est donc sans aucun doute une alternative intéressante aux autre méthodes d'estimation de la RND.

1.6.2.2 SVD des opérateurs de prix restreints. Définissons tout d'abord l'opérateur d'option d'achat restreint sur l'intervalle $\mathcal{I} = [0, B]$ comme l'opérateur γ de $\mathbb{L}_2\mathcal{I}$ dans $\mathbb{L}_2\mathcal{I}$ tel que,

$$(\gamma f)(\xi) = \int_{\mathcal{I}} \theta(\xi, x) f(x) dx, \qquad \xi \in \mathcal{I}, f \in \mathbb{L}_2\mathcal{I},$$
$$\theta(\xi, x) = (x - \xi)^+.$$

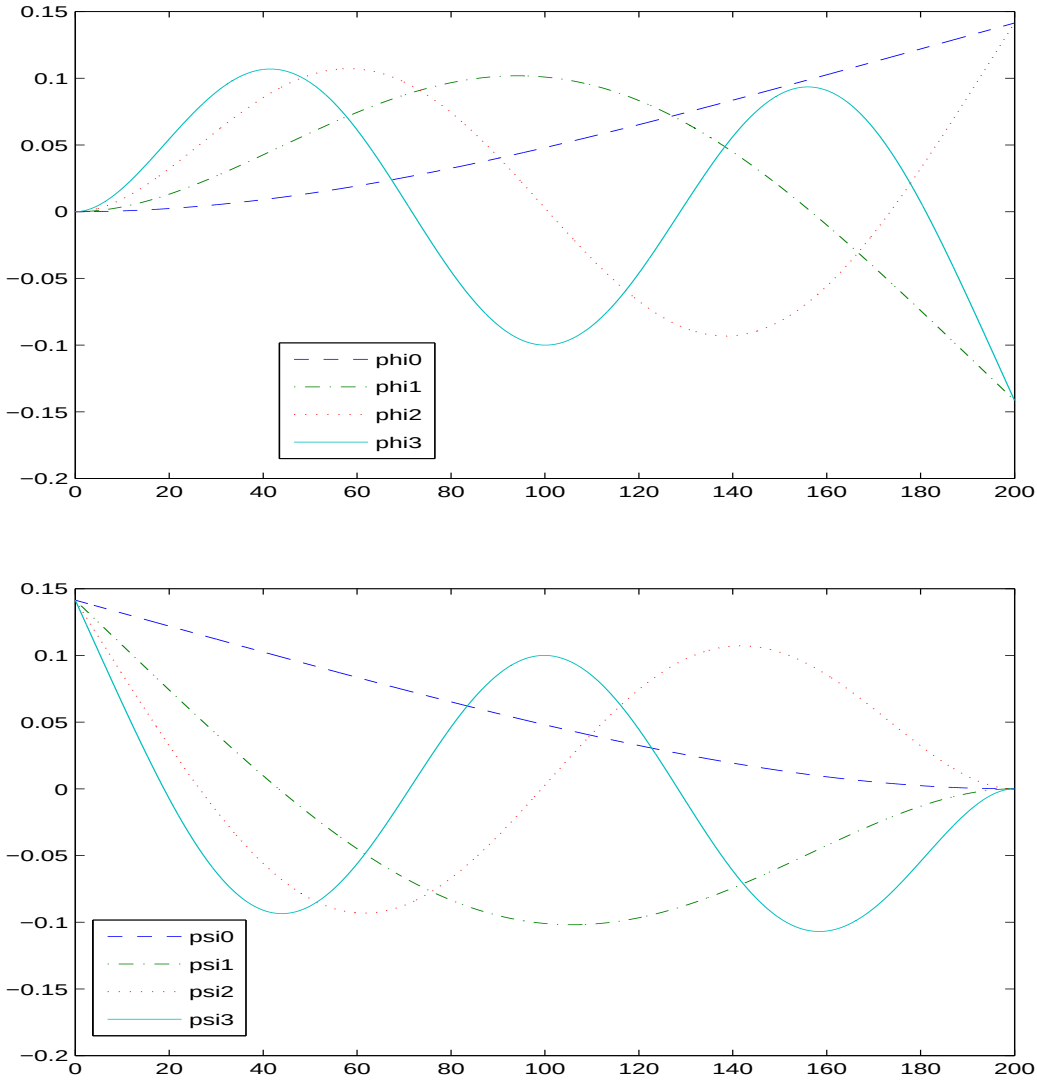

FIGURE *1.9 – Cette figure représente les quatre premiers éléments des deux bases de vecteurs singuliers* (φ_k) *et* (ψ_k)*. En haut, on représente* φ_k*,* $k = 0, \dots, 3$*. En bas, on représente* (ψ_k)*,* $k = 0, \dots, 3$*.*

Il est évident que γf appartient bien à $\mathbb{L}_2\mathcal{I}$. Notons $\langle ., . \rangle$ le produit scalaire usuel de $\mathbb{L}_2\mathcal{I}$ et par $\|.\|_{\mathbb{L}_2\mathcal{I}}$ la norme associée. L'opérateur adjoint γ^* de γ est tel que, pour tout $f, g \in \mathbb{L}_2\mathcal{I}$,

$$\begin{aligned}\langle \gamma^* f, g \rangle &= \langle f, \gamma g \rangle \\ &= \int_{\mathcal{I}} du f(u) \int_{\mathcal{I}} dx \theta(u,x) g(x) \\ &= \int_{\mathcal{I}} dx g(x) \int_{\mathcal{I}} du \theta(u,x) f(u).\end{aligned}$$

De fait

$$\gamma^* f(\xi) = \int_{\mathcal{I}} \theta^*(\xi, x) f(x) dx, \qquad \xi \in \mathcal{I}, f \in \mathbb{L}_2\mathcal{I},$$
$$\theta^*(\xi, x) = \theta(x, \xi).$$

De sorte que γ^* n'est rien d'autre que l'opérateur d'option de vente restreint à $\mathcal{I}$. On prouve que les vecteurs singuliers (φ_k) et (ψ_k) de γ et γ^* forment des bases orthonormées de $\mathbb{L}_2\mathcal{I}$ au Chapter 7. De plus elles peuvent être calculées de manière explicite ainsi que les valeurs singulières (λ_k) associées. Écrivons

$$f_{k,1}(\xi) = e^{\rho_k \xi / B}, \qquad f_{k,2}(\xi) = e^{-\rho_k \xi / B},$$
$$f_{k,3}(\xi) = \cos(\rho_k \xi / B), \qquad f_{k,4}(\xi) = \sin(\rho_k \xi / B),$$

où

$$\rho_k = \frac{\pi}{2} + k\pi + (-1)^k \beta_k, \qquad k \in \mathbb{N}, \tag{1.14}$$

et, pour tout $k \in \mathbb{N}$, β_k est la plus petite solution positive u de l'équation du point fixe suivante,

$$\exp(\pi/2 + k\pi + (-1)^k u) = \frac{1 + \cos(u)}{\sin(u)}.$$

De manière intéressante, la séquence (β_k) décroît à vitesse exponentielle vers zéro comme détaillé dans Lemma 7.6.3. De plus, on écrit,

$$h_{k,1} = a_{k,1} f_{k,1} + a_{k,2} f_{k,2}, \qquad h_{k,2} = a_{k,3} f_{k,3} + a_{k,4} f_{k,4},$$

où les coefficients $a_{k,i}, i = 1, \dots, 4$ sont tels que,

$$a_{k,1} = \frac{1}{\sqrt{B}} \frac{(-1)^k}{e^{\rho_k} + (-1)^k},$$
$$a_{k,2} = (-1)^k e^{\rho_k} a_{k,1} = \frac{1}{\sqrt{B}} \frac{1}{1 + (-1)^k e^{-\rho_k}},$$
$$a_{k,3} = -\frac{1}{\sqrt{B}},$$
$$a_{k,4} = \frac{1}{\sqrt{B}} \frac{1 - (-1)^k e^{-\rho_k}}{1 + (-1)^k e^{-\rho_k}}.$$

Alors le résultat suivant est tiré du Theorem 7.6.1.

Theorem 1.6.1. *Les vecteurs propres (φ_k) de $\gamma^*\gamma$ et (ψ_k) de $\gamma\gamma^*$ sont tels que*

$$\varphi_k = h_{k,1} + h_{k,2}, \qquad \psi_k = h_{k,1} - h_{k,2}.$$

Des représentations graphiques de ces vecteurs singuliers sont données en Figure 1.9. Ils sont liés les uns aux autres par les relations suivantes,

$$\gamma \varphi_k = \lambda_k \psi_k, \qquad \gamma^* \psi_k = \lambda_k \varphi_k,$$

où nous avons écrit

$$\lambda_k = \left(\frac{B}{\rho_k} \right)^2,$$

et ρ_k est définit en eq. (1.14). De plus, ils vérifient $\|\varphi_k\|_{\mathbb{L}_2\mathcal{I}} = \|\psi_k\|_{\mathbb{L}_2\mathcal{I}} = 1$.

1.6.2.3 Programme quadratique destiné à recouvrer la RND. On montre au Chapter 7 que cette SVD offre un cadre théorique propice à l'estimation de la RND q à partir des prix d'options de vente cotés sur le marché. En particulier, la RND peut être obtenue comme la solution d'un simple programme quadratique bâtit sur cette SVD et qui prend les prix d'options de vente cotés sur le marché comme seuls paramètres en entrée.
Pour être plus précis, on se donne $N \in \mathbb{N}$ et on cherche la fonction de prix d'option de vente (en fonction du strike) $P_N(\xi) = \omega_0\varphi_0(\xi) + \ldots + \omega_N\varphi_N(\xi)$ la plus régulière possible qui vérifie un jeux de contraintes de non-arbitrage sur une grille de points (ξ_i), $1 \leq i \leq n$ de $\mathcal{I}$ et soit comprise entre les prix à l'achat et à la vente des options de put cotées sur le marché.

Les contraintes de non-arbitrage. On rappelle que le prix $P(\xi)$ des options d'achat de maturité τ, comme fonction du strike ξ, vérifie les contraintes de non-arbitrage suivantes,

$$\max(0, \xi e^{-r\tau} - S_0 e^{-\delta\tau}) \leq P(\xi) \leq \xi e^{-r\tau}, \tag{1.15}$$

$$0 \leq \partial_\xi P(\xi) \leq e^{-r\tau}, \tag{1.16}$$

$$0 \leq \partial_\xi^2 P(\xi). \tag{1.17}$$

où S_0 désigne le prix aujourd'hui d'un sous-jacent qui paye un taux de dividende continu δ. Comme détaillé au Chapter 7, ces contraintes admettent un équivalent discret sur une grille (ξ_i), $0 \leq i \leq N$, de strikes de $\mathcal{I}$. De plus, si l'on admet que la fonction de prix $P(\xi)$ peut s'écrire sous la forme $P_N(\xi)$, alors ce jeux de contraintes discrètes peut s'écrire sous la forme d'une contrainte affine sur le vecteur des (ω_i), $0 \leq i \leq N$. En plus de ces contraintes de non arbitrage, on voudrait que les prix d'option de vente $P_N(\xi)$ soient localisés entre les prix à l'achat et à la vente cotés sur le marché. Ce qui impose des contraintes d'inégalité supplémentaires. On résume l'ensemble de ces contraintes en Figure 1.10. À chaque $P_N(\xi)$ correspond une unique densité risque neutre $q_N(\xi)$, comme décrit dans le paragraphe suivant. Par conséquent, on cherche la fonction $P_N(\xi)$ qui vérifie les contraintes discrètes décrites ci-dessus et telle que la densité q_N associée soit la plus régulière possible. On mesure la régularité de q_N par la norme $\mathbb{L}_2\mathcal{I}$ au carré de sa dérivée seconde sur $\mathcal{I}$, laquelle peut s'écrire comme une forme quadratique des (ω_i), $0 \leq i \leq N$. Si bien que l'estimation d'un continuum de prix $P_N(\xi)$, $\xi \in \mathcal{I}$, qui soit cohérent avec les prix cotés sur le marché et associé à la RND q_N la plus régulière sur $\mathcal{I}$ se réduit à la résolution d'un simple programme quadratique en les (ω_i), $0 \leq i \leq N$.

Des prix d'option à la densité risque neutre. On note $P_N^\bigstar$ la fonction de prix associée aux poids $(\omega_i^\bigstar)$, $0 \leq i \leq N$, solutions du problème quadratique décrit ci-dessus, en supposant qu'une solution existe. La RND correspondante $q_N^\bigstar$ s'en déduit directement puisque elle est l'image réciproque de $P_N^\bigstar$ par l'opérateur de prix d'option de vente réactualisé. On peut en fait écrire,

$$q_N^\bigstar(\xi) = e^{r\tau} \sum_{i=0}^{N} \omega_i^\bigstar \lambda_i^{-1} \psi_i(\xi), \qquad \xi \in \mathcal{I}.$$

On calcule la RND obtenue à partir de prix d'options de vente réels sur le $S\&P500$ cotés au 01/05/2005 et expirant 72 jours plus tard (voir Chapter 7). On obtient la RND représentée en Figure 1.11 pour $N = 26$. Comme on peut le voir, $q_{26}^\bigstar$ rend compte de la queue gauche épaisse de la RND, un phénomène bien connu des praticiens mais difficilement capturé par des méthodes paramétriques plus traditionnelles.

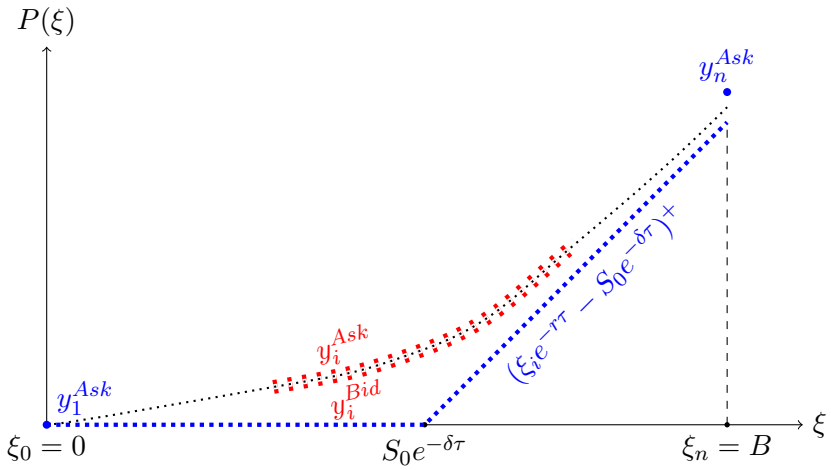

FIGURE *1.10 – Cette figure résume l'ensemble des contraintes vérifiées par la fonction de prix d'option de vente* $P^\star(\xi)$ *solution du problème d'optimisation quadratique décrit en Section 1.6.2.3. On travaille sur une grille discrète de strikes* $0 = \xi_1 < \ldots < \xi_n = B$ *qui contient comme sous-ensemble les strikes cotés sur le marché, que l'on note* $\xi_{i_1}, \ldots, \xi_{i_s}$*, et qui est "relativement" dense dans* $\mathcal{I} = [0, B]$*. Les prix d'option de vente estimés* $P_N^\star(\xi_1), \ldots, P_N^\star(\xi_n)$ *sur la grille de strikes* $\xi_1, \ldots, \xi_n$ *apparaissent sous la forme de pointillés noirs. Ils se trouvent entre les prix à la vente* y_k^{Ask} *et l'achat* y_k^{Bid} *qui sont représentés par de gros points rouges au niveau des strikes* $\xi_{i_1}, \ldots, \xi_{i_s}$ *cotés sur le marché. D'autre part, les* $P_N^\star(\xi_i)$*,* $1 \leq i \leq n$*, vérifient les versions discrètes des contraintes décrites en eq. (1.15), eq. (1.16), eq. (1.17).*

Du choix de N et de l'existence d'une solution au problème d'optimisation quadratique. Remarquons simplement ici que les vecteurs singuliers (φ_k) forment en fait une base orthonormée de $\mathbb{L}_2\mathcal{I}$. Par conséquent, si l'ensemble des fonctions de $\mathbb{L}_2\mathcal{I}$ qui vérifient les contraintes du problème d'optimisation quadratique n'est pas vide, alors le problème admet une solution à partir d'un N assez grand. En pratique, on choisit N comme le plus petit entier naturel à partir duquel le problème admet une solution (voir Chapter 7 pour plus de détails).

1.6.2.4 Commentaires. De manière intéressante, les vecteurs singuliers φ_0 et ψ_0 correspondant à la plus grande valeur singulière λ_0 de γ et γ^* ressemblent eux-mêmes très fortement à des fonctions de prix d'options d'achat et de vente comme fonction de leur strike ξ (voir Figure 1.9). C'est pourquoi ils seront à même de capturer l'essentiel de la forme de la section transverse des prix d'option, à laquelle les vecteurs singuliers suivants se contenteront d'apporter des corrections. C'est une propriété fondamentale de cette SVD qui nous laisse penser que les vecteurs singuliers des opérateurs de prix restreints sont des outils appropriés pour estimer la RND q. De plus, les performances pratiques de l'algorithme de programmation quadratique sont plutôt convaincantes (voir Chapter 7 pour les détails).

1.6.2.5 Perspectives. Remarquons que la SVD décrite ci-dessus n'est valide que pour un intervalle de la forme $[0, B]$. En fait, il est aussi possible de dériver une SVD explicite pour un intervalle de la forme $[-B, B]$. Nous pensons que cela devrait nous permettre d'extrapoler la

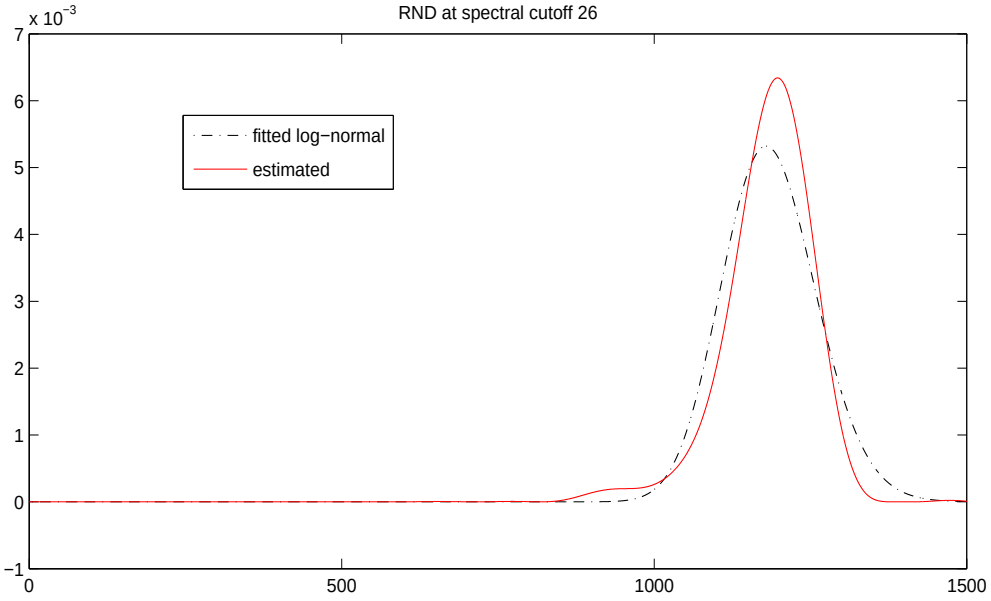

FIGURE *1.11 – Cette figure représente la RND* $q_{26}^{\bigstar}$ *(ligne continue) estimée à partir de prix d'options de vente réels (bid et ask) sur le* $S\&P500$*. On choisit* $B = 1.4 * F_0 = 1.4 * S_0 * e^{(r-\delta)\tau} = 1660$*. De plus, on représente la meilleure approximation log-normale de* q *obtenue par moindres carrés par rapport aux prix d'options cotés moyens (ligne pointillée).*

méthode décrite ci-dessus à l'estimation de RND bivariées via les prix cotés d'options de spread. C'est l'objet d'un travail de recherche en cours.
De plus, et d'un point de vue plus théorique, il est possible de se contenter d'une procédure d'estimation non paramétrique q_n de q plus conventionnelle de manière à pouvoir contrôler la vitesse de convergence de la perte $\mathbb{E}\|q_n - q\|^2_{\mathbb{L}_2\mathcal{I}}$ sur des classes de régularité construites à partir des espaces singuliers des opérateurs de prix restreints. C'est aussi l'objet d'un travail de recherche en cours.

1.7 Appendice.

1.7.1 L'estimateur par polynômes locaux. Commençons dans un premier temps par rappeler la construction de l'estimateur par polynômes locaux (LPE) avant de s'attarder sur ses performances théoriques.

Construction du LPE. Le LPE a été utilisé pour la première fois en régression non paramétrique dans [67]. Pour une revue des développements historiques relatifs au LPE, voir [67, 68, 69, 2, 3, 70, 71, 72]. Ici nous rappelons la définition du LPE telle qu'elle est donnée, par exemple, dans [35].

Definition 1.7.1. *Soient* $h > 0$*,* $x \in \mathbb{R}^d$*,* $l \in \mathbb{N}$ *et une fonction* $K : \mathbb{R}^d \mapsto \mathbb{R}^+$*. On note* $\hat{p}_x$ *un*

polynôme de degré l sur $\mathbb{R}^d$ qui minimise

$$\sum_{i=1}^{n}[Y_i - \hat{p}_x(X_i - x)]^2 K\left(\frac{X_i - x}{h}\right). \tag{1.18}$$

L'estimateur par polynômes locaux $f_n^{LP}(x)$ d'ordre l, noté aussi estimateur LP(l) de la fonction de régression $f(x)$ évaluée au point x est définit par $f_n^{LP}(x) := \hat{p}_x(0)$ si $\hat{p}_x$ est l'unique minimiseur de eq. (1.18) et $f_n^{LP}(x) := 0$ autrement. La valeur h est appelée la "largeur de bande" et la fonction K est appelée le noyau de l'estimateur LP(l).

Seuillage spectral en design aléatoire. Supposons que f appartienne à l'espace de Hölder $\mathscr{C}^s(\Omega)$ pour un $s > 0$ (voir Chapter 3 pour plus de détails). Dans ce qui suit nous noterons f_n^{LP} l'estimateur LP($\lfloor s \rfloor$) associé. Rappelons brièvement les résultats obtenus avec le LPE en design aléatoire. Supposons avant tout que K soit suffisamment régulier, en ce sens qu'il vérifie les conditions (3.3) à (3.6) énoncées dans [35]. Comme détaillé dans cette dernière référence, le calcul de l'estimateur LP($\lfloor s \rfloor$) est étroitement lié à l'inversion de la matrice de régression $\bar{B} := (\bar{B}_{s_1,s_2})_{|s_1|,|s_2| \leq \lfloor s \rfloor}$, où

$$\bar{B}_{s_1,s_2} = \frac{1}{nh^d}\sum_{i=1}^{n}\left(\frac{X_i - x}{h}\right)^{s_1+s_2} K\left(\frac{X_i - x}{h}\right).$$

De telle manière qu'il est possible de définir une version f_n^{LP*} de f_n^{LP} via un seuillage spectral de $\bar{B}$. Plus précisément, si la plus petite valeur propre $\lambda_{\min}(\bar{B})$ est plus grande que $\pi_n^{-1} = (\log n)^{-1}$, on pose $f_n^{LP*}(x) = f_n^{LP}(x)$, et autrement, on pose $f_n^{LP*}(x) = 0$.

Résultats théoriques. Les performances théoriques du LPE sont étudiées sous (**CS1**) dans [3]. Toutefois, des résultats équivalents sont démontrés dans [35] sous des hypothèse plus faibles. En effet, [35] se place sous (**D1**) mais remplace (**S1**) par une hypothèse sur la régularité du support que nous notons (**S2′**) et que nous rappelons ici. Elle est détaillée dans [35, p.613] et s'énonce ainsi. Soient deux constantes $c_0, r_0 > 0$. Nous dirons qu'un sous-ensemble Lebesgue mesurable $\mathcal{A}$ de $\mathbb{R}^d$ est (c_0, r_0)-**régulier** si

$$\lambda(\mathcal{A} \cap B(x,r)) \geq c_0 \lambda(B(x,r)), \qquad \forall 0 < r \leq r_0, \forall x \in \mathcal{A}.$$

Notons en particulier que les boules unités de $\ell^q(\mathbb{R}^d)$ sont (c_0, r_0)-régulières pour des constantes $c_0, r_0 > 0$ déterminées et pour $q \geq 1$, alors que ce n'est plus le cas dès que $q \in (0,1)$.
On définit donc l'hypothèse (**S2′**) comme suit, pour deux constantes $c_0, r_0 > 0$.
(**S2′**) $\mathcal{A}$ est (c_0, r_0)-régulier.
Notons au passage que le cube unité de $\mathbb{R}^d$ correspond au cas $q = \infty$ et est donc (c_0, r_0)-régulier, si bien que l'hypothèse (**S1**) est un cas particulier de (**S2′**). De plus on fait référence aux deux hypothèses (**D1**) et (**S2′**) par (**CS2′**) et, sous l'hypothèse (**CS2′**), on a le résultat suivant qui s'obtient aisément en modifiant légèrement la preuve de [35, Theorem 3.2].

Theorem 1.7.1. *Supposons que la fonction de régression f appartienne à une boule $\mathcal{B}(\mathscr{C}^s(\Omega), M)$ de rayon M de la classe de Hölder $\mathscr{C}^s(\Omega)$ et que (**CS2′**) soit vérifiée. Alors, pour n'importe quel*

$0 < h < r_0/c$, n'importe quels δ tels que $Ch^s\pi_n < \delta$ et n'importe quel $n \geq 1$, l'estimateur f_n^{LP*} vérifie, pour tout $x \in \mathcal{A}$,

$$\sup_{f\in\mathcal{B}(\mathscr{C}^s(\Omega),M)} \mathbb{P}_f^{\otimes n}(|f_n^{LP*}(x) - f(x)| \geq \delta)$$
$$\leq C\exp(-Cnh^d/\pi_n)\mathbb{1}_{\{\delta\leq M\}} + C\exp\left(-C\frac{nh^d\delta^2/\pi_n^2}{1+C\delta/\pi_n}\right).$$

En particulier, si on choisit $h = n^{-\frac{1}{2s+d}}$, on obtient, pour tout $x \in \mathcal{A}$,

$$\sup_{f\in\mathcal{B}(\mathscr{C}^s(\Omega),M)} \mathbb{P}_f^{\otimes n}(|f_n^{LP*}(x) - f(x)| \geq \delta)$$
$$\leq C\exp(-Cn^{\frac{2s}{2s+d}}/\pi_n)\mathbb{1}_{\{\delta\leq M\}} + C\exp\left(-Cn^{\frac{2s}{2s+d}}\frac{\delta^2/\pi_n^2}{1+C\delta/\pi_n}\right).$$

Les constantes absolues C (qui varient d'une occurence à l'autre) ne dépendent que de s, d, M, $c_0, r_0, \mu_{\min}, \mu_{\max}$ et du noyau K.

Il est intéressant de remarquer que la procédure d'estimation linéaire localisée en ondelettes présente de grandes similarités avec la procédure d'estimation par polynômes locaux, modulo les avantages calculatoires discutés en Section 1.3. En particulier, (**S2′**) est à mettre en vis-à-vis de (**S2**) et ces deux hypothèses permettent d'obtenir les résultats de concentration exponentielle similaires décrits en Théorème 1.7.1 et Théorème 1.3.1.

2

Optimal wavelet regression on a uniform design

Contents

2.1 Minimax risk analysis. Let us recall that the minimax framework has been defined at inception of Chapitre 1. Let us here focus on the minimax risk $R_n(\mathcal{F})$ over a function space $\mathcal{F}$. $\mathcal{F}$ will essentially refer to a Besov space $B^s_{\tau,q}(\Omega)$ on a subset Ω of $\mathbb{R}^d$ (see Chapter 3 for a proper definition of Besov spaces). As described in Chapitre 1, we can think of Ω as the unit-cube $[0,1]^d$ of $\mathbb{R}^d$. The study of the minimax rate $R_n(\mathcal{F})$ most often divides into two distinct steps. It consists indeed on the one hand in determining a lower bound $n^{-\gamma}$ on the minimax risk $R_n(\mathcal{F})$ and, on the other hand, in showing that a specific estimation procedure reaches this very same estimation rate (modulo a constant or/and $\log n$ factor). In this Chapter, we will focus on wavelet estimation procedures and recall that they are (nearly) minimax optimal over Besov spaces.

2.1.1 Upper-bound method, bias variance trade-off. Let us assume that we dispose of a multi-resolution analysis (MRA) constituted of a sequence of approximation spaces $(V_j)_{j\geq 0}$ such that $\dim V_j = N = 2^{jd}$. In addition, we denote by f_j^* the best linear approximation of f onto V_j in $\mathbb{L}_p$-norm. Denote by f_n an estimator of f_j^* in V_j such that $\mathbb{E}f_n = f_j^*$ and built upon the n sample points (X_i, Y_i)s. The error which results from the estimation of f by f_n breaks down into two bits.

$$2^{1-p}\mathbb{E}\|f_n - f\|^p_{\mathbb{L}_p} \leq \mathbb{E}\|f_n - f_j^*\|^p_{\mathbb{L}_p} + \|f - f_j^*\|^p_{\mathbb{L}_p}.$$

By extension from the case where $p = 2$, the first term on the rhs is known as the variance term while the second term is known as the bias term. Notice that the bias term is deterministic so that no expectation is needed there. As detailed in Section 3.2.3 below, the bias term is a decreasing function of the model complexity, that is of $\dim V_j$. On the contrary, the variance

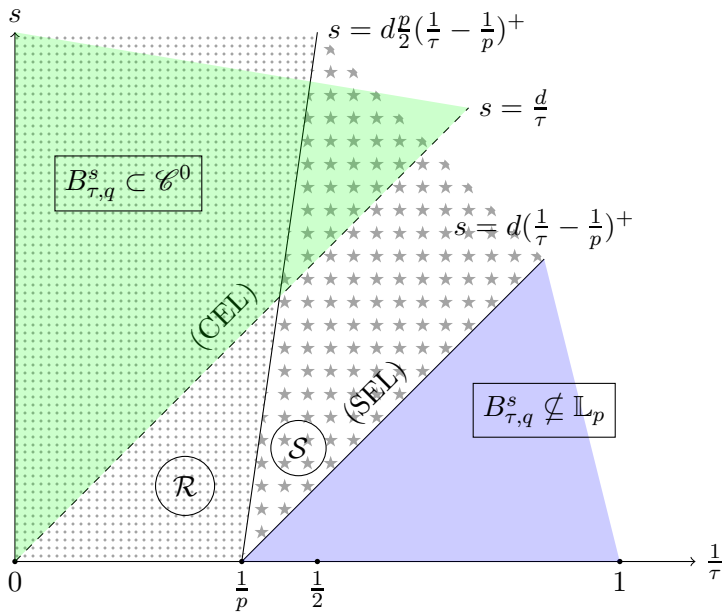

Figure 2.1: This graph displays the main distinct Besov smoothness zones as a function of the coordinates $(1/\tau, s)$ of $B^s_{\tau,q}(\Omega)$. Notice that q does not appear in this graph since it is of secondary importance. (SEL) stands for the Sobolev embedding line under which $B^s_{\tau,q}(\Omega)$ does not embed into $\mathbb{L}_p(\Omega)$ anymore. (CEL) stands for the (dashed) continuous embedding line above which $B^s_{\tau,q}(\Omega)$ embeds into $\mathscr{C}^0(\Omega)$. Finally, $\mathcal{R}$ (dotted area) and $\mathcal{S}$ (starred area) stand for the regular and sparse zone, respectively, when the estimation loss is measured in $\mathbb{L}_p$-norm. More details can be found in Proposition 3.1.1 below.

term is an increasing function of the model complexity. In this linear estimation framework, statisticians look for the model complexity $N = 2^{jd}$ that ideally balances bias with variance, that is the optimal model complexity N_s or, equivalently, the optimal resolution level j_s, which typically depends on the smoothness s of f.

2.1.2 Lower bound methods, regular versus sparse case. Roughly speaking, the lower-bound toolbox consists of Fano's and Assouad's lemma (see [73, Chap. 2]) as well as the Bayesian minimax theorem (see [74, Chap. 4]). In particular, the study of (a lower-bound on) $R_n(B^s_{\tau,q})$ leads to two different regimes termed the sparse case and the regular case. Assume that f belongs to the unit-ball $U(B^s_{\tau,q})$ of the Besov space $B^s_{\tau,q}$ and write $\nu = s - (dp/2)(1/\tau - 1/p)$. All the results that follow are also valid for f in a ball of finite radius M, but for ease of notations, we will stick to the unit-ball in the sequel. Then two cases arise, whether $\nu > 0$ or $\nu \leq 0$. A lower bound on the minimax risk can be found in [75, Theorem 2] in the density estimation setting for $\Omega = \mathbb{R}^d$. In the density estimation setting still, a similar result has been obtained in [47, Theorem 11] with needlet frames for $\Omega = \mathbb{S}^d$, where $\mathbb{S}^d$ stands for the hypersphere of $\mathbb{R}^{d+1}$. Needlet frames have been introduced previously in Chapitre 1 and are further detailed in Chapter 6.

Theorem 2.1.1. *Let $p, q \in [1, \infty]$, $\tau \in (0, \infty]$ and write*

$$R_n(B^s_{\tau,q}) = \inf_{f_n} \sup_{f \in U(B^s_{\tau,q})} \left(\mathbb{E} \|f_n - f\|^p_{\mathbb{L}_p} \right)^{1/p},$$

where $\inf_{f_n}$ *stands for the* inf *over all the measurable functions f_n of the data points. Then, we have*

$$R_n(B^s_{\tau,q}) \geq \begin{cases} Cn^{-\frac{s}{2s+d}}, & \nu > 0 \quad \textit{(regular case)} \\ Cn^{-\frac{s-d(\frac{1}{\tau}-\frac{1}{p})}{2(s-d[\frac{1}{\tau}-\frac{1}{2}])}}, & \nu \leq 0 \textit{ and } s > d/\tau \quad \textit{(sparse case)} \end{cases}$$

Interestingly, notice that the demarcation line $\nu = 0$, that is $s = (dp/2)(1/\tau - 1/p)$, is steeper than the Sobolev embedding line $s = d(1/\tau - 1/p)^+$ if and only if $1/p < 1/2$. So that the sparse zone exists if and only if $p \in (2, \infty]$. The reader is referred to Chapter 3 and Proposition 3.1.1 for details relative to Besov spaces and the Sobolev embedding line.

2.2 Optimal wavelet estimation on a uniform design. Over the last two decades, linear and non-linear wavelet estimators have proved to be very powerful tools in a wide range of applications and in particular in statistical estimation. From a practical standpoint, these estimators are built upon an euclidean lattice, which makes them computationally very appealing. In fact, the computation of a wavelet estimator everywhere on Ω boils down to the estimation of a finite number of wavelet coefficients. This is a definitive advantage over kernel estimators, which must be recomputed at each single evaluation. On the flip side, and as detailed in Chapter 5, wavelet estimators loose some of the flexibility that is offered by kernel estimators due to this very same underlying lattice structure.
From a theoretical standpoint, wavelet estimators have been proved to be (nearly) minimax optimal over wide Besov scales in the density estimation setting. As stated previously, these results extend naturally to the nonparametric regression on a random design setting, provided the design density μ is uniform on Ω. We will therefore quote results from the density estimation setting, being well understood that they are equally valid in the regression on a uniform design setting, under appropriate assumptions on the regression noise.

2.2.1 Multi-resolution analysis, wavelets and notations. First results on multi-resolution analysis (MRA) and wavelets basis (see [76, 77]) emerged in the nonparametric statistics literature in the early 1990's (see [78, 79, 80, 81, 75]). Multi-resolution analysis (MRA) and associated wavelets are detailed below in Section 3.2.1. For reader's convenience, we recall here the main notations. Fix $r \in \mathbb{N}$ and consider the Daubechies' r-MRA built upon the corresponding Daubechies' scaling functions $\varphi_{j,k}$ and associated wavelets $\psi_{j,k}$ (see Section 3.2.1 for terminology). Recall that it consists in nested approximation spaces $(V_j)_{j \geq 0}$ that reproduce polynomials up to degree $r-1$. Furthermore, we denote by $\mathscr{P}_j$ the orthogonal projection operator onto the approximation space V_j (see eq. (3.4)) and by $\mathscr{R}_j = I - \mathscr{P}_j$ the corresponding remainder operator. Finally we define by $\mathscr{W}_j$ the projector onto the detail spaces up to level $j-1$ (see eq. (3.5)). Recall that $\mathscr{P}_j f$ and $\mathscr{W}_j f$ are two representations of the projection of f onto V_j, the former in term of scaling function coefficients $\alpha_{j,k} = \langle f, \varphi_{j,k} \rangle$ and the latter in term of wavelet coefficients $\beta_{j,k} = \langle f, \psi_{j,k} \rangle$.

2.2.2 Linear and non-linear wavelet estimation procedures. The linear estimator $\mathscr{P}_j f_n$ of f is built upon the first representation and reduces in fact to the estimation of $N = 2^{jd}$ scaling function coefficients $\alpha_{j,k}^{(n)}$ at level j and writes as,

$$\mathscr{P}_j f_n = \sum_{k \in \mathcal{Z}_j} \alpha_{j,k}^{(n)} \varphi_{j,k}. \tag{2.1}$$

The non-linear estimator is obtained via the second representation by the estimation and thresholding of $N \asymp 2^{Jd}$ wavelet coefficients $\beta_{j,k}^{(n)}$ up to a cut-off level J and writes as,

$$\mathscr{W}_J f_n = \sum_{j=-1}^{J-1} \sum_{k \in \Lambda_j} \eta(\beta_{j,k}^{(n)}) \psi_{j,k}, \tag{2.2}$$

for some function $\eta(x) = \mathbb{1}_{\{x \geq \varepsilon\}}$, where ε stands for a (fixed) thresholding level. As we will see below, ε will be of the form $\kappa\sqrt{\log n/n}$, for some well-chosen (constant) factor κ. It is noteworthy that the resolution level j in eq. (2.1) and the cutoff level J in eq. (2.2) play very different roles (see Section 2.2.7 for details).

2.2.3 Best linear approximations in $\mathbb{L}_p(\Omega)$-norm. As stated in [82], wavelets are natural unconditional bases of $\mathbb{L}_2(\Omega)$ and remain unconditional bases of $\mathbb{L}_p(\Omega)$ because of their tremendous localization properties, which are at the root of their universality. In the Hilbert space setting of $\mathbb{L}_2(\Omega)$, the best approximation of f in V_j is trivially obtained by the projection $\mathscr{P}_j f$ of f onto the approximation space V_j or, alternatively, by the projection $\mathscr{W}_j f$ of f onto the corresponding detail spaces. In that context, we dispose of natural estimates $\alpha_{j,k}^{(n)}$ and $\beta_{j,k}^{(n)}$ of the coefficients $\alpha_{j,k} = \langle f, \varphi_{j,k} \rangle$ and $\beta_{j,k} = \langle f, \psi_{j,k} \rangle$ in the regression problem, which are

$$\alpha_{j,k}^{(n)} = \frac{|\Omega|}{n} \sum_{i=1}^{n} Y_i \varphi_{j,k}(X_i), \qquad \beta_{j,k}^{(n)} = \frac{|\Omega|}{n} \sum_{i=1}^{n} Y_i \psi_{j,k}(X_i). \tag{2.3}$$

The law of large numbers ensures that they converge to the true coefficients $\alpha_{j,k}$ and $\beta_{j,k}$, provided μ is the uniform distribution on Ω. So that $\mathscr{P}_j f_n$ and $\mathscr{W}_J f_n$ are readily constructed upon these estimates. In a non-Hilbertian setting, that is for an $\mathbb{L}_p(\Omega)$-norm loss with $p \neq 2$, it is not clear how to compute the best approximation of f into V_j. It is a striking result that $\mathscr{P}_j f$ is as good as the best approximation of f in V_j measured with an $\mathbb{L}_p$-norm loss. As shown in Lemma 3.2.1, the error estimate $\|f - \mathscr{P}_j f\|_{\mathbb{L}_p}$ is optimal in V_j in the sense that

$$\|f - \mathscr{P}_j f\|_{\mathbb{L}_p} \asymp \inf_{g \in V_j} \|f - g\|_{\mathbb{L}_p}.$$

This important result allows us to resort to the use of $\mathscr{P}_j f_n$ as the best approximation of f into V_j even when $p \neq 2$ and is therefore of crucial importance. As detailed in the proof of Lemma 3.2.1, it hinges on the uniform boundedness of $\mathscr{P}_j$ in $\mathbb{L}_p(\Omega)$, which is in turn connected to the fine localization properties of wavelets and scaling functions (see proof of Theorem 3.2.1).

2.2.4 Optimality of linear wavelet estimators when $1/\tau \leq 1/p$**.** The following result follows from [78, Theorem 2].

Theorem 2.2.1. *Let* $s > 0$, $\tau, p, q \in [1, \infty)$, $1/\tau \leq 1/p$, *then*

$$\sup_{f \in U(B^s_{\tau,q})} \left(\mathbb{E} \| \mathscr{P}_{j_s} f_n - f \|^p_{\mathbb{L}_p} \right)^{1/p} \leq C n^{-\frac{s}{2s+d}},$$

where $2^{j_s d} = \lfloor n^{\frac{d}{2s+d}} \rfloor$. *Notice that the condition* $s > d/\tau$, *which corresponds to the embedding* $B^s_{\tau,q}(\Omega) \subset \mathscr{C}^0(\Omega)$, *is not needed here (see Proposition 3.1.1 for details and notations).*

It is noteworthy that the dimension $N_s = 2^{j_s d}$ of the model which balances bias and variance depends on the smoothness parameter s. So that $\mathscr{P}_{j_s} f_n$ is minimax optimal when $1/\tau \leq 1/p$ and for all $s > 0$. Unfortunately, linear estimation procedures become suboptimal as soon as $1/\tau > 1/p$, as described in the next section.

2.2.5 Sub-optimality of linear procedures when $1/\tau > 1/p$**.** In the case where the $\mathbb{L}_p$-norm of the loss is coarser that the $\mathbb{L}_\tau$-norm with which the smoothness of the underlying function f is measured, that is $1/\tau > 1/p$, Besov spaces $B^s_{\tau,q}$ contain functions f whose smoothness is spatially inhomogeneous, as seen through the goggles of the $\mathbb{L}_p$-norm loss. This setting is thus sometimes referred to as the case of inhomogeneous smoothness, and in that case, linear wavelet procedures become suboptimal. This result is proved in [75, Theorem 1] in the density estimation setting with $d = 1$ and $\Omega = \mathbb{R}$. However, it generalizes to any dimension d as follows,

Theorem 2.2.2. *Let* $\tau, q, p \in [1, \infty]$, $1/\tau \geq 1/p$, $s > d/\tau$

$$R^L_n(B^s_{\tau,q}) = \inf_{f_n \in \mathcal{L}} \sup_{f \in U(B^s_{\tau,q})} \left(\mathbb{E} \| f_n - f \|^p_{\mathbb{L}_p} \right)^{1/p},$$

where $\inf_{f_n \in \mathcal{L}}$ *stands for the infinimum over all measurable functions of the data points that are built upon linear estimation procedures, meaning that for any* $a \in (0,1)$, *then* $\mathbb{E}_{af+(1-a)g} f_n = a\mathbb{E}_f f_n + (1-a)\mathbb{E}_g f_n$. *Then, we obtain,*

$$C_1 n^{-\frac{t}{2t+d}} \leq R^L_n \leq C_2 n^{-\frac{t}{2t+d}},$$

where $t = s - d(1/\tau - 1/p)$ *(and with an additional* $\log n$ *factor when* $p = \infty$*). This rate is strictly slower than the optimal rates in the regular and sparse zones as soon as* $1/\tau > 1/p$.

2.2.6 Optimality of thresholded wavelet estimators when $1/\tau \leq s/d + 1/p$**.** The problem of the inefficiency of linear wavelet procedures in the case of inhomogeneous smoothness is tackled by non-linear wavelet procedures. Non-linear wavelet estimators are indeed optimal almost all the way down to the Sobolev embedding line, left aside the constraint $s > d/\tau$, which corresponds to the embedding $B^s_{\tau,q}(\Omega) \subset \mathscr{C}^0(\Omega)$. It was initially proved in [75] in the density estimation setting for $d = 1$ and $\Omega = \mathbb{R}$. It was then proved in the nonparametric regression setting under (**CS1**) and in the particular case where μ is the uniform distribution on Ω in [83]. The result has been detailed again for the density estimation problem with needlet frames in the case where Ω stands for the hypersphere $\mathbb{S}^d$ of $\mathbb{R}^{d+1}$ in [47].

Theorem 2.2.3. *Let* $s > 0$, $p \in [1, \infty]$ *and* $\tau \in (0, \infty]$. *Furthermore, assume that*

i) $2^J = n/\log n$ *and* $\|f\|_{\mathbb{L}_\infty} \leq M$ *for some absolute constant* M *if* $p \in [1,2]$,
ii) $2^J = (n/\log n)^{\frac{p}{p-2}}$ *if* $p \in (2,\infty]$.
Then, for a well chosen thresholding constant κ *in eq. (2.2), we have the following results,*

$$\sup_{f\in U(B^s_{\tau,q})} \left(\mathbb{E}\|\mathscr{W}_J f_n - f\|^p_{\mathbb{L}_p}\right)^{1/p} \leq \begin{cases} C(\log n) n^{-\frac{s}{2s+d}}, & \nu > 0 \\ C(\log n) n^{-\frac{s-d(\frac{1}{\tau}-\frac{1}{p})}{2(s-d[\frac{1}{\tau}-\frac{1}{2}])}}, & \nu \leq 0 \text{ and } s > d/\tau \end{cases}$$

where $C(\log n)$ *stands for a multiplicative constant that only depends on* n *via a multiplicative* $\log n$ *factor. Recall that it is necessary to have* $p \in [2,\infty]$, *that is* $1/p \leq 1/2$, *for the sparse zone to exist, that is* $\nu \leq 0$.

2.2.7 Linear versus nonlinear wavelet estimators. Roughly speaking, the superiority of non-linear wavelet estimators over linear ones stems from the fact that they adapt to inhomogeneous smoothness thanks to thresholding. From a technical point of view, the analytical treatment of thresholded wavelet estimators differs from their linear version. To be more precise, in the linear estimation case, the bias between the estimate $\mathscr{P}_j f_n$ and f is isolated in $\mathscr{R}_j f$. So that bias and variance can each benefit from a specific treatment. In the non-linear case, however, part of the bias between $\mathscr{W}_J f_n$ and f remains into the variance term, due to the presence of thresholding, so that bias and variance must be handled both at once. Interestingly, in the non-linear case, the cutoff level J is chosen so high that the actual remainder $\mathscr{R}_J f$ is always negligible in front of the "pseudo" variance term and thus of secondary importance. While in the linear case, j is of primary importance since it must be chosen equal to j_s for bias and variance to be properly balanced. In that sense, the choice of the resolution level for linear wavelet estimators is comparable to the choice of the bandwidth for kernel estimators.

2.3 Adaptation. As described above, minimax linear wavelet procedures on $B^s_{\tau,q}$ require the knowledge of the regularity s of the unknown function f. However, the smoothness parameter s might be unknown itself, so that one might want to adopt an other estimation strategy.

2.3.1 Wavelet thresholding. As detailed previously, non-linear wavelet estimators are nearly optimal almost all the way down to the Sobolev embedding line (see Figure 2.2). In addition, their construction is adaptive since it does not require the knowledge of any of the unknown parameters s, τ, q. As is well known, the regularity r of the underlying r-MRA is tightly connected to the range of smoothness that can be recovered by corresponding wavelet estimation methods. To be more precise, non-linear wavelet procedures built upon a r-MRA for some $r \in \mathbb{N}$ can approximate functions of smoothness s, provided $s \in (0,r)$. In that sense, non-linear wavelet procedures are said to be adaptive over the large Besov scale $\cup_{0<t<r} B^t_{\tau,q}(\Omega)$. The price to pay for adaptation is a deterioration of the estimation rate by a $\log n$ factor.

2.3.2 Lepski's method. Linear wavelet and alternative kernel estimators can be made adaptive thanks to the so-called Lepski's method. Although it does not benefit from the computational efficiency of wavelet thresholding, it has the merit of being flexible enough to allow a wide range of linear estimation procedures to be made adaptive. Consider the case of the linear wavelet estimator $\mathscr{P}_j f_n$ and assume that we dispose of a resolution grid $\mathcal{J} = \{j_r, \dots, J\}$ large

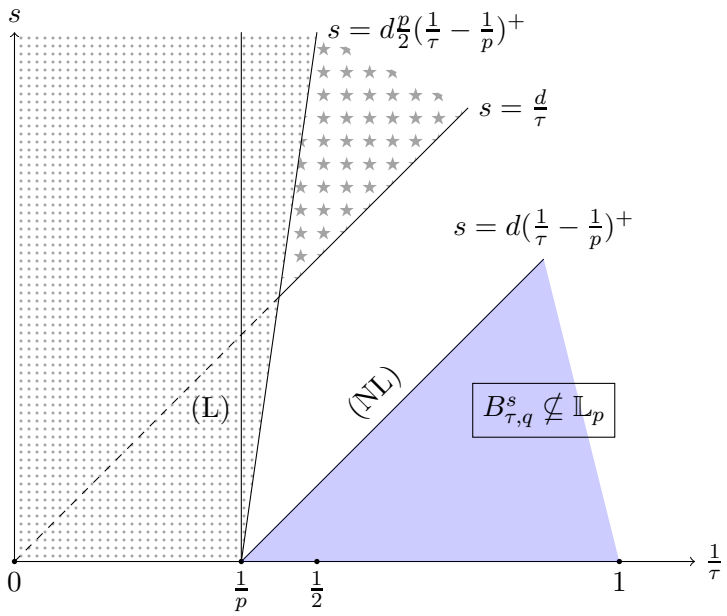

Figure 2.2: This graph displays the main estimation zones as a function of the coordinates $(1/\tau, s)$ of $B^s_{\tau,q}(\Omega)$ when estimation loss is measured in $\mathbb{L}_p$-norm. (NL) stands for the non-linear line down to which the best N-term wavelet approximation (but not estimation !) procedures are optimal. It superimposes with the Sobolev embedding line. (L) stands for the linear line on the right of with linear estimation procedures become suboptimal. Finally, the doted area corresponds to the regular zone. And the starred area corresponds to the part of the sparse zone, on which thresholded wavelet estimation procedures are optimal. It is noteworthy that minimax optimality is not valid anymore below the (CEL) line $s = d/\tau$ (see Figure 2.1).

enough so that $j_s \in \mathcal{J}$, which is always possible as soon as $s \in (0, r)$. Roughly speaking, and as detailed in [84], Lepski's method amounts to choosing the coarsest resolution level $j^@(x)$ at each point $x \in \Omega$ for which the estimator $\mathscr{P}_{j^@(x)} f_n(x)$ displays a "similar" behavior as at any finer resolution level $j > j^@(x), j \in \mathcal{J}$. More details about Lepski's method can be found in Chapter 5.

3

Function spaces, wavelet bases and approximation theory

Contents

3.1 Function spaces on a domain Ω. This part is inspired from [85, 86, 87]. In what follows, Ω will stand for $\mathbb{R}^d$ itself or a bounded subset of $\mathbb{R}^d$. In order to fix the ideas, we can choose Ω to be $[0,1]^d$, the unit-cube of $\mathbb{R}^d$. Here we report standard material relative to function spaces on Ω. Roughly speaking, the function spaces we will define below tie up functions whose moduli of smoothness present a similar behavior.

3.1.1 Spaces of integrable functions $\mathbb{L}_p(\Omega)$**.** Let $\mathcal{X}$ stand for a proper subset of $\Omega \subset \mathbb{R}^d$ and denote by ν a Borel measure on $\mathcal{X}$. We will denote by $\mathbb{L}_p(\mathcal{X},\nu)$ the space of functions $f : \mathcal{X} \mapsto \mathbb{R}$ such that

$$\|f\|^p_{\mathbb{L}_p(\mathcal{X},\nu)} := \int_{\mathcal{X}} |f(x)|^p \nu(dx) < \infty.$$

Let us denote by λ the Lebesgue measure on $\mathcal{X}$. In order to alleviate notations, we will write $\|.\|_{\mathbb{L}_p(\mathcal{X})}$ in place of $\|.\|_{\mathbb{L}_p(\mathcal{X},\lambda)}$, or even $\|.\|_{\mathbb{L}_p}$ when it will be clear from the context that the underlying space is $\mathcal{X}$.

3.1.2 Spaces of continuously differentiable functions $\mathscr{C}^m(\Omega)$**.** Let $m \in \mathbb{N}$. $\mathscr{C}^m(\Omega)$ is defined to be the space of continuous functions which have bounded and continuous partial derivatives $\partial^\gamma f$ for $\gamma \in \mathbb{N}^d$ such that $|\gamma| := \gamma_1 + \ldots + \gamma_d \leq m$. This space is a Banach space for the norm

$$\|f\|_{\mathscr{C}^m(\Omega)} := \|f\|_{\mathbb{L}_\infty(\Omega)} + \sum_{|\alpha|=m} \|\partial^\alpha f\|_{\mathbb{L}_\infty(\Omega)}.$$

3.1.3 Sobolev spaces $W^{m,p}(\Omega)$**.** An immediate extension of $\mathscr{C}^m(\Omega)$ is obtained by measuring smoothness in an average sense. To be more precise, the Sobolev space $W^{m,p}(\Omega)$ consists of all functions which are in $\mathbb{L}_p(\Omega)$ and whose partial derivatives up to order m are in $\mathbb{L}_p(\Omega)$. It is a Banach space for the norm

$$\|f\|_{W^{m,p}(\Omega)} := \|f\|_{\mathbb{L}_p(\Omega)} + |f|_{W^{m,p}(\Omega)},$$

where the rhs stands for the semi-norm defined as follows

$$|f|_{W^{m,p}(\Omega)} := \sum_{|\alpha|=m} \|\partial^\alpha f\|_{\mathbb{L}_p(\Omega)}.$$

Remark that, although $\|f\|_{\mathscr{C}^m(\Omega)}$ coincides with $\|f\|_{W^{m,\infty}(\Omega)}$, these spaces are different.

3.1.4 Hölder spaces $\mathscr{C}^s(\Omega)$**.** These spaces introduce fractional order of smoothness into the picture. For any $h \in \mathbb{R}^d$, let us denote denote by T_h the corresponding translation operator defined by $T_h f(.) = f(. + h)$ and by I the identity operator. Following [86], for any integer r, we define the r^{th} difference operator with step h by $\Delta_h^r = (T_h - I)^r$. It is immediate that $\Delta_h^r = \Delta_h^1(\Delta_h^{r-1})$ and

$$\Delta_h^r(f,x) = \sum_{k=0}^{r} (-1)^{r-k} \binom{r}{k} f(x+kh).$$

Throughout the sequel, we use the convention that $\Delta_h^r(f,x)$ is defined to be zero whenever any of the points $x, x+h, \ldots, x+rh$ is not in Ω. Let us write $\lceil s \rceil$ the smallest integer larger or equal to s. Hölder spaces $\mathscr{C}^s(\Omega)$ are defined as follows

$$\mathscr{C}^s(\Omega) = \{f \in \mathscr{C}^0(\Omega) : \sup_{x\in\Omega} |\Delta_h^{\lceil s \rceil}(f,x)| \leq C\|h\|^s\}, \qquad s \in \mathbb{R}^+\backslash\mathbb{N} \tag{3.1}$$

It can be shown that an equivalent definition is (see [85, p. 160]),

$$\mathscr{C}^s(\Omega) = \{f \in \mathscr{C}^{\lfloor s \rfloor}(\Omega) : \partial^\gamma f \in \mathscr{C}^{s-\lfloor s \rfloor}(\Omega), |\gamma| = \lfloor s \rfloor\}, \qquad s \in \mathbb{R}^+\backslash\mathbb{N}$$

where $\mathscr{C}^{s-\lfloor s \rfloor}(\Omega)$ inside the brackets is defined above in eq. (3.1). It is clear that, for $s \in \mathbb{N}$, this latter definition of Hölder space coincides with the space of continuously differentiable functions $\mathscr{C}^s(\Omega)$ defined previously. This is the reason why we have used the same letter $\mathscr{C}$ to refer to both function spaces. In the sequel, we will thus refer to any space $\mathscr{C}^s(\Omega)$, $s \in \mathbb{R}^+$, by the name of Hölder space.

3.1.5 Fractional Sobolev spaces $W^{s,p}(\Omega)$**.** Lipschitz spaces can in turn be extended to fractional Sobolev spaces by measuring smoothness in an average sense. We in fact define the fractional Sobolev spaces $W^{s,p}(\Omega)$ to be the Besov space $B^s_{p,\infty}(\Omega)$ for $s \in \mathbb{R}^+\backslash\mathbb{N}$ and $p \in (0,\infty]$. Let us now turn to Besov spaces, which will be central to the subsequent developments.

3.1.6 Besov spaces $B^s_{p,q}(\Omega)$**.** As we will see below, Besov spaces contain all the previous function spaces. Besov spaces regroup in fact functions whose moduli of smoothness have a similar behavior. To be more precise, we define the r^{th} order modulus of smoothness of $f \in \mathbb{L}_p(\Omega)$, $p \in (0,\infty]$, by

$$\omega_r(f,t)_p = \sup_{\|h\|\leq t} \|\Delta^r_h(f,.)\|_{\mathbb{L}_p(\Omega)},$$

where $\mathbb{L}_\infty(\Omega)$ is replaced by $\mathscr{C}^0(\Omega)$, the space of uniformly continuous functions on Ω, when $p=\infty$. Notice that $\omega_r(f,t)_p \to 0$ as $t \to 0$ and the smoother f the faster it converges to 0. Besov spaces are characterized by three parameters $s \in (0,\infty)$ and $p,q \in (0,\infty]$. s corresponds to the order of smoothness and p to the $\mathbb{L}_p(\Omega)$-norm in which the smoothness is to be measured. The role of q is secondary and will allow to make subtle distinctions between smoothness spaces with same primary parameters. Let us write $r = \lfloor s \rfloor + 1$ the smallest integer larger than s. We say that $f \in B^s_{p,q}(\Omega)$ is and only if the semi-norm

$$|f|_{B^s_{p,q}(\Omega)} := \begin{cases} \left(\int_0^\infty [t^{-s}\omega_r(f,t)_p]^q \frac{dt}{t}\right)^{\frac{1}{q}}, & q \in (0,\infty) \\ \sup_{t>0} t^{-s}\omega_r(f,t)_p, & q=\infty \end{cases} \tag{3.2}$$

is finite. And $B^s_{p,q}(\Omega)$ is a Banach space for the norm

$$\|f\|_{B^s_{p,q}(\Omega)} := \|f\|_{\mathbb{L}_p(\Omega)} + |f|_{B^s_{p,q}(\Omega)}.$$

In fact, it results from the monotonicity of the modulus of smoothness ($\omega_r(f,t)_p \leq \omega_r(f,t')_p$ for $t' > t$) that the semi-norm $|f|_{B^s_{p,q}(\Omega)}$ admits the following discrete equivalent

$$|f|_{B^s_{p,q}(\Omega)} \asymp \begin{cases} \left(\sum_{j\geq 0} [2^{js}\omega_r(f,2^{-j})_p]^q\right)^{\frac{1}{q}}, & q \in (0,\infty) \\ \sup_{j\geq 0} 2^{js}\omega_r(f,2^{-j})_p, & q=\infty \end{cases} \tag{3.3}$$

From now on, $\|f\|_{B^s_{p,q}(\Omega)}$ will refer to the Besov norm defined upon the latter discrete version of the Besov semi-norm.

3.1.6.1 Besov spaces and Lipschitz spaces. We define Lipschitz spaces on Ω as $Lip^s(\Omega) = B^s_{\infty,\infty}(\Omega)$ for $s \in \mathbb{R}^+$. It can be shown that $Lip^s(\Omega) = \mathscr{C}^s(\Omega)$ for $s \in \mathbb{R}^+\backslash\mathbb{N}$, while $Lip^s(\Omega)$ is strictly larger than the space $\mathscr{C}^s(\Omega)$ for $s \in \mathbb{N}$. This is due to the fact that $Lip^s(\Omega)$ uses $\omega_{\lfloor s \rfloor+1}$ in its definition, while $\mathscr{C}^s(\Omega)$ uses $\omega_{\lceil s \rceil}$ and the fact that, for $s \in \mathbb{N}$, $\omega_{s+1}(f,t)_p \leq 2\omega_s(f,t)_p$, $p \in (0,\infty]$, as described in [88, eq.(7.5)].

3.1.6.2 Besov spaces and Sobolev spaces. In the same way, it follows from the definition of fractional Sobolev spaces given above that $B^s_{p,\infty}(\Omega) = W^{s,p}(\Omega)$ for any $s \in \mathbb{R}^+\backslash\mathbb{N}$ and $B^s_{p,\infty}(\Omega)$ is slightly larger than $W^{s,p}(\Omega)$ otherwise. In fact the later inclusion is always strict except for $p=2$ where it can be shown that $B^s_{2,\infty}(\Omega) = W^{s,2}(\Omega)$.

3.1.6.3 Properties of Besov spaces. In this section we describe some well-known facts relative to Besov spaces. Let $(Y, \|.\|_Y)$ and $(X, \|.\|_X)$ be two normed vector spaces such that $Y \subseteq X$. We will say that Y embeds continuously in X if and only if $\|.\|_X \leq C\|.\|_Y$ for some absolute constant C and we will denote it by $Y \hookrightarrow X$.

Proposition 3.1.1. *We have the following results, for all $\tau, p \in [1, \infty]$ and $s > 0$,*

(i) $B^s_{p,q} \subset \mathscr{C}^0(\Omega)$ *for* $s > d/p$.
(ii) $B^s_{p,q_1}(\Omega) \hookrightarrow B^s_{p,q_2}(\Omega)$ *for* $q_1 < q_2$.
(iii) Regardless of the values q_1, q_2, we have $B^{s_1}_{p,q_1}(\Omega) \hookrightarrow B^{s_2}_{p,q_2}(\Omega)$ *for* $s_1 \geq s_2$. *This shows in particular that q is of secondary importance with respect to s.*
(iv) $B^s_{\tau,q} \hookrightarrow B^s_{p,q}$ *for* $1/\tau \leq 1/p$.
(v) $B^s_{\tau,q} \hookrightarrow B^{s-d(1/\tau-1/p)}_{p,q}$ *for* $1/\tau \geq 1/p$ *and* $s > d(1/\tau - 1/p)$.
(vi) $B^s_{\tau,q}(\Omega) \hookrightarrow \mathbb{L}_p(\Omega)$ *provided* $s > d(1/\tau - 1/p)^+$. *The inclusion never holds when* $s < d(1/\tau - 1/p)^+$ *and may or may not hold when* $s = d(1/\tau - 1/p)^+$. *The line* $s = d(1/\tau - 1/p)^+$ *is known as the Sobolev embedding line.*

Proof. Item ii follows directly from the nestedness of the ℓ_q spaces with increasing values of q. Item iii can be found in [85]. Item v is the Sobolev embedding theorem (see [87, 89]). Item vi is a consequence of the Sobolev embedding theorem. □

3.2 Besov spaces, wavelet bases and multi-resolution analysis. The advent of wavelets in applied mathematics dates back to the early 1980's. Since then they have proved to be a powerful tool for data compression, numerical analysis, function estimation, to quote a few. Detailed depictions of the construction of wavelet frames, Riesz and orthonormal bases can be found in textbooks such as [77, 90, 91, 85, 92, 93] and references therein. A nice textbook on wavelets with statistical applications in view is [94]. For reader's convenience, an overview of frames and Riesz bases is given in Chapter 4. The construction of wavelet bases has been facilitated by the introduction of multi-resolution analyses (MRA) by [76].

3.2.1 Multiresolution analysis. The proper definition of MRA can be found in [76] or [85, Definition 2.2.1]. In Chapter 5, we will make use of MRAs generated by Daubechies' scaling function φ, to which we will refer as Daubechies' MRA. We therefore only focus on this particular case here. Recall first that we work on the bounded domain $\Omega = [0,1]^d$. For such a domain, a boundary corrected MRA is given in [95]. We make an extensive use of it in Chapter 5 and recall the details of its construction there. At this point, our sole aim is to fix notations and remind the reader of the essential properties of MRAs, which are needed in Chapitre 1 and Chapter 2. Let us denote by φ the multivariate Daubechies' scaling function, obtained by tensorial product of univariate versions (see [85, Remark 1.4.5] and Section 3.2.2 for more details). Let us denote by $\varphi_{j,k}$ the dilated and translated version of φ, meaning $\varphi_{j,k}(x) = 2^{jd/2}\varphi(2^j x - k)$ (or its boundary corrected version, when necessary) for $k \in \mathcal{Z}_j^d$, where $\mathcal{Z}_j = \{0, 1, \dots 2^j - 1\}$. Now, recall that Daubechies' MRA is constituted of nested approximation spaces $(V_j)_{j\geq 0}$ such that (i) V_j is a closed subspace of $\mathbb{L}_2(\Omega)$; (ii) $(\varphi_{j,k})_{k\in\mathcal{Z}_j^d}$ is an orthonormal basis of V_j; (iii) $\cup_{j\geq 0} V_j$ is dense in $\mathbb{L}_2(\Omega)$. Therefore, each nested approximation space V_j is of dimension 2^{jd}. Notice as an aside that scaling functions $\varphi_{j,k}$ (also known as father wavelets) and associated wavelets $\psi_{j,k}$ (also known as mother wavelets) come in a wide range of flavors and can be tuned to constitute frames, Riesz bases as well as orthonormal bases of the (V_j) or $\mathbb{L}_2(\Omega)$, respectively. To further

clarify the matter, we give a brief refresher on bases and frames in Chapter 4.
Let us now come back to the Daubechies' MRA of Ω introduced above. We denote by $\mathscr{P}_j$ the projector onto V_j, meaning

$$\mathscr{P}_j f = \sum_{k \in \mathcal{Z}_j^d} \alpha_{j,k} \varphi_{j,k}, \qquad \alpha_{j,k} = \langle f, \varphi_{j,k} \rangle, \tag{3.4}$$

and denote by $\mathscr{R}_j f = f - \mathscr{P}_j f$ the corresponding remainder. We also denote by $\mathscr{Q}_j = \mathscr{P}_{j+1} - \mathscr{P}_j$ the projector onto the detail space $W_j = V_{j+1} \ominus V_j$. Recall in particular that the Daubechies' wavelets $\psi_{j,k}$ associated to Daubechies' scaling function constitute orthonormal basis of the detail spaces. To be more precise, there exists a set of indices $\Lambda_j \subset \mathbb{Z}^d$ such that $\#\Lambda_j \asymp 2^{jd}$ and $(\psi_{j,k})_{k \in \Lambda_j}$ constitutes an orthonormal family of W_j for all $j \geq 0$. Notice interestingly that V_j decomposes into finer and finer details, or equivalently, the projection operator $\mathscr{P}_j$ decomposes as a sum of projections onto detail spaces,

$$\begin{aligned} V_j &= W_{j-1} \oplus \ldots \oplus W_0 \oplus V_0, \\ \mathscr{P}_j &= \mathscr{Q}_{j-1} + \ldots + \mathscr{Q}_0 + \mathscr{P}_0. \end{aligned}$$

So that the projection $\mathscr{P}_j$ of f onto V_j made explicit in eq. (3.4) writes equivalently as a wavelet expansion $\mathscr{W}_j f$,

$$\mathscr{W}_j f = \sum_{\ell \geq -1}^{j-1} \sum_{k \in \Lambda_\ell} \beta_{\ell,k} \psi_{\ell,k}, \qquad \beta_{\ell,k} = \langle f, \psi_{\ell,k} \rangle, \tag{3.5}$$

where, for the sake of concision, we have written $\Lambda_0 = \mathcal{Z}_0^d = \{0\}$, $\beta_{-1,0} = \alpha_{0,0}$ and $\psi_{-1,0} = \varphi_{0,0}$. Let us now recall the following results (see [77] or [85, Theorem 3.3.1]),

Theorem 3.2.1. *Let $p, q \in [1, \infty]$ and assume that $\varphi \in \mathbb{L}_p \cap \mathbb{L}_q$ where q is such that $1/p + 1/q = 1$. Then the projectors $\mathscr{P}_j$ are uniformly bounded in $\mathbb{L}_p$. Moreover the basis $\varphi_{j,k}$ is $\mathbb{L}_p$-stable in the sense that*

$$\| \sum_{k \in \mathcal{Z}_j^d} c_k \varphi_{j,k} \|_{\mathbb{L}_p} \asymp 2^{jd(\frac{1}{2} - \frac{1}{p})} \| (c_k)_{k \in \mathcal{Z}_j^d} \|_{\ell^p}, \tag{3.6}$$

with constants that do not depend on j.

Proof. The proof of the uniform-boundedness of $\mathscr{P}_j$ follows directly from eq. (3.6) above. Notice indeed that Hölder inequality leads to

$$|\langle f, \varphi_{j,k} \rangle| \leq \|f\|_{\mathbb{L}_p(\mathrm{Supp}\varphi_{j,k})} \|\varphi_{j,0}\|_{\mathbb{L}_q} \leq 2^{jd(\frac{1}{2} - \frac{1}{q})} \|f\|_{\mathbb{L}_p(\mathrm{Supp}\varphi_{j,k})}.$$

Taking the p^{th} power, summing over k and remarking that

$$\#\{k' : \mathrm{Supp}\varphi_{j,k} \cap \mathrm{Supp}\varphi_{j,k'} \neq \emptyset\} \leq C,$$

for some absolute constant C independent of j and k, we obtain

$$\| (\langle f, \varphi_{j,k} \rangle)_{k \in \mathbb{Z}^d} \|_{\ell^p} \lesssim 2^{jd(\frac{1}{2} - \frac{1}{q})} \|f\|_{\mathbb{L}_p}.$$

The result follows by combining this last inequality with eq. (3.6). □

This result allows to conclude readily that $\mathscr{P}_j f$ provides us with a best approximation of f into V_j measured in $\mathbb{L}_p$-norm. Notice indeed that

Lemma 3.2.1. *The error estimate $\|f - \mathscr{P}_j f\|_{\mathbb{L}_p}$ is optimal in V_j, that is*

$$\|f - \mathscr{P}_j f\|_{\mathbb{L}_p} \asymp E_{2^{-j}}(f)_p := \inf_{g \in V_j} \|f - g\|_{\mathbb{L}_p}.$$

Proof. One side is obvious. Te other side follows readily from the uniform boundedness of $\mathscr{P}_j$. Notice indeed that, for any $g \in V_j$,

$$\begin{aligned}\|f - \mathscr{P}_j f\|_{\mathbb{L}_p} &\leq \|f - g\|_{\mathbb{L}_p} + \|\mathscr{P}_j f - \mathscr{P}_j g\|_{\mathbb{L}_p} \\ &\leq (1 + \|\mathscr{P}_j\|)\|f - g\|_{\mathbb{L}_p},\end{aligned}$$

and the results follows after taking the inf over all $g \in V_j$ on the right side and noticing that $\|\mathscr{P}_j\| \leq C$ for some absolute constant C independent of j. □

Finally, we have the following result, which can be found in [92, Theorem 8.4]. It is stated for $\Omega = \mathbb{R}^d$ with an adequately chosen MRA, but holds equally as well in our setting $\Omega = [0,1]^d$ with a boundary corrected MRA.

Theorem 3.2.2. *Fix $\Omega = \mathbb{R}^d$. Suppose $f \in \mathbb{L}_p(\Omega)$ if $p \in [1, \infty)$, or $f \in \mathscr{C}^0(\Omega)$ if $p = \infty$, then $\|\mathscr{P}_j f - f\|_{\mathbb{L}_p} \to 0$ as $j \to \infty$.*

3.2.2 Polynomial exactness. Polynomial exactness is a crucial feature of nested approximation spaces and, ultimately, of the scaling function φ, which relates directly to the smoothness that can be explained by the MRA. It is possible to choose φ such that approximation spaces V_j reproduce polynomials up to order $r-1$ for some arbitrary $r \in \mathbb{N}$. We will refer to such a MRA as a r-MRA. Interestingly, r-MRAs can explain smoothness s for any $s \in (0, r)$. Notice also that the volume of Suppφ grows with r. Daubechies' scaling function φ associated to a r-MRA is indeed supported on the hypercube $[-r+1, r]^d$. Notice also that the volume of Suppφ is the same as the volume of Suppψ. As described in [90], Daubechies' scaling functions have minimal volume support among scaling functions that reproduce polynomials up to order $r-1$.

3.2.3 Multiresolution analysis and Besov spaces. It appears, maybe surprisingly, that MRAs and associated wavelet bases are tightly intertwined with Besov spaces. In fact, it can be shown that Besov spaces can be exactly characterized by the behavior of the remainder $\mathscr{R}_j$ associated to a given r-MRA. The following theorem can be found in the proof of [85, Theorem 3.6.1].

Theorem 3.2.3. *r-MRAs built upon $\varphi \in B^\gamma_{p,q_0}$, for some q_0, characterize exactly Besov spaces in the sense that, for $s < \gamma \wedge r$,*

$$\|f\|_{B^s_{p,q}} \asymp \|f\|_{\mathbb{L}_p} + \|(2^{js}\|\mathscr{R}_j f\|_{\mathbb{L}_p})_{j \geq 0}\|_{\ell^q}.$$

Furthermore, we have the following equivalence, which explains the link between approximation spaces $\mathcal{A}^s_{p,q}$ of approximation theory (see [86] for details) and Besov spaces. It can also be found in the proof of [85, Theorem 3.6.1],

Theorem 3.2.4. *Under the assumptions of Theorem 3.2.3, we have got*

$$\begin{aligned}\|\mathscr{R}_j f\|_{\mathbb{L}_p} &\lesssim \omega_r(f, 2^{-j})_p \\ 2^{js}\omega_r(f, 2^{-j})_p &\lesssim \|f\|_{\mathbb{L}_p} + \sum_{t=0}^{j} 2^{st}\|\mathscr{R}_t f\|_{\mathbb{L}_p}\end{aligned}$$

Moreover, Theorem 3.2.3 leads directly to a norm equivalence expressed in term of the projection $\mathscr{Q}_j f$ of f onto the detail spaces and hence in term of its wavelet coefficients. We have the following result.

Corollary 3.2.1. *Notice that, under the assumptions of Theorem 3.2.3,*

$$\|f\|_{B^s_{p,q}} \asymp \|(2^{js}2^{jd(\frac{1}{2}-\frac{1}{p})}\|(\langle f,\psi_{j,k}\rangle)_{k\in\Lambda_j}\|_{\ell^p})_{j\geq 0}\|_{\ell^q}.$$

Proof. This results directly from the fact that

$$\|f\|_{\mathbb{L}_p} + \|(2^{js}\|\mathscr{R}_j f\|_{\mathbb{L}_p})_{j\geq 0}\|_{\ell^q} \asymp \|\mathscr{P}_0 f\|_{\mathbb{L}_p} + \|(2^{js}\|\mathscr{Q}_j f\|_{\mathbb{L}_p})_{j\geq 0}\|_{\ell^q},$$

and, similarly to Theorem 3.2.1,

$$\|\mathscr{Q}_j f\|_{\mathbb{L}_p} \asymp 2^{jd(\frac{1}{2}-\frac{1}{p})}\|(\langle f,\psi_{j,k}\rangle)_{k\in\Lambda_j}\|_{\ell^p}.$$

□

3.3 Linear and nonlinear approximation theory. It is the aim of approximation theory to come up with approximation spaces that allow to control the bias term $\mathscr{R}_j f$ in an optimal fashion. It is well known that N-dimensional linear (resp. non-linear) wavelet approximation spaces are able to approximate functions f of a Besov space $B^s_{\tau,q}$ at a rate $N^{-s/d}$ in $\mathbb{L}_p(\Omega)$-norm, as long as $1/\tau \leq 1/p$ (resp. $1/\tau \leq s/d + 1/p$). The optimality of linear (res. non-linear) wavelet approximation procedures, among all linear (resp. non-linear) approximation procedures, is proved via the study of linear (resp. non-linear) N-widths.

3.3.1 Lower estimate for linear approximation. In order to show that no linear approximation method on a N dimensional subspace X_N of $\mathbb{L}_p(\Omega)$ can do better than an approximation rate of order $N^{-s/d}$, one uses Kolmogorov N-widths. They measure the approximation performance of the best N-dimensional linear space on a compact subset K of a given smoothness class. For any compact subset K of $\mathbb{L}_p(\Omega)$, they are defined as

$$d_N(K) := \inf_{\dim(X_N)=N} \sup_{f\in K} \inf_{g\in X_N} \|f-g\|_{\mathbb{L}_p(\Omega)}.$$

Let us denote by $U(B^s_{\tau,q}(\Omega))$ the unit-ball of $B^s_{\tau,q}(\Omega)$ and fix the domain Ω to be the unit-interval of $\mathbb{R}$, meaning $\Omega = [0,1)$ and $d = 1$. In addition, we fix the ambient space X to be $\mathbb{L}_p(\Omega)$, so that $X_N \subseteq X = \mathbb{L}_p(\Omega)$. As described in [86, 96], the unit-balls $U(B^s_{\tau,q}(\Omega))$ are compact subsets of $\mathbb{L}_p(\Omega)$ provided $1/\tau < s + 1/p$, that is when we are on the left of the Sobolev embedding line. As detailed in the latter references, $d_N(U(B^s_{\tau,q}(\Omega)))$ is never better than $O(N^{-s})$. In fact, we have $d_N(U(B^s_{\tau,q}(\Omega))) \asymp N^{-s}$ on the line (L) and also for all $1/\tau \leq 1/p$. Surprisingly, for $p \in (2,\infty)$ and $s > 1/\tau$, there is always a range of τ on the right of (L) (see Figure 3.1), namely $1/2 \geq 1/\tau > 1/p$, for which $d_N(U(B^s_{\tau,q}(\Omega))) \asymp N^{-s}$. We know however that conventional linear approximation spaces are unable to reach this approximation rate in that smoothness area (see Figure 3.1). In fact, in order to reach such rates in that area, we must resort to non-linear approximation methods. Hence, there are linear spaces that can perform as well as non-linear ones on this particular domain. Unfortunately, we are unable to construct them explicitely (see [86]).

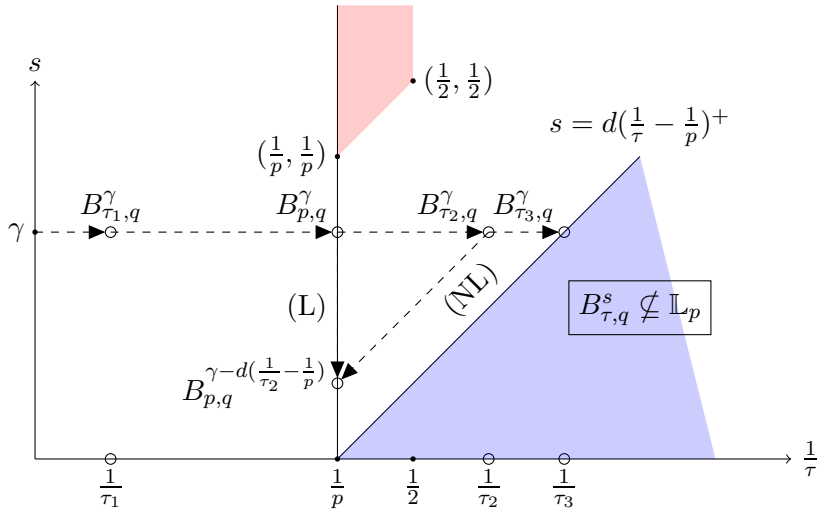

Figure 3.1: This graph represents properties of Besov spaces $B^s_{\tau,q}$ in the coordinate system $(1/\tau, s)$. We give ourselves $\tau_1 > p > \tau_2 > \tau_3$ in $[1,\infty]$. The dashed arrows represent paths of continuous embedding of Besov spaces into one another. When the approximation error is measured in $\mathbb{L}_p$-norm, the vertical line (L) stands for the right limit beyond which linear approximation procedures become suboptimal. (NL) superimposes with the Sobolev embedding line and, roughly speaking, stands for the right limit down to which non-linear approximation procedures are optimal. The small colored area at the top of the figure represents the so-called super-approximation zone, where there exist linear procedures that are optimal but are yet to be discovered.

3.3.2 Lower estimate for non-linear approximation. We know that classical non-linear methods approximate functions in $B^s_{\tau,\infty}(\Omega)$ with accuracy N^{-s} for $1/\tau < s + 1/p$. But could it be that other non-linear methods do better? This question is answered through the study of nonlinear N-widths $\delta_N(U(B^s_{\tau,q}(\Omega)))$ (see [86] and references therein for more details). In particular, it can be shown that $\delta_N(U(B^s_{\tau,q}(\Omega))) \asymp N^{-s}$ on the left of (NL), so that, among all non-linear approximation methods, best N-terms wavelet approximation methods are optimal.

3.3.3 Link between approximation and estimation rates. The link between estimation and approximation has been thoroughly studied by Albert Cohen, Ronald DeVore, Gérard Kerkyacharian, Dominique Picard and their co-authors and can be found in papers such as [82].

4

From orthonormal bases to frames

This material is for the most part borrowed from [97, Chap. 3-5]. Other relevant material relative to frames in the context of statistical estimation and noise reduction can be found in [91, Chap. 5] and [90, Chap. 3]. In what follows, proofs are most often not given and the reader is rather referred to the above references for detailed proofs.

Contents

4.1 Bases and their limitations. In a signal processing context, bases have often been criticized for their lack of flexibility: (i) it is indeed often impossible to construct a basis with additional special properties, (ii) and even a slight modification of a basis element might destroy the basis property. In addition, it is noteworthy that situations differ drastically between a finite-dimensional vector space and an infinite dimensional Hilbert space $\mathcal{H}$. In a finite-dimensional vector space, we know that every family of vectors that spans it contains a basis. In an infinite-dimensional vector space, one can prove the existence of a sequence (f_k) such that (i) Each $f \in \mathcal{H}$ admits an unconditionally convergent expansion $f = \sum c_k f_k$ with $(c_k) \in \ell^2(\mathbb{N})$, while (ii) no subsequence of (f_k) is a basis for $\mathcal{H}$. These are the major motivations for the study of over-complete families of $\mathcal{H}$.

4.2 Bessel sequences, orthonormal bases, Riesz bases and frames. Let $\mathcal{H}$ stand for a separable Hilbert space with inner product $\langle ., . \rangle$. As is customary, we refer to the sequence $\{f_k\}_{k \geq 1}$ to mean the countable ordered set $\{f_1, f_2, ...\}$. For ease of notations, we often drop the subscript and simply write $\{f_k\}$.

4.2.1 Bessel sequences. Let us first introduce the concept of Bessel sequence, which is closely related to the property of unconditional basis. We start by a useful lemma/definition.

Lemma 4.2.1. *Let $\{f_k\}$ be a sequence in $\mathcal{H}$ and suppose that $\sum_{k=1}^{\infty} c_k f_k$ is convergent for all*

$\{c_k\} \in \ell^2(\mathbb{N})$. *Then the* ***pre-frame or synthesis operator*** T,

$$T : \ell^2(\mathbb{N}) \mapsto \mathcal{H},$$
$$T(\{c_k\}) = \sum c_k f_k,$$

defines a bounded linear operator. Its adjoint T^*, *also known as the* ***analysis operator****, is given by*

$$T^* : \mathcal{H} \mapsto \ell_2(\mathbb{N}),$$
$$T^*(f) = \{\langle f, f_k\rangle\}.$$

Furthermore, we have

$$\sum |\langle f, f_k\rangle|^2 = \|T^* f\|^2_{\ell^2(\mathbb{N})} \leq \|T\|^2 \|f\|^2_{\mathcal{H}}.$$

Finally, we define the ***frame operator*** *by* $S = TT^*$, *so that*

$$S : \mathcal{H} \mapsto \mathcal{H},$$
$$S(f) = \sum_k \langle f, f_k\rangle f_k.$$

As described below, the boundedness of the operator T on $\ell^2(\mathbb{N})$ associated to a family $\{f_k\}$ guarantees that the order of summation is irrelevant. Such sequences will be termed Bessel sequences.

Definition 4.2.1. *A sequence* $\{f_k\}$ *in* $\mathcal{H}$ *is called a Bessel sequence if there exists a constant* $B > 0$ *such that*

$$\sum_{k=1}^{\infty} |\langle f, f_k\rangle|^2 \leq B\|f\|^2, \qquad \forall f \in \mathcal{H}.$$

Theorem 4.2.1. *The sequence* $\{f_k\}$ *is a Bessel sequence of Bessel bound* B *if and only if the associated synthesis operator* T *defines a bounded operator from* $\ell^2(\mathbb{N})$ *into* $\mathcal{H}$ *and* $\|T\| \leq \sqrt{B}$.

Corollary 4.2.1. *If* $\{f_k\}$ *is a Bessel sequence in* $\mathcal{H}$, *then* $\sum c_k f_k$ *converges unconditionally for all* $\{c_k\} \in \ell^2(\mathbb{N})$, *meaning that for any permutation* σ *of* $\mathbb{N}$, $\sum c_k f_k = \sum c_{\sigma(k)} f_{\sigma(k)}$.

As we will see in the sequel, all orthonormal bases, Riesz bases and frames are Bessel sequences and therefore unconditional bases of $\mathcal{H}$. We will only work with these unconditional families in what follows, so that we will write (f_k) in place of $\{f_k\}$ and (c_k) in place of $\{c_k\}$ to stress the fact that the order of summation is of no importance.

4.2.2 Bases and orthonormal bases.

We start by a definition.

Definition 4.2.2. *A sequence* (e_k) *is a (Schauder) basis for* $\mathcal{H}$ *if for each* $f \in \mathcal{H}$, *there exist unique scalar coefficients* $(c_k(f))$ *such that*

$$f = \sum c_k(f) e_k. \tag{4.1}$$

Orthonormal bases can be characterized in a wide range of ways, as described by the following result.

Theorem 4.2.2. *For an orthonormal system (e_k), the following are equivalent:*
1) (e_k) is an orthonormal basis,
2) $f = \sum \langle f, e_k \rangle e_k$ for all $f \in \mathcal{H}$,
3) $\langle f, g \rangle = \sum \langle f, e_k \rangle \langle g, e_k \rangle$ for all $f, g \in \mathcal{H}$,
4) $\sum |\langle f, e_k \rangle|^2 = \|f\|^2$ for all $f \in \mathcal{H}$,
5) The closure of Span(e_k) in $\mathcal{H}$ equals $\mathcal{H}$ itself,
6) If $\langle f, e_k \rangle = 0$ for all $k \in \mathbb{N}$, then $f = 0$.

Notice that Item 4 ensures that an orthonormal basis is a Bessel sequence and thus an unconditional basis.

Theorem 4.2.3. *Every separable Hilbert space $\mathcal{H}$ admits an orthonormal basis*

Theorem 4.2.4. *Every separable infinite-dimensional Hilbert space is isometrically isomorphic to $\ell^2(\mathbb{N})$.*

As described below, unitary operators on $\mathcal{H}$ allow to recover all orthonormal bases on $\mathcal{H}$. Let us first recall the definition of a unitary operator.

Theorem 4.2.5. *Let $\mathcal{H}$ be a Hilbert space and $U : \mathcal{H} \mapsto \mathcal{H}$ a bounded linear operator. We have the following equivalences,*
1) U is unitary,
2) $U^*U = UU^* = Id$,
3) U preserves the inner product and is onto,
4) U preserves the inner product and its range is dense in $\mathcal{H}$.

Then we have the following result.

Theorem 4.2.6. *Let (e_k) be an orthonormal basis for $\mathcal{H}$. Then the orthonormal basis of $\mathcal{H}$ are exactly the (Ue_k), where $U : \mathcal{H} \mapsto \mathcal{H}$ is a unitary operator.*

4.2.3 Riesz bases. Let us now turn to Riesz bases, which are still unconditional bases of $\mathcal{H}$ and offer a bit more flexibility than orthonormal bases. They appear by weakening the condition on the operator U above.

Definition 4.2.3. *A Riesz basis for $\mathcal{H}$ is a family of the form (Ue_k), where (e_k) is an orthonormal basis for $\mathcal{H}$ and $U : \mathcal{H} \mapsto \mathcal{H}$ is a bounded bijective operator.*

Theorem 4.2.7. *If (f_k) is a Riesz basis for $\mathcal{H}$, there exists a unique sequence (g_k) in $\mathcal{H}$ such that*

$$f = \sum \langle f, g_k \rangle f_k, \qquad \forall f \in \mathcal{H}. \tag{4.2}$$

The sequence (g_k) is also a Riesz basis called the dual Riesz basis of (f_k). Furthermore, a Riesz basis is also a Bessel sequence, so that eq. (4.2) converges unconditionally.

Corollary 4.2.2. *For a pair of dual Riesz bases (f_k) and (g_k), we have*
1) (f_k) and (g_k) are bi-orthogonal,
2) For all $f \in \mathcal{H}$,

$$f = \sum \langle f, g_k \rangle f_k = \sum \langle f, f_k \rangle g_k.$$

As detailed below, Riesz bases can be characterized by conditions imposed on the associated synthesis operator. This characterization will prove useful in forthcoming developments relative to frames.

Theorem 4.2.8. *For a sequence (f_k) in $\mathcal{H}$, the following conditions are equivalent:*
1) (f_k) is a Riesz basis for $\mathcal{H}$,
2) (f_k) is complete in $\mathcal{H}$ and there exists constants $A, B > 0$ such that, for every finite scalar sequence (c_k), one has

$$A \sum |c_k|^2 \leq \| \sum c_k f_k \|^2 \leq B \sum |c_k|^2. \tag{4.3}$$

Furthermore, if $A = B = 1$ in item 2, then (f_k) is an orthonormal basis of $\mathcal{H}$.

4.2.4 Frames in Hilbert spaces. As will be detailed below a frame (f_k) in $\mathcal{H}$ is a sequence such that every $f \in \mathcal{H}$ admits an expansion of the form described in eq. (4.1), except that the coefficient functionals $(c_k(f))$ are not unique anymore. Let us first give a formal definition of frames.

Definition 4.2.4. *A sequence (f_k) of elements in $\mathcal{H}$ is a frame for $\mathcal{H}$ if there exist constants $A, B > 0$ such that*

$$A\|f\|^2 \leq \sum |\langle f, f_k \rangle|^2 \leq B\|f\|^2, \qquad \forall f \in \mathcal{H}. \tag{4.4}$$

In the case where $A = B$, (f_k) is said to be a tight frame. Obviously, the rhs of eq. (4.4) guarantees that a frame is also a Bessel sequence of $\mathcal{H}$.

It is noteworthy that the above definition of frames is similar to the characterization of Riesz bases given in eq. (4.3). However, and as detailed in Theorem 4.2.10 below, eq. (4.4) is weaker than eq. (4.3), which explains why frames offer more flexibility than Riesz bases.

Lemma 4.2.2. *Let (f_k) be a frame with frame operator S and (optimal) frame bounds A, B. Then, the following holds,*
1) S is bounded, invertible, self-adjoint and positive.
2) $(S^{-1} f_k)$ is a frame with frame operator S^{-1} and (optimal) frame bounds B^{-1}, A^{-1}.

Furthermore, we have the following result,

Theorem 4.2.9. *Let (f_k) be a frame with frame operator S. Then $(S^{-1} f_k)$ is a dual frame of (f_k) in the sense that*

$$f = \sum \langle f, S^{-1} f_k \rangle f_k, \qquad \forall f \in \mathcal{H},$$
$$f = \sum \langle f, f_k \rangle S^{-1} f_k, \qquad \forall f \in \mathcal{H}.$$

and both series converge unconditionally.

Proof. The fact that S is invertible follows from eq. (4.4). Now, simply notice that

$$f = S S^{-1} f = \sum \langle S^{-1} f, f_k \rangle f_k,$$

and repeat the same argument with $S^{-1} S$. □

Among frames, tight frames play a very particular role. They are the frames for which frame bounds A, B as equal, so that eq. (4.4) transforms into a sequence of equalities. As detailed below, tight frames are interesting in the sense that they are equal to their canonical dual frame, modulo a renormalization constant, which has the merit of making computations as simple as with orthonormal bases. As described in Chapter 6, it is a crucial feature of needlet frames that they are a tight frame of the space of square integrable functions on the sphere.

Corollary 4.2.3. *If (f_k) is a tight frame with frame bound A, then the canonical dual frame is (f_k/A) and thus*

$$f = \frac{1}{A}\sum \langle f, f_k\rangle f_k, \qquad \forall f \in \mathcal{H}.$$

Thus a tight frame can be used at no additional computational cost compared with an orthonormal basis.

Let us now come back to the comparison of frames and Riesz bases.

Theorem 4.2.10. *A Riesz basis (f_k) for $\mathcal{H}$ is also a frame for $\mathcal{H}$. The dual Riesz basis equals the canonical dual frame $(S^{-1}f_k)$. Conversely, a frame is a Riesz basis if and only if the synthesis operator T is injective.*

Proof. The first part is immediate. For the second part, notice that T is bounded and surjective by construction, since (f_k) is a frame. Let us denote by $\Phi : \mathcal{H} \mapsto \ell^2(\mathbb{N})$ the isometric isomorphism defined by $\Phi e_k = \delta_k$, where δ_k is the sequence of coordinates in $\ell^2(\mathbb{N})$ with zeros everywhere, except at coordinate k, where it is worth 1. If T is also injective, then it is bijective, so that $f_k = T\delta_k = T\Phi e_k$ is the image of an orthonormal basis of $\mathcal{H}$ by a bounded bijective operator and hence a Riesz basis. □

A frame that is not a Riesz basis is said to be **over-complete** or called a **redundant frame**. Interestingly, frames can be seen to be images of orthonormal bases by an operator U, which satisfies weaker conditions than for Riesz bases (see Definition 4.2.3).

Theorem 4.2.11. *Let (e_k) be an orthonormal basis for $\mathcal{H}$. The frames for $\mathcal{H}$ are exactly the families (Ue_k), where $U : \mathcal{H} \mapsto \mathcal{H}$ is a bounded and surjective operator.*

An other interesting feature of over-complete frames is that they admit many representations in term of the frame elements (f_k), as shown by the following result.

Theorem 4.2.12. *Assume that (f_k) is an over-complete frame. Then there exist frames $(g_k) \neq (S^{-1}f_k)$ such that*

$$f = \sum \langle f, g_k\rangle f_k, \qquad \forall f \in \mathcal{H}.$$

This can eventually contribute to simplify computations when the inversion of the frame operator is too complicated and there exists a simpler alternative dual frame. However, it is noteworthy that the frame coefficients computed with the canonical dual frame have smallest $\ell^2(\mathbb{N})$-norm.

Lemma 4.2.3. *Let (f_k) be a frame for $\mathcal{H}$ and $f \in \mathcal{H}$. If f has a representation $f = \sum c_k f_k$ for some coefficients (c_k), then*

$$\|(c_k)\|^2 = \|(\langle f, S^{-1}f_k\rangle)\|^2 + \|(c_k - \langle f, S^{-1}f_k\rangle)\|^2.$$

In other words, the sequence $(\langle f, S^{-1}f_k\rangle)$ has minimal $\ell^2(\mathbb{N})$-norm among all sequences representing f.

4.3 Frames and signal processing. This is an example borrowed from [97, §5.9] and [91, p.135] which helps to understand how frames can be helpful in a noise reduction context.

4.3.1 Preliminary results. Let us start with two technical results.

Proposition 4.3.1. *Let T stand for a bounded operator from $\mathcal{H}$ into $\ell^2(\mathbb{N})$ and T^* for its adjoint operator. As is well-known, one has got*

$$\mathcal{N}(T^*) \oplus^\perp \mathcal{R}(T) = \mathcal{H}, \qquad \mathcal{N}(T) \oplus^\perp \mathcal{R}(T^*) = \ell^2(\mathbb{N}).$$

So that
1) T surjective $\Leftrightarrow$ T^* injective,
2) T^* surjective $\Leftrightarrow$ T injective.

Proof. Let $f \in \mathcal{N}(T^*)$ and $x \in \ell^2(\mathbb{N})$, then $\langle f, Tx\rangle = \langle T^* f, x\rangle = 0$. So that $\mathcal{N}(T^*) \subset \mathcal{R}(T)^\perp$. Furthermore, if $f \in \mathcal{R}(T)^\perp$, then for all $x \in \ell^2(\mathbb{N})$, one obtains $\langle x, T^* f\rangle = \langle Tx, f\rangle = 0$ so that $T^* f = 0$, that is $f \in \mathcal{N}(T^*)$. The symmetric results for T follow the same lines. This concludes the proof. □

Let us recall that for an operator U, $U^\dagger$ stands for its pseudo-inverse. The reader is referred to [97, §2.5] for an exact definition.

Lemma 4.3.1. *The orthogonal projector from $\ell^2(\mathbb{N})$ onto $\mathcal{R}(T^*)$ writes $P = T^*(T^*)^\dagger$. And for any $x \in \ell^2(\mathbb{N})$, $(T^*)^\dagger x = (TT^*)^{-1}Tx = S^{-1}Tx$.*

Proof. Indeed, any $z \in \ell^2(\mathbb{N})$ writes $z = x + y$ where $x \in \mathcal{R}(T^*)$ and $y \in \mathcal{R}(T^*)^\perp$. Obviously, $Px = x$ and $Py = 0$, so that $Pz = Px + Py = Px = x$.
Since S is invertible, this is equivalent to proving $S(T^*)^\dagger x = Tx$. However, if $x \in \mathcal{R}(T^*)$, this is obvious. On the other hand, if $x \in \mathcal{R}(T^*)^\perp$, then $x \in \mathcal{N}(T)$ so that $Tx = 0$. This concludes the proof. □

4.3.2 Application to noise reduction. As detailed in Theorem 4.2.10 above, a frame is redundant if and only if the associated synthesis operator T is not injective. It follows therefore from Proposition 4.3.1, that a frame is redundant if and only if the associated analysis operator T^* is not surjective. Suppose now that we are forwarded the frame coefficients θ_k of $f \in \mathcal{H}$ along a noisy transmission line. So that the θ_ks actually stand for the original frame coefficients $\langle f, S^{-1}f_k\rangle$ contaminated with some random noise ξ_k. Let us denote by P the orthogonal projector onto $\mathcal{R}(T^*)$. As we know the frame (f_k) that has been used to code f, we also know $\mathcal{R}(T^*)$ and thus P. We can therefore project the noisy coefficients (θ_k) onto $\mathcal{R}(T^*)$. So that

$$P[(\theta_k)_{k\geq 0}] = (\langle f, S^{-1}f_k\rangle) + P[(\xi_k)_{k\geq 0}],$$

where $\|P[(\xi_k)_{k\geq 0}]\| \leq \|(\xi_k)\|$ since P is an orthogonal projection. Obviously, the more redundant the frame (f_k), the larger $\mathcal{R}(T^*)^\perp$ and hence the larger the component of the noise (ξ_k) that is removed by P. To be more specific, we know from Lemma 4.3.1 that $P = T^*S^{-1}T$. Therefore

$$\begin{aligned} P[(\xi_k)_{k\geq 0}] &= T^*S^{-1}\sum \xi_j f_j \\ &= T^*\sum \xi_j S^{-1} f_j \\ &= (\langle \sum \xi_j S^{-1} f_j, f_k\rangle)_{k\geq 0}. \end{aligned}$$

In particular, if (ξ_k) is a zero-mean normal noise with variance $\mathbb{E}\xi_k^2 = \sigma^2$, then

$$\begin{aligned}\mathbb{E}[P[(\xi_t)_{t\geq 0}]]_k^2 &= \mathbb{E}\langle \sum \xi_j S^{-1} f_j, f_k\rangle^2 \\ &= \mathbb{E}\sum_{p,q} \xi_p \xi_q \langle S^{-1} f_p, f_k\rangle \langle S^{-1} f_q, f_k\rangle \\ &= \sigma^2 \sum_p \langle S^{-1} f_p, f_k\rangle^2 \leq \frac{\sigma^2}{A}\|f_k\|^2.\end{aligned}$$

So that the projection operation shrinks the noise when $A > \|f_k\|^2$.

5

Classification via local multi-resolution projections

Abstract. We focus on the supervised binary classification problem, which consists in guessing the label Y associated to a co-variate $X \in \mathbb{R}^d$, given a set of n independent and identically distributed co-variates and associated labels (X_i, Y_i). We assume that the law of the random vector (X, Y) is unknown and the marginal law of X admits a density supported on a set $\mathcal{A}$. In the particular case of plug-in classifiers, solving the classification problem boils down to the estimation of the regression function $\eta(X) = \mathbb{E}[Y|X]$. Assuming first $\mathcal{A}$ to be known, we show how it is possible to construct an estimator of η by localized projections onto a multi-resolution analysis (MRA). In a second step, we show how this estimation procedure generalizes to the case where $\mathcal{A}$ is unknown. Interestingly, this novel estimation procedure presents similar theoretical performances as the celebrated local-polynomial estimator (LPE). In addition, it benefits from the lattice structure of the underlying MRA and thus outperforms the LPE from a computational standpoint, which turns out to be a crucial feature in many practical applications. Finally, we prove that the associated plug-in classifier can reach super-fast rates under a margin assumption. ■

Key-Words: Nonparametric regression; Random design; Multi-resolution analysis; Supervised binary classification; Margin assumption.

Contents

5.1 Introduction.

5.1.1 Setting. The supervised binary classification problem is directly related to a wide range of applications such as spam detection or assisted medical diagnosis (see [98, chap. 1] for more details). It can be described as follows.

The supervised binary classification problem. Let Ω stand for a subset of $\mathbb{R}^d$ and write $\mathcal{Y} = \{0, 1\}$. Assume we observe n co-variates $X_i \in \Omega$ and associated labels $Y_i \in \mathcal{Y}$ such that the elements of $\mathcal{D}_n = \{(X_i, Y_i), i = 1, \dots, n\}$ are n independent realizations of the random vector $(X, Y) \in \Omega \times \mathcal{Y}$ of unknown law $\mathbb{P}_{X,Y}$. Given $\mathcal{D}_n$ and a new co-variate X_{n+1}, we want to predict the associated label Y_{n+1} so as to minimize the probability of making a mistake.

In other words, we want to build a **classifier** $h_n : \Omega \mapsto \mathcal{Y}$ upon the data $\mathcal{D}_n$, which minimizes $\mathbb{P}(h_n(X) \neq Y | \mathcal{D}_n)$. It is well known that the Bayes classifier $h^*(\tau) := \mathbb{1}_{\{\eta(\tau) \geq 1/2\}}$, where $\eta(\tau) := \mathbb{E}[Y|X = \tau] = \mathbb{P}(Y = 1|X = \tau)$ (unknown in practice), is optimal among all classifiers since, for any other classifier h_n, we have $\ell(h_n, h^*) := \mathbb{P}(h_n(X) \neq Y|\mathcal{D}_n) - \mathbb{P}(h^*(X) \neq Y) \geq 0$ (see [1]). As a consequence, we measure the classification risk $\mathscr{T}(h_n)$ associated to a classifier h_n as its average relative performance over all data sets $\mathcal{D}_n$, $\mathscr{T}(h_n) = \mathbb{E}^{\otimes n}\ell(h_n, h^*)$. As described in [1, Chap. 7], there is no classifier h_n such that $\mathscr{T}(h_n)$ goes to zero with n at a specified rate for all distributions $\mathbb{P}_{X,Y}$. We therefore make the assumption that $\mathbb{P}_{X,Y}$ belongs to a class of distributions $\mathcal{P}$ (as large as possible) and aim at constructing a classifier h_n such that

$$\inf_{\theta_n} \sup_{\mathbb{P}_{X,Y} \in \mathcal{P}} \mathscr{T}(\theta_n) \lesssim \sup_{\mathbb{P}_{X,Y} \in \mathcal{P}} \mathscr{T}(h_n) \lesssim (\log n)^{\delta} \inf_{\theta_n} \sup_{\mathbb{P}_{X,Y} \in \mathcal{P}} \mathscr{T}(\theta_n), \qquad n \geq 1, \tag{5.1}$$

where the infinimum is taken over all measurable maps θ_n from Ω into $\mathcal{Y}$ and $\lesssim$ means lesser or equal up to a multiplicative constant factor independent of n. Any classifier h_n verifying eq. (5.1) will be said to be **(nearly) minimax optimal** when $\delta = 0$ ($\delta > 0$). $\mathcal{P}$ will stand for the set of all distributions such that the marginal law $\mathbb{P}_X$ of X admits a density μ on Ω and η belongs to a given smoothness class. Throughout the paper, we will denote by μ the density of $\mathbb{P}_X$.

Many classifiers have been suggested in the literature, such as k-nearest neighbors, neural networks, support vector machine (SVM) or decision trees (see [1, 98]). In this paper, we will exclusively focus on **plug-in classifiers** $h_n(\tau) := \mathbb{1}_{\{\eta_n(\tau) \geq 1/2\}}$, where η_n stands for an estimator of η. With such classifiers, it is shown in [99] that,

$$\mathscr{T}(h_n) \leq 2\mathbb{E}^{\otimes n}\mathbb{E}|\eta_n(X) - \eta(X)|, \tag{5.2}$$

where the term on the rhs is known as the regression loss (of the estimator η_n of η) in $\mathbb{L}_1(\Omega, \mu)$-norm. Eq. (5.2) shows in particular that rates of convergence on the classification risk of a plug-in classifier h_n can be readily derived from rates of convergence on the regression loss of η_n. This prompts us to focus on the regression problem, which can be stated in full generality as follows.

The regression on a random design problem. Let $\Omega, \mathcal{Y}$ stand for subsets of $\mathbb{R}^d$ and $\mathbb{R}$, respectively. Assume we dispose of n co-variates $X_i \in \Omega$ and associated observations $Y_i \in \mathcal{Y}$ such that the

elements of $\mathcal{D}_n = \{(X_i, Y_i), i = 1, \dots, n\}$ are n independent realizations of the random vector $(X, Y) \in \Omega \times \mathcal{Y}$ of unknown law $\mathbb{P}_{X,Y}$. We define $\xi := Y - \eta(X)$, where $\eta(\tau) := \mathbb{E}[Y|X = \tau]$, so that by construction $\mathbb{E}[\xi|X] = 0$. Given $\mathcal{D}_n$ and under the assumption that $\mathbb{P}_{X,Y}$ belongs to a large class of distributions $\mathcal{P}$, we want to come up with an estimator η_n of η, which is as accurate as possible for the wide range of losses $\mathscr{S}_p(\eta_n) = \mathbb{E}^{\otimes n}\mathbb{E}|\eta_n(X) - \eta(X)|^p$, $p \geq 1$.

As described previously, in the particular case where $\mathcal{Y} = \{0, 1\}$, we fall back on the regression problem associated to the classification problem with plug-in classifiers. In this case, ξ is bounded such that $|\xi| \leq 1$. Notice however that the regression on a random design problem stated above permits for $\mathcal{Y}$ to be any subset of $\mathbb{R}$ (including $\mathbb{R}$ itself). To be more precise, and by analogy with eq. (5.1), our aim is to build an estimator η_n of η such that, for all $p \geq 1$,

$$\inf_{\theta_n} \sup_{\mathbb{P}_{X,Y} \in \mathcal{P}} \mathscr{S}_p(\theta_n) \lesssim \sup_{\mathbb{P}_{X,Y} \in \mathcal{P}} \mathscr{S}_p(\eta_n) \lesssim (\log n)^{\delta} \inf_{\theta_n} \sup_{\mathbb{P}_{X,Y} \in \mathcal{P}} \mathscr{S}_p(\theta_n), \qquad n \geq 1, \tag{5.3}$$

where the infinimum is taken over all measurable maps θ_n from Ω into $\mathcal{Y}$. And η_n will be said to be (nearly) minimax optimal when $\delta = 0$ ($\delta > 0$).

5.1.2 Motivations. Many estimators η_n of η have been suggested in the literature to solve the regression on a random design problem. Among them, the celebrated local polynomial estimator (LPE) has been praised for its flexibility and strong theoretical performances (see [2, 3]). As is well known, the LPE is minimax optimal in any dimension $d \in \mathbb{N}$ and for any $\mathscr{S}_p$-loss, $p \in (0, \infty]$, over the set of laws $\mathcal{P}$ such that (i) μ is bounded from above and below on its support $\mathcal{A} := \text{Supp}\mu = \{\tau : \mu(\tau) > 0\}$, (ii) η belongs to a Hölder ball $\mathscr{C}^s(\Omega, M)$ of radius M and (iii) ξ has sub-Gaussian tails. As a drawback, the LPE is computationally expansive since it requires to perform a new regression at every single point $x \in \mathcal{A}$ where we want to estimate η.
Computational efficiency is however of primary importance in many practical applications. In this paper, we show that it is possible to construct a novel estimator η_n of η by localized projections onto multi-resolution analysis (MRA) of $\mathbb{L}_2(\mathbb{R}^d, \lambda)$ (where λ stands for the Lebesgue measure on Ω), which presents similar theoretical performances and is computationally more efficient than the LPE.

5.1.3 The hypotheses. In this section, we summarize the assumptions on μ, $\mathcal{A}$, η and ξ that will be used throughout the paper.

Assumption on μ. Let us denote by $\mu_{\min}, \mu_{\max}$ two real numbers such that $0 < \mu_{\min} \leq \mu_{\max} < \infty$. As is standard in the regression on a random design setting, we assume that the density μ is bounded above and below on its support $\mathcal{A}$.
(**D1**) $\mu_{\min} \leq \mu(\tau) \leq \mu_{\max}$ for all $\tau \in \mathcal{A}$.
This guarantees that we have enough information at each point $x \in \mathcal{A}$ in order to estimate η with best accuracy. For a study with weaker assumptions on μ, the reader is referred to [100, 26], for example, and the references therein.

Assumption on $\mathcal{A}$. We first assume that,
(**S1**) $\mathcal{A} = \Omega = [0, 1]^d$.

Therefore $\mathcal{A}$ is known under (**S1**). We will deal with the case where $\mathcal{A}$ is unknown in Section 5.9.

Assumption on η. Fix $r \in \mathbb{N}$. In the sequel, we will assume that,

(**$\mathbf{H}^{\mathbf{r}}_{\mathbf{s}}$**) The regression function η belongs to the generalized Lipschitz ball $\mathscr{L}^s(\Omega, M)$ of radius M, for some $s \in (0, r)$.

Unless otherwise sated, s is **unknown** but belongs to the interval $(0, r)$, where r is **known**. For a detailed review of generalized Lipschitz classes, the reader is referred to Section 5.13.1 below.

Assumptions on the noise ξ. We will consider the two following assumptions,

(**N1**) Conditionally on X, the noise ξ is uniformly bounded, meaning that there exists an absolute constant $K > 0$ such that $|\xi| \leq K$.

(**N2**) The noise ξ is independent of X and normally distributed with mean zero and variance σ^2, which we will denote by $\xi \sim \Phi(0, \sigma^2)$.

Assumption (**N1**) is adapted to the supervised binary classification setting, where $\mathcal{Y} = \{0, 1\}$, while (**N2**) is more common in the regression on a random design setting, where $\mathcal{Y} = \mathbb{R}$.

Combination of assumptions. In the sequel, we will conveniently refer by (**CS1**) to the set of assumptions (**D1**), (**S1**), (**N1**) or (**N2**). As detailed below in Section 5.3, configuration (**CS1**) is comparable to what is customary in the regression on a random design setting.

5.2 Our results. Assuming at first $\mathcal{A}$ to be known, we introduce a novel nonparametric estimator $\eta^{@}$ of η built upon local regressions against a multi-resolution analysis (MRA) of $\mathbb{L}_2(\mathbb{R}^d, \lambda)$ and show that, under (**CS1**), it is adaptive nearly minimax optimal over a wide generalized Lipschitz scale and across the wide range of losses $\mathbb{L}_p(\Omega, \mu), p \in [1, \infty)$. We subsequently show that these results generalize to the case where $\mathcal{A}$ is unknown but belongs to a large class of (eventually disconnected) subsets of $\mathbb{R}^d$, provided we modify the estimator $\eta^{@}$ accordingly. We denote by $\eta^{\maltese}$ this latter estimator and prove that $\eta^{\maltese}$ can be used to build an adaptive nearly minimax optimal plug-in classifier, which can reach super-fast rates under a margin assumption. The above results essentially hinge on an exponential upper-bound on the probability of deviation of $\eta^{@}$ from η at a point, as detailed in Theorem 5.7.1. These results either improve on the current literature or are interesting in their own right for the following reasons.

1) They show that it is possible to use MRAs to construct an adaptive nearly minimax optimal estimator $\eta^{@}$ of η under the sole set of assumptions (**CS1**). More precisely, our results (i) hold in any dimension d; (ii) over the wide range of $\mathbb{L}_p(\Omega, \mu)$-losses, $p \in [1, \infty)$; (iii) and a large Lipschitz scale; (iv) and do not require any assumption on μ beyond (**D1**). It is noteworthy that, in contrary to most alternative MRA-based estimation methods, no smoothness assumption on μ is needed.
2) From a computational perspective, $\eta^{@}$ outperforms other estimators of η under (**D1**) since it takes full advantage of the lattice structure of the underlying MRA. In particular it requires at most as many regressions as there are data points to be computed everywhere on Ω, while alternative kernel estimators must be recomputed at each single point of Ω. We illustrate this latter feature through simulation.
3) Furthermore, and in contrary to alternative MRA-based estimators, the local nature of $\eta^{@}$ allows to relax the assumption that $\mathcal{A}$ is known. This latter configuration allows for μ to cancel on Ω as long as it remains bounded on its support $\mathcal{A}$, which is particularly appropriate

to the supervised binary classification problem under a margin assumption.

4) In the regression on a random design setting, $\eta^{@}$ bridges in fact the gap between usual linear wavelet estimators and alternative kernel estimators, such as the LPE. On the one hand, $\eta^{@}$ inherits its computational efficiency from the lattice structure of the underlying MRA. On the other hand, it features similar theoretical performances as the LPE in the random design setting. In particular, it remains a (locally) linear estimator of the data (modulo a spectral thresholding of the local regression matrix), and cannot discriminate finer smoothness than the one described by (generalized) Lipschitz spaces.

Here is the paper layout. We start by a literature review in Section 5.3. We give a hand-waving introduction to the main ideas that underpin the local multi-resolution estimation procedure in Section 5.4. We define notations that will be used throughout the paper and introduce MRAs in Section 5.5. Our actual estimation procedure is described in Section 5.6 and the results are detailed in Section 5.7. We show how these results can be fine-tuned under additional assumptions in Section 5.8. Assumption (**S1**) is relaxed and the properties of $\eta^{\maltese}$ are detailed in Section 5.9. We show how these latter results spread to the classification setting in Section 5.10. Results of a simulation study with $\eta^{@}$ under (**CS1**) are given in Section 5.11. Proofs of the regression results can be found in Section 5.12. The proofs of the classification results are simple modifications of the proofs given in [35] and thus detailed in the Appendix in Section 5.13. In addition, the Appendix contains a detailed review of generalized Lipschitz spaces and MRAs in Section 5.13.1 and Section 5.13.2, respectively.

5.3 Literature review. Both the regression on a random design problem and the classification problem have a long-standing history in nonparametric statistics. We will therefore limit ourselves to a brief account of the corresponding literature that is relevant to the present paper.

5.3.1 Classification with plug-in classifiers. Let us start with a review of some of the classification literature dedicated to plug-in classifiers. The seminal work [32] showed that plug-in rules are asymptotically optimal. It has been subsequently pointed out in [33] that the classification problem is in fact only sensitive to the behavior of $\mathbb{P}_{X,Y}$ near the boundary line $\mathscr{M} := \{\tau \in \Omega : \eta(\tau) = 1/2\}$. So that assumptions on the behavior of $\mathbb{P}_{X,Y}$ away from this boundary are in fact unnecessary. Subsequent works such as [34] have shown that convex combinations of plug-in classifiers can reach fast rates (meaning faster than $n^{-1/2}$, and thus faster than nonparametric estimation rates). More recently, it has been shown in [35] that plug-in classifiers can reach super fast rates (that is faster than n^{-1}) under suitable conditions. All these results are derived under some sort of smoothness assumption on the regression function η (see [36]) and a margin assumption (**MA**) (see Section 5.10 for details). This latter assumption clarifies the behavior of $\mathbb{P}_{X,Y}$ in a neighborhood of $\mathscr{M}$ and kicks in naturally through the computation

$$\mathscr{T}(h_n) \leq \delta \mathbb{P}(0 < |2\eta(X) - 1| \leq \delta) + \mathbb{E}|\eta_n(X) - \eta(X)| \mathbb{1}_{\{|\eta_n(X) - \eta(X)| > \delta\}},$$

where δ is chosen such that it balances the two terms on the rhs. Finally, [35] exhibited optimal convergence rates under smoothness and margin assumptions and showed that they are attained with plug-in classifiers. Let us now turn to the regression on a random design problem.

5.3.2 Regression on a random design with wavelets. First results on multi-resolution analysis (MRA) and wavelet bases (see [76, 77]) emerged in the nonparametric statistics literature in the early 1990's (see [78, 79, 80, 81, 75]). It has been proved that, under (**CS1**) and in the particular case where μ is the uniform distribution on Ω, thresholded wavelet estimators of η are nearly minimax optimal over a wide Besov scale and range of $\mathbb{L}_p(\Omega,\mu)$-losses (see [83]). In order to leverage on the power of MRAs and associated wavelet bases, several authors attempted to transpose these latter results to more general design densities μ. This, however, led to a considerable amount of difficulties.

The literature relative to the study of wavelet estimators on an **unknown** random design breaks down into two main streams. (i) The first one aims at constructing new wavelet bases adapted to the (empirical) measure of the design (see [4, 5, 6, 7]). (ii) The second one aims at coming up with new algorithms to estimate the coefficients of the expansion of η on traditional wavelet bases (see [8, 9, 10, 11, 12]). The present paper belongs to this second line of research.

As described in [9], the success of the LPE on a random design results from the fact that it is built as a "ratio", which cancels out most of the influence of the design. In a wavelet context, a first suggestion has therefore been to use the ratio estimator of η (see [14, 15], for example), well known from the statistics literature on orthogonal series decomposition (see [16, 17] and [1, Chap. 17] and the references therein). Roughly speaking, the ratio estimator is the wavelet equivalent of the Nadaraya-Watson estimator (see [18, 19]). It is elaborated on the simple observation that $\eta(x)=\eta(x)\mu(x)/\mu(x)$ for all $x\in\mathcal{A}$, where both $g(.)=\eta(.)\mu(.)$ and $\mu(.)$ are easily estimated via traditional wavelet methods. The ratio estimator relies thus unfortunately on the estimation of μ itself and must therefore assume as much smoothness on μ as on η.

To address that issue, an other approach has been introduced in [20, 21]. They work with $d=1$ and take Ω to be the unit interval $[0,1]$. Their approach relies on the wavelet estimation of $\eta\circ G^{-1}$, where G stands for the cumulative distribution of the design and G^{-1} for its generalized inverse. Results are therefore stated in term of regularity of $f\circ G^{-1}$. Unfortunately, this method does not readily generalize to the the multi-dimensional case, where G admits no inverse.

Finally, [22] obtains adaptive near-minimax optimal wavelet estimators over a wide Besov scale under (**CS1**) by means of model selection techniques. His results are hence valid for the $\mathbb{L}_2(\Omega,\mu)$-loss only.

Other relevant references that proceed with hybrid estimators (LPE and kernel estimator or LPE and wavelet estimator) are [25] and [101]. They both work under (**CS1**), with $d=1$ and assume that μ is at least continuous.

5.4 A primer on local multi-resolution estimation under (CS1). In order to fix the ideas, let us now give a hand-waving introduction to the local multi-resolution estimation method. Throughout the paper, we will work with r-MRAs of $\mathbb{L}_2(\mathbb{R}^d,\lambda)$, for some $r\in\mathbb{N}$, consisting of nested approximation spaces $\mathcal{V}_j\subset\mathcal{V}_{j+1}$ built upon compactly supported scaling functions (see Section 5.5.2 and [90, 91, 85, 94]). Under the assumption that η belongs to the generalized Lipschitz ball $\mathscr{L}^s(\Omega,M)$ of radius M, the essential supremum of the remainder of the orthogonal projection $\mathscr{P}_j\eta$ of η onto $\mathcal{V}_j$ decreases like 2^{-js} (see Section 5.13.1). The regression function η can therefore be legitimately approximated by $\mathscr{P}_j\eta$. As an element of $\mathcal{V}_j$, $\mathscr{P}_j\eta$ may be written as an infinite linear combination of scaling functions at level j. In particular, there exists a partition $\mathcal{F}_j$ of Ω into hypercubes of edge-length 2^{-j} such that, for all $\mathcal{H}\in\mathcal{F}_j$ and all $x\in\mathcal{H}$, we can write $\mathscr{P}_j\eta(x)=\sum_{k\in\mathcal{S}_j(\mathcal{H})}\alpha_{j,k}\varphi_{j,k}(x)$, where $\mathcal{S}_j(\mathcal{H})$ stands for a finite subset of

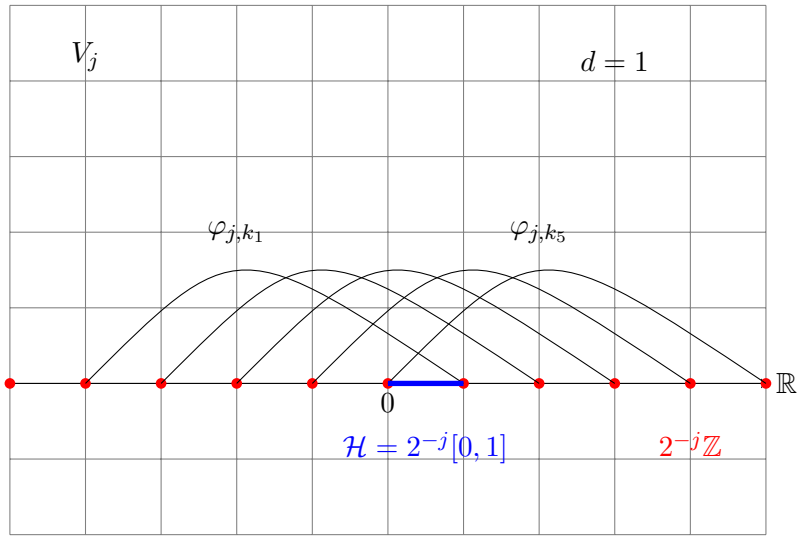

Figure 5.1: Description of the localization cells $\mathcal{H}$ and their relations to the Supp$\varphi_{j,k}$.

$\mathbb{Z}^d$ (see Figure 5.1). This leaves us in turn with the estimation of coefficients $(\alpha_{j,k})_{k\in\mathcal{S}_j(\mathcal{H})}$ for all $\mathcal{H} \in \mathcal{F}_j$, which is achieved by least-squares and provides us with the estimator $\eta_j^{@}$ of η on $\mathcal{H}$. It is noteworthy that the local estimator $\eta_j^{@}$ of η is exclusively built upon scaling functions and does not require the estimation of wavelet coefficients. In particular, it does not involve any sort of wavelet coefficient thresholding. To the best of the author knowledge, this is the first time that this local estimation procedure is proposed and studied from both a theoretical and computational perspective. In addition, we show that Lepski's method (see [84], for example) can be used to adaptively choose the resolution level j. Notice that Lepski's method has already been used in a MRA setting in [31]. In what follows, we detail the local multi-resolution estimation method and establish the near minimax optimality of $\eta^{@}$.

5.5 Notations.

5.5.1 Preliminary notations. In the sequel, we will denote by $\mathcal{B}_p(z,\rho)$ the closed ℓ_p-ball of $\mathbb{R}^d$ of center z and radius ρ. More generally, we adopt the following notations: for any subset $\mathcal{S}$ of a topological space Ω, Closure$(\mathcal{S})$ will stand for its closure, Inter$(\mathcal{S})$ for its interior, $\mathcal{S}^c$ for its complement in Ω and $\partial\mathcal{S} = \text{Closure}(\mathcal{S}) \cap \text{Inter}(\mathcal{S})^c$ for its boundary. Besides, for any two $\mathcal{S}_1, \mathcal{S}_2 \subset \mathbb{R}^d$, we will denote the relative complement of $\mathcal{S}_2$ in $\mathcal{S}_1$ by $\mathcal{S}_1 \backslash \mathcal{S}_2$ $(= \mathcal{S}_1 \cap \mathcal{S}_2^c)$ and their symmetric difference $\mathcal{S}_1 \backslash \mathcal{S}_2 \cup \mathcal{S}_2 \backslash \mathcal{S}_1$ by $\mathcal{S}_1 \Delta \mathcal{S}_2$. For any subset $\mathcal{S}$ of $\mathbb{R}^d$, $z \in \mathbb{R}^d$ and $\tau \in \mathbb{R}^+$, we will write $z + \mathcal{S}$ and $\tau\mathcal{S}$ to mean the sets $\{z + u : u \in \mathcal{S}\}$ and $\{\tau u : u \in \mathcal{S}\}$, respectively. Finally, given a set (of functions) $\mathcal{R}$, Span$\mathcal{R}$ will denote the set of finite linear combinations of elements of $\mathcal{R}$.

For any $p \in \mathbb{N}$, vectors v of $\mathbb{R}^p$ will be seen as elements of $\mathcal{M}_{p,1}$, that is matrix with p rows and one column. For any two $u, v \in \mathbb{R}^p$, $\langle u, v\rangle$ will denote their Euclidean scalar product. In addition, for any $p, q \in \mathbb{N}$ and $M \in \mathcal{M}_{p,q}$, M^t will stand for the transpose of M. For any two matrices M, P, $M \cdot P$ will denote their matrix product when it makes sense. $[M]_{k,\ell}$ and $[M]_{k,\bullet}$

will respectively stand for the element of M located at line k, column ℓ and the k^{th} row of M. Finally, $\|M\|_S$ will denote the spectral norm of M (see [102, §5.6.6]).
We denote by $\lfloor z \rfloor$ the integer part of $z \in \mathbb{R}$ defined as $\max\{a \in \mathbb{Z} : a \leq z\}$. More generally, given $z \in \mathbb{R}^d$, we write $\lfloor z \rfloor$ the integer part of z, meant in a coordinate-wise sense. In the same way, we denote by $\lceil z \rceil$ the smallest integer greater than z (in a coordinate-wise sense). We write rhs (resp. lhs) to mean *right-* (resp. *left-*) *hand-side* and sometimes write $:=$ to mean *equal by definition*. Throughout the paper, we will refer to constants independent of n as *absolute constants* and c, C will stand for absolute constants whose value may vary from line to line. For any two sequences a_n, b_n of n, we will write $a_n \lesssim b_n$ to mean $a_n \leq C b_n$ for some absolute constant C and $a_n \approx b_n$ to mean that there exist two constants c, C independent of n such that $c b_n \leq a_n \leq C b_n$.

5.5.2 The polynomial reproduction property. In what follows, we will exclusively consider MRAs built upon Daubechies' scaling functions $\varphi_{j,k}$ (see Section 5.13.2). Given a natural integer r, we will refer by r-MRA to a MRA whose nested approximation spaces $\mathcal{V}_j$ reproduce polynomials up to order $r-1$. Daubechies' scaling functions are appealing in the estimation framework since they are compactly supported and have minimal volume supports among scaling functions that give rise to r-MRAs. Recall that a r-MRA can explain Lipschitz smoothness s for any $s \in (0, r)$. Obviously, the usefulness of the 1-MRA, also known as the Haar MRA, is fairly limited when dealing with the estimation of smooth functions. However, the simple geometry of the Haar scaling function brings a great deal of simplification in the proofs, which will allow us to highlight the key points of our estimation procedure and hopefully clarify our arguments. This is the unique reason why we have treated the two cases $r = 1$ and $r \geq 2$ distinctly in the proofs. The reader is referred to the Appendix in Section 5.13.2 for a detailed review of MRAs of $\mathbb{R}^d$.

5.5.3 General notations. Consider the Daubechies' r-MRA of $\mathbb{L}_2(\mathbb{R}^d, \lambda)$ built upon Daubechies' scaling function φ, as described in Section 5.13.2. We will denote by $\mathrm{Supp}\varphi_{j,k} = \{\tau \in \mathbb{R}^d : \varphi_{j,k}(\tau) > 0\}$ the support of $\varphi_{j,k}$. Recall that $\mathrm{Supp}\varphi = [-(r-1), r]^d$. To alleviate notations, we will write φ_k in place of $\varphi_{0,k}$ and φ_j in place of $\varphi_{j,0}$. Notice that $\mathrm{Closure}(\mathrm{Supp}\varphi_{j,k})$ is in fact a closed hyper-cube of $\mathbb{R}^d$ whose corners lie on the lattice $2^{-j}\mathbb{Z}^d$ (see Section 5.13.2). Moreover, for any $x \in \mathcal{A}$, write

$$\mathcal{S}_j(x) = \{\nu \in \mathbb{Z}^d : x \in \mathrm{Supp}\varphi_{j,\nu}\}.$$

Furthermore, we write $\mathcal{F}_j := 2^{-j}((0,1)^d + \mathbb{Z}^d) \cap \Omega$. It defines a partition of Ω into 2^{jd} hypercubes of edge length 2^{-j}, modulo a λ-null set. For the sake of concision, we write $R = 2r - 1$ in the sequel. We have the following proposition, whose proof is straightforward and thus left to the reader.

Proposition 5.5.1. *$\mathcal{S}_j$ verifies the following properties,*

1. *$\mathcal{S}_j$ is constant on each element $\mathcal{H} \in \mathcal{F}_j$. We will denote by $\mathcal{S}_j(\mathcal{H})$ its value on $\mathcal{H}$.*
2. *Moreover, for any two $\mathcal{H}_1, \mathcal{H}_2 \in \mathcal{F}_j$, $\mathcal{H}_1 \neq \mathcal{H}_2$, $\mathcal{S}_j(\mathcal{H}_1)$ differs from $\mathcal{S}_j(\mathcal{H}_2)$ by at least one element.*
3. *Finally, for any $\mathcal{H} \in \mathcal{F}_j$, $\#\mathcal{S}_j(\mathcal{H}) = R^d$*

It is a direct consequence of Proposition 5.5.1 that in the case where $r = 1$, we have $\#\mathcal{S}_j(\mathcal{H}) = 1$ for all $\mathcal{H} \in \mathcal{F}_j$. We denote its single element by $\nu(\mathcal{H})$. It is in fact easy to show that $\nu(\mathcal{H}) = \lfloor 2^j x \rfloor$ for any $x \in \mathcal{H}$. For any $\mathcal{H} \in \mathcal{F}_j$, we write

$$\alpha_{\mathcal{H}} = (\alpha_{j,\nu})_{\nu \in \mathcal{S}_j(\mathcal{H})} \in \mathbb{R}^{R^d},$$
$$\varphi_{\mathcal{H}}(.) = (\varphi_{j,\nu}(.)\mathbb{1}_{\mathcal{H}}(.))_{\nu \in \mathcal{S}_j(\mathcal{H})} \in \mathbb{R}^{R^d}.$$

and denote by $Y_{\mathcal{H}} = (Y_i \mathbb{1}_{\mathcal{H}}(X_i))_{1 \le i \le n}$. Moreover, we write $\mathcal{I}_{\mathcal{H}} = \{i : X_i \in \mathcal{H}\}$ and $n_{\mathcal{H}} = \#\mathcal{I}_{\mathcal{H}}$.

5.6 Construction of the local estimator $\eta^{@}$. Assume we are under (**CS1**) and work with the Daubechies' r-MRA of $\mathbb{L}_2(\mathbb{R}^d, \lambda)$ (see Section 5.13.2). The estimation procedure is local, so that we start by selecting a point $x \in \mathcal{A}$ (see Section 5.13.3 for a technical remark). By construction, there exists $\mathcal{H} \in \mathcal{F}_j$ such that $x \in \mathcal{H}$. We want to estimate η at point x. As detailed in Section 5.13.2, an estimator of η can be reduced to an estimator of the orthogonal projection $\mathscr{P}_j\eta$ of η onto $\mathcal{V}_j$, modulo an error $\mathscr{R}_j\eta$, such that $|\mathscr{R}_j\eta| \le M 2^{-js}$ when η belongs to the generalized Lipschitz ball $\mathscr{L}^s(\Omega, M)$ of radius M. Now, we can write

$$\mathscr{P}_j\eta(x) = \sum_{k \in \mathbb{Z}^d} \alpha_{j,k}\varphi_{j,k}(x) = \sum_{k \in \mathcal{S}_j(\mathcal{H})} \alpha_{j,k}\varphi_{j,k}(x) = \langle \alpha_{\mathcal{H}}, \varphi_{\mathcal{H}}(x) \rangle.$$

This leaves us with exactly R^d coefficients $\alpha_{j,\nu}, \nu \in \mathcal{S}_j(\mathcal{H})$ to estimate, which are valid for any $x \in \mathcal{H}$. We evaluate these coefficients by least-squares. Denote by $B_{\mathcal{H}} \in \mathcal{M}_{n,R^d}$ the matrix whose rows are the vectors $\varphi_{\mathcal{H}}(X_i)^t$ for $1 \le i \le n$. Let us denote by $k_1, \dots, k_{R^d}$ the elements of $\mathcal{S}_j(\mathcal{H})$. Then we choose

$$\begin{aligned} \alpha^{\diamond}_{\mathcal{H}} &\in \arg\min_{a \in \mathbb{R}^{R^d}} \sum_{i=1}^{n} \left(Y_i - \sum_{t=1}^{R^d} a_t \varphi_{j,k_t}(X_i) \right)^2 \mathbb{1}_{\mathcal{H}}(X_i) \\ &= \arg\min_{a \in \mathbb{R}^{R^d}} \|Y_{\mathcal{H}} - B_{\mathcal{H}} \cdot a\|^2_{\ell_2(\mathbb{R}^n)}, \end{aligned} \tag{5.4}$$

where we set $\alpha^{\diamond}_{\mathcal{H}} = 0$ if the arg min above contains more than one element. Let us write $Q_{\mathcal{H}} = B^t_{\mathcal{H}} \cdot B_{\mathcal{H}}/n \in \mathcal{M}_{R^d,R^d}$. As is well known, when $Q_{\mathcal{H}}$ is invertible, the arg min on the rhs of eq. (5.4) admits one single element which writes as follows,

$$\alpha^{\diamond}_{\mathcal{H}} = Q^{-1}_{\mathcal{H}} \cdot \frac{1}{n} B^t_{\mathcal{H}} \cdot Y_{\mathcal{H}}. \tag{5.5}$$

Naturally, we will denote the corresponding estimator of $\mathscr{P}_j\eta$ at point x by $\eta^{\diamond}_{\mathcal{H}}(x) = \langle \alpha^{\diamond}_{\mathcal{H}}, \varphi_{\mathcal{H}}(x) \rangle$. We now introduce a thresholded version of $\eta^{\diamond}_{\mathcal{H}}$ based on the spectral thresholding of $Q_{\mathcal{H}}$. We denote by $\lambda_{\min}(Q_{\mathcal{H}})$ the smallest eigenvalue of $Q_{\mathcal{H}}$ in the case where $r \ge 2$, when $Q_{\mathcal{H}}$ is actually a matrix, and $Q_{\mathcal{H}}$ itself in the case where $r = 1$, when it is a real number. Furthermore, we define

$$\eta^{@}_{\mathcal{H}}(x) = \begin{cases} 0 & \text{if } \pi_n^{-1} > \lambda_{\min}(Q_{\mathcal{H}}) \\ \eta^{\diamond}_{\mathcal{H}}(x) & \text{otherwise} \end{cases}, \tag{5.6}$$

where π_n is a tuning parameter. In practice, and unless otherwise stated, we choose $\pi_n = \log n$. Moreover, we assume throughout the paper that n is large enough so that $\pi_n^{-1} \leq \min(\frac{g_{\min}}{2}, 1)$, where, for reasons that will clarified later, we have denoted,

$$g_{\min} := \mu_{\min} c_{\min}, \tag{5.7}$$

and $c_{\min}$ stands for the strictly positive constant defined in the proof of Proposition 5.12.4. Ultimately, the estimator $\eta_j^{@}$ of $\mathscr{P}_j\eta$ is defined as,

$$\eta_j^{@}(x) = \sum_{\mathcal{H}\in\mathcal{F}_j} \eta_{\mathcal{H}}^{@}(x)\mathbb{1}_{\mathcal{H}}(x), \qquad x \in \Omega. \tag{5.8}$$

5.7 The results. Let r be a natural integer, denote by $\mathcal{P}$ the set of all distributions on $\Omega \times \mathcal{Y}$ and write

$$\mathcal{P}(\mathbf{CS1}, \mathbf{H_s^r}) := \{\mathbb{P} \in \mathcal{P} : \ (\mathbf{CS1}) \text{ and } (\mathbf{H_s^r}) \text{ hold true}\}. \tag{5.9}$$

Furthermore, we define j_r, j_s, J and $t(n)$ such that,

$$2^{j_r} = \lfloor n^{\frac{1}{2r+d}} \rfloor, \qquad 2^{j_s} = \lfloor n^{\frac{1}{2s+d}} \rfloor,$$
$$2^{Jd} = \lfloor nt(n)^{-2} \rfloor, \qquad t(n)^2 = \kappa\pi_n^2 \log n,$$

where κ is a positive real number to be chosen later. In addition, we write $\mathcal{J}_n = \{j_r, j_r + 1, \ldots, J-1, J\}$. Notice that j_s strikes the balance between bias and variance in the sense that, for $\log n \geq (2s+d)\log 2$ and $s \in (0, r)$, one has got

$$n^{-\frac{1}{2}} 2^{j_s \frac{d}{2}} \leq 2^{-j_s s}, \tag{5.10a}$$
$$2^{-j_s s} \leq 2^{r+\frac{d}{2}} 2^{j_s \frac{d}{2}} n^{-\frac{1}{2}}, \tag{5.10b}$$
$$2^{-j_s s} \leq 2^r n^{-\frac{s}{2s+d}}. \tag{5.10c}$$

Throughout the sequel, we assume that n is large enough so that the latter inequalities hold true. Our first result gives an upper bound on the probability of deviation of $\eta_j^{@}$ form η at a point $x \in \mathcal{A}$.

Theorem 5.7.1. *Fix $r \in \mathbb{N}$ and assume we are under $(\mathbf{CS1})$ and $(\mathbf{H_s^r})$. Recall that $\eta_j^{@}$ is defined in eq. (5.8). Then, for all $j \in \mathcal{J}_n$, all $\delta > 2M2^{-j_s}\max(1, 3\pi_n R^d \mu_{\max})$ and all $x \in \mathcal{A}$, we have got*

$$\sup_{\mathbb{P}\in\mathcal{P}(\mathbf{CS1},\mathbf{H_s^r})} \mathbb{P}^{\otimes n}(|\eta(x) - \eta_j^{@}(x)| \geq \delta)$$
$$\leq 2R^{2d} \exp\left(-n2^{-jd} \frac{\pi_n^{-2}}{2\mu_{\max}R^{4d} + \frac{4}{3}R^{2d}\pi_n^{-1}}\right) \mathbb{1}_{\{\delta \leq M\}} + R^d \Lambda\left(\frac{\delta 2^{-j\frac{d}{2}}}{2\pi_n R^d}\right), \tag{5.11}$$

where Λ is defined as follows,

$$\Lambda(\delta) = \begin{cases} 2\exp\left(-\dfrac{n\delta^2}{18K^2\mu_{\max} + 4K2^{j\frac{d}{2}}\delta}\right), & \text{under } (\mathbf{N1}) \\ 1 \wedge \left\{\dfrac{2\sigma(\mu_{\max} + 2^{j\frac{d}{2}}\delta)^{\frac{1}{2}}}{\delta\sqrt{2\pi n}} \exp\left(-\dfrac{n\delta^2\sigma^{-2}}{\mu_{\max} + 2^{j\frac{d}{2}}\delta}\right)\right\} & \\ \quad +2\exp\left(-\dfrac{n\delta^2}{2\mu_{\max} + \frac{4}{3}2^{j\frac{d}{2}}\delta}\right), & \text{under } (\mathbf{N2}) \end{cases}$$

As a consequence of the above theorem, we can deduce the (near) minimax optimality of $\eta^{@}_{j_s}$ over generalized Lipschitz balls.

Corollary 5.7.1. *Fix $r \in \mathbb{N}$ and assume we are under* (**CS1**) *and* ($\mathbf{H}^{\mathbf{r}}_{\mathbf{s}}$). *Then, for any $p \in [1,\infty)$ and $j \in \mathcal{J}_n$, one has got*

$$\sup_{\mathbb{P}\in\mathcal{P}(\mathbf{CS1},\mathbf{H}^{\mathbf{r}}_{\mathbf{s}})} \mathbb{E}^{\otimes n}\|\eta - \eta^{@}_{j}\|^p_{\mathbb{L}_p(\Omega,\mu)} \leq C(p)\pi_n^p \max\left(2^{-js}, \frac{2^{j\frac{d}{2}}}{\sqrt{n}}\right)^p, \tag{5.12}$$

*where $\eta^{@}_j$ and $C(p)$ are defined in eq. (5.8) and Proposition 5.12.1 below, respectively. A fortiori, when s is **known**, we can choose $j = j_s$ and apply eq. (5.10a) and eq. (5.10c) above to obtain*

$$\sup_{\mathbb{P}\in\mathcal{P}(\mathbf{CS1},\mathbf{H}^{\mathbf{r}}_{\mathbf{s}})} \mathbb{E}^{\otimes n}\|\eta - \eta^{@}_{j_s}\|^p_{\mathbb{L}_p(\Omega,\mu)} \leq C(p)2^{rp}\pi_n^p n^{-\frac{sp}{2s+d}}.$$

This, together with the lower-bound of Theorem 5.7.3, proves that $\eta^{@}_{j_s}$ is (nearly) minimax optimal over the generalized Lipschitz ball $\mathscr{L}^s(\Omega, M)$ of radius M.

The next Theorem shows that the approximation level j can be determined from the data $\mathcal{D}_n$ so that we obtain adaptation over a wide generalized Lipschitz scale.

Theorem 5.7.2. *Fix $r \in \mathbb{N}$ and assume we are under* (**CS1**) *and* ($\mathbf{H}^{\mathbf{r}}_{\mathbf{s}}$). *We define*

$$g(j,k) := \left(\frac{2^{j\frac{d}{2}}}{\sqrt{n}}t(n) + \frac{2^{k\frac{d}{2}}}{\sqrt{n}}t(n)\right),$$
$$j^{@}(x) := \inf\{j \in \mathcal{J}_n : |\eta^{@}_j(x) - \eta^{@}_k(x)| \leq g(j,k), \forall k \in \mathcal{J}_n, k > j\}, \quad x \in \mathcal{A},$$

where $\eta^{@}_j$ is defined in eq. (5.8) and $\inf\emptyset = \max(\mathcal{J}_n) = J$. If κ is chosen large enough, meaning $\kappa \geq \frac{p}{2}C_9^{-1}$, where C_9 is defined in Proposition 5.12.2, then we obtain

$$\sup_{\mathbb{P}\in\mathcal{P}(\mathbf{CS1},\mathbf{H}^{\mathbf{r}}_{\mathbf{s}})} \mathbb{E}^{\otimes n}\|\eta^{@}_{j^{@}(.)}(.) - \eta(.)\|^p_{\mathbb{L}_p(\Omega,\mu)} \leq 5^p 2^{rp} t(n)^p n^{-\frac{sp}{2s+d}}.$$

So that $\eta^{@}_{j^{@}(.)}(.)$ is a nearly minimax adaptive estimator of η over the generalized Lipschitz scale $\bigcup_{0<s<r} \mathscr{L}^s(\Omega, M)$.

Finally, we prove that $\eta^{@}$ is indeed (nearly) minimax optimal by giving the corresponding lower-bound result.

Theorem 5.7.3. *Assume we are under* (**CS1**) *and* ($\mathbf{H}^{\mathbf{r}}_{\mathbf{s}}$). *We write* $\inf_{\theta_n}$ *the infinimum over all estimators* θ_n *of* η, *that is all measurable functions of the data* $\mathcal{D}_n$. *Then, for* $d \geq 1$, $s > 0$, *we have, for all* $1 \leq p < \infty$,

$$\inf_{\theta_n} \sup_{\mathbb{P} \in \mathcal{P}(\mathbf{CS1}, \mathbf{H}^{\mathbf{r}}_{\mathbf{s}})} \mathbb{E}^{\otimes n} \|\theta_n - \eta\|^p_{\mathbb{L}_p(\Omega,\mu)} \gtrsim n^{-\frac{sp}{2s+d}}.$$

The next section shows how these results can be improved in the case where we benefit from additional information on μ or η.

5.8 Refinement of the results. As can be seen from Corollary 5.7.1 and Theorem 5.7.2 above, π_n appears as a multiplicative factor in the upper-bounds and thus deteriorates them by a multiplicative $\log n$ term. However, this needs not be the case, and under appropriate additional assumptions, π_n can be chosen to be a constant. Consider indeed the following two assumptions.

(**O1**) We know $\mu^*_{\min} \in \mathbb{R}$, such that $0 < \mu^*_{\min} \leq \mu_{\min}$.

(**O2**) We know a finite positive real number M such that $\|\eta\|_{\mathbb{L}_\infty(\Omega,\lambda)} \leq M$.

Under (**O1**), we know a lower bound $\mu^*_{\min}$ of $\mu_{\min}$, and therefore a lower bound $g^*_{\min}$ of $g_{\min}$ (see eq. (5.7)). Under (**O1**), we will thus choose $\pi_n^{-1} = \min(\frac{g^*_{\min}}{2}, 1)$. It is straightforward to show that Theorem 5.7.1 is still valid with this new value of π_n (see Remark 1 in the proof of Theorem 5.7.1), and thus all the subsequent results follow as well. Under (**O2**), we know an upper bound M of the essential supremum of η on Ω. In that case, we redefine

$$\eta^{@}_{\mathcal{H}}(x) = T_M(\eta^{\diamond}_{\mathcal{H}}(x)) \mathbb{1}_{\{\lambda_{\min}(Q_{\mathcal{H}}) > 0\}}, \tag{5.13}$$

where, for any $z \in \mathbb{R}$, we have written $T_M(z) = z\mathbb{1}_{\{|z| \leq M\}} + M\text{sign}(z)\mathbb{1}_{\{|z|>M\}}$. Once again, it is straightforward to show that Theorem 5.7.1 is now valid with $\pi_n^{-1} = \min(\frac{g_{\min}}{2}, 1)$ and $2M$ in place of M in the indicator function on the rhs of eq. (5.11) (see Remark 1 in the proof of Theorem 5.7.1), and thus all the subsequent results follow as well.

Notice that π_n is an absolute constant under (**O1**) and (**O2**), while it is an increasing sequence of n to be fine-tuned by the statistician otherwise. Hence π_n appears to be the price to pay for not knowing a lower bound of $\mu_{\min}$ or an upper bound of the essential supremum of η on Ω.

5.9 Relaxation of assumption (S1).

5.9.1 The problem. Now, we would like to relax assumption (**S1**) and allow for $\mathcal{A}$ to be an unknown subset of Ω, eventually disconnected. Under (**CS1**), the success of $\eta^{@}$ stems from the fact that it is constructed upon an approximation grid of the form $2^{-j}\mathbb{Z}^d \cap [0,1]^d$, whose edges coincide exactly with the boundary of $\mathcal{A}$. In the case where $\mathcal{A}$ is unknown, some cells of the lattice might straddle the boundary of $\mathcal{A}$ and thus require a new treatment.

In order to handle this new configuration, we will need to make a smoothness assumption on the boundary of $\mathcal{A}$ and allow for the estimation cells to move with the point at which we want to estimate η. Ultimately, we devise a new estimator $\eta^{\maltese}$ of η which is built upon a moving approximation grid. In fact, this new estimation method ensures that the point x at which we

want to estimate η always belongs to a cell $\mathcal{H}$ of $\mathcal{F}_j$ at resolution level j, whose center belongs to $\mathcal{A}$. This will ensure that local regressions performed on cells that straddle the boundary of $\mathcal{A}$ are still meaningful.
The smoothness assumption we will make on $\mathcal{A}$ might be compared to the support assumption made in [35, eq. (2.1)] in the classification context. In substance, it is assumed in [35] that $\mathcal{A}$ is locally ball-shaped to be compatible with the ball-shaped support of the LPE kernel, which they use to estimate η. In our case, we perform estimation with multi-dimensional scaling functions whose supports are cube-shaped and will thus assume that $\mathcal{A}$ is locally cube-shaped.

5.9.2 Smoothness assumption on $\mathcal{A}$. Let us now make these informal arguments more precise. To that end we introduce assumption (**S2**) as an alternative to (**S1**) above. Fix an absolute constant $\mathfrak{m}_0 \in (0,1)$ and recall that $2^{j_s} = \lfloor n^{\frac{1}{2s+d}} \rfloor$. With these notations, (**S2**) goes as follows,

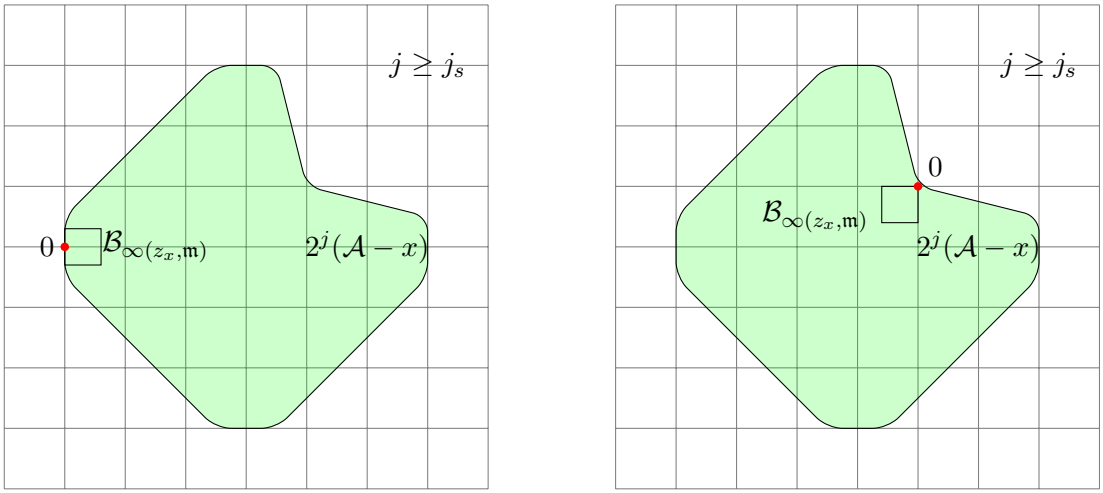

Figure 5.2: (**S2**) *allows for $\mathcal{A}$ to be non-convex and eventually disconnected.*

(**S2**) $\Omega = \mathbb{R}^d$ and $\mathcal{A}$ belongs to $\mathscr{A}_{j_s}$, where

$$\mathscr{A}_{j_s} := \{\mathcal{A} \subset \mathbb{R}^d : \exists \mathfrak{m} \geq \mathfrak{m}_0, \forall x \in \mathcal{A}, \\ \exists z_x \in \mathbb{R}^d, 0 \in \mathcal{B}_\infty(z_x, \mathfrak{m}) \subset 2^{j_s}(\mathcal{A}-x)\},$$

In words, (**S2**) means that if we zoom close enough to any $x \in \mathcal{A}$, we can find a hypercube $\mathcal{B}_\infty(z_x, \mathfrak{m})$ that contains x and is a subset of $\mathcal{A}$. Notice readily that for all $j_1 \geq j_2$, the component of $2^{j_2}(\mathcal{A}-x)$ that contains 0 is a subset of the component of $2^{j_1}(\mathcal{A}-x)$ that contains 0, so that $\mathscr{A}_{j_2} \subset \mathscr{A}_{j_1}$. Therefore $\mathscr{A}_{j_s}$ grows with n and shrinks with s. Of course, (**S1**) is a particular case of (**S2**). Setting (**S2**) allows $\mathcal{A}$ to be unknown and belong to a wide class of subsets of $\mathbb{R}^d$, eventually disconnected (see Figure 5.2).
In the sequel, we will conveniently refer by (**CS2**) to the set of assumptions (**D1**), (**S2**), (**N1**) or (**N2**).

***5.9.3 Moving local estimation under* (CS2).** As detailed above, η^{Φ} is obtained by local regression on a moving approximation grid. Let us describe the construction of η^{Φ} more precisely.

First of all, we split the sample into two pieces. For simplicity, let us assume that we dispose of $2n$ data points. The first half of the sample points, which we denote by $\mathcal{D}'_n = \{(X'_i, Y'_i), i = 1, \dots, n\}$, will be used to identify the support $\mathcal{A}$ of μ, while the second half, which we denote by $\mathcal{D}_n = \{(X_i, Y_i), i = 1, \dots, n\}$, will be used to estimate the scaling functions coefficients by local regressions.

Let us denote by $\mathcal{H}_0$ the cell $2^{-j}[0,1]^d$ of the lattice $2^{-j}\mathbb{Z}^d$ at resolution j. And denote by $\mathcal{H}_0(x)$ the same cell centered in x, that is $\mathcal{H}_0(x) = x - 2^{-j-1} + 2^{-j}[0,1]^d$. Then, the construction of $\eta_j^{\Phi}(x)$ at a point $x \in \mathbb{R}^d$ goes as follows. (i) If none of the design points (X'_i) of the sample $\mathcal{D}'_n$ lie in $\mathcal{H}_0(x)$, then take $\eta^{\Phi}(x) = 0$. (ii) If one or more design points of the sample $\mathcal{D}'_n$ lie in $\mathcal{H}_0(x)$, we select one of them and denote it by X'_{i_x} (the selection procedure is of no importance beyond computational considerations). By construction, x belongs to the cell $\mathcal{H}_0(X'_{i_x})$ centered in $X'_{i_x} \in \mathcal{A}$. Since X'_{i_x} belongs to $\mathcal{A}$, it makes sense to perform a local regression on $\mathcal{H}_0(X'_{i_x})$ with the sample points $\mathcal{D}_n$, which gives rise to an estimator η^{Φ} of η valid at any point of $\mathcal{H}_0(X'_{i_x}) \cap \mathcal{A}$. It is noteworthy that this procedure uses the sample $\mathcal{D}'_n$ to identify the support $\mathcal{A}$ of μ.

Interestingly, the above estimation procedure requires at most as many regressions as there are data points in $\mathcal{D}'_n$ to return an estimator η^{Φ} of η at every single point $x \in \mathcal{A}$. It is therefore computationally more efficient than any other kernel estimator, such as the LPE. The computational performance of η^{Φ} can in fact be further improved in the sense that the local regression on the cell $\mathcal{H}_0(X'_i)$ can be omitted if the cell $\mathcal{H}_0(X'_i)$ is itself included in the union of cells centered at other design points of $\mathcal{D}'_n$. In particular, we can choose X'_{i_x} to be a design point X'_i of $\mathcal{D}'_n$ that belongs to $\mathcal{H}_0(x)$ and for which a local regression has already been performed, if it exists, or any one of the X'_i that belong to $\mathcal{H}_0(x)$ otherwise.

Intuitively, the computational efficiency of η^{Φ} stems from the fact that the design points (X'_i) provide some valuable information on the unknown support $\mathcal{A}$ of μ, which can be exploited under (**CS2**). In particular, and as we will see below, (**D1**) guarantees that the design points of $\mathcal{D}'_n$ populate $\mathcal{A}$ densely enough so that, as long as $j \leq J$, the cells $\mathcal{H}_0(X'_i)$, $1 \leq i \leq n$, form a cover of $\mathcal{A}$, modulo a set whose μ-measure decreases almost exponentially fast toward zero with n.

5.9.4 Construction of the local estimator η^{Φ}. Assume we are under (**S2**) and work with the Daubechies' r-MRA of $\mathbb{L}_2(\mathbb{R}^d, \lambda)$. Obviously, shifting the approximation grid is equivalent to shifting the data points (X_i) of $\mathcal{D}_n$ and keeping the lattice fixed. For ease of notations and clarity, we adopt this second point of view. In order to compute η^{Φ} at a point $x \in \mathcal{H}_0(X'_{i_x}) \cap \mathcal{A}$, we want to shift the design points in such a way that X'_{i_x} falls right in the middle of $\mathcal{H}_0$. In other words, we want X'_{i_x} to be shifted at point $2^{-j-1} \in \mathbb{R}^d$ (whose coordinates are worth $2^{-j-1} \in \mathbb{R}$). This corresponds to the change of variable $\widetilde{X}_i = X_i - (X'_{i_x} - 2^{-j-1})$, where we have denoted by X_i and $\widetilde{X}_i$ the representations of a same data point in the canonical and shifted coordinate systems of $\mathbb{R}^d$, respectively. In order to compute η^{Φ} at point $x \in \mathcal{H}_0(X'_{i_x}) \cap \mathcal{A}$, it is therefore enough to perform a local regression on $\mathcal{H}_0$ against the shifted data points,

$$\widetilde{\mathcal{D}}_x = \{(\widetilde{X}_i, Y_i), i = 1, \dots, n\}.$$

For the sake of concision, we will denote by $\widetilde{u} = u - (X'_{i_x} - 2^{-j-1})$ the coordinate representation of a point u in the shifted coordinate system of $\mathbb{R}^d$. Let us denote by $k_1, \ldots, k_{R^d}$ the elements of $\mathcal{S}_j(\mathcal{H}_0)$. With these notations, eq. (5.4) must be corrected and written as

$$\alpha^{\diamond}_{\mathcal{H}_0} \in \arg\min_{a\in\mathbb{R}^{R^d}} \sum_{i=1}^{n} \left(Y_i - \sum_{t=1}^{R^d} a_t \varphi_{j,k_t}(\widetilde{X}_i) \right)^2 \mathbb{1}_{\mathcal{H}}(\widetilde{X}_i), \tag{5.14}$$

where we set $\alpha^{\diamond}_{\mathcal{H}_0} = 0$ if the arg min above contains more than one element. The notations introduced in Section 5.5.3 can be updated to this new setting as follows. $B_{\mathcal{H}_0}$ stands now for the random matrix of $\mathcal{M}_{n,R^d}$ whose rows are the $\varphi_{\mathcal{H}_0}(\widetilde{X}_i)^t$, $i = 1, \ldots, n$. In addition, we recall that we have defined $Q_{\mathcal{H}_0} = B^t_{\mathcal{H}_0} \cdot B_{\mathcal{H}_0}/n \in \mathcal{M}_{R^d,R^d}$. Its coefficients write thus as

$$[Q_{\mathcal{H}_0}]_{\nu,\nu'} = \frac{1}{n}\sum_{i=1}^{n} \varphi_{j,\nu}(\widetilde{X}_i)\varphi_{j,\nu'}(\widetilde{X}_i)\mathbb{1}_{\mathcal{H}_0}(\widetilde{X}_i), \qquad \nu,\nu' \in \mathcal{S}_j(\mathcal{H}_0).$$

Notice here that $\mathcal{S}_j(\mathcal{H}_0) = \{\nu \in \mathbb{Z}^d : 2^{-1} \in \mathrm{Supp}\varphi_\nu\}$, which neither depends on j nor x. Therefore, and for later reference, we denote

$$\mathfrak{S} := \{\nu \in \mathbb{Z}^d : 2^{-1} \in \mathrm{Supp}\varphi_\nu\}, \tag{5.15}$$

In addition, if we write $Y_{\mathcal{H}_0} = (Y_i \mathbb{1}_{\mathcal{H}_0}(\widetilde{X}_i))_{1\le i\le n}$, then eq. (5.5) still holds true when the solution to eq. (5.14) is unique. So that, for all $x \in \mathcal{H}_0(X_{i_x}) \cap \mathcal{A}$, we can write $\eta^{\diamond}_{\mathcal{H}_0}(\widetilde{x}) = \langle \alpha^{\diamond}_{\mathcal{H}_0}, \varphi_{\mathcal{H}_0}(\widetilde{x})\rangle$. Finally eq. (5.6) remains valid with X_i replaced by $\widetilde{X}_i$ and $\mathcal{H}$ by $\mathcal{H}_0$, $\eta^{@}_{\mathcal{H}_0}$ redefined as $\eta^{\maltese}_{\mathcal{H}_0}$ and $g_{\min}$ redefined as

$$g_{\min} = \mu_{\min} c_{\min}, \tag{5.16}$$

where $c_{\min}$ is the strictly positive constant defined in Lemma 5.12.1 below. So that ultimately, the estimator $\eta^{\maltese}_j$ of $\mathscr{P}_j\eta$ at a point $x \in \mathbb{R}^d$ writes as

$$\eta^{\maltese}_j(x) = \eta^{\maltese}_{\mathcal{H}_0}(\widetilde{x}), \qquad x \in \Omega. \tag{5.17}$$

Notice that by contrast with eq. (5.8) above, the sum over the hypercubes of $\mathcal{F}_j$ has disappeared. This is due to the fact that the approximation grid moves with x so that we end up virtually always performing estimation on the same hypercube $\mathcal{H}_0$.

5.9.5 The results. Interestingly, $\eta^{\maltese}$ still verifies similar results as the ones described in Section 5.7. To be more precise, recall that we work with a sample of size $2n$ broken up into two pieces $\mathcal{D}_n$ and $\mathcal{D}'_n$ of size n. Let us redefine $\mathcal{J}_n$ so that $\mathcal{J}_n = \{j_s, j_s+1, \ldots, J-1, J\}$ where $2^{j_s} = \lfloor n^{\frac{1}{2s+d}} \rfloor$. Then, we obtain the following result in place of Theorem 5.7.1.

Theorem 5.9.1. *Fix $r \in \mathbb{N}$ and assume we are under* (**CS2**) *and* ($\mathbf{H}^{\mathbf{r}}_{\mathbf{s}}$). *Recall that $\eta^{\maltese}_j$ is defined in eq. (5.17). Then, for all $j \in \mathcal{J}_n$, all $\delta > 2M2^{-js}\max(1, 3\pi_n R^d \mu_{\max})$ and all $x \in \mathcal{A}$, we have*

got

$$\sup_{\mathbb{P}\in\mathcal{P}(\mathbf{CS2},\mathbf{H_s^r})} \mathbb{P}^{\otimes n}(|\eta(x)-\eta_j^{\maltese}(x)|\geq\delta)$$
$$\leq 3R^{2d}\exp\left(-n2^{-jd}\frac{\pi_n^{-2}}{2\mu_{\max}R^{4d}+\frac{4}{3}R^{2d}\pi_n^{-1}}\right)\mathbb{1}_{\{\delta\leq M\}}$$
$$+R^d\Lambda\left(\frac{\delta 2^{-j\frac{d}{2}}}{2\pi_n R^d}\right),$$

where Λ has been defined in Theorem 5.7.1.

Left aside the fact that $\eta^{\maltese}$ is constructed upon a sample of size $2n$, the sole difference with the result of Theorem 5.7.1 is that the leading constant in front of the exponential on the second line has changed from $2R^d$ to $3R^d$. Furthermore, it is straightforward to deduce from Theorem 5.9.1 results similar to Corollary 5.7.1, Theorem 5.7.2 and Theorem 5.7.3, and a fortiori the refined results obtained in Section 5.8, for $\eta^{\maltese}$ under (**CS2**). The proofs of these results for $\eta^{\maltese}$ under the set of assumptions (**CS2**) follow, for the most part, exactly the same lines as the proofs given for $\eta^{@}$ under (**CS1**). Details can be found in Section 5.12.2.

5.10 Classification via local multi-resolution projections. Recall from [35] that the margin assumption can be written as,
(**MA**) There exist constants $C_*>0$ and $\vartheta\geq 0$ such that

$$\mathbb{P}(0<|2\eta(X)-1|\leq t)\leq C_* t^{\vartheta},\quad \forall t>0.$$

The binary classification setting corresponds to (**CS2**), under assumptions (**N1**) and (**O2**). Notice besides that we have $K=1$ in (**N1**) and $M=1$ in ($\mathbf{H_s^r}$). Since we are under (**O2**), it follows from Section 5.8 that $\pi_n=\pi_0=\min(1,\frac{g_{\min}}{2})$ is independent of n and $\eta^{\maltese}$ is capped at $M=1$ as in eq. (5.13). For the sake of coherence, we denote by $j^{\maltese}$ the adaptive resolution level built upon $\eta^{\maltese}$, as described in Theorem 5.7.2, and define $\mathcal{P}(\mathbf{CS2},\mathbf{H_s^r})$ by analogy with eq. (5.9) above. Finally, we recall that $\eta^{\maltese}$ is built upon a sample of size $2n$ split into two sub-samples $\mathcal{D}_n$ and $\mathcal{D}_n'$ of size n. In this context, we have the following Proposition.

Proposition 5.10.1. *Fix $r\in\mathbb{N}$ and assume we are in the binary classification setting. Assume moreover that ($\mathbf{H_s^r}$) holds true. Then, for all $j\in\mathcal{J}_n$, all $x\in\mathcal{A}$ and any $1\geq\delta>2\ 2^{-js}\max(1,3\pi_0 R^d\mu_{\max})$, we have got*

$$\sup_{\mathbb{P}\in\mathcal{P}(\mathbf{CS2},\mathbf{H_s^r})} \mathbb{P}^{\otimes n}(|\eta(x)-\eta_j^{\maltese}(x)|\geq\delta)$$
$$\leq 3R^{2d}n^{-\kappa C_{10}'}+2R^d\exp(-C_{10}a_n(j)\delta^2), \tag{5.18}$$

and for $1\geq\delta>62^r t(n)n^{-\frac{s}{2s+d}}$,

$$\sup_{\mathbb{P}\in\mathcal{P}(\mathbf{CS2},\mathbf{H_s^r})} \mathbb{P}^{\otimes n}(|\eta(x)-\eta_{j^{\maltese}(x)}^{\maltese}(x)|\geq\delta)$$
$$\leq 11R^{2d}(\log n)^2 n^{-\kappa C_6'}+2R^d\exp(-C_{11}n^{\frac{2s}{2s+d}}\delta^2), \tag{5.19}$$

where we have written $a_n(j):=n2^{-jd}$ and the constants $C_6',C_{10}',C_{10},C_{11}$ are all defined in the proof, eq. (5.38) and eq. (5.39).

The proof of this latter result is a straightforward consequence of Theorem 5.7.1 and Theorem 5.7.2. It is detailed in the Appendix. All the results that follow can be easily derived from [35]. Their proofs are therefore not reported in this Section but delayed to the Appendix as well. The first result derives an upper-bound on the classification loss from an upper bound on the probability of deviation of a classifier η_n from η at a point $x \in \mathcal{A}$. It is similar to [35, Theorem 3.1] in scope and proof.

Theorem 5.10.1. *Fix $r \in \mathbb{N}$ and assume we are in the binary classification setting. Assume moreover that $(\mathbf{H}_\mathbf{S}^\mathbf{r})$ and $(\mathbf{MA})$ hold true. Let η_n be an estimator of η and assume there exists $\delta_n \in (0,1)$ and strictly positive constants C_{11}, C_{12}, C_{13} such that, for all $1 \geq \delta \geq \delta_n$ and almost all $x \in \mathcal{A}$, we have*

$$\sup_{\mathbb{P} \in \mathcal{P}(\mathbf{CS2}, \mathbf{H}_\mathbf{S}^\mathbf{r}, \mathbf{MA})} \mathbb{P}^{\otimes n}(|\eta_n(x) - \eta(x)| \geq \delta) \leq C_{11} b_n + C_{12} \exp(-C_{13} a_n \delta^2), \tag{5.20}$$

for some positive sequences a_n and b_n. Consider the plug-in classifier $h_n(.) := \mathbb{1}_{\{\eta_n(.) \geq \frac{1}{2}\}}$. Then, we have got

$$\sup_{\mathbb{P} \in \mathcal{P}(\mathbf{CS2}, \mathbf{H}_\mathbf{S}^\mathbf{r}, \mathbf{MA})} \mathscr{T}(h_n) \leq 2C_* \delta_n^{1+\vartheta} \Big(1 + C_{11} b_n \delta_n^{-(1+\vartheta)} + C_{12} \sum_{k \geq 1} 2^{k(1+\vartheta)} \exp(-C_{13} a_n \delta_n^2 2^{2(k-1)}) \Big).$$

As a consequence of Theorem 5.10.1, we can use the plug-in classifier built upon $\eta^{\maltese}$ to obtain similar results as the ones given in [35, Lemma 3.1] for LPE based plug-in classifiers.

Corollary 5.10.1. *Fix $r \in \mathbb{N}$ and assume we are in the binary classification setting. Assume moreover that $(\mathbf{H}_\mathbf{S}^\mathbf{r})$ and $(\mathbf{MA})$ hold true. Consider the plug-in classifiers $h_{j_s}^{\maltese}(.) = \mathbb{1}_{\{\eta_{j_s}^{\maltese}(.) \geq \frac{1}{2}\}}$ and $h_{j^{\maltese}}^{\maltese}(.) = \mathbb{1}_{\{\eta_{j^{\maltese}(.)}^{\maltese}(.) \geq \frac{1}{2}\}}$. Then, we have*

$$\sup_{\mathbb{P} \in \mathcal{P}(\mathbf{CS2}, \mathbf{H}_\mathbf{S}^\mathbf{r}, \mathbf{MA})} \mathscr{T}(h_{j_s}^{\maltese}) \leq C_{15} n^{-\frac{s}{2s+d}(1+\vartheta)}, \quad \text{as soon as } \kappa > \tfrac{1+\vartheta}{2C'_{10}}, \tag{5.21}$$

$$\sup_{\mathbb{P} \in \mathcal{P}(\mathbf{CS2}, \mathbf{H}_\mathbf{S}^\mathbf{r}, \mathbf{MA})} \mathscr{T}(h_{j^{\maltese}}^{\maltese}) \leq C_{16} (\log n)^{\frac{1+\vartheta}{2}} n^{-\frac{s}{2s+d}(1+\vartheta)}, \quad \text{as soon as } \kappa > \tfrac{1+\vartheta}{2C'_6}, \tag{5.22}$$

where C'_6, C'_{10} have been defined in Proposition 5.10.1 above and C_{15}, C_{16} are defined in the proof in eq. (5.40) and eq. (5.42).

In addition, the lower bound of [35, Theorem 3.5] carries over to the present setting after minor modifications. We have indeed the following Theorem.

Theorem 5.10.2. *Fix $r \in \mathbb{N}$ and assume we are in the binary classification setting. Assume moreover that $(\mathbf{H}_\mathbf{S}^\mathbf{r})$ and $(\mathbf{MA})$ hold true and $s\vartheta \leq d$. Then there exists a constant $c > 0$ such that for any classifier θ_n, that is any $\{0,1\}$-valued measurable function θ_n of the data $\mathcal{D}_n$, we have*

$$\sup_{\mathbb{P} \in \mathcal{P}(\mathbf{CS2}, \mathbf{H}_\mathbf{S}^\mathbf{r}, \mathbf{MA})} \mathscr{T}(\theta_n) \gtrsim n^{-\frac{s}{2s+d}(1+\vartheta)}.$$

So that, under the above assumptions, the classifiers $h^{\maltese}$ defined in Corollary 5.10.1 are (nearly) minimax optimal.

5.11 Simulation study. In order to illustrate the performance of $\eta^{@}_{j^{@}}$, we have carried out a simulation study in the regression setting in the one-dimensional case, that is with $d = 1$. As detailed earlier, the sole purpose of this simulation is to show that (1) $\eta^{@}$ can be easily implemented and is computationally efficient, (2) $\eta^{@}$ works well in practice in the case where the density of the design μ is discontinuous, (3) and to give an intuitive visual feel for $\eta^{@}$, which is built upon the juxtaposition of local regressions against a set of scaling functions. In particular, we run our simulation against benchmark signals, which allows to compare them with the ones detailed in the literature for alternative kernel estimators (see simulation study in [84], for example). We have run them under (**CS1**), which corresponds to the case where $\eta^{@}_{j}$ can be completely computed with exactly 2^j regressions. We have in particular $\Omega = [0,1] = \mathcal{A}$. We focus on the functions η introduced in [79] and used as a benchmark in numerous subsequent simulation studies. They are made available through the Wavelab850 library freely available at `http://www-stat.stanford.edu/~wavelab/`. In addition we have chosen the noise ξ to be standard normal, that is we are working under (**N2**) with $\sigma = 1$. In all cases, we have chosen the signal-to-noise ratio (SNR) to be equal to 7. To be more specific, we are working on a dyadic grid G of $[0,1]$ of resolution 2^{-15}. We compute the root-mean-squared-error (RMSE) of both the signal and the noise on that grid and rescale the signal so that its RMSE be seven times bigger than the one of the noise.

Let us now give details about the simulation of the sample points and the computation of the estimator. We divide the unit-interval into ten sub-segments $A_k := 10^{-1}[k, k+1]$ for $k = 0, \dots, 9$. We define the density of X as follows.

$$\mu(x) = \sum_{k=0}^{9} p_k \lambda(A_k)^{-1} \mathbb{1}_{A_k}(x).$$

We choose the p_k's at random. To that end, we denote by $(u_k)_{0 \le k \le 9}$ ten realizations of the uniform random variable on $[.25, 1]$, write $v = u_0 + \ldots + u_9$ and set $p_k = u_k v^{-1}$. Notice that this guarantees that $\mu \ge \min_{0 \le k \le 9} 10 p_k \ge \mu_{\min} = 0.25$ on $[0,1]$. We then simulate 3000 sample points X_i according to μ. Finally, we bring the points back on the grid G by assimilating them to their nearest grid node. Since the X_i's are supposed to be drawn from a law that is absolutely continuous with respect to the Lebesgue measure on $[0,1]$, we must keep only one data point per grid node. This reduces the number of data points from 3000 to the number that is reported on top of each of the histograms.

In order to compute the adaptive estimator at sample points X_i, we use the boundary-corrected scaling functions coded into Wavelab850 for $r = 3$ and for which we must have $j \ge 3$. We set $J = \lceil \log(n/\log n)/\log 2 \rceil$. The elimination of redundant sample points on the grid removes on average 150 points so that we obtain $J = 10$. We therefore have $\mathcal{J}_n = \{3, 4, \dots, 10\}$. Notice interestingly that the computation of $\eta^{@}_3$ requires only 8 regressions and $\eta^{@}_{10}$ requires $1,024$ of them. This is much smaller than for the LPE whose computation necessitates as many regressions as there are sample points at each resolution level. In practice, we compute the minimum eigenvalues of all regression matrices across partitions and resolution levels and choose π_n^{-1} to be the first decile of this set of values. When proving theoretical results, we have chosen $\eta^{@}_j$ to be zero on the small probability event where the minimum eigenvalue of the regression matrix is smaller than π_n^{-1}. In practice we can choose it to be an average value of the nearby cells in order to get an estimator that is overall more appealing to the eye. In our

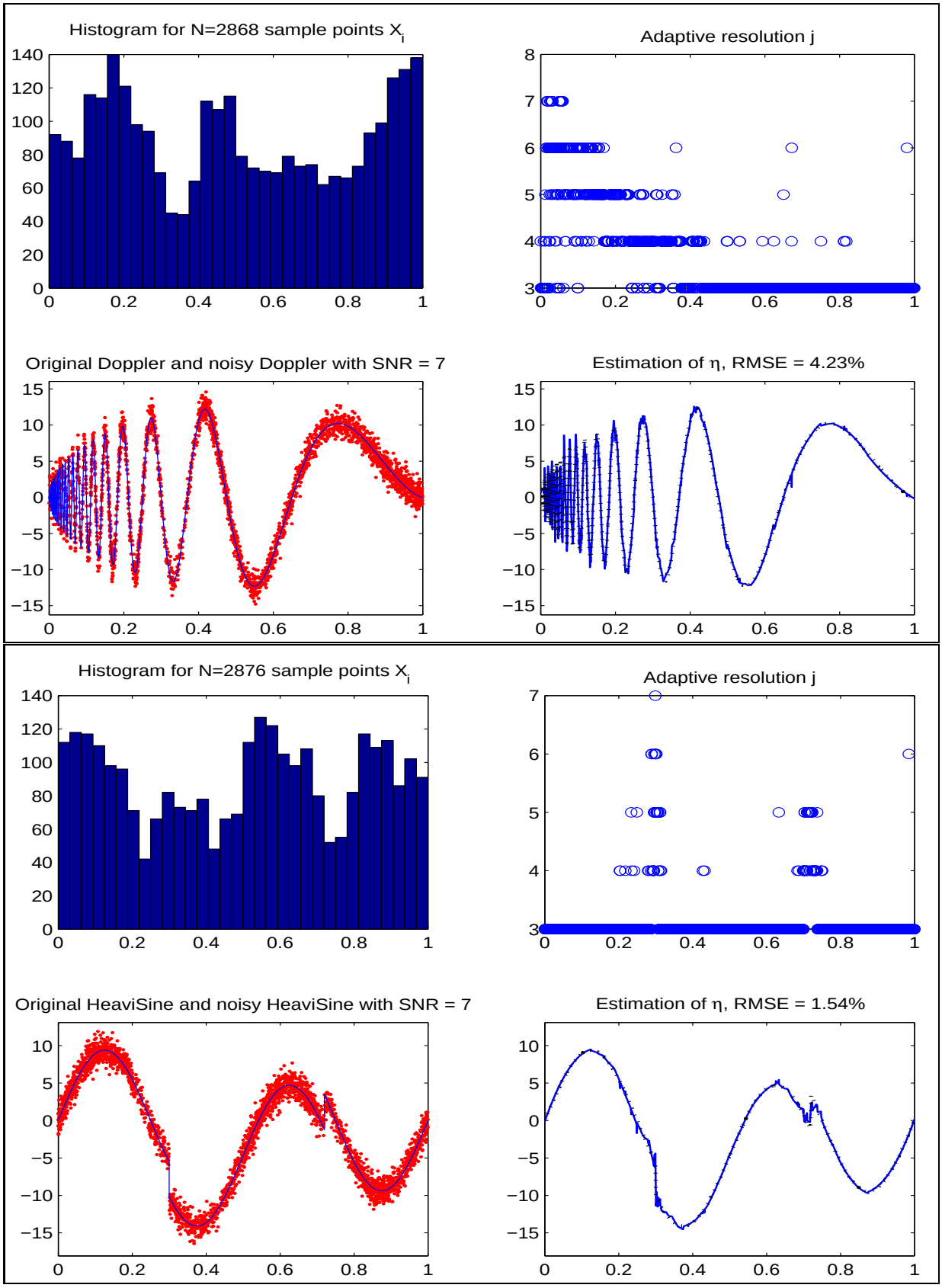

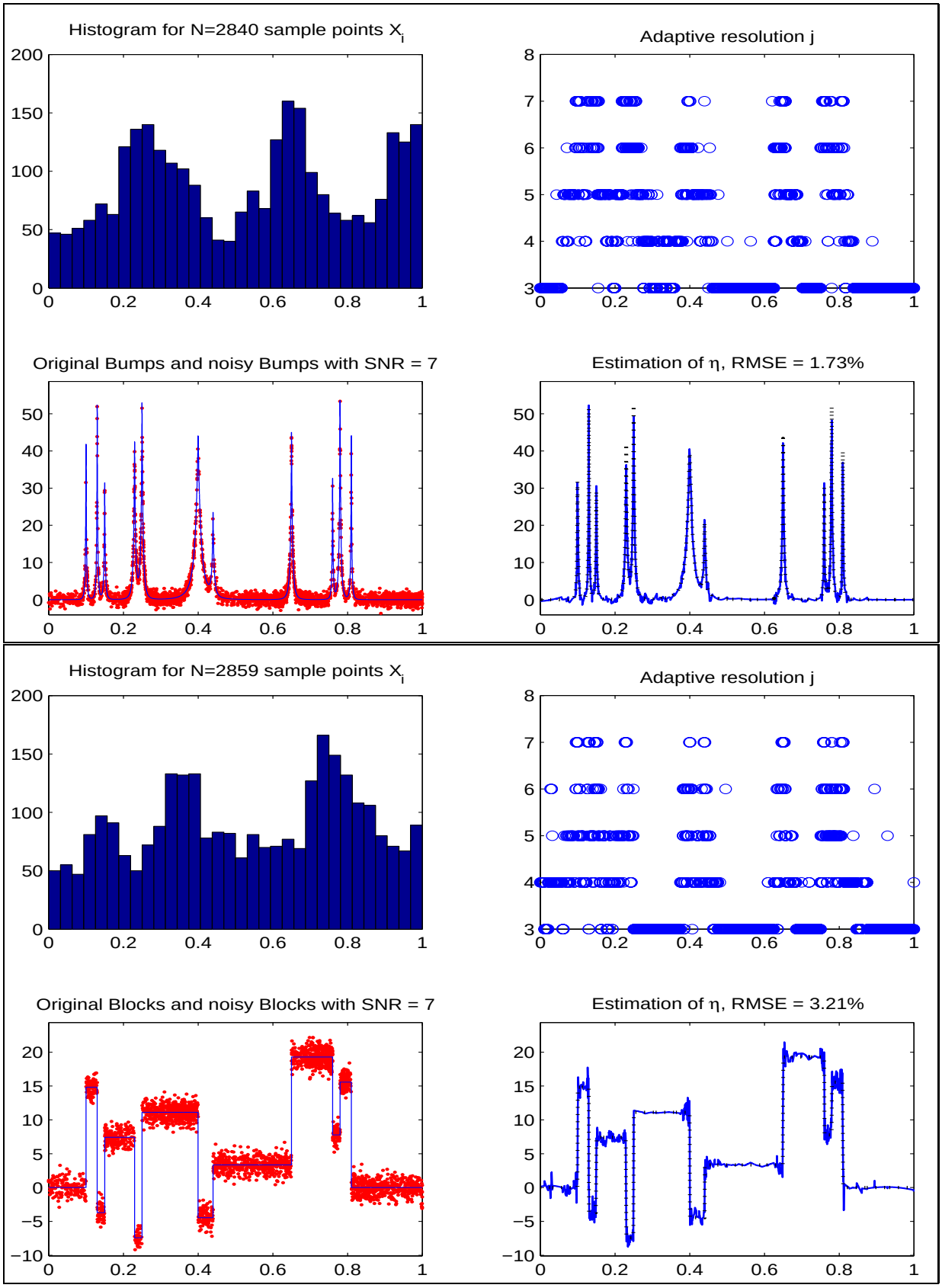

simulation, we in fact do not use that modification. Instead, we modify $j^{@}$ to be the highest $j \in \{3, \dots, j^{@}\}$ such that $\eta_{j^{@}}^{@}$ has been computed from a valid regression matrix, meaning a regression matrix whose smallest eigenvalue is greater than the threshold π_n^{-1}.
In practice, for a given signal, we generate μ at random and compute $\eta_{j^{@}}^{@}$ for 100 samples drawn from μ. We quantify the performance $\eta_{j^{@}}^{@}$ by its relative RMSE, meaning its RMSE computed at sample points X_i divided by the amplitude of the true signal, that is its maximal absolute value on the underlying dyadic grid. We display results for "Doppler", "HeaviSine", "Bumps" and "Blocks" corresponding to the median performance among the 100 trials. Each figure displays four graphs. Clockwise from the top left corner, they display in turn, an histogram of sample points X_i; the adaptive level $j^{@}$ at sample points X_i; the true signal (black dots) and the estimator $\eta_{j^{@}}^{@}$ at sample points X_i (solid blue line) and its corresponding relative RMSE in the title; and finally the original signal (solid blue line) with its noisy version at sample points X_i (red dots).

5.12 Proofs.

5.12.1 Proof of the upper-bound results under (**CS1**).

5.12.1.1 Proof of Corollary 5.7.1. Consider the term

$$I = \int_{\mathcal{A}} \mathbb{E}[|\eta(x) - \eta_j^{@}(x)|^p]\mu(x)dx.$$

Now, apply Proposition 5.12.1 and notice that $\int_{\mathcal{A}} \mu(x)dx = 1$ to show that I is upper-bounded by the term that appears on the rhs of eq. (5.12) stated in Corollary 5.7.1. In particular, for all $1 \leq p < \infty$, we obtain $I \leq C(p)\pi_n^p t(n)^{-p} \leq C(p) < \infty$. This in turn proves that we can apply the Fubini-Tonelli theorem to get

$$I = \mathbb{E}[\|\eta - \eta_j^{@}\|_{\mathbb{L}_p(\Omega,\mu)}^p],$$

and concludes the proof. □

5.12.1.2 Proof of Theorem 5.7.1.

Local estimation under (**CS1**) *in the case where* $r = 1$.. Let $x \in \mathcal{A}$ and $j \in \mathcal{J}_n$. There exists $\mathcal{H} \in \mathcal{F}_j$ such that $x \in \mathcal{H}$. Recall that with Haar MRAs, we have $\mathcal{S}_j(\mathcal{H}) = \{\nu(\mathcal{H})\}$ so that $B_{\mathcal{H}} \in \mathcal{M}_{n,1}$ and for any $i \in \mathcal{I}_{\mathcal{H}}$, $[B_{\mathcal{H}}]_i = \varphi_{j,\nu(\mathcal{H})}(X_i)\mathbb{1}_{\mathcal{H}}(X_i) = \varphi_{j,\nu(\mathcal{H})}(X_i)$ since $\mathcal{H} = \mathrm{Supp}\varphi_{j,\nu(\mathcal{H})}$. So that

$$Q_{\mathcal{H}} = \frac{1}{n}\sum_{i\in\mathcal{I}_{\mathcal{H}}} \varphi_{j,\nu(\mathcal{H})}(X_i)^2 = 2^{jd}\frac{n_{\mathcal{H}}}{n}.$$

On $\{Q_{\mathcal{H}} \geq \pi_n^{-1}\}$, we can divide by $Q_{\mathcal{H}}$ and thus write

$$\alpha_{j,\nu(\mathcal{H})}^{\diamond} = \frac{\sum_{i=1}^n Y_i\varphi_{j,\nu(\mathcal{H})}(X_i)}{\sum_{i=1}^n \varphi_{j,\nu(\mathcal{H})}(X_i)^2} = 2^{-jd/2}\frac{\sum_{i=1}^n Y_i\mathbb{1}_{\{X_i\in\mathrm{Supp}\varphi_{j,\nu(\mathcal{H})}\}}}{\sum_{i=1}^n \mathbb{1}_{\{X_i\in\mathrm{Supp}\varphi_{j,\nu(\mathcal{H})}\}}} = 2^{-jd/2}\frac{1}{n_{\mathcal{H}}}\sum_{i\in\mathcal{I}_{\mathcal{H}}} Y_i.$$

On this event, the estimation error can hence be written as

$$\begin{aligned}
|\mathscr{P}_j\eta(x) - \eta^{\diamond}_{\mathcal{H}}(x)| &= 2^{jd/2}|\alpha_{j,\nu(\mathcal{H})} - \alpha^{\diamond}_{j,\nu(\mathcal{H})}| \\
&= \frac{1}{n_{\mathcal{H}}}|\sum_{i\in\mathcal{I}_{\mathcal{H}}} \alpha_{j,\nu(\mathcal{H})}\varphi_{j,\nu(\mathcal{H})}(X_i) - \sum_{i\in\mathcal{I}_{\mathcal{H}}} Y_i| \\
&= \frac{1}{n_{\mathcal{H}}}|\sum_{i\in\mathcal{I}_{\mathcal{H}}} (\mathscr{P}_j\eta(X_i) - Y_i)| \\
&= \frac{1}{n_{\mathcal{H}}}|\sum_{i\in\mathcal{I}_{\mathcal{H}}} (\mathscr{R}_j\eta(X_i) + \xi_i)| \\
&= \frac{n}{n_{\mathcal{H}}}2^{-jd/2}\frac{1}{n}|\sum_{i=1}^{n}(\varphi_{j,\nu(\mathcal{H})}(X_i)(\mathscr{R}_j\eta(X_i) + \xi_i))| \\
&\leq 2^{j\frac{d}{2}}\pi_n\frac{1}{n}|\sum_{i=1}^{n}(\varphi_{j,\nu(\mathcal{H})}(X_i)(\mathscr{R}_j\eta(X_i) + \xi_i))|,
\end{aligned}$$

since $Q_{\mathcal{H}}^{-1} \leq \pi_n$. Write

$$W_{j,\nu(\mathcal{H})} = \frac{1}{n}|\sum_{i=1}^{n}(\varphi_{j,\nu(\mathcal{H})}(X_i)(\mathscr{R}_j\eta(X_i) + \xi_i))|.$$

By definition, we have $\eta^{@}_j(x) = \eta^{@}_{\mathcal{H}}(x)$, so that we have

$$\begin{aligned}
\mathbb{P}(|\eta(x) - \eta^{@}_j(x)| \geq \delta) &= \mathbb{P}(|\eta(x) - \eta^{@}_{\mathcal{H}}(x)| \geq \delta, Q_{\mathcal{H}} \geq \pi_n^{-1}) \\
&\quad + \mathbb{P}(|\eta(x) - \eta^{@}_{\mathcal{H}}(x)| \geq \delta, Q_{\mathcal{H}} < \pi_n^{-1}).
\end{aligned} \tag{5.23}$$

By construction, $\eta^{@}_{\mathcal{H}}(x) = \eta^{\diamond}_{\mathcal{H}}(x)$ on the event $\{Q_{\mathcal{H}} \geq \pi_n^{-1}\}$ and $\eta^{@}_{\mathcal{H}}(x) = 0$ on its complement. So that we obtain $|\eta(x) - \eta^{@}_{\mathcal{H}}(x)| = |\eta(x)| \leq M$ on the rhs of eq. (5.23). Notice in addition that $M2^{-js} \geq |\mathscr{R}_j\eta(x)|$ under $(\mathbf{H}^{\mathbf{r}}_{\mathbf{s}})$ (see Section 5.13.1). Finally, we obtain, for $\frac{\delta}{2} > M2^{-js} \geq |\mathscr{R}_j\eta(x)|$,

$$\begin{aligned}
&\mathbb{P}(|\eta(x) - \eta^{@}_j(x)| \geq \delta) \\
&\quad\leq \mathbb{P}(|\mathscr{P}_j\eta(x) - \eta^{\diamond}_{\mathcal{H}}(x)| \geq \frac{\delta}{2}, Q_{\mathcal{H}} \geq \pi_n^{-1}) + \mathbb{P}(Q_{\mathcal{H}} < \pi_n^{-1})\mathbb{1}_{\{\bar{M}\geq\delta\}} \\
&\quad\leq \mathbb{P}(W_{j,\nu(\mathcal{H})} \geq 2^{-jd/2-1}\delta\pi_n^{-1}) + \mathbb{P}(Q_{\mathcal{H}} < \pi_n^{-1})\mathbb{1}_{\{\bar{M}\geq\delta\}}.
\end{aligned}$$

where we have written $\bar{M} = M$. The term on the rhs is tackled thanks to Proposition 5.12.5. Regarding the lhs, a direct application of Proposition 5.12.6 allows to write, for all $\delta > 2M2^{-js}\max(1, 3\pi_n\mu_{\max})$,

$$\mathbb{P}(W_{j,\nu(\mathcal{H})} \geq 2^{-jd/2-1}\delta\pi_n^{-1}) \leq \Lambda(2^{-j\frac{d}{2}-1}\delta\pi_n^{-1}).$$

This concludes the proof.

Remark 1. Under (**O2**), we have $|\eta^{@}_{\mathcal{H}}(x)| \leq M$, and since $\eta \in \mathscr{L}^s(\Omega, M)$, we obtain $|\eta(x) - \eta^{@}_{\mathcal{H}}(x)| \leq 2M$ on the rhs of eq. (5.23). While on the lhs, it is straightforward that (see [103, Chap. 10])

$$|\eta(x) - \eta^{@}_{\mathcal{H}}(x)| = |\eta(x) - T_M(\eta^{\diamond}_{\mathcal{H}}(x))| \leq |\eta(x) - \eta^{\diamond}_{\mathcal{H}}(x)|.$$

Under (**O1**), the proof remains unchanged. So that the proof still holds with

$$\bar{M} = \begin{cases} 2M, & \text{under } (\mathbf{O2}), \\ M, & \text{otherwise.} \end{cases}$$

□

Local estimation under (**CS1**) *in the case where* $r \geq 2$.. The proof follows the same lines as above, except that $Q_{\mathcal{H}}$ is now a matrix. Let $x \in \mathcal{A}$ and $j \in \mathcal{J}_n$. There exists $\mathcal{H} \in \mathcal{F}_j$ such that $x \in \mathcal{H}$. Let us work on the set $\{\lambda_{\min}(Q_{\mathcal{H}}) \geq \pi_n^{-1}\}$ on which $Q_{\mathcal{H}}$ is invertible. On that set, we can write

$$\begin{aligned} |\mathscr{P}_j\eta(x) - \eta^{\diamond}_{\mathcal{H}}(x)| &= |\langle \alpha_{\mathcal{H}} - \alpha^{\diamond}_{\mathcal{H}}, \varphi_{\mathcal{H}}(x)\rangle| \\ &= |\langle Q_{\mathcal{H}}^{-1} \cdot \left(\frac{B^t_{\mathcal{H}}}{n} \cdot (B_{\mathcal{H}} \cdot \alpha_{\mathcal{H}} - Y_{\mathcal{H}}) \right), \varphi_{\mathcal{H}}(x)\rangle| \\ &\leq \|Q_{\mathcal{H}}^{-1}\|_S \| \frac{B^t_{\mathcal{H}}}{n} \cdot (B_{\mathcal{H}} \cdot \alpha_{\mathcal{H}} - Y_{\mathcal{H}})\|_{\ell^2(\mathbb{R}^{R^d})} \|\varphi_{\mathcal{H}}(x)\|_{\ell^2(\mathbb{R}^{R^d})} \\ &\leq R^{\frac{d}{2}} 2^{j\frac{d}{2}} \lambda_{\min}(Q_{\mathcal{H}})^{-1} \| \frac{B^t_{\mathcal{H}}}{n} \cdot (B_{\mathcal{H}} \cdot \alpha_{\mathcal{H}} - Y_{\mathcal{H}})\|_{\ell^2(\mathbb{R}^{R^d})}. \end{aligned}$$

Now, notice that for all $X_i \in \mathcal{H}$, we have $Y_i = \langle \alpha_{\mathcal{H}}, \varphi_{\mathcal{H}}(X_i)\rangle + \mathscr{R}_j\eta(X_i) + \xi_i$. Write $\mathscr{R}_{\mathcal{H}} = (\mathscr{R}_j\eta(X_i)\mathbb{1}_{\mathcal{H}}(X_i))_{1\leq i\leq n}$ and $\xi_{\mathcal{H}} = (\xi_i \mathbb{1}_{\mathcal{H}}(X_i))_{1\leq i\leq n}$. Then, we have,

$$W_{\mathcal{H}} = |\frac{B^t_{\mathcal{H}}}{n} \cdot (B_{\mathcal{H}} \cdot \alpha_{\mathcal{H}} - Y_{\mathcal{H}})| = |\frac{B^t_{\mathcal{H}}}{n} \cdot (\xi_{\mathcal{H}} + \mathscr{R}_{\mathcal{H}})| \in \mathbb{R}^{R^d}.$$

Thus, a direct application of Proposition 5.12.6 allows to write, for $\delta > 2M2^{-js}\max(1, 3\pi_n R^d \mu_{\max})$,

$$\begin{aligned} \mathbb{P}(|\eta(x) - \eta^{\diamond}_{\mathcal{H}}(x)| \geq \delta, \lambda_{\min}(Q_{\mathcal{H}}) \geq \pi_n^{-1}) & \\ &\leq \mathbb{P}(\|W_{\mathcal{H}}\|_{\ell_2(\mathbb{R}^{R^d})} \geq \frac{\delta 2^{-j\frac{d}{2}}}{2\pi_n R^{\frac{d}{2}}}) \\ &\leq R^d \sup_{k\in\mathcal{S}_j(\mathcal{H})} \mathbb{P}\left([W_{\mathcal{H}}]_k \geq \frac{\delta 2^{-j\frac{d}{2}}}{2\pi_n R^d} \right) \\ &\leq R^d \Lambda\left(\frac{\delta 2^{-j\frac{d}{2}}}{2\pi_n R^d} \right). \end{aligned}$$

At last, using exactly the same arguments as in the case where $r = 1$ above, we obtain

$$\begin{aligned} \mathbb{P}(|\eta(x) - \eta^{@}_j(x)| \geq \delta) \leq \mathbb{P}(|\eta(x) - \eta^{\diamond}_{\mathcal{H}}(x)| \geq \delta, \lambda_{\min}(Q_{\mathcal{H}}) \geq \pi_n^{-1}) & \\ + \mathbb{P}(\lambda_{\min}(Q_{\mathcal{H}}) < \pi_n^{-1}) \mathbb{1}_{\{\delta \leq \bar{M}\}}, & \end{aligned}$$

where $\bar{M}$ has been defined in Remark 1. The term on the lhs has been dealt with above. The term on the rhs is tackled using Proposition 5.12.3. This concludes the proof. □

5.12.1.3 Proof of Theorem 5.7.2 . This result is obtained after a slight modification of [84, Proposition 3.4]. In the same way as in the proof of Theorem 5.7.1, we are brought back to controlling $\mathbb{E}|\eta^{@}_{j^{@}(x)}(x) - \eta(x)|^p$ for all $x \in \mathcal{A}$. To that end, we split this term as follows

$$\begin{aligned}\mathbb{E}|\eta^{@}_{j^{@}(x)}(x) - \eta(x)|^p &= \mathbb{E}|\eta^{@}_{j^{@}(x)}(x) - \eta(x)|^p(\mathbb{1}_{\{j^{@}(x)\leq j_s\}} + \mathbb{1}_{\{j^{@}(x)>j_s\}}) \\ &= I + II.\end{aligned}$$

Let us first deal with I. Notice that

$$2^{1-p}|\eta^{@}_{j^{@}(x)}(x) - \eta(x)|^p \leq |\eta^{@}_{j^{@}(x)}(x) - \eta^{@}_{j_s}(x)|^p + |\eta^{@}_{j_s}(x) - \eta(x)|^p.$$

The last term is of the good order since

$$\begin{aligned}\mathbb{E}|\eta^{@}_{j_s}(x) - \eta(x)|^p &\leq C(p)\pi_n^p \max\left(2^{-j_s s}, \frac{2^{j_s\frac{d}{2}}}{\sqrt{n}}\right)^p \\ &= \frac{C(p)}{(\kappa\log n)^{\frac{p}{2}}}\left(t(n)2^r n^{-\frac{s}{2s+d}}\right)^p,\end{aligned}$$

according to Proposition 5.12.1, eq. (5.10a) and eq. (5.10c). Regarding the first term, notice that on the event $\{j^{@}(x) \leq j_s\}$, one has got

$$\begin{aligned}|\eta^{@}_{j^{@}(x)}(x) - \eta^{@}_{j_s}(x)| \leq g(j^{@}(x), j_s) &\leq \sup_{j_\varpi \leq k \leq j_s} g(k, j_s) \\ &\leq g(j_s, j_s) = 2t(n)\frac{2^{j_s\frac{d}{2}}}{\sqrt{n}} \leq 2t(n)2^r n^{-\frac{s}{2s+d}},\end{aligned}$$

where we have used eq. (5.10a) and eq. (5.10c) and which is of the good order too. Let us now turn to II. For any two $j < k$, we write

$$\mathcal{G}(x, j, k) = \{|\eta^{@}_j(x) - \eta^{@}_k(x)| > g(j, k)\}.$$

Write $\mathcal{J}_n(j) = \{k \in \mathcal{J}_n : k > j\}$. Notice first that we have the following inclusions

$$\begin{aligned}\{j^{@}(x) = j\} &\subseteq \bigcup_{k\in\mathcal{J}_n(j-1)} \mathcal{G}(x, j-1, k), \\ \{j^{@}(x) > j_s\} = \bigcup_{j\in\mathcal{J}_n(j_s)} \{j^{@}(x) = j\} &\subseteq \bigcup_{j\in\mathcal{J}_n(j_s)} \bigcup_{k\in\mathcal{J}_n(j-1)} \mathcal{G}(x, j-1, k).\end{aligned}$$

Therefore, we can write

$$\begin{aligned}II &\leq \sum_{j\in\mathcal{J}_n(j_s)} \mathbb{E}|\eta^{@}_{j^{@}(x)}(x) - \eta(x)|^p \mathbb{1}_{\{j^{@}(x)=j\}} \\ &\leq \sum_{j\in\mathcal{J}_n(j_s)} \sum_{k\in\mathcal{J}_n(j-1)} \mathbb{E}|\eta^{@}_j(x) - \eta(x)|^p \mathbb{1}_{\mathcal{G}(x,j-1,k)}.\end{aligned}$$

Now, we notice that

$$|\eta^{@}_j(x) - \eta^{@}_k(x)| \leq |\eta^{@}_j(x) - \eta(x)| + |\eta(x) - \eta^{@}_k(x)|.$$

So that

$$\begin{aligned}\mathcal{G}(x,j,k) &= \{|\eta_j^{@}(x) - \eta_k^{@}(x)| > g(j,k)\} \\ &\subset \left\{|\eta_j^{@}(x) - \eta(x)| > \frac{2^{j\frac{d}{2}}}{\sqrt{n}} t(n)\right\} \bigcup \left\{|\eta_k^{@}(x) - \eta(x)| > \frac{2^{k\frac{d}{2}}}{\sqrt{n}} t(n)\right\}, \\ \mathbb{P}(\mathcal{G}(x,j,k)) &\leq \mathbb{P}\left(|\eta_j^{@}(x) - \eta(x)| > \frac{2^{j\frac{d}{2}}}{\sqrt{n}} t(n)\right) + \mathbb{P}\left(|\eta_k^{@}(x) - \eta(x)| > \frac{2^{k\frac{d}{2}}}{\sqrt{n}} t(n)\right).\end{aligned}$$

So that a direct application of the Cauchy-Schwarz inequality leads to

$$\mathbb{E}|\eta_j^{@}(x) - \eta(x)|^p \mathbb{1}_{\mathcal{G}(x,j-1,k)} \leq (\mathbb{E}|\eta_j^{@}(x) - \eta(x)|^{2p})^{\frac{1}{2}} \mathbb{P}(\mathcal{G}(x,j-1,k))^{\frac{1}{2}}.$$

Now, a direct application of Proposition 5.12.1 for $j_s \leq j \leq J$ gets us

$$(\mathbb{E}|\eta_j^{@}(x) - \eta(x)|^{2p})^{\frac{1}{2}} \leq \sqrt{C(2p)} \pi_n^p \max\left(2^{-js}, \frac{2^{j\frac{d}{2}}}{\sqrt{n}}\right)^p \leq \sqrt{C(2p)} (\kappa \log n)^{-\frac{p}{2}}.$$

Besides, notice that for $j_s \leq j < k \leq J$, we can apply Proposition 5.12.2 with $\kappa \geq \frac{p}{2} C_9^{-1}$ to obtain

$$\mathbb{P}\left(|\eta_j^{@}(x) - \eta(x)| > \frac{2^{j\frac{d}{2}}}{\sqrt{n}} t(n)\right) \vee \mathbb{P}\left(|\eta_k^{@}(x) - \eta(x)| > \frac{2^{k\frac{d}{2}}}{\sqrt{n}} t(n)\right) \leq 5R^{2d} n^{-\frac{p}{2}}.$$

To conclude the proof, it remains to notice that $\#\mathcal{J}_n \leq \log n$ and remark that the multiplicative constant in the upper-bound of Theorem 5.7.2 is indeed smaller than, say, 5 for n large enough. □

5.12.1.4 A few useful Propositions and Lemmas.

Proposition 5.12.1. *Fix $r \in \mathbb{N}$ and assume we are under* (**CS1**) *and* ($\mathbf{H}_\mathbf{s}^\mathbf{r}$). *Then, For any $x \in \mathcal{A}$ and $j \in \mathcal{J}_n$, one has got*

$$\mathbb{E}[|\eta(x) - \eta_j^{@}(x)|^p] \leq C(p) \pi_n^p \max\left(2^{-js}, \frac{2^{j\frac{d}{2}}}{\sqrt{n}}\right)^p,$$

where

$$C(p) = 3^p M^p \max(1, R^{2d} \mu_{\max})^p + C_5(r,d,p,\mu_{\max}; K, \sigma) + 2M^p R^{2d},$$

and C_5 is made explicit in the proof at eq. (5.24).

Proof. For any $x \in \mathcal{A}$, take $\delta = 3M 2^{-js} \max(1, 3\pi_n R^d \mu_{\max})$. Notice first that $\max(1, 3\pi_n R^d \mu_{\max}) \leq \pi_n \max(1, 3R^d \mu_{\max})$ since, by construction, $\pi_n^{-1} \leq 1$ in any case. Now, write

$$\begin{aligned}\mathbb{E}[|\eta(x) - \eta_j^{@}(x)|^p] &= \int_{\mathbb{R}^+} p t^{p-1} \mathbb{P}(|\eta(x) - \eta_j^{@}(x)| \geq t) dt \\ &\leq \delta^p + \int_\delta^{+\infty} p t^{p-1} \mathbb{P}(|\eta(x) - \eta_j^{@}(x)| \geq t) dt.\end{aligned}$$

As δ has been fixed, we only need to tackle the rhs above, which we will denote by II. Using Theorem 5.7.1, we can write

$$II \leq 2R^{2d} \exp\left(-n2^{-jd} \frac{\pi_n^{-2}}{2\mu_{\max} R^{4d} + \frac{4}{3} R^{2d} \pi_n^{-1}}\right) \int_0^M p t^{p-1} dt + R^d \int_0^\infty p t^{p-1} \Lambda\left(\frac{t 2^{-j\frac{d}{2}}}{2\pi_n R^d}\right) dt.$$

Denote by II_1 and II_2 the lhs and rhs terms above, respectively. Now, recall that $j \leq J$, where $2^{Jd} \leq nt(n)^{-2}$ and $t(n)^2 = \kappa \pi_n^2 \log n$. Therefore, as soon as

$$\kappa \geq \frac{p}{2}\left(2\mu_{\max} R^{4d} + \frac{4}{3} R^{2d} \pi_n^{-1}\right),$$

we have $II_1 \leq 2M^p R^{2d} n^{-\frac{p}{2}}$. Let us now turn to II_2. Assume first that we are working under the bounded noise assumption, (**N1**). In that case, we have

$$\begin{aligned} II_2 &\leq 2R^d \int_0^\infty p t^{p-1} \exp\left(-\frac{n 2^{-jd} t^2 \pi_n^{-2}}{64K^2 R^{2d} \mu_{\max} + 8KR^d \pi_n^{-1} t}\right) dt \\ &\leq C_2(r, d, p, \mu_{\max}, K) \left(\pi_n \frac{2^{j\frac{d}{2}}}{\sqrt{n}}\right)^p. \end{aligned}$$

where the last inequality results from the change of variable $u = \sqrt{n} 2^{-j\frac{d}{2}} \pi_n^{-1} t$ together with the fact that $2^{jd} \leq n$ and we have written

$$C_2 := 2R^d \int_0^\infty p t^{p-1} \exp\left(-\frac{t^2}{64K^2 R^{2d} \mu_{\max} + 8KR^d t}\right) dt.$$

Assume now that we are working under the Gaussian noise assumption (**N2**). In that case, we have

$$\begin{aligned} II_2 \leq R^d \int_0^\infty p t^{p-1} \Bigg(1 \wedge \Bigg\{ &\frac{2\sigma R^{\frac{d}{2}} (4R^d \mu_{\max} + 2t\pi_n^{-1})^{\frac{1}{2}}}{t \pi_n^{-1} 2^{-j\frac{d}{2}} \sqrt{2\pi n}} \\ &\exp\left(-\frac{n 2^{-jd} \pi_n^{-2} t^2 \sigma^{-2}}{4R^{2d} \mu_{\max} + 2R^d \pi_n^{-1} t}\right) \Bigg\}\Bigg) dt \\ + 2R^d \int_0^\infty p t^{p-1} &\exp\left(-\frac{n 2^{-jd} \pi_n^{-2} t^2}{8R^{2d} \mu_{\max} + \frac{8}{3} R^d \pi_n^{-1} t}\right) dt. \end{aligned}$$

Denote by II_3 and II_4 the first and second term, respectively. They can both be handled in the exact same way as II_2, which leads to

$$II_4 \leq C_4(r, d, p, \mu_{\max}) \left(\pi_n \frac{2^{j\frac{d}{2}}}{\sqrt{n}}\right)^p,$$

where we have written

$$C_4 := 2R^d \int_0^\infty pt^{p-1} \exp\left(-\frac{t^2}{8R^{2d}\mu_{\max} + \frac{8}{3}R^d t}\right) dt,$$

and

$$II_3 \leq C_3(r, d, p, \mu_{\max}, \sigma) \left(\pi_n \frac{2^{j\frac{d}{2}}}{\sqrt{n}}\right)^p,$$

where we have written

$$C_3 := R^d \int_0^\infty pt^{p-1} \left(1 \wedge \left\{ \frac{2\sigma R^{\frac{d}{2}}(4R^d\mu_{\max} + 2t)^{\frac{1}{2}}}{t\sqrt{2\pi}} \right.\right.$$
$$\left.\left. \exp\left(-\frac{t^2\sigma^{-2}}{4R^{2d}\mu_{\max} + 2R^d t}\right)\right\}\right) dt.$$

To conclude, let us write

$$C_5(r, d, p, \mu_{\max}; K, \sigma) = \begin{cases} C_2(r, d, p, \mu_{\max}, K) & \text{under } (\mathbf{N1}) \\ C_3(r, d, p, \mu_{\max}, \sigma) + C_4(r, d, p, \mu_{\max}) & \text{under } (\mathbf{N2}) \end{cases} \tag{5.24}$$

Therefore, we ultimately obtain

$$\mathbb{E}[|\eta(x) - \eta_j^{@}(x)|^p] \leq \left(3^p M^p \max(1, 3R^d\mu_{\max})^p + C_5 + 2M^p R^{2d}\right)$$
$$\pi_n^p \max\left(2^{-js}, \frac{2^{j\frac{d}{2}}}{\sqrt{n}}\right)^p,$$

which concludes the proof. □

Proposition 5.12.2. *Fix r in $\mathbb{N}$ and assume we are under* (**CS1**) *and* ($\mathbf{H}_\mathbf{s}^\mathbf{r}$). *This means in particular that $s \in (0, r)$. Let j be such that $j_s \leq j \leq J$. Let $t(n)^2 = \kappa\pi_n^2 \log n$, and define*

$$C_9(r, d, \mu_{\max}, \pi_n; K, \sigma) := \begin{cases} C_6(r, d, \mu_{\max}, K, \pi_n), & \textit{under } (\mathbf{N1}) \\ C_6(r, d, \mu_{\max}, \sigma, \pi_n), & \textit{under } (\mathbf{N2}) \end{cases},$$

where C_6 is defined in eq. (5.25) below. Then we have, for n large enough,

$$\mathbb{P}\left(|\eta_j^{@}(x) - \eta(x)| > \frac{2^{j\frac{d}{2}}}{\sqrt{n}} t(n)\right) \leq 5R^{2d} n^{-\kappa C_9}.$$

Proof. The proof relies on a direct application of Theorem 5.7.1. Write $C_0 = 2M \max(1, 3\pi_n R^d \mu_{\max})$ and notice indeed that the theorem applies since for $j \geq j_s$, we get $2^{j\frac{d}{2}} n^{-\frac{1}{2}} \geq 2^{-(r+\frac{d}{2})} 2^{-j_s s}$ (see eq. (5.10b)) and, as soon as n is large enough, we have $t(n) \geq 2^{r+\frac{d}{2}} C_0$. This leads us to

$$\mathbb{P}\left(|\eta_j^{@}(x) - \eta(x)| > \frac{2^{j\frac{d}{2}}}{\sqrt{n}} t(n)\right) \leq 2R^{2d} \exp\left(-n2^{-jd} \frac{\pi_n^{-2}}{2\mu_{\max} R^{4d} + \frac{4}{3}R^{2d}\pi_n^{-1}}\right)$$
$$+ R^d \Lambda\left(\frac{t(n)}{2\pi_n R^d \sqrt{n}}\right).$$

Let us denote the first term by I and the second one by II. I is easily tackled noticing that for $j \leq J$, $n2^{-jd} \geq n2^{-Jd} \geq t(n)^2 = \kappa\pi_n^2 \log n$. So that, we obtain $I \leq 2R^{2d}n^{-\kappa C_6}$, where we have written

$$C_6(r,d,\mu_{\max},K,\pi_n) := \frac{\min(1,K^{-2})}{64\mu_{\max}R^{2d} + 8R^d\pi_n^{-1}}. \tag{5.25}$$

Let us now turn to II. Assume first we work under (**N1**). Then we can write

$$II \leq 2R^d \exp\left(-\frac{t(n)^2\pi_n^{-2}}{64R^{2d}K^2\mu_{\max} + 8R^dK\pi_n^{-1}\frac{2^{j\frac{d}{2}}t(n)}{\sqrt{n}}}\right).$$

Notice first that $2^{j\frac{d}{2}}t(n) \leq \sqrt{n}$. Therefore, we obtain $II \leq 2R^dn^{-\kappa C_6}$. Assume now that we work under (**N2**). In that case, we obtain

$$\begin{aligned} II \leq R^d\Bigg(1 \wedge \Bigg\{ & \frac{2R^{\frac{d}{2}}\sigma(4R^d\mu_{\max} + 2\pi_n^{-1}\frac{2^{j\frac{d}{2}}t(n)}{\sqrt{n}})^{\frac{1}{2}}}{t(n)\pi_n^{-1}\sqrt{2\pi}} \\ & \exp\left(-\frac{t(n)^2\pi_n^{-2}\sigma^{-2}}{4R^{2d}\mu_{\max} + 2R^d\pi_n^{-1}\frac{2^{j\frac{d}{2}}t(n)}{\sqrt{n}}}\right)\Bigg\}\Bigg) \\ & + 2R^d\exp\left(-\frac{t(n)^2\pi_n^{-2}}{8R^{2d}\mu_{\max} + \frac{8}{3}R^d\pi_n^{-1}\frac{2^{j\frac{d}{2}}t(n)}{\sqrt{n}}}\right). \end{aligned}$$

We proceed exactly as under (**N1**). So that we obtain $II \leq C_7n^{-\kappa C_8}$, where

$$\begin{aligned} C_8(r,d,\mu_{\max},\sigma,\pi_n) &:= \frac{\min(1,\sigma^{-2})}{4R^{2d}\mu_{\max} + 2R^d\pi_n^{-1}}, \\ C_7(r,d,\mu_{\max},\sigma,\pi_n,t(n)) &= R^d\frac{2R^{\frac{d}{2}}\sigma(4R^d\mu_{\max} + 2\pi_n^{-1})^{\frac{1}{2}}}{t(n)\pi_n^{-1}\sqrt{2\pi}} + 2R^d. \end{aligned}$$

So that $C_7 \leq 3R^d$ for n large enough. Notice finally that $C_8(r,d,\mu_{\max},t,\pi_n) \geq C_6(r,d,\mu_{\max},t,\pi_n)$. This concludes the proof. □

Proposition 5.12.3. *Fix an integer $r \geq 2$ and assume we are under (**CS1**). Let $x \in \mathcal{A}$ and $j \in \mathcal{J}_n$. By construction, there exists $\mathcal{H} \in \mathcal{F}_j$ such that $x \in \mathcal{H}$. Recall besides that $\#\mathcal{S}_j(\mathcal{H}) = R^d$, where $R = 2r-1$ is obviously independent of both x and j. Write $\|.\| = \|.\|_{\ell_2(\mathbb{R}^{R^d})}$ and assume there exists a strictly positive constant $g_{\min}$ independent of x and j such that*

$$\lambda_{\min}(\mathbb{E}Q_{\mathcal{H}}) = \min_{u\in\mathbb{R}^{R^d}:\|u\|=1} \langle u, \mathbb{E}Q_{\mathcal{H}}u\rangle \geq g_{\min}. \tag{5.26}$$

Then, for any real number t such that $0 < t \leq \frac{g_{\min}}{2}$, we have

$$\mathbb{P}(\lambda_{\min}(Q_{\mathcal{H}}) \leq t) \leq 2R^{2d}\exp\left(-n2^{-jd}\frac{t^2}{2\mu_{\max}R^{4d} + \frac{4}{3}R^{2d}t}\right).$$

Proof. Under the assumption described in eq. (5.26), we get

$$\begin{aligned}\lambda_{\min}(Q_{\mathcal{H}}) &\geq \min_{u\in\mathbb{R}^{R^d}:\|u\|=1} \langle u, \mathbb{E}Q_{\mathcal{H}} u\rangle + \min_{u\in\mathbb{R}^{R^d}:\|u\|=1} \langle u, (Q_{\mathcal{H}} - \mathbb{E}Q_{\mathcal{H}})u\rangle \\ &\geq 2t - \sum_{\nu,\nu'\in\mathcal{S}_j(\mathcal{H})} |[Q_{\mathcal{H}}]_{\nu,\nu'} - [\mathbb{E}Q_{\mathcal{H}}]_{\nu,\nu'}|.\end{aligned}$$

Write $T_i = \varphi_{j,\nu}(X_i)\varphi_{j,\nu'}(X_i)\mathbb{1}_{\mathcal{H}}(X_i) - \mathbb{E}\varphi_{j,\nu}(X)\varphi_{j,\nu'}(X)\mathbb{1}_{\mathcal{H}}(X)$, so that $\mathbb{E}T_i = 0$, $\mathbb{V}\mathrm{ar}T_i \leq \mu_{\max}2^{jd}$ and $|T_i| \leq 2^{jd+1}$. A direct application of Bernstein inequality for any $\delta > 0$ leads to

$$\begin{aligned}&\mathbb{P}(|[Q_{\mathcal{H}}]_{\nu,\nu'} - [\mathbb{E}Q_{\mathcal{H}}]_{\nu,\nu'}| \geq \delta) \\ &= \mathbb{P}(|\frac{1}{n}\sum_{i=1}^{n} \varphi_{j,\nu}(X_i)\varphi_{j,\nu'}(X_i)\mathbb{1}_{\mathcal{H}}(X_i) - \mathbb{E}\varphi_{j,\nu}(X)\varphi_{j,\nu'}(X)\mathbb{1}_{\mathcal{H}}(X)| \geq \delta) \\ &\leq 2\exp\left(-\frac{n2^{-jd}\delta^2}{2\mu_{\max} + \frac{4}{3}\delta}\right).\end{aligned}$$

To conclude, we write

$$\begin{aligned}\mathbb{P}(\lambda_{\min}(Q_{\mathcal{H}}) \leq t) &\leq \mathbb{P}(\sum_{\nu,\nu'\in\mathcal{S}_j(\mathcal{H})} |[Q_{\mathcal{H}}]_{\nu,\nu'} - [\mathbb{E}Q_{\mathcal{H}}]_{\nu,\nu'}| \geq t) \\ &\leq 2R^{2d}\exp\left(-n2^{-jd}\frac{t^2}{2\mu_{\max}R^{4d} + \frac{4}{3}R^{2d}t}\right).\end{aligned}$$

□

Proposition 5.12.4. *Fix an integer $r \geq 2$ and assume we are under* (**CS1**). *For any $x \in \mathcal{A}$ and $j \in \mathcal{J}_n$, we denote by $\mathcal{H}$ the unique hypercube of $\mathcal{F}_j$ such that $x \in \mathcal{H}$. Then, there exists a strictly positive absolute constant $g_{\min}$ independent of both x and j such that, for all $j \in \mathcal{J}_n$ and all $x \in \mathcal{A}$, we have $\lambda_{\min}(\mathbb{E}Q_{\mathcal{H}}) \geq g_{\min} > 0$.*

Proof. For any $u \in \mathbb{R}^{R^d}$ such that $\|u\|_{\ell_2(\mathbb{R}^{R^d})} = 1$, we can write

$$\begin{aligned}\langle u, \mathbb{E}Q_{\mathcal{H}} \cdot u\rangle &= \int_{\mathcal{A}} \left(\sum_{\nu\in\mathcal{S}_j(\mathcal{H})} u_\nu \varphi_{j,\nu}(w)\mathbb{1}_{\mathcal{H}}(w)\right)^2 \mu(w)dw \\ &\geq \mu_{\min}\int_{\mathcal{H}} \left(\sum_{\nu\in\mathcal{S}_j(\mathcal{H})} u_\nu\varphi_{j,\nu}(w)\right)^2 dw, \qquad (5.27) \\ &= \mu_{\min}\int_{[0,1]^d} \left(\sum_{\nu\in\mathfrak{S}} u_\nu\varphi_\nu(w)\right)^2 dw, \qquad (5.28)\end{aligned}$$

where $\mathfrak{S}$ has been defined in eq. (5.15) and the last equality results from the fact that the value of the integral on the rhs of eq. (5.27) is invariant with $\mathcal{H}$, meaning that for any $\mathcal{H} \in \mathcal{F}_j$ and

$u \in \mathbb{R}^{R^d}$,

$$\begin{aligned}
&\int_{\mathcal{H}} \left(\sum_{\nu \in \mathcal{S}_j(\mathcal{H})} u_\nu \varphi_{j,\nu}(w) \right)^2 dw \\
&= \int_{2^{-j}[0,1]^d} \left(\sum_{\nu \in \mathcal{S}_j(2^{-j}[0,1]^d)} u_\nu \varphi_{j,\nu}(w) \right)^2 dw \\
&= \int_{[0,1]^d} \left(\sum_{\nu \in \mathfrak{S}} u_\nu \varphi_\nu(w) \right)^2 dw.
\end{aligned}$$

Let us denote by $\mathbb{S}^{R^d-1}$ the unit-sphere of $\mathbb{R}^{R^d}$. As detailed in the proof of Lemma 5.12.1, the map

$$u \in \mathbb{S}^{R^d-1} \mapsto \int_{[0,1]^d} \left(\sum_{\nu \in \mathfrak{S}} u_\nu \varphi_\nu(w) \right)^2 dw,$$

is absolutely continuous with respect to u on the compact subset $\mathbb{S}^{R^d-1}$ of $\mathbb{R}^{R^d}$. It therefore reaches its minimum at some point $u^* \in \mathbb{S}^{R^d-1}$. It is a direct consequence of the **local linear independence property** of the scaling functions (φ_k) (see Proposition 5.12.8) that

$$\int_{[0,1]^d} \left(\sum_{\nu \in \mathfrak{S}} u^*_\nu \varphi_\nu(w) \right)^2 dw = c_{\min} > 0,$$

where $c_{\min}$ is a constant that is both independent from x and j. This concludes the proof with $g_{\min} = \mu_{\min} c_{\min}$. □

Proposition 5.12.5. *Fix $r = 1$ and assume we are under (**CS1**). Let $x \in \mathcal{A}$, $j \in \mathcal{J}_n$ and $\mathcal{H} \in \mathcal{F}_j$ such that $x \in \mathcal{H}$. Then, for any real number t such that $0 < t \leq \frac{g_{\min}}{2}$, we have $2^{jd}\frac{n_{\mathcal{H}}}{n} \geq t$ on the event $\Omega^c_{j,\nu(\mathcal{H})}(t)$, where $\Omega_{j,\nu(\mathcal{H})}(t) := \{\frac{1}{n}\sum_{i=1}^n \varphi_{j,\nu(\mathcal{H})}(X_i)^2 < t\}$. In addition, we have got*

$$\mathbb{P}(\Omega_{j,\nu(\mathcal{H})}(t)) \leq 2\exp\left(-n2^{-jd} \frac{t^2}{2\mu_{\max} + \frac{4}{3}t} \right).$$

Recall that the constant $g_{\min}$ has been defined in Proposition 5.12.4.

Proof. Notice that

$$\int \varphi_{j,\nu(\mathcal{H})}(w)^2 \mu(w) dw \geq \mu_{\min} \geq 2t. \tag{5.29}$$

On $\Omega^c_{j,\nu(\mathcal{H})}(t)$, we have

$$2^{jd}\frac{n_{\mathcal{H}}}{n} \geq \frac{1}{n}\sum_{i=1}^n \varphi_{j,\nu(\mathcal{H})}(X_i)^2 \geq t.$$

For any $\delta > 0$, we write

$$\mathcal{C}_{j,k}(\delta) = \left\{ |\frac{1}{n}\sum_{i=1}^{n} \varphi_{j,k}(X_i)^2 - \mathbb{E}\varphi_{j,k}(X)^2| \leq \delta \right\}. \tag{5.30}$$

Notice now that

$$\Omega_{j,\nu(\mathcal{H})}(t) \subset \{\frac{1}{n}\sum_{i=1}^{n} \varphi_{j,\nu(\mathcal{H})}(X_i)^2 - \mathbb{E}\varphi_{j,\nu(\mathcal{H})}(X_i)^2 < -t\} \subset \mathcal{C}^c_{j,\nu(\mathcal{H})}(t),$$

where $\mathcal{C}_{j,\nu(\mathcal{H})}(t)$ is defined in eq. (5.30). Finally, it is straightforward that $\mathcal{C}^c_{j,\nu(\mathcal{H})}(t)$ has very small probability thanks to Bernstein inequality (see [94, p. 165] for example). Write indeed $T_i = \varphi_{j,\nu(\mathcal{H})}(X_i)^2 - \mathbb{E}\varphi_{j,\nu(\mathcal{H})}(X)^2$. Then $\mathbb{E}T_i = 0$, $\mathbb{V}\mathrm{ar}T_i \leq \mu_{\max} 2^{jd}$ and $|T_i| \leq 2^{jd+1}$. Thus, we can write

$$\mathbb{P}(\mathcal{C}^c_{j,\nu(\mathcal{H})}(t)) \leq 2\exp\left(-n2^{-jd}\frac{t^2}{2\mu_{\max} + \frac{4}{3}t}\right),$$

which concludes the proof. □

Proposition 5.12.6. *Let $(X_i)_{i=1,\dots,n}$ and $(\xi_i)_{i=1,\dots,n}$ be sequences of independent random variables such that $\mathbb{E}(\xi|X) = 0$. Take any $j \geq j_r$. Moreover, assume we are given a function $\mathscr{R}_j(.)$ such that $\|\mathscr{R}_j(.)\|_{\mathbb{L}_\infty(\Omega,\lambda)} \leq M2^{-js}$, a subset $\mathcal{H}$ of Ω and a scaling function $\varphi_{j,k}$. Write*

$$W_{j,k} = \frac{1}{n}\sum_{i=1}^{n} \varphi_{j,k}(X_i)\mathbb{1}_{\mathcal{H}}(X_i)(\mathscr{R}_j(X_i) + \xi_i),$$

and define

$$\Lambda(\delta) = \begin{cases} 2\exp\left(-\dfrac{n\delta^2}{18K^2\mu_{\max} + 4K2^{j\frac{d}{2}}\delta}\right), & \text{under } (\mathbf{N1}) \\ 1 \wedge \left\{\dfrac{2\sigma(\mu_{\max} + 2^{j\frac{d}{2}}\delta)^{\frac{1}{2}}}{\delta\sqrt{2\pi n}}\exp\left(-\dfrac{n\delta^2\sigma^{-2}}{\mu_{\max} + 2^{j\frac{d}{2}}\delta}\right)\right\} & \\ \quad +2\exp\left(-\dfrac{n\delta^2}{2\mu_{\max} + \frac{4}{3}2^{j\frac{d}{2}}\delta}\right), & \text{under } (\mathbf{N2}) \end{cases}$$

Then, for all $\delta > 3\mu_{\max}M2^{-j(s+\frac{d}{2})}$, we have

$$\mathbb{P}(|W_{j,k}| \geq \delta) \leq \Lambda(\delta).$$

Proof. Notice indeed that

$$\begin{aligned} W_{j,k} &\leq |\frac{1}{n}\sum_{i=1}^{n}\varphi_{j,k}(X_i)\xi_i\mathbb{1}_{\mathcal{H}}(X_i)| \\ &+ |\frac{1}{n}\sum_{i=1}^{n}\varphi_{j,k}(X_i)\mathscr{R}_j(X_i)\mathbb{1}_{\mathcal{H}}(X_i) - \mathbb{E}\varphi_{j,k}(X)\mathscr{R}_j(X)\mathbb{1}_{\mathcal{H}}(X)| \\ &+ |\mathbb{E}\varphi_{j,k}(X)\mathscr{R}_j(X)\mathbb{1}_{\mathcal{H}}(X)| \\ &= I + II + III. \end{aligned}$$

So that we can write

$$\mathbb{P}(|W_{j,k}| \geq \delta) \leq \mathbb{P}(I \geq \delta/3) + \mathbb{P}(II \geq \delta/3) + \mathbb{P}(III \geq \delta/3).$$

Now it is enough to notice that

$$\begin{aligned} III &\leq \int |\varphi_{j,k}(w)\mathscr{R}_j(w)|\mathbb{1}_{\mathcal{H}}(w)\mu(w)dw \\ &\leq \mu_{\max}\int_{\Omega}|\varphi_{j,k}(w)\mathscr{R}_j(w)|dw \\ &\leq \mu_{\max}\|\varphi_{j,k}\|_{\mathbb{L}_1(\Omega,\lambda)}\|\mathscr{R}_j\|_{\mathbb{L}_\infty(\Omega,\lambda)} \\ &\leq \mu_{\max}M2^{-j(s+\frac{d}{2})}. \end{aligned}$$

So that $\mathbb{P}(III \geq \delta/3) = 0$ as soon as $\delta > 3\mu_{\max}M2^{-j(s+\frac{d}{2})}$.
Now, turn to II and write $II = |\sum T_i/n|$ with $T_i = \varphi_{j,k}(X_i)\mathscr{R}_j(X_i)\mathbb{1}_{\mathcal{H}}(X_i) - \mathbb{E}\varphi_{j,k}(X)\mathscr{R}_j(X)\mathbb{1}_{\mathcal{H}}(X)$. Obviously $\mathbb{E}T_i = 0$, $\mathbb{V}\mathrm{ar}T_i \leq \mathbb{E}(\varphi_{j,\nu}(X)\mathscr{R}_j(X)\mathbb{1}_{\mathcal{H}}(X))^2 \leq \mu_{\max}M^2 2^{-2js}$ and $|T_i| \leq M2^{-js}2^{j\frac{d}{2}+1}$. So that we can apply Bernstein inequality to get

$$\mathbb{P}(II \geq \delta/3) \leq 2\exp\left(-\frac{n2^{2js}\delta^2}{18\mu_{\max}M^2 + 4M2^{j\frac{d}{2}}2^{js}\delta}\right).$$

And finally, turn to III. Assume first that the noise ξ is bounded by K. We have obviously $\mathbb{E}\varphi_{j,k}(X_i)\xi_i\mathbb{1}_{\mathcal{H}}(X_i) = 0$, $\mathbb{V}\mathrm{ar}(\varphi_{j,k}(X_i)\xi_i\mathbb{1}_{\mathcal{H}}(X_i)) \leq K^2\mu_{\max}$ and $|\varphi_{j,k}(X_i)\xi_i\mathbb{1}_{\mathcal{H}}(X_i)| \leq K2^{j\frac{d}{2}+1}$, so that

$$\mathbb{P}(I \geq \delta/3) \leq 2\exp\left(-\frac{n\delta^2}{18K^2\mu_{\max} + 4K2^{j\frac{d}{2}}\delta}\right).$$

Now, it is enough to notice that for all $s > 0$ and j such that $j \geq \frac{1}{s}\log_2\frac{M}{K}$ (which becomes a constraint for $K < M$ only),

$$\frac{n2^{2js}\delta^2}{18\mu_{\max}M^2 + 4M2^{j\frac{d}{2}}2^{js}\delta} \geq \frac{n\delta^2}{18K^2\mu_{\max} + 4K2^{j\frac{d}{2}}\delta},$$

which concludes the proof under (**N1**). When $j \geq \frac{1}{s}\log_2 3M$, the conclusion under (**N2**) is a direct consequence of Proposition 5.12.7. □

Proposition 5.12.7. *Let $\varphi_{j,k}$ be a scaling function and $\mathcal{H}$ a subset of Ω. Define*

$$I = \frac{1}{n}\sum_{i=1}^{n} \varphi_{j,k}(X_i)\xi_i \mathbb{1}_{\mathcal{H}}(X_i).$$

Assume now that the noise ξ is conditionally Gaussian, that is we are under (**N2**). *Then, we notice that, conditionally on $X_1,\dots,X_n$, $I \sim \Phi(0, \sigma\rho_{j,k}/\sqrt{n})$, where $\rho_{j,k}^2 = n^{-1}\sum_{i=1}^n \varphi_{j,k}(X_i)^2\mathbb{1}_{\mathcal{H}}(X_i)$. Then, for all $\delta > 0$, one can write*

$$\mathbb{P}(|I| \geq \delta) \leq 1 \wedge \left\{ \frac{2\sigma(\mu_{\max} + 2^{j\frac{d}{2}}\delta)^{\frac{1}{2}}}{\delta\sqrt{2\pi n}} \exp\left(-\frac{n\delta^2\sigma^{-2}}{\mu_{\max} + 2^{j\frac{d}{2}}\delta}\right)\right\} + 2\exp\left(-\frac{n\delta^2}{2\mu_{\max} + \frac{4}{3}2^{j\frac{d}{2}}\delta}\right).$$

Proof. For any $\delta > 0$, we write

$$\mathcal{C}_{j,k}(\delta) = \left\{ |\frac{1}{n}\sum_{i=1}^{n} \varphi_{j,k}(X_i)^2\mathbb{1}_{\mathcal{H}}(X_i) - \mathbb{E}\varphi_{j,k}(X)^2\mathbb{1}_{\mathcal{H}}(X)| \leq \delta \right\}.$$

Notice first that

$$\mathcal{C}_{j,k}(2^{j\frac{d}{2}}\delta) \subset \{\rho_{j,k}^2 \leq \mu_{\max} + 2^{j\frac{d}{2}}\delta\}.$$

So that

$$\begin{aligned}\mathbb{1}_{\{|I|\geq\delta\}} &\leq \mathbb{1}_{\{|I|\geq\delta\}}\mathbb{1}_{\{\rho_{j,k}^2 \leq \mu_{\max}+2^{j\frac{d}{2}}\delta\}} + \mathbb{1}_{\{|I|\geq\delta\}}\mathbb{1}_{\mathcal{C}_{j,k}^c(2^{j\frac{d}{2}}\delta)} \\ &\leq \mathbb{1}_{\{|I|\geq\delta\}}\mathbb{1}_{\{\rho_{j,k}^2 \leq \mu_{\max}+2^{j\frac{d}{2}}\delta\}} + \mathbb{1}_{\mathcal{C}_{j,k}^c(2^{j\frac{d}{2}}\delta)}.\end{aligned}$$

The first term is handled thanks to a regular Gaussian tail inequality. Notice indeed that

$$\begin{aligned}&\mathbb{P}(|I| \geq \delta | X_1,\dots,X_n)\mathbb{1}_{\{\rho_{j,k}^2 \leq \mu_{\max}+2^{j\frac{d}{2}}\delta\}} \\ &\quad\leq 1 \wedge \left\{ \frac{2\rho_{j,k}\sigma}{\delta\sqrt{2\pi n}} \exp\left(-\frac{n\delta^2}{\rho_{j,k}^2\sigma^2}\right)\right\}\mathbb{1}_{\{\rho_{j,k}^2 \leq \mu_{\max}+2^{j\frac{d}{2}}\delta\}} \\ &\quad\leq 1 \wedge \left\{ \frac{2\sigma(\mu_{\max} + 2^{j\frac{d}{2}}\delta)^{\frac{1}{2}}}{\delta\sqrt{2\pi n}} \exp\left(-\frac{n\delta^2\sigma^{-2}}{\mu_{\max} + 2^{j\frac{d}{2}}\delta}\right)\right\}.\end{aligned}$$

In addition, notice that $\mathbb{E}\varphi_{j,k}(X)^4\mathbb{1}_{\mathcal{H}}(X) \leq \mu_{\max}2^{jd}$ and $|\varphi_{j,k}(X)^2\mathbb{1}_{\mathcal{H}}(X_i) - \mathbb{E}\varphi_{j,k}(X)^2\mathbb{1}_{\mathcal{H}}(X)| \leq 2^{jd+1}$, so that a direct application of Bernstein inequality leads to

$$\mathbb{P}(\mathcal{C}_{j,k}(2^{j\frac{d}{2}}\delta)^c) \leq 2\exp\left(-\frac{n2^{jd}\delta^2}{2^{jd}(2\mu_{\max} + \frac{4}{3}2^{j\frac{d}{2}}\delta)}\right) = 2\exp\left(-\frac{n\delta^2}{2\mu_{\max} + \frac{4}{3}2^{j\frac{d}{2}}\delta}\right),$$

which concludes the proof. □

***5.12.2 Proof of the upper-bound results under* (CS2).** Recall that under (**CS2**), we work with a sample of size $2n$ split into two pieces denoted by $\mathcal{D}_n$ and $\mathcal{D}'_n$. As detailed previously, similar results as the ones described in Section 5.7, Section 5.8 and Section 5.12.1.4 are still valid with $\eta^{\maltese}$ under (**CS2**). They in fact all stem from Theorem 5.9.1. The proofs remain for the most part unchanged, with $\mathcal{J}_n$ redefined as $\mathcal{J}_n = \{j_s, j_s+1, \dots, J-1, J\}$ where $2^{j_s} = \lfloor n^{\frac{1}{2s+d}} \rfloor$, $\eta^{\maltese}$ in place of $\eta^{@}$, $\widetilde{X}_i$ in place of X_i (where we have written $\widetilde{u} = u - X'_{i_x} + 2^{-j-1}$), and $\mathcal{H}_0$ in place of $\mathcal{H}$. The sole differences appear in the proofs of Theorem 5.9.1, Proposition 5.12.4 and Proposition 5.12.5. Let us start with the proof of Theorem 5.9.1.

Proof of Theorem 5.9.1. Assume we are under (**CS2**) and want to control the probability of deviation of $\eta_j^{\maltese}(x)$ from $\eta(x)$ at a point $x \in \mathcal{A}$, for some $j \in \mathcal{J}_n$. Recall that $\mathcal{H}_0(x)$ stands for the cell $\mathcal{H}_0 = 2^{-j}[0,1]^d$ centered in x at level j, that is $\mathcal{H}_0(x) = x - 2^{-j-1} + 2^{-j}[0,1]^d$ and denote by $\mathcal{O}_x$ the event

$$\mathcal{O}_x = \{\#\{i : X'_i \in \mathcal{H}_0(x)\} \geq 1\}.$$

We can write

$$\begin{aligned}\mathbb{P}(|\eta(x) - \eta_j^{\maltese}(x)| \geq \delta) &= \mathbb{P}(|\eta(x) - \eta_j^{\maltese}(x)| \geq \delta, \mathcal{O}_x) \\ &\quad + \mathbb{P}(|\eta(x) - \eta_j^{\maltese}(x)| \geq \delta, \mathcal{O}_x^c).\end{aligned}$$

Focus first on what happens on the event $\mathcal{O}_x^c$. The last term can be controlled easily since the probability that no single design point X'_i of $\mathcal{D}'_n$ belongs to $\mathcal{H}_0(x)$ decreases exponentially fast with n. Notice indeed that, under (**CS2**),

$$\begin{aligned}\mathbb{P}(\mathcal{O}_x^c) &= (\mathbb{P}(X'_1 \notin \mathcal{H}_0(x)))^n \\ &= (1 - \mathbb{P}(X'_1 \in \mathcal{H}_0(x)))^n \\ &= \left(1 - \int_{\mathcal{A} \cap \mathcal{H}_0(x)} \mu(w)dw\right)^n \\ &\leq \left(1 - \mu_{\min} 2^{-jd} \lambda\left(2^j(\mathcal{A} - x) \cap [-2^{-1}, 2^{-1}]^d\right)\right)^n \\ &\leq (1 - \mu_{\min} 2^{-jd} \min(2\mathfrak{m}_0, 2^{-1})^d)^n \\ &\leq \exp(-\mu_{\min} \min(2\mathfrak{m}_0, 2^{-1})^d n 2^{-jd}),\end{aligned}$$

where the before last inequality is a direct consequence of (**S2**) and the last one comes from the fact that for any $x \in [0,1)$, $\ln(1-x) \leq -x$. Now, recall that $\eta_j^{\maltese}(x) = 0$ on $\mathcal{O}_x^c$ and $|\eta(x)| \leq M$ since $\eta \in \mathscr{L}^s(\mathbb{R}^d, M)$. So that we obtain

$$\mathbb{P}(|\eta(x) - \eta_j^{\maltese}(x)| \geq \delta, \mathcal{O}_x^c) \leq \exp(-\mu_{\min} \min(2\mathfrak{m}_0, 2^{-1})^d n 2^{-jd}) \mathbb{1}_{\{\delta \leq M\}},$$

which is smaller than the first term in the upper-bound of Theorem 5.9.1. Now focus on what happens on the event $\mathcal{O}_x$. We can write

$$\begin{aligned}\mathbb{P}(|\eta(x) - \eta_j^{\maltese}(x)| \geq \delta, \mathcal{O}_x) &= \mathbb{P}(\mathcal{O}_x)\mathbb{E}[\mathbb{P}(|\eta(x) - \eta_j^{\maltese}(x)| \geq \delta | X'_{i_x}) | \mathcal{O}_x] \\ &\leq \mathbb{E}[\mathbb{P}(|\eta(x) - \eta_j^{\maltese}(x)| \geq \delta | X'_{i_x}) | \mathcal{O}_x].\end{aligned}$$

Therefore, it is enough to control the probability of deviation of $\eta_j^{\maltese}(x)$ from $\eta(x)$ on $\mathcal{O}_x$, conditionally on X'_{i_x}. It is controlled in exactly the same way as the probability of deviation of $\eta_j^{@}(x)$ from $\eta(x)$ under (**CS1**), except that we now work with conditional probabilities and expectations with respect to X'_{i_x}. Interestingly, the random variable X'_{i_x} is independent of the points of $\mathcal{D}_n$ since it is built upon the design points (X'_i) of $\mathcal{D}'_n$ which are themselves independent of the points of $\mathcal{D}_n$. This is a key feature that makes theoretical computations tractable under (**CS2**) and allows to handle $\eta^{\maltese}$ in a similar way as $\eta^{@}$ under (**CS1**). As announced above, Proposition 5.12.4 and Proposition 5.12.5 are the sole results that are not obviously true under (**CS2**). However we show below that they can indeed be extended to setting (**CS2**) without much trouble. Ultimately, this proves that, on the event $\mathcal{O}_x$ and conditionally on X'_{i_x}, the probability of deviation of $\eta_j^{\maltese}(x)$ from $\eta(x)$ verifies Theorem 5.7.1. So that finally, it remains to put everything together to obtain the results announced in Theorem 5.9.1, which concludes the proof. □

Let us now show how the proofs of Proposition 5.12.4 and Proposition 5.12.5 can be extended to setting (**CS2**), thanks to the **local linear independence property** of the scaling functions (see Proposition 5.12.8) and a compactness argument.

Proof of Proposition 5.12.4 under (**CS2**). The proof of Proposition 5.12.4 under (**CS1**) breaks down under (**CS2**) at boundary points of $\mathcal{A}$. Eq. (5.28) is indeed not valid anymore under (**CS2**) since μ eventually cancels on the cell $\mathcal{H}_0(X'_{i_x})$ centered in X'_{i_x}. Recall however that $\mathcal{S}_j(\mathcal{H}_0) = \mathfrak{S} = \{\nu \in \mathbb{Z}^d : 2^{-1} \in \mathrm{Supp}\varphi_\nu\}$ is a set of indexes which is independent of both x and j. Recall that all computations at point x are performed conditionally on X'_{i_x} under (**CS2**). Recall that we write $\widetilde{w} = w - X'_{i_x} + 2^{-j-1}$. Given the independence of X'_{i_x} from the points of $\mathcal{D}_n$, we can write

$$
\begin{aligned}
&\langle u, \mathbb{E}[Q_{\mathcal{H}_0}|X'_{i_x}] \cdot u\rangle \\
&= \int_{\mathbb{R}^d} \left(\sum_{\nu\in\mathfrak{S}} u_\nu \varphi_{j,\nu}(\widetilde{w}) \mathbb{1}_{\mathcal{H}_0}(\widetilde{w})\right)^2 \mu(w)dw \\
&\geq \mu_{\min} \int_{\mathcal{A}\cap\mathcal{H}_0(X'_{i_x})} \left(\sum_{\nu\in\mathfrak{S}} u_\nu 2^{jd/2} \varphi(2^j(w - X'_{i_x}) + 2^{-1} - \nu)\right)^2 dw \\
&= \mu_{\min} \int_{2^j(\mathcal{A}-X'_{i_x})\cap[-2^{-1},2^{-1}]^d} \left(\sum_{\nu\in\mathfrak{S}} u_\nu \varphi_\nu(w + 2^{-1})\right)^2 dw \\
&\geq \mu_{\min} \inf_{\mathfrak{m}\geq\mathfrak{m}_0} \inf_{z\in\mathcal{B}_\infty(0,\mathfrak{m})} \int_{\mathcal{B}_\infty(z,\mathfrak{m})\cap[-2^{-1},2^{-1}]^d} \left(\sum_{\nu\in\mathfrak{S}} u_\nu \varphi_\nu(w + 2^{-1})\right)^2 dw \\
&= \mu_{\min} \inf_{\mathfrak{m}\geq\mathfrak{m}_0} \inf_{z\in\mathcal{B}_\infty(2^{-1},\mathfrak{m})} \int_{\mathcal{B}_\infty(z,\mathfrak{m})\cap[0,1]^d} \left(\sum_{\nu\in\mathfrak{S}} u_\nu \varphi_\nu(w)\right)^2 dw.
\end{aligned}
$$

Thus, a direct application of Lemma 5.12.1 leads to $\lambda_{\min}(\mathbb{E}[Q_{\mathcal{H}_0}|X'_{i_x}]) \geq \mu_{\min} c_{\min}$. This concludes the proof with $g_{\min} = \mu_{\min} c_{\min}$. □

Proof of Proposition 5.12.5 under (**CS2**). Recall first that $\widetilde{x} \in \mathcal{H}_0 = 2^{-j}[0,1]^d$ and $\nu(\mathcal{H}_0) = 0$. At points x located at the boundary of $\mathcal{A}$, the cell $\mathcal{H}_0(X'_{i_x}) = X'_{i_x} + 2^{-j}[-2^{-1}, 2^{-1}]^d$ centered in X'_{i_x} is eventually not a subset of $\mathcal{A}$ anymore, so that the proof of Proposition 5.12.5 breaks down at the level of eq. (5.29). Using the independence of X'_{i_x} from the points of $\mathcal{D}_n$, we can write

$$\begin{aligned}
\mathbb{E}[Q_{\mathcal{H}_0}|X'_{i_x}] &= \int \varphi_{j,\nu(\mathcal{H}_0)}(\widetilde{w})^2 \mu(w) dw \\
&\geq \mu_{\min} \int_{\mathcal{A}} 2^{jd} \varphi_{\nu(\mathcal{H}_0)}(2^j(w - X'_{i_x}) + 2^{-1})^2 dw \\
&= \mu_{\min} \int_{2^j(\mathcal{A} - X'_{i_x})} \varphi(w + 2^{-1})^2 dw \\
&\geq \mu_{\min} \inf_{\mathfrak{m} \geq \mathfrak{m}_0} \inf_{z \in \mathcal{B}_\infty(0,\mathfrak{m})} \int_{\mathcal{B}_\infty(z,\mathfrak{m})} \varphi(w + 2^{-1})^2 dw \\
&= \mu_{\min} \inf_{\mathfrak{m} \geq \mathfrak{m}_0} \inf_{z \in \mathcal{B}_\infty(2^{-1},\mathfrak{m})} \int_{\mathcal{B}_\infty(z,\mathfrak{m})} \varphi(w)^2 dw \\
&\geq \mu_{\min} c_{\min} \geq 2t,
\end{aligned}$$

where the before last inequality comes as a direct application of Lemma 5.12.1, eq. (5.32). The end of the proof follows the same lines as previously, under setting (**CS1**). □

The updated proofs hinge on the following results.

Lemma 5.12.1. *Let $r \in \mathbb{N}$. Let φ be the Daubechies' scaling function of regularity r and $\mathfrak{S} = \{\nu \in \mathbb{Z}^d : 2^{-1} \in Supp\varphi_\nu\}$. Then, there exists a strictly positive absolute constant $c_{\min}$ such that*

$$\inf_{u \in \mathbb{S}^{R^d - 1}} \inf_{\mathfrak{m} \geq \mathfrak{m}_0} \inf_{z \in \mathcal{B}_\infty(2^{-1},\mathfrak{m})} \int_{\mathcal{B}_\infty(z,\mathfrak{m}) \cap [0,1]^d} \left(\sum_{\nu \in \mathfrak{S}} u_\nu \varphi_\nu(w) \right)^2 dw \geq c_{\min}, \tag{5.31}$$

$$\inf_{\mathfrak{m} \geq \mathfrak{m}_0} \inf_{z \in \mathcal{B}_\infty(2^{-1},\mathfrak{m})} \int_{\mathcal{B}_\infty(z,\mathfrak{m})} \sum_{\nu \in \mathfrak{S}} \varphi_\nu(w)^2 dw \geq c_{\min}. \tag{5.32}$$

Proof. The proof of eq. (5.32) follows the same lines as the one of eq. (5.31). Therefore, we will only prove eq. (5.31). Now write $u = (u_\nu)_{\nu \in \mathfrak{S}}$ and $\varphi_{\mathfrak{S}}(.) = (\varphi_\nu(.))_{\nu \in \mathfrak{S}}$. Denote by $\mathbb{S}^{R^d - 1}$ the unit sphere of $\mathbb{R}^{R^d}$. Consider the map defined by

$$\begin{aligned}
f_{\mathfrak{m}} :& \mathcal{B}_\infty(2^{-1}, \mathfrak{m}) \times \mathbb{S}^{R^d - 1} \mapsto \mathbb{R}, \\
f_{\mathfrak{m}}(z, u) &= \int_{\mathcal{B}_\infty(z,\mathfrak{m}) \cap [0,1]^d} \langle u, \varphi_{\mathfrak{S}}(w) \rangle^2 dw.
\end{aligned}$$

Notice first that, u being fixed, $\inf_{z \in \mathcal{B}_\infty(2^{-1},\mathfrak{m})} f_{\mathfrak{m}}(z,u)$ is an increasing function of $\mathfrak{m}$, since the integrand is positive and for $\mathfrak{m}_1 \geq \mathfrak{m}_2$, for all $z_1 \in \mathcal{B}_\infty(2^{-1}, \mathfrak{m}_1)$, we can find $z_2 \in \mathcal{B}_\infty(2^{-1}, \mathfrak{m}_2)$ such that $\mathcal{B}_\infty(z_2, \mathfrak{m}_2) \subset \mathcal{B}_\infty(z_1, \mathfrak{m}_1)$. So that $\inf_{\mathfrak{m} \geq \mathfrak{m}_0} \inf_{z \in \mathcal{B}_\infty(2^{-1},\mathfrak{m})} f_{\mathfrak{m}}(z,u)$ reduces in fact to $\inf_{z \in \mathcal{B}_\infty(2^{-1},\mathfrak{m}_0)} f_{\mathfrak{m}_0}(z,u)$. From now on, let us write f in place of $f_{\mathfrak{m}_0}$ and prove that f is continuous on its domain. We have indeed

$$|f(z_2,u_2) - f(z_1,u_1)| \leq |f(z_2,u_2) - f(z_1,u_2)| + |f(z_1,u_2) - f(z_1,u_1)|.$$

And

$$|f(z_1,u_2)-f(z_1,u_1)| \leq \int_{\mathcal{B}_\infty(z_1,\mathfrak{m}_0)\cap[0,1]^d} |\langle u_2-u_1,\varphi_{\mathfrak{S}}(w)\rangle||\langle u_2+u_1,\varphi_{\mathfrak{S}}(w)\rangle| dw$$
$$\leq 2R^d \|\varphi\|^2_{\mathbb{L}_\infty(\mathbb{R}^d)} \|u_2-u_1\|_{\ell_2(\mathbb{R}^{R^d})}.$$

Besides, noticing that

$$\mathbb{1}_{\mathcal{B}_\infty(z_1,\mathfrak{m}_0)}(w) = \mathbb{1}_{[0,2\mathfrak{m}_0]^d}(w-z_1+\mathfrak{m}_0) = \mathbb{1}_{[0,1]^d}(\frac{w-z_1+\mathfrak{m}_0}{2\mathfrak{m}_0}),$$

we can write

$$\begin{aligned}
&|f(z_2,u_2)-f(z_1,u_2)| \\
&\leq \int_{[0,1]^d} |\mathbb{1}_{\mathcal{B}_\infty(z_2,\mathfrak{m}_0)}(w)-\mathbb{1}_{\mathcal{B}_\infty(z_1,\mathfrak{m}_0)}(w)|\langle u_2,\varphi_{\mathfrak{S}}(w)\rangle dw \\
&\leq R^{d/2}\|\varphi\|_{\mathbb{L}_\infty(\mathbb{R}^d)} 2\mathfrak{m}_0 \int_{\mathbb{R}^d} |\mathbb{1}_{[0,1]^d}(w+\frac{\mathfrak{m}_0-z_2}{2\mathfrak{m}_0}) - \mathbb{1}_{[0,1]^d}(w+\frac{\mathfrak{m}_0-z_1}{2\mathfrak{m}_0})| dw \\
&\leq 2R^{d/2}\|\varphi\|_{\mathbb{L}_\infty(\mathbb{R}^d)} \|z_2-z_1\|_{\ell_1(\mathbb{R}^d)},
\end{aligned}$$

where the last inequality comes as a direct application of Lemma 5.12.2. Since f is continuous and its domain is compact, it is in particular lower bounded and reaches its lower bound in $(z^*,u^*) \in \mathcal{B}_\infty(2^{-1},\mathfrak{m}_0)\times\mathbb{S}^{r,d}$. Now, since $u^* \neq 0$, it is a direct consequence of the local linear independence of the scaling functions $(\varphi_{j,k})_{k\in\mathbb{Z}^d}$ described in Proposition 5.12.8 that $f(z^*,u^*) > 0$. This concludes the proof. □

Proposition 5.12.8. *Let $\mathfrak{m}$ be a constant such that $\mathfrak{m} > 0$ and fix $z \in \mathbb{R}^d$ such that $z \in \mathcal{B}_\infty(2^{-1},\mathfrak{m})$. Write $\mathfrak{S}_d := \{k \in \mathbb{Z}^d : 2^{-1} \in Supp\varphi_k\}$, the set of indexes corresponding to the scaling functions whose support $Supp\varphi_k$ contains the point $2^{-1} \in \mathbb{R}^d$. The scaling functions (φ_k) verify the **local linear independence property** in the sense that $\sum_{k\in\mathfrak{S}} \alpha_k\varphi_k = 0$ on the domain $\mathcal{B}_\infty(z,\mathfrak{m})$ if and only if $\alpha_k = 0$ for all $k \in \mathfrak{S}$.*

Proof. The proof follows the same lines as the proof of Theorem 3.7.1 and Remark 3.7.1 in [85] and relies on arguments detailed in [30] and the references therein. For completeness, we detail the proof here.
In the one-dimensional case, the proof is given in [30, Corollaire 3]. Notice indeed that for $d=1$, $\lambda(\text{Supp}\varphi_k) = R := 2r-1$ and $\cup_{k\in\mathfrak{S}}\text{Supp}\varphi_k = [-R+1,R]$. Set $\mathbb{1}_{[a,b]} = 0$ and $[a,b] = \emptyset$ as soon as $a > b$. Now, $\sum_{k\in\mathfrak{S}} \alpha_k\varphi_k = 0$ on $[z-\mathfrak{m},z+\mathfrak{m}]$ implies that both restrictions $\mathbb{1}_{[-R+1,z-\mathfrak{m}]}\sum_{k\in\mathfrak{S}} \alpha_k\varphi_k$ and $\mathbb{1}_{[z+\mathfrak{m},R]}\sum_{k\in\mathfrak{S}} \alpha_k\varphi_k$ belong to $\mathcal{V}_0$, according to [30, Proposition 1]. However $z \in [1/2-\mathfrak{m},1/2+\mathfrak{m}]$, therefore $\lambda([-R+1,z-\mathfrak{m}]) < R$ and $\lambda([z+\mathfrak{m},R]) < R$, which leads to a contradiction thanks to [30, Lemme 1, (ii)]. Therefore, both restrictions must be zero as well, which leads to $\sum_{k\in\mathfrak{S}} \alpha_k\varphi_k = 0$ and thus $\alpha_k = 0$ for all $k \in \mathfrak{S}$, since the $(\varphi_k)_{k\in\mathbb{Z}}$ have disjoint supports.
The generalization to the d-dimensional case follows by induction as in the proof of Theorem 3.7.1 in [85]. Assume the property holds in dimension $d-1$ and let us work in dimension d. Let $z \in \mathcal{B}_\infty(2^{-1},\mathfrak{m})$ and, for any $x \in \mathbb{R}^d$, write $x = (x_{1,d-1},x_d)$, where $x_{1,d-1}$ is the element of $\mathbb{R}^{d-1}$ consisting of the first $d-1$ coordinates of x and x_d is its last coordinate. Assume now that

$\sum_{k\in\mathfrak{S}_d}\alpha_k\varphi_k(x)=0$ on $\mathcal{B}_\infty(z,\mathfrak{m})$. We can integrate this latter expression against a test function $g(x_{1,d-1})$ supported on $\mathcal{B}_\infty(z_{1,d-1},\mathfrak{m})$ along the first $d-1$ dimensions. Using the fact that for all $x\in\mathbb{R}^d$ and $k\in\mathbb{Z}^d$, $\varphi_k(x)=\varphi^{(d-1)}_{k_{1,d-1}}(x_{1,d-1})\varphi^{(1)}_{k_d}(x_d)$, we obtain

$$\begin{aligned}0&=\sum_{k_d\in\mathfrak{S}_1}a_{k_d}\varphi^{(1)}_{k_d}(x_d),\quad \text{on } \mathcal{B}_\infty(z_d,\mathfrak{m}),\\ a_{k_d}&=\sum_{m\in\mathfrak{S}_{d-1}}\int\alpha_{(m,k_d)}g(x_{1,d-1})\varphi^{(d-1)}_m(x_{1,d-1})dx_{1,d-1}.\end{aligned}$$

However, the linear independence property in one dimension triggers $a_{k_d}=0$ for all $k_d\in\mathfrak{S}_1$. Since the test function g is chosen arbitrarily, this latter result leads in turn to

$$\sum_{m\in\mathfrak{S}_{d-1}}\alpha_{(m,k_d)}\varphi^{(1,d-1)}_m(x_{1,d-1})=0,\quad \text{for all } k_d\in\mathfrak{S}_1 \text{ and } x_{1,d-1}\in\mathcal{B}_\infty(z_{1,d-1},\mathfrak{m}).$$

Finally, using the induction hypothesis, we obtain $\alpha_k=0$ for all $k\in\mathfrak{S}_d$. □

Lemma 5.12.2. *Define the function f as follows*

$$\begin{aligned}f&:\mathbb{R}^d\mapsto\mathbb{R}^+,\\ f(y)&\triangleq\int_{\mathbb{R}^d}\mathbb{1}_{\{w+y\in[0,1]^d\}}dw.\end{aligned}$$

Then, f is Lipschitz-continuous on $\mathbb{R}^d$, such that, for any two $y,z\in\mathbb{R}^d$,

$$|f(y)-f(z)|\leq 2\|y-z\|_{\ell_1(\mathbb{R}^d)}.$$

Proof. The result is easily obtained by induction. We have indeed obviously for $d=1$,

$$\begin{aligned}|f(y)-f(z)|&\leq\int_{\mathbb{R}}|\mathbb{1}_{\{w+y\in[0,1]\}}-\mathbb{1}_{\{w+z\in[0,1]\}}|dw\\ &\leq\lambda([[0,1]-y]\Delta[[0,1]-z])\leq 2|y-z|.\end{aligned}$$

Now, write $\mathfrak{T}(y)=[0,1]^d-y$ and $\mathfrak{T}_i(y)=[0,1]-y_i$ for $1\leq i\leq d$, where y_i stands for the i^{th} coordinate of y. In addition, for $1\leq p\leq q\leq d$, we write

$$\mathfrak{T}_{p,q}(y)=\Pi_{i=p}^q\mathfrak{T}_i(y).$$

Recall that, for any $y,z\in\mathbb{R}^d$, we have the following relationships

$$\begin{aligned}\mathfrak{T}(y)\Delta\mathfrak{T}(z)&=(\mathfrak{T}(y)\cap\mathfrak{T}(z)^c)\cup(\mathfrak{T}(y)^c\cap\mathfrak{T}(z)),\\ \mathfrak{T}(y)&=(\mathfrak{T}_{1,d-1}(y)\times\mathbb{R})\cap(\mathbb{R}^{d-1}\times\mathfrak{T}_d(y)),\\ (\mathfrak{T}_{1,d-1}(y)\times\mathbb{R})^c&=\mathfrak{T}_{1,d-1}(y)^c\times\mathbb{R},\\ (\mathbb{R}^{d-1}\times\mathfrak{T}_d(y))^c&=\mathbb{R}^{d-1}\times\mathfrak{T}_d(y)^c.\end{aligned}$$

Making a repeated use of them, we can write

$$\begin{aligned}\mathfrak{T}(y)\Delta\mathfrak{T}(z)&=(\mathfrak{T}_{1,d-1}(y)\times\mathbb{R}\cap\mathbb{R}^{d-1}\times\mathfrak{T}_d(y))\Delta(\mathfrak{T}_{1,d-1}(z)\times\mathbb{R}\cap\mathbb{R}^{d-1}\times\mathfrak{T}_d(z))\\ &=(\mathfrak{T}(y)\cap(\mathfrak{T}_{1,d-1}(z)\times\mathbb{R})^c)\cup(\mathfrak{T}(y)\cap(\mathbb{R}^{d-1}\times\mathfrak{T}_d(z))^c)\\ &\cup(\mathfrak{T}(z)\cap(\mathfrak{T}_{1,d-1}(y)\times\mathbb{R})^c)\cup(\mathfrak{T}(z)\cap(\mathbb{R}^{d-1}\times\mathfrak{T}_d(y))^c)\end{aligned}$$

$$
\begin{aligned}
&= (\mathfrak{T}(y) \cap (\mathfrak{T}_{1,d-1}(z)^c \times \mathbb{R})) \cup (\mathfrak{T}(y) \cap (\mathbb{R}^{d-1} \times \mathfrak{T}_d(z)^c)) \\
&\cup (\mathfrak{T}(z) \cap (\mathfrak{T}_{1,d-1}(y)^c \times \mathbb{R})) \cup (\mathfrak{T}(z) \cap (\mathbb{R}^{d-1} \times \mathfrak{T}_d(y)^c)) \\
&= (\mathfrak{T}_{1,d-1}(y) \cap \mathfrak{T}_{1,d-1}(z)^c) \times \mathfrak{T}_d(y) \cup \mathfrak{T}_{1,d-1}(y) \times (\mathfrak{T}_d(y) \cap \mathfrak{T}_d(z)^c) \\
&\cup (\mathfrak{T}_{1,d-1}(z) \cap \mathfrak{T}_{1,d-1}(y)^c) \times \mathfrak{T}_d(z) \cup \mathfrak{T}_{1,d-1}(z) \times (\mathfrak{T}_d(z) \cap \mathfrak{T}_d(y)^c).
\end{aligned}
$$

Now remark that each of the four above sets define hyper-rectangles of $\mathbb{R}^d$. Denote by λ^k the Lebesgue measure of $\mathbb{R}^k$ and notice that $\lambda^k(\mathfrak{T}_{1,k}(y)) = \lambda(\mathfrak{T}_k(y)) = 1$ for all $1 \leq k \leq d$. Therefore, we obtain

$$
\begin{aligned}
\lambda^d(\mathfrak{T}(y)\Delta\mathfrak{T}(z)) &\leq \lambda^{d-1}(\mathfrak{T}_{1,d-1}(y) \cap \mathfrak{T}_{1,d-1}(z)^c) + \lambda(\mathfrak{T}_d(y) \cap \mathfrak{T}_d(z)^c) \\
&+ \lambda^{d-1}(\mathfrak{T}_{1,d-1}(z) \cap \mathfrak{T}_{1,d-1}(y)^c) + \lambda(\mathfrak{T}_d(z) \cap \mathfrak{T}_d(y)^c) \\
&= \lambda^{d-1}(\mathfrak{T}_{1,d-1}(y)\Delta\mathfrak{T}_{1,d-1}(z)) + \lambda(\mathfrak{T}_d(y)\Delta\mathfrak{T}_d(z)).
\end{aligned}
$$

Consequently, we obtain immediately by induction that

$$
|f(y) - f(z)| \leq \sum_{i=1}^{d} 2|y_i - z_i| = 2\|y - z\|_{\ell_1(\mathbb{R}^d)}.
$$

□

5.12.3 Proof of the lower-bound. In this section, we show that the proof of Theorem 5.7.3 under both settings (**CS1**) and (**CS2**) hinges on the well-known arguments of the proof of the lower-bound in the uniform design case. The arguments that follow are for the most part standard. Nonetheless, we report them here for completeness.

5.12.3.1 Preliminary results. First recall the definition of the Kullback-Leibler divergence for two probabilities $\mathbb{P}$ and $\mathbb{Q}$ on some measurable space $(\Omega, \mathcal{F})$:

$$
\mathscr{K}(\mathbb{P}, \mathbb{Q}) = \begin{cases} \int_\Omega \log\left\{\frac{d\mathbb{P}}{d\mathbb{Q}}(\omega)\right\} \mathbb{P}(d\omega) & \text{if } \mathbb{P} \ll \mathbb{Q} \\ +\infty & \text{otherwise} \end{cases}
$$

Here we use a version of Fano's lemma that is due to [104]. It can be stated as follows

Theorem 5.12.1 (Fano's Lemma)**.** *Let $\mathcal{F}$ be a σ-algebra on the space Ω. Let $G_i \in \mathcal{F}, i \in \{0, 1, \dots m\}$ such that $\forall i \neq j, G_i \cap G_j = \emptyset$. Let $\{\mathbb{P}_i\}_{i=0,\dots m}$ be probability measures on $(\Omega, \mathcal{F})$. If we write*

$$
\kappa(\mathbb{P}_0, \dots, \mathbb{P}_m) \triangleq \inf_{j=0,\dots m} \frac{1}{m} \sum_{i \neq j} \mathscr{K}(\mathbb{P}_i, \mathbb{P}_j),
$$

then, with $C = e^{\frac{3}{e}}$,

$$
\max_{i=0,\dots m} \mathbb{P}_i(G_i^c) \geq \frac{1}{2} \wedge C \left\{\sqrt{m} e^{-\kappa(\mathbb{P}_0,\dots,\mathbb{P}_m)}\right\}.
$$

Furthermore, we will need the following two Propositions that give upper bounds on the Kullback-Leibler divergence under specific sets of assumptions.

Proposition 5.12.9. *Assume we work under* (**S2**) *and the Gaussian noise hypothesis* (**N2**). *Then, for any two* $(\Omega, \mathscr{B}(\Omega))$*-measurable maps* η_1, η_2*, we have*

$$\mathscr{K}(\mathbb{P}_{\eta_1}, \mathbb{P}_{\eta_2}) \leq \frac{1}{2}\|\eta_1 - \eta_2\|^2_{\mathbb{L}_2(\Omega,\mu)}.$$

Proof. The proof is straightforward and can be found in [105, Lemma 3.3]. □

Proposition 5.12.10. *Assume we work under any of the two settings* (**S1**) *and* (**S2**) *and the bounded noise assumption* (**N1**). *Assume moreover* ξ *to be independent of* X *and such that, for any Borel subset* B *of* $[-K, K]$*,*

$$\mathbb{P}(\xi \in B) = C_K \int_B e^{-\frac{1}{2}u^2} du, \qquad\qquad C_K^{-1} = \int_{-K}^{K} e^{-\frac{1}{2}u^2} du.$$

Then for any two $(\Omega, \mathscr{B}(\Omega))$*-measurable maps* η_1, η_2*, we obtain*

$$\mathscr{K}(\mathbb{P}_{\eta_1}, \mathbb{P}_{\eta_2}) \leq \max(4, 2K) C_K \|\eta_1 - \eta_2\|_{\mathbb{L}_2(\Omega,\mu)},$$

where $\mathscr{B}(\Omega)$ *stands for the Borel* σ*-field of* Ω*.*

Proof. The proof is straightforward and hence reported to the Appendix. □

5.12.3.2 Lower bound under setting (**CS1**). We choose $\mu(.) = 1$, so that we are brought back to the case of a regression on a uniform design. Notice that, under (**S1**), such a μ verifies (**D1**) since $\mu_{\min}, \mu_{\max}$ must be such that $\mu_{\min} \leq 1 \leq \mu_{\max}$. In the case of a Gaussian noise such as under (**N2**), the proof of the lower-bound is well known and can be found in [106, 47, 105], to quote a few. In the case of a bounded noise, the same reasoning still applies thanks to Proposition 5.12.10 above.

5.12.3.3 Lower bound under setting (**CS2**). In that case, a bit more work is needed. Let $r \in \mathbb{N}$ and recall that $2^{j_s} = \lfloor n^{\frac{1}{2s+d}} \rfloor$. Let us write $\Omega = \mathbb{R}^d$ and denote by $(\mathcal{V}_j)_{j\geq 0}$ the Daubechies' r-MRA of $\mathbb{L}_2(\mathbb{R}^d, \lambda)$. For any subset $\mathcal{X}$ of $\mathbb{Z}^d$, write $\nabla(\mathcal{X}) := [\{0,1\}\backslash\{(0,\ldots,0)\}] \times \mathcal{X}$ and $\nabla := \nabla(\mathbb{Z}^d)$. We recall that the multivariate Daubechies' wavelets $\psi_\nu, \nu \in \nabla$ associated with the r-MRA above are supported on hypercubes of volume R^d. We define the grid

$$G_{2^{j_\zeta}} := \left\{(k_1, \ldots, k_d) : k_i \in \{0, \ldots, \lfloor \mathfrak{m} 2^{j_s} \rfloor - 1\}\right\},$$

for some absolute constant $\mathfrak{m}$ to be chosen later. Obviously, we have $\# G_{2^{j_s}} = \lfloor \mathfrak{m} 2^{j_s} \rfloor^d$. In addition, we take

$$\mathcal{A} = \bigcup_{k \in G_{2^{j_s}}} \mathcal{B}_\infty(k, \frac{1}{2}\lfloor \mathfrak{m} 2^{j_s} \rfloor^{-1}).$$

Now, choose $\mathfrak{m}$ such that $2^{j_s} 2^{-1} \lfloor \mathfrak{m} 2^{j_s} \rfloor^{-1} \geq R$, that is, say, $\mathfrak{m} = (2R)^{-1}$. We assume that n is large enough, that is $2^{j_s} \geq 2R$, so that the grid is not degenerate. It is immediate that $\mathcal{A}$ verifies (**S2**). Now, define $\bar{\mu}$ on $\mathbb{R}^d$ to be

$$\bar{\mu}(.) = \sum_{k \in G_{2^{j_s}}} \mathbb{1}_{\mathcal{B}_\infty(k, \frac{1}{2}\lfloor \mathfrak{m} 2^{j_s} \rfloor^{-1})}(.).$$

By construction, we obtain $\int_{\mathcal{A}} \bar{\mu}(w)dw = 1$. And finally, $\bar{\mu}$ verifies (**D1**) since $\mu_{\min} \leq 1 \leq \mu_{\max}$, as desired. Let $j \geq j_s$. Notice now that for any $k \in G_{2^{js}}$, we can find a subset $G^*_{j,k}$ of $\mathbb{Z}^d$ such that $\#G^*_{j,k} = 2^{(j-j_s)d}$ and such that for all $\nu \in \nabla(G^*_{j,k})$, Supp$\psi_{j,\nu} \subset \mathcal{B}_\infty(k, \frac{1}{2}\lfloor \mathfrak{m} 2^{j_s} \rfloor^{-1})$.
We write

$$\bar{G}_j := \bigcup_{k \in G_{2^{j_s}}} G^*_{j,k}.$$

In addition, we denote by $\boldsymbol{a} := (a_\nu)_{\nu \in \nabla(\bar{G}_j)}$ an element of $\{0,1\}^{\nabla(\bar{G}_j)}$. With these notations, we define

$$\Upsilon(\bar{G}_j) := \left\{ \eta \in \mathscr{L}^s(\mathbb{R}^d, M) : \eta = \gamma_j \sum_{\nu \in \nabla(\bar{G}_j)} a_\nu \psi_{j,\nu},\ \boldsymbol{a} \in \{0,1\}^{\bar{G}_j} \right\}, \quad j \geq j_s.$$

Now, we just need to remark that $\#\nabla(\bar{G}_j) \approx 2^{jd}$ and for any two $\eta_1, \eta_2 \in \Upsilon(\bar{G}_j)$,

$$\|\eta_1 - \eta_2\|_{\mathbb{L}_p(\Omega,\bar{\mu})} = \|\eta_1 - \eta_2\|_{\mathbb{L}_p(\mathbb{R}^d,\lambda)}. \tag{5.33}$$

This last result together with both Proposition 5.12.9 and Proposition 5.12.10 above allows us to conclude once more using the well known arguments of the proof of the lower bound in a uniform design, under both assumptions (**N1**) and (**N2**). For completeness, we detail the end of the reasoning below. We denote by (**Ind**) the assumption that ξ is independent of X and write

$$\mathcal{P}^*(\bar{G}_j) := \{\mathbb{P} \in \mathcal{P}(\mathbb{R}^d \times \mathbb{R}) : \eta \in \Upsilon(\bar{G}_j), \mu = \bar{\mu}, (\textbf{Ind}) \text{ holds true}\}.$$

We denote by $\eta_{\boldsymbol{a}}$ the elements of $\Upsilon(\bar{G}_j)$, where we write $\boldsymbol{a} \in \{0,1\}^{\nabla(\bar{G}_j)}$. It appears that, for $\eta_{\boldsymbol{a}} \in \Upsilon(\bar{G}_j)$,

$$\|\eta_{\boldsymbol{a}}\|_{\mathscr{L}^s(\mathbb{R}^d)} \leq C|\gamma_j| 2^{j(s+\frac{d}{2})} \sup_{\nu \in \nabla(\bar{G}_j)} a_\nu \leq C|\gamma_j| 2^{j(s+\frac{d}{2})},$$

where the first inequality is a direct application of eq. (5.37). Thus, in order to have $\eta_{\boldsymbol{a}} \in \mathscr{L}^s(\mathbb{R}^d, M)$, it is enough to choose $|\gamma_j| \leq CM2^{-j(s+\frac{d}{2})}$. With this constraint on γ_j, we obtain

$$\mathcal{P}(\mathbf{CS2}, \mathbf{H^r_s}) \supset \mathcal{P}^*(\bar{G}_j).$$

Besides, for any two $\boldsymbol{a}, \boldsymbol{a'} \in \{0,1\}^{\nabla(\bar{G}_j)}$, a direct application of [85, eq. (3.6.16)] leads to

$$\|\eta_{\boldsymbol{a}} - \eta_{\boldsymbol{a'}}\|_{\mathbb{L}_p(\Omega,\bar{\mu})} \geq c|\gamma_j| 2^{jd(\frac{1}{2}-\frac{1}{p})} \left(\sum_{\nu \in \nabla(\bar{G}_j)} |a_\nu - a'_\nu|^p \right)^{\frac{1}{p}}. \tag{5.34}$$

The Varshamov-Gilbert Lemma (see [107, Lemma 2.9]) ensures there exists a subset $\nabla(A_j) \subset \nabla(\bar{G}_j)$ such that $\#\nabla(A_j) \geq \frac{\#\nabla(\bar{G}_j)}{8}$ and $\sum_{\nu \in \nabla(A_j)} |a_\nu - a'_\nu| \geq \frac{\#\nabla(\bar{G}_j)}{8}$. Write $\Gamma_j := \{(a_\nu)_{\nu \in \nabla(\bar{G}_j)} : a_\nu \in \{0, \mathbb{1}_{\{\nu \in \nabla(A_j)\}}\}\}$. Now, if we pick $|\gamma| = c2^{-j(s+\frac{d}{2})}$ and $\boldsymbol{a}, \boldsymbol{a'} \in \Gamma_j$, eq. (5.34) together with the latter results leads to

$$\|\eta_{\boldsymbol{a}} - \eta_{\boldsymbol{a'}}\|_{\mathbb{L}_p(\Omega,\bar{\mu})} \geq c|\gamma| 2^{jd(\frac{1}{2}-\frac{1}{p})} \left(\frac{2^{jd}}{8} \right)^{\frac{1}{p}} = c2^{-js}. \tag{5.35}$$

Now we can write $\delta := \frac{1}{2}c2^{-js}$ and $G_{\boldsymbol{a}} = \{\|\theta - \eta_{\boldsymbol{a}}\|_{\mathbb{L}_p(\Omega,\bar{\mu})} < \delta\}$. It results from eq. (5.35) that, for $\boldsymbol{a} \in \Gamma_j$, the $G_{\boldsymbol{a}}$'s are mutually exclusive. Let us denote by $\mathbb{P}_{\eta_{\boldsymbol{a}},\bar{\mu}}$ the law of (X,Y) under the assumption that $\eta = \eta_{\boldsymbol{a}}$ and $\mu = \bar{\mu}$ and $\mathbb{E}_{\eta_{\boldsymbol{a}},\bar{\mu}}$ the corresponding expectation. We will add the superscript $\otimes n$ when dealing with their n^{th} tensorial product. Thus we can apply Theorem 5.12.1 to obtain

$$\begin{aligned}\max_{\mathbb{P}\in\mathcal{P}^*(\Upsilon(A_j))} \mathbb{E}\|\theta-\eta\|^p_{\mathbb{L}_p(\Omega,\bar{\mu})} &= \max_{\boldsymbol{a}\in\Gamma_j} \mathbb{E}^{\otimes n}_{\eta_{\boldsymbol{a}},\bar{\mu}}\|\theta-\eta_{\boldsymbol{a}}\|^p_{\mathbb{L}_p(\mathcal{A},\bar{\mu})} \\ &\geq \delta^p \max_{\boldsymbol{a}\in\Gamma_j} \mathbb{P}^{\otimes n}_{\eta_{\boldsymbol{a}},\bar{\mu}}(\|\theta-\eta_{\boldsymbol{a}}\|_{\mathbb{L}_p(\Omega,\bar{\mu})} \geq \delta) \\ &= \delta^p \max_{\boldsymbol{a}\in\Gamma_j} \mathbb{P}^{\otimes n}_{\eta_{\boldsymbol{a}},\bar{\mu}}(G^c_{\boldsymbol{a}}) \\ &\geq \delta^p \left\{\frac{1}{2} \wedge C\sqrt{2^{\#\Gamma_j}-1}e^{-\kappa((\mathbb{P}^{\otimes n}_{\eta_{\boldsymbol{a}},\bar{\mu}})_{\boldsymbol{a}\in\Gamma_j})}\right\}.\end{aligned} \tag{5.36}$$

In addition both Proposition 5.12.9 and Proposition 5.12.10 lead to

$$\begin{aligned}\mathscr{K}(\mathbb{P}^{\otimes n}_{\eta_{\boldsymbol{a}},\bar{\mu}}, \mathbb{P}^{\otimes n}_{\eta_{\boldsymbol{a}'},\bar{\mu}}) &= n\mathscr{K}(\mathbb{P}_{\eta_{\boldsymbol{a}},\bar{\mu}}, \mathbb{P}_{\eta_{\boldsymbol{a}'},\bar{\mu}}) \leq Cn\|\eta_{\boldsymbol{a}} - \eta_{\boldsymbol{a}'}\|^2_{\mathbb{L}_2(\Omega,\bar{\mu})} \\ &= Cn|\gamma_j|^2\|\sum_{\nu\in\nabla(A_j)}(a_\nu - a'_\nu)\psi_{j,\nu}\|^2_{\mathbb{L}_2(\Omega,\lambda)} \\ &\leq Cn|\gamma_j|^2 \sum_{\nu\in\nabla(A_j)}|a_\nu - a'_\nu|^2 \leq Cn|\gamma_j|^2 2^{jd} = Cn2^{-2js},\end{aligned}$$

where the second equality makes use of eq. (5.33). As a consequence

$$\sqrt{2^{\#\Gamma_j}-1}e^{-\kappa((\mathbb{P}^{\otimes n}_{\eta_{\boldsymbol{a}},\bar{\mu}})_{\boldsymbol{a}\in\Gamma_j})} \geq 2^{c2^{jd}}e^{-cn2^{-2js}}.$$

In order to balance this last term, it is enough to choose j such that $n2^{-2js} = c2^{jd}$, which leads to $n^{-\frac{1}{2}} = c2^{-j(s+\frac{d}{2})}$. Combining this value with eq. (5.36) and the inclusion $\mathscr{L}^s(\mathbb{R}^d, M) \supset \Upsilon(\bar{G}_j) \supset \Upsilon(A_j)$ gives

$$\sup_{\mathbb{P}\in\mathcal{P}(\mathbf{CS2},\mathbf{H^r_s})} \mathbb{E}\|\theta-\eta\|^p_{\mathbb{L}_p(\Omega,\bar{\mu})} \geq \max_{\mathbb{P}\in\mathcal{P}^*(\Upsilon(A_j))} \mathbb{E}\|\theta-\eta\|^p_{\mathbb{L}_p(\Omega,\bar{\mu})} \geq c(2^{-j})^{sp} = cn^{-\frac{sp}{2s+d}}.$$

This concludes the proof of Theorem 5.7.3. □

5.13 Appendix.

5.13.1 Generalized Lipschitz spaces. Here, we sum up relevant facts about Lipschitz and Besov spaces on $\mathbb{R}^d$ as stated in [85, Chap. 3] for any $d \in \mathbb{N}$ and [88, Chap. 2, §9] for $d = 1$. Let us denote by $\mathscr{C}(\mathbb{R}^d)$ and $\widetilde{\mathscr{C}}(\mathbb{R}^d)$ the spaces of continuous and absolutely continuous functions on $\mathbb{R}^d$, respectively. Let us denote by $\|.\|$ the Euclidean norm of $\mathbb{R}^d$, f a function defined on $\mathbb{R}^d$ and write $\Delta^1_h(f,x) = |f(x+h) - f(x)|$ for any $x \in \mathbb{R}^d$. For any $r \in \mathbb{N}$ and all $x \in \mathbb{R}^d$, we further define the r^{th}-finite difference by induction as follows,

$$\Delta^r_h(f,x) = \Delta^1_h(\Delta^{r-1}_h(f,x)),$$

and the r^{th}-modulus of smoothness of $f \in \mathscr{C}(\mathbb{R}^d)$ as follows

$$\omega_r(f,t)_\infty = \sup_{0\leq\|h\|\leq t} \|\Delta_h^r(f,.)\|_{\mathbb{L}_\infty(\mathbb{R}^d,\lambda)}.$$

Write $s > 0$ and $r = \lfloor s \rfloor + 1$. The Besov space $B^s_{\infty,\infty}$ on $\mathbb{R}^d$, also known as the generalized Lipschitz space $\mathscr{L}^s(\mathbb{R}^d)$, is the collection of all functions $f \in \widetilde{\mathscr{C}}(\mathbb{R}^d) \cap \mathbb{L}_\infty(\mathbb{R}^d,\lambda)$ such that the semi-norm

$$|f|_{\mathscr{L}^s(\mathbb{R}^d)} := \sup_{t>0} \left(t^{-s}\omega_r(f,t)_\infty\right),$$

is finite. The norm for $\mathscr{L}^s(\mathbb{R}^d)$ is subsequently defined as

$$\|f\|_{\mathscr{L}^s(\mathbb{R}^d)} := \|f\|_{\mathbb{L}_\infty(\mathbb{R}^d,\lambda)} + |f|_{\mathscr{L}^s(\mathbb{R}^d)}.$$

Fix a real number $M > 0$. Throughout the paper, $\mathscr{L}^s(\mathbb{R}^d, M)$ refers to the ball of $\mathscr{L}^s(\mathbb{R}^d)$ of radius M. Obviously, the elements of $\mathscr{L}^s(\mathbb{R}^d, M)$ are λ-a.e. uniformly bounded by M on $\mathbb{R}^d$.
As described in [88, 85], there exists an alternative definition of Lipschitz spaces $\mathscr{C}^s(\mathbb{R}^d)$, also known as Hölder spaces, which goes as follows. For any integer d, multi-index $q = (q_1, \ldots, q_d) \in \mathbb{N}^d$ and $x = (x_1, \ldots, x_d) \in \mathbb{R}^d$, we define the differential operator ∂^q as usual by $\partial^q := \frac{\partial^{q_1+\ldots+q_d}}{\partial^{q_1}x_1 \ldots \partial^{q_d}x_d}$.
For any positive integer s, $\mathscr{C}^s(\mathbb{R}^d)$ consists of the functions f on $\mathbb{R}^d$ such that $\partial^q f$ is bounded and absolutely continuous on $\mathbb{R}^d$, for all $q \in \mathbb{N}^d$ such that $|q|_1 := q_1 + \ldots + q_d \leq s$. This definition is extended to non-integer s as follows,

$$\begin{aligned}
\mathscr{C}^s(\mathbb{R}^d) &:= \{f \in \widetilde{\mathscr{C}}(\mathbb{R}^d) \cap \mathbb{L}_\infty(\mathbb{R}^d,\lambda) : \sup_{x\in\mathbb{R}^d} \Delta_h^1(f,x) \leq C|h|^s\}, \quad 0 < s < 1,\\
\mathscr{C}^s(\mathbb{R}^d) &:= \{f \in \widetilde{\mathscr{C}}(\mathbb{R}^d) \cap \mathbb{L}_\infty(\mathbb{R}^d,\lambda) :\\
&\qquad \partial^q f \in \mathscr{C}^{s-m}(\mathbb{R}^d), |q|_1 = m\}, \quad m < s < m+1,\ m \in \mathbb{N}.
\end{aligned}$$

It can be shown that, for all non-integer $s > 0$, $\mathscr{C}^s(\mathbb{R}^d) = \mathscr{L}^s(\mathbb{R}^d)$, while $\mathscr{C}^s(\mathbb{R}^d)$ is a strict subset of $\mathscr{L}^s(\mathbb{R}^d)$ when $s \in \mathbb{N}$ (see [88, p. 52] for examples of functions that belong to $\mathscr{L}^1([0,1])$ but not to $\mathscr{C}^1([0,1])$ in the particular case where $d = 1$).
Furthermore, we define these function spaces on the subset Ω of $\mathbb{R}^d$ as the restriction of their elements to Ω. As explained in [85, Remark 3.2.4], function spaces on Ω can be defined by restriction or, alternatively, in an intrinsic way, and both definitions coincide for fairly general domains Ω of $\mathbb{R}^d$.
Looking at function spaces on Ω as function spaces on $\mathbb{R}^d$ restricted to Ω justifies the use of MRAs of $\mathbb{L}_2(\mathbb{R}^d,\lambda)$ in our local analysis.

5.13.2 MRAs and smoothness analysis.

5.13.2.1 Generalities. In order to estimate η on Ω, we will work with MRAs of $\mathbb{L}_2(\mathbb{R}^d,\lambda)$ built upon a compactly supported scaling function φ. Multivariate MRAs will always be assumed to be obtained from a tensorial product of one-dimensional MRAs, as described in [85, §1.4, eq. (1.4.10)] and recalled below. We will denote by $\varphi_{j,k}(.) = 2^{jd/2}\varphi(2^j. - k)$ the translated and dilated version of φ with $k \in \mathbb{Z}^d$. As usual, we denote $\mathcal{V}_j = \text{Closure}(\text{Span}\{\varphi_{j,k}, k \in \mathbb{Z}^d\})$, so

that Closure$(\cup_{j\geq 0}\mathcal{V}_j) = \mathbb{L}_2(\mathbb{R}^d,\lambda)$ (where the closures are taken with respect to the $\mathbb{L}_2(\mathbb{R}^d,\lambda)$-metric). As we are interested in finer and finer approximations of an objective function as the sample size grows, we can in fact truncate the MRA at resolution scales 2^{-j}, $j \geq 0$. In the sequel, we will still refer to it as a MRA.
Here, let us simply recall that, for any $k = (k_1,\ldots,k_d) \in \mathbb{Z}^d$ and $x = (x_1,\ldots,x_d) \in \mathbb{R}^d$, the multivariate scaling functions write as

$$\varphi_{j,k}(x) = \varphi_{j,k_1}(x_1)\ldots\varphi_{j,k_d}(x_d).$$

Let us denote by ψ the univariate wavelet associated to the univariate scaling function φ. Then the multivariate wavelets $\psi_{j,\nu}$ are indexed by $j \geq 0$ and the double index $\nu = (\varepsilon,k) \in \nabla = [\{0,1\}^d\backslash\{(0,\ldots,0)\}] \times \mathbb{Z}^d$ and write as

$$\psi_{j,\nu}(x) = \psi_{j,k}^{(\varepsilon_1)}(x_1)\ldots\psi_{j,k}^{(\varepsilon_d)}(x_d),$$

where we have written $\psi^{(0)} = \varphi$, $\psi^{(1)} = \psi$ and $\varepsilon = (\varepsilon_1,\ldots,\varepsilon_d)$.

5.13.2.2 Connection between MRAs and generalized Lipschitz spaces. The r-MRAs defined in Section 5.5.2 are intimately connected with generalized Lipschitz spaces. Assume we are given a r-MRA with $r \in \mathbb{N}$ and $\eta \in \mathscr{L}^s(\mathbb{R}^d,M)$, where $s \in (0,r)$ and $M > 0$. Denote by $\mathscr{P}_j\eta$ the projection of η onto $\mathcal{V}_j$ and by $\mathscr{R}_j\eta = \eta - \mathscr{P}_j\eta$ the corresponding remainder. Then, we have for all $x \in \mathbb{R}^d$, $\eta(x) = \mathscr{P}_j\eta(x) + \mathscr{R}_j\eta(x)$ where $\|\mathscr{R}_j\eta\|_{\mathbb{L}_\infty(\mathbb{R}^d,\lambda)} \leq M2^{-js}$, as detailed in [85, Corollary 3.3.1]. It is noteworthy that the above approximation results remain valid in the particular case where we work on the subset Ω of $\mathbb{R}^d$ and consider η to be the restriction to Ω of an element of $\mathscr{L}^s(\mathbb{R}^d)$.
Let us denote by $\{\varphi_k : k \in \mathbb{Z}^d\} \cup \{\psi_{j,\nu} : j \geq 0, \nu \in \nabla\}$ the Daubechies' wavelet basis associated to a r-MRA (see Section 5.13.2 for notations and [90, Chap. 5, 6] for a detailed review of wavelet bases and [85, §1.4,Remark 1.4.5] for the construction of their multi-dimensional isotropic version). For any $\eta \in \mathscr{L}^s(\mathbb{R}^d)$, we write $\alpha_k := \langle\eta,\varphi_k\rangle_{\mathbb{L}_2(\mathbb{R}^d,\lambda)}$ and $\beta_{j,\nu} := \langle\eta,\psi_{j,\nu}\rangle_{\mathbb{L}_2(\mathbb{R}^d,\lambda)}$. Then, we have the following well-known norm equivalence

$$\|\eta\|_{\mathscr{L}^s(\mathbb{R}^d)} \approx \sup_{k\in\mathbb{Z}^d}|\alpha_k| + \sup_{j\geq 0}2^{j(s+\frac{d}{2})}\sup_{\nu\in\nabla}|\beta_{j,\nu}|, \quad s \in (0,r). \tag{5.37}$$

This latter result happens to be useful in the proof of the lower bound (see Section 5.12.3).

5.13.3 A technical comment relative to the lattice structure of the MRA under (CS1). Assume we work under (**CS1**) with the Daubechies' r-MRA of $\mathbb{L}_2(\mathbb{R}^d,\lambda)$. Let $x \in [0,1]^d$. Notice that the scaling functions $\varphi_{j,k}, k \in \mathbb{Z}^d$ are supported on hypercubes of the form $\text{Supp}\varphi_{j,k} = 2^{-j}(N_{1,k},N_{2,k})$, where $N_{1,k},N_{2,k} \in \mathbb{Z}^d$. When doing estimation at point x at resolution 2^{-j}, we have to differentiate two cases according to whether x belongs to Inter(Supp$\varphi_{j,k}$) or ∂Supp$\varphi_{j,k}$. This is due to the fact that $\#\mathcal{S}_j(x)$ is constant on each open hypercube of $2^{-j}[\mathbb{Z}^d + (0,1)^d]$ while it raises ($r = 1$) or drops ($r \geq 2$) at their boundary. However, notice that it is only necessary to focus on the case where $x \in$ Inter(Supp$\varphi_{j,k}$), since we are interested in results that hold $\mathbb{P}_X$-almost surely. $\mathbb{P}_X$ is indeed absolutely continuous with respect to the

Lebesgue measure λ on $\mathbb{R}^d$ (with density μ) and for any $j \geq 0$, $k \in \mathbb{Z}^d$, $\lambda(\partial \text{Supp}\varphi_{j,k}) = 0$. Consequently

$$\mathbb{P}_X \left(\bigcup_{j\geq 0, k\in\mathbb{Z}^d} \partial \text{Supp}\varphi_{j,k} \right) = 0.$$

When working under (**S1**), we implicitly assume throughout the paper that

$$\mathcal{A} = [0,1]^d \backslash \bigcup_{j\geq 0, k\in\mathbb{Z}^d} \partial \text{Supp}\varphi_{j,k}.$$

Notice that this problem does not occur under (**CS2**) where, by construction, x is always located inside $\mathcal{H}_0(X_{i_x})$.

5.13.4 Proof of Proposition 5.12.10.

Proof of Proposition 5.12.10. For any two Borel subsets A and B of $\mathbb{R}$ and Ω, respectively, and any $(\Omega, \mathscr{B}(\Omega))$-measurable map η, a straightforward computation leads to

$$\mathbb{P}_\eta(Y \in A, X \in B) = \int_B \mu(x)dx \int_A du C_K e^{-\frac{1}{2}(u-\eta(x))^2}.$$

Therefore, for any two $(\Omega, \mathscr{B}(\Omega))$-measurable maps η_1, η_2, one can write

$$\begin{aligned}
&\mathscr{K}(\mathbb{P}_{\eta_1}, \mathbb{P}_{\eta_2}) \\
&= \int_\Omega \log\left(\frac{d\mathbb{P}_{\eta_1}}{d\mathbb{P}_{\eta_2}}(\omega)\right) d\mathbb{P}_{\eta_1}(\omega) \\
&= \frac{1}{2}\int_{\mathcal{A}} dx\mu(x) \int_{-K}^{K} du C_K [(u-\eta_2(x))^2 - (u-\eta_1(x))^2] e^{-\frac{1}{2}(u-\eta_1(x))^2} \\
&= \frac{1}{2}\int_{\mathcal{A}} dx\mu(x)(\eta_1(x)-\eta_2(x))^2 \int_{-K}^{K} du C_K e^{-\frac{1}{2}(u-\eta_1(x))^2} \\
&+ \int_{\mathcal{A}} dx\mu(x)(\eta_1(x)-\eta_2(x)) \int_{-K}^{K} du C_K (u-\eta_1(x)) e^{-\frac{1}{2}(u-\eta_1(x))^2}.
\end{aligned}$$

Now, notice first that

$$\int_{-K}^{K} du C_K e^{-\frac{1}{2}(u-\eta_1(x))^2} \leq 2KC_K.$$

In addition, notice that

$$\left| \int_{-K}^{K} du C_K (u-\eta_1(x)) e^{-\frac{1}{2}(u-\eta_1(x))^2} \right| = C_K \left| e^{-\frac{1}{2}(K-\eta_1(x))^2} - e^{-\frac{1}{2}(K-\eta_1(x))^2} \right| \leq 2C_K.$$

Consequently, we end up with the desired result

$$\begin{aligned}
\mathscr{K}(\mathbb{P}_{\eta_1}, \mathbb{P}_{\eta_2}) &= 2C_K \|\eta_1 - \eta_2\|_{\mathbb{L}_1(\Omega,\mu)} + KC_K \|\eta_1 - \eta_2\|_{\mathbb{L}_2(\Omega,\mu)} \\
&\leq \max(4, 2K) C_K \|\eta_1 - \eta_2\|_{\mathbb{L}_2(\Omega,\mu)}.
\end{aligned}$$

□

5.13.5 Proof of the classification results.

Proof of Proposition 5.10.1. Notice first that eq. (5.18) is a direct consequence of Theorem 5.9.1. The proof of eq. (5.19) follows the same lines as the proof of Theorem 5.7.2. The reader is therefore advised to read the latter proof before this one. Notice that

$$\begin{aligned}\mathbb{P}(|\eta^{\Phi}_{j^{\Phi}(x)}(x) - \eta(x)| \geq \delta) \leq\ & \mathbb{P}(|\eta^{\Phi}_{j_s}(x) - \eta(x)| \geq \delta/3) \\ & + \mathbb{P}(|\eta^{\Phi}_{j^{\Phi}(x)}(x) - \eta^{\Phi}_{j_s}(x)| \geq \delta/3, j^{\Phi}(x) \leq j_s) \\ & + \mathbb{P}(|\eta^{\Phi}_{j^{\Phi}(x)}(x) - \eta^{\Phi}_{j_s}(x)| \geq \delta/3, j^{\Phi}(x) > j_s).\end{aligned}$$

Let us denote the three terms on the rhs from top to bottom by I, II and III. I is upper bounded using eq. (5.18) above with $j = j_s$ and $\delta > 6\ 2^{-j_s s} \max(1, 3\pi_0 R^d \mu_{\max})$. This leads to

$$I \leq 3R^{2d} n^{-\kappa C'_{10}} + 2R^d \exp(-C_{10} a_n(j_s) \delta^2),$$

where C'_{10} and C_{10} are such that

$$C'_{10} := \frac{1}{4\mu_{\max} R^{4d} + \frac{8}{3} R^{2d} \pi_0^{-1}}, \qquad C_{10} := \frac{C_6(r, d, \mu_{\max}, 1, \pi_0)}{2\pi_0^2}, \tag{5.38}$$

and C_6 is defined in eq. (5.25). Now, recall from the proof of Theorem 5.7.2 that, on the event $\{j^{\Phi} \leq j_s\}$, $II = 0$ as soon as $\delta > 6t(n)2^{j_s \frac{d}{2}} n^{-\frac{1}{2}}$. Let us finally turn to III. With the same notations as in the proof of Theorem 5.7.2, we obtain

$$\begin{aligned}III &\leq \sum_{j \in \mathcal{J}_n(j_s)} \sum_{k \in \mathcal{J}_n(j-1)} \mathbb{P}(\mathcal{G}(x, j-1, k)) \\ &\leq (\log n)^2 10 R^{2d} n^{-\kappa C_6},\end{aligned}$$

where the last inequality uses Proposition 5.12.2 and the fact that $\#\mathcal{J}_n \leq \log n$. Denote moreover,

$$C'_6 = \frac{1}{64\mu_{\max} R^{4d} + 8R^{2d} \pi_0^{-1}}, \qquad C_{11} := 2^{-2r} C_{10}, \tag{5.39}$$

and notice finally that $C'_{10} \wedge C_6 > C'_6$. Besides, recall from eq. (5.10c) that $2^{-j_s s} \leq 2^r n^{-\frac{s}{2s+d}}$, so that for n large enough, $6\ 2^{-j_s s} \max(1, 3\pi_0 R^d \mu_{\max}) \leq 62^r t(n) n^{-\frac{s}{2s+d}}$ and a direct application of eq. (5.10c) leads to $C_{10} a_n(j_s) \geq C_{11} n^{\frac{2s}{2s+d}}$. This concludes the proof. □

Proof of Theorem 5.10.1. It follows closely the proof of [35, Theorem 3.1]. Consider the sets A_k defined as

$$\begin{aligned}A_0 &:= \{\tau \in \Omega : 0 < |\eta(x) - \frac{1}{2}| \leq \delta_n\}, \\ A_k &:= \{\tau \in \Omega : 2^{k-1}\delta_n < |\eta(x) - \frac{1}{2}| < 2^k \delta_n\}, \quad 1 \leq k \leq \bar{k},\end{aligned}$$

where we define $\bar{k}$ by $2^{\bar{k}+1} = \lceil \delta_n^{-1} \rceil$. Notice indeed that $2^{k-1}\delta_n \geq 2^{-1}$, that is $A_k = \emptyset$ for $k \geq \bar{k}+1$. Therefore, we can write

$$\begin{aligned}\mathscr{R}(h_n) &= \sum_{0\leq k\leq \bar{k}} \mathbb{E}(|2\eta(X)-1|\mathbb{1}_{\{h_n(X)\neq h^*(X)\}}\mathbb{1}_{\{X\in A_k\}}) \\ &\leq 2\delta_n \mathbb{P}(0 < |\eta(X) - \frac{1}{2}| \leq \delta_n) \\ &+ \sum_{1\leq k\leq \bar{k}} \mathbb{E}(|2\eta(X)-1|\mathbb{1}_{\{h_n(X)\neq h^*(X)\}}\mathbb{1}_{\{X\in A_k\}}).\end{aligned}$$

Notice now that we have $|\eta - \frac{1}{2}| \leq |\eta_n - \eta|$ on the event $\{h_n \neq h^*\}$. So that, for any $1 \leq k \leq \bar{k}$, we obtain

$$\begin{aligned}&\mathbb{E}(|2\eta(X)-1|\mathbb{1}_{\{h_n(X)\neq h^*(X)\}}\mathbb{1}_{\{X\in A_k\}}) \\ &\leq 2^{k+1}\delta_n \mathbb{E}(\mathbb{1}_{\{|\eta_n(X)-\eta(X)|\geq 2^{k-1}\delta_n\}}\mathbb{1}_{\{0<|\eta(X)-\frac{1}{2}|\leq 2^k\delta_n\}}) \\ &= 2^{k+1}\delta_n \mathbb{E}\mathbb{P}^{\otimes n}(|\eta_n(X)-\eta(X)| \geq 2^{k-1}\delta_n | X)\mathbb{1}_{\{0<|\eta(X)-\frac{1}{2}|\leq 2^k\delta_n\}} \\ &\leq 2^{k+1}\delta_n \mathbb{P}(0 < |\eta(X) - \frac{1}{2}| \leq 2^k\delta_n)(C_{11}b_n + C_{12}\exp(-C_{13}a_n(2^{k-1}\delta_n)^2)) \\ &\leq 2C_*(2^k\delta_n)^{1+\vartheta}(C_{11}b_n + C_{12}\exp(-C_{13}a_n(2^{k-1}\delta_n)^2)),\end{aligned}$$

where the before last inequality uses eq. (5.20), which is possible since $2^{k-1}\delta_n \leq 1$ as long as $k \leq \bar{k}$, and the last one uses (**MA**). So that putting everything together, we obtain

$$\begin{aligned}\mathscr{R}(h_n) &\leq 2C_*\delta_n^{1+\vartheta} + 2C_*C_{11}(2^{\bar{k}}\delta_n)^{1+\vartheta}b_n \\ &+ 2C_*C_{12}\delta_n^{1+\vartheta}\sum_{1\leq k\leq \bar{k}} 2^{k(1+\vartheta)}\exp(-C_{13}a_n\delta_n^2 2^{2(k-1)}).\end{aligned}$$

It remains to notice that $2^{\bar{k}}\delta_n \leq 1$ to conclude the proof. □

Proof of Corollary 5.10.1. The proof of eq. (5.21) and eq. (5.22) are straightforward consequences of Proposition 5.10.1 and Theorem 5.10.1. Start with eq. (5.21) and choose $\delta_n = 32^{-j_s s}\max(1, 3\pi_0 R^d \mu_{\max})$. Notice first that eq. (5.10a) leads to

$$a_n(j_s)\delta_n^2 \geq 9\max(1, 3\pi_0 R^d \mu_{\max})^2$$

Besides, eq. (5.10c) leads to $2^{-j_s s} \leq 2^r n^{-\frac{s}{2s+d}}$. Finally, notice that

$$\delta_n^{-(1+\vartheta)} n^{-\kappa C'_{10}} \leq C n^{\frac{s}{2s+d}(1+\vartheta)-\kappa C'_{10}}$$

which goes to zero as soon as, say, $\kappa > \frac{1+\vartheta}{2C'_{10}}$. This concludes the proof of eq. (5.21) with

$$C_{15} := 2C_*C_{14}^{1+\vartheta}2^{r(1+\vartheta)}\left(2 + 2R^d\sum_{k\geq 1}2^{k(1+\vartheta)}\exp(-C_{10}C_{14}^2 2^{2(k-1)})\right), \tag{5.40}$$

$$C_{14} := 3\max(1, 3\pi_0 R^d \mu_{\max}), \tag{5.41}$$

where C_{10} is defined in eq. (5.38) above. Let us now turn to eq. (5.22) and choose $\delta_n = t(n)n^{-\frac{s}{2s+d}}$. Notice now that

$$n^{\frac{2s}{2s+d}}\delta_n^2 \geq t(n)^2$$

and $2R^d \sum_{k\geq 1} 2^{k(1+\vartheta)} \exp(-C_{11}t(n)^2 2^{2(k-1)})$ can be made as small as we want for n large enough. Finally, notice that

$$(\log n)^2 \delta_n^{-(1+\vartheta)} n^{-\kappa C_6'} \leq C(\log n)^2 t(n)^{-(1+\vartheta)} n^{\frac{s}{2s+d}(1+\vartheta)-\kappa C_6'}$$

which goes to zero as soon as, say, $\kappa > \frac{1+\vartheta}{2C_6'}$. This concludes the proof with

$$C_{16} := 2C^*. \tag{5.42}$$

□

Proof of Theorem 5.10.2. Notice first that for all $s > 0$, $\mathscr{L}^s(\mathbb{R}^d) \supset \mathscr{C}^s(\mathbb{R}^d)$ so that we can rely on the proof of [35, Theorem 3.5]. This latter proof carries over word for word to the present setting after replacing ℓ_2-balls by ℓ_∞-balls in the definition of the support of μ. □

Acknowledgements. *The author would like to thank Dominique Picard for many fruitful discussions and suggestions. He would also like to acknowledge interesting conversations with Gérard Kerkyacharian. Finally, he would like to thank two anonymous referees and an associate editor whose constructive comments led to a full refactoring of the paper and largely contributed to improve it.*

6

Nonparametric regression on the hypersphere with uniform design

Abstract. This paper deals with the estimation of a function f defined on the sphere $\mathbb{S}^d$ of $\mathbb{R}^{d+1}$ from a sample of noisy observation points. We introduce an estimation procedure based on wavelet-like functions on the sphere called needlets and study two estimators $f^{\circledast}$ and $f^{\bigstar}$ respectively made adaptive through the use of a stochastic and deterministic needlet-shrinkage method. We show hereafter that these estimators are nearly-optimal in the minimax framework, explain why $f^{\circledast}$ outperforms $f^{\bigstar}$ and run finite sample simulations with $f^{\circledast}$ to demonstrate that our estimation procedure is easy to implement and fares well in practice. We are motivated by applications in geophysical and atmospheric sciences. ■

Key-Words: Non-parametric regression; Uniform design; Minimax rate; Needlets; Needlet-shrinkage; Stochastic thresholding.

Contents

6.1 Introduction. Many branches of applied sciences call upon simple and powerful statistical methods to efficiently analyze spherical data. This is precisely the case of geophysical and atmospheric sciences, where data are usually collected via satellite or ground stations around the globe. Although there exists a basis of spherical harmonics in $\mathbb{L}^2(\mathbb{S}^2)$, its elements are poorly localized, which makes them of little use to represent locally-supported or multi-scale functions on the sphere (see [42, p. 32]). Furthermore, the direct or indirect transposition of Euclidean wavelets to the sphere inherently leads to artificial distortions. This problem has been addressed

by a proliferating literature leading to the creation of a wide variety of wavelet frames intrinsic to the sphere (see [41, 42] for example). These spherical wavelet frames have since then found many applications in modeling the Earth's magnetic field ([108, 109, 110]), atmospheric flows ([111]), oceanographic flows ([112]) or ionospheric currents ([113]). At the same time, [114] introduced spherical basis functions (SBFs) and used them to design multi-resolution analysis MRA of spherical signals. SBFs were successfully applied in modeling the regional gravity field ([115, 116]) or the global temperature field ([117, 118]). However, the issue was raised that SBFs are actually single-scale (see [117] for example), which, from a practical perspective, makes it difficult for the MRA construct given by [114] to discriminate global from local phenomena. To address that problem, [117] proposed a multi-scale statistical method built upon SBFs of varying bandwidths, which led to new questions of bandwidth selection.

More recently, [40, 39] have shown it is possible to construct well concentrated frames on the hyper-sphere called needlets, which outperform previous spherical wavelet frames and SBFs in many ways. These needlets are very natural building blocks on the sphere and although they are not exactly an orthogonal basis, they behave almost like one ([39]). They are in fact semi-orthogonal in the sense that any two needlets that are at least two levels apart are orthogonal. Besides each needlet is localized around a center point of $\mathbb{S}^d$ and decaying almost exponentially away from this point. Needlets improve in fact considerably on other spherical basis since, similarly to Euclidean wavelets, they characterize Besov spaces on the sphere and provide us with Jackson estimates of best approximations with needlets ([39, Theorem 6.2]). In addition, needlets are truly multi-scale since they concentrate more and more around their center along increasing needlet levels (see Figure 6.1). As will be highlighted underneath, these fine features turn needlets into a powerful alternative to existing spherical wavelet frames or SBFs in performing sensible multi-scale modeling of spherical functions. They are indeed already extensively used for applications in astrophysics (e.g. [44, 45, 46]).

In this paper, we consider the problem of recovering f from the observation of n independent and identically distributed (iid) realizations $(Y_i, T_i), i = 1, \dots, n$ of the random vector (Y, T) generated by the model

$$Y = f(T) + \sigma V, \qquad T \sim \mathcal{U}(\mathbb{S}^d), \quad V \sim \mathcal{N}(0,1) \tag{6.1}$$

where T is uniformly distributed on the hyper-sphere: $T \sim \mathcal{U}(\mathbb{S}^d)$, V is a real-valued standard normal random variable: $V \sim \mathcal{N}(0,1)$, $\sigma \in \mathbb{R}^{+*}$ quantifies the magnitude of the error and f is a real-valued map of a wide Besov scale. In the sequel, we introduce an estimation procedure, which features multi-scale capabilities and is robust and easy to implement, since it rests in practice on the calibration of one single parameter (see Section 6.7). It is noteworthy that our results hold under the assumption that the data are uniformly scattered on the sphere, which is however not the case in most of the practical situations mentioned earlier. Further research is needed in order to circumvent that problem and show that our results eventually generalize to a warped needlets setting ([21]).

We prove in this paper that two well chosen needlet estimators $f^{\circledast}$ and $f^{\bigstar}$ allow to reconstruct with near-minimax-optimality a very wide range of functions f defined on the sphere. In the sequel, we will write $f^{\diamond}$ to refer indifferently to $f^{\circledast}$ or $f^{\bigstar}$, unless stated otherwise. This will prove very convenient in statements that apply to both estimators. As is well-known, we mean by "near-optimality" that the approximation loss between $f^{\diamond}$ and f is within a logarithmic factor of the optimal minimax rate for a given *a priori* class. Optimal estimators tend to be

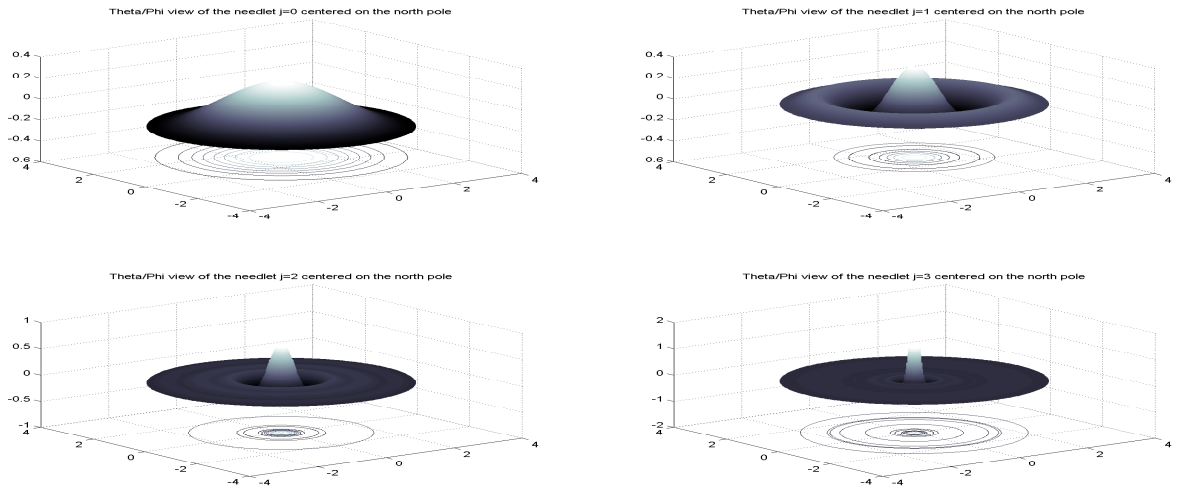

Figure 6.1: These graphs represent the needlets $\psi_{j,\eta}$ for $\eta = \eta_0 \triangleq (0,0,1)$ (Cartesian coordinates), and $j \in \{0,1,2,3\}$. We display a polar view of the needlets, that is $\psi_{j,\eta_0} = \psi_{j,\eta_0}(\varphi,\theta)$, where φ and θ stand respectively for the spherical coordinates colatitude and longitude. In this polar representation, we let φ play the role of the length of the radius vector, while θ stands for the angle between the latter radius and the x-axis

overwhelmingly specific to the smoothness class and the loss for which they are optimal and become irrelevant to any other setting. However, by relaxing the requirement of optimality to near-optimality, it becomes possible to choose $f^\diamond$ to be nearly-optimal over a wide range of losses and smoothness classes ([81]). In this paper, near-minimaxity is thus not only obtained for the celebrated $\mathbb{L}^2$-loss but also for the $\mathbb{L}^\infty$-loss, which means that $f^\diamond$ converges uniformly to f as the sample size grows. Besides, the near-optimality of $f^\diamond$ holds over a wide range of smoothness classes, which makes these results particularly interesting in practice, when there is only scarce information available on the objective function f.
The two needlet estimators $f^\circledast$ and $f^\bigstar$ are respectively made adaptive through the use of a stochastic and deterministic thresholding method. Although they verify a wide range of similar properties, the proofs of their near-optimality differ slightly. We run numerical simulations on $f^\circledast$ and show how the stochastic thresholding outperforms the deterministic one. As described in Section 6.7, this is due to the fact that the stochastic thresholding parameter adjusts to the magnitude of the sample noise at each sample coefficient $\hat{\beta}_{j,\eta}$ (see Section 6.5). Furthermore, we study the impact of the dimension d on both estimators. Despite the well-known deterioration of minimax rates as the dimension d increases, we show that working on a higher dimensional underlying unit sphere $\mathbb{S}^d$ sharpens the constants in our minimaxity results and makes the construction of both estimators easier.
This paper extends the optimality results of [119] to the regression setting, which is essentially made possible thanks to the sharp localization properties of needlets, as will be made precise in the proof of Lemma 6.10.3.
The plan of the paper is as follows. In Section 6.2 and Section 6.3 we review some background material on needlets and Besov spaces on the sphere. Readers familiar with these latter matters may jump directly to Section 6.4, where we introduce the model and set notations that will be

used throughout the paper. Section 6.5 presents our thresholding estimators, whose minimax performances are stated in Section 6.6. Section 6.7 describes the performance of the estimators on some simulated data. Finally, Section 6.8–Section 6.10 contain the proofs.
In the sequel, the symbol $\triangleq$ stands for *equal by definition*. In addition, for two functions A, a of the variable γ, we write $A(\gamma) \approx a(\gamma)$ when there exist constants c, C independent of γ such that $ca(\gamma) \leq A(\gamma) \leq Ca(\gamma)$ for all values of γ. Furthermore, we will write $C(\beta)$ to mean that the constant C depends on parameter β.

6.2 Needlets and their properties. In this section, we give an overview of the needlets construction and describe some of their properties. It is inspired from [39] where the needlets were originally introduced and presents similar material as in [119, Section 2]. We first introduce spherical harmonics. We then detail the needlet construction. It is essentially divided into two steps: a Littlewood-Paley decomposition and a quadrature formula.

6.2.1 Spherical harmonics. In what follows, we write $\mathfrak{M}$ the surface measure of $\mathbb{S}^d$, that is the unique positive measure on $\mathbb{S}^d$ which is invariant under rotation and has the area ω_d of $\mathbb{S}^d$ as total mass, that is $\omega_d = 2\pi^{(d+1)/2}/\Gamma(\frac{d+1}{2})$. Denote by $\mathcal{H}_l$ the set of spherical harmonics of degree l ([43, Chap. 4]). We can consider $\mathcal{H}_l$ as a subspace of $\mathbb{L}^2(\mathbb{S}^d)$ with inner product $(f,g) = \int_{\mathbb{S}^d} f(x)g(x)\mathfrak{M}(dx)$ and show that $\mathcal{H}_k \perp \mathcal{H}_l$ for $k \neq l$ and the collection of finite linear combinations of $\cup\mathcal{H}_l$ is dense in $\mathbb{L}^2(\mathbb{S}^d)$. Moreover we can compute $a_{l,d} \triangleq \dim \mathcal{H}_l = \mathcal{O}(l^{d-1})$ and exhibit an orthonormal basis $\{Y_{l,m}; m = 1, \ldots, a_{l,d}\}$ of $\mathcal{H}_l$ and, subsequently, an orthonormal basis $\cup_{l\geq 0}\{Y_{l,1}, \ldots, Y_{l,a_{l,d}}\}$ of $\mathbb{L}^2(\mathbb{S}^d)$. Thus, for any $f \in \mathbb{L}^2(\mathbb{S}^d)$, the orthogonal projector on $\mathcal{H}_l$ is given by

$$P_{\mathcal{H}_l} f(\xi) = \sum_{m=1}^{a_{l,d}} (f, Y_{l,m}) Y_{l,m}(\xi) = \int_{\mathbb{S}^d} P_l(\xi, x) f(x) \mathfrak{M}(dx)$$

where we have written $P_l(\xi, x) = \sum_{m=1}^{a_{l,d}} Y_{l,m}(\xi)Y_{l,m}(x)$ the projection kernel on $\mathcal{H}_l$. Thanks to the addition theorem [120, Theorem 2], we have $P_l(\xi, x) = c_{l,d}L_l(\xi \centerdot x)$ where $c_{l,d} \triangleq a_{l,d}/\omega_d$, the operator "$\centerdot$" stands for the usual Euclidean scalar product of $\mathbb{R}^{d+1}$, and L_l is the Legendre polynomial of degree l and dimension $d+1$ ([120, p 16]). From now on, we will write $P_l(\xi \centerdot x)$ in place of $P_l(\xi, x)$.

Remark 2. For practical implementation, let's recall that we have

$$\int_{-1}^{1} L_l(t)L_k(t)(1-t^2)^{\frac{d-2}{2}} dt = \widetilde{c}_{l,d}\delta_{l,k}, \qquad \widetilde{c}_{l,d} = \frac{\omega_d}{\omega_{d-1}} \frac{1}{a_{l,d}} = \frac{\sqrt{\pi}\Gamma(\frac{d}{2})}{a_{l,d}\Gamma(\frac{d+1}{2})}$$

In Section 6.7, we will run simulations on the sphere of $\mathbb{R}^3$. In this case, $d = 2$, so that we have $\omega_2 = 4\pi$, $\widetilde{c}_{l,2} = \frac{2}{2l+1}$ and we can write $N_l = \sqrt{\frac{2l+1}{2}}L_l$ the normalized Legendre polynomials. Besides $c_{l,2} = \frac{2l+1}{4\pi}$ and we will therefore use kernels of the form $P_l(\xi \centerdot x) = \frac{2l+1}{4\pi}L_l(\xi \centerdot x) = \sqrt{\frac{2l+1}{8\pi^2}}N_l(\xi \centerdot x)$ for simulations.

A direct application of Parseval's formula in $\mathbb{L}^2(\mathbb{S}^d)$ leads to

$$\int_{\mathbb{S}^d} P_l(\xi \centerdot x)P_k(x \centerdot \tau)\mathfrak{M}(dx) = \delta_{l,k}P_l(\xi \centerdot \tau) \tag{6.2}$$

Let's write $\mathscr{P}_l$ the space of spherical harmonics of degree at most l. Obviously, the kernel $K_l = \sum_{k=0}^{l} P_k$ stands for the orthogonal projector on $\mathscr{P}_l$. Unfortunately, the poor localization properties of K_l are a major obstacle to its use for function decomposition outside the $\mathbb{L}^2$ framework. This problem is circumvented in [40] by the introduction of a new kernel whose construction is based on the Littlewood-Paley decomposition.

6.2.2 Littlewood-Paley decomposition. Let φ be a C^∞ function on $\mathbb{R}$, symmetric and decreasing on $\mathbb{R}^+$ such that $\text{supp}\varphi \subset [-1,1]$, $\varphi(z) = 1$ if $|z| \leq \frac{1}{2}$ and $0 \leq \varphi(z) \leq 1$ otherwise. We set $b^2(z) \triangleq \varphi(z/2) - \varphi(z)$ so that $b^2(z) \geq 0$ and $b(z) \neq 0$ only if $\frac{1}{2} \leq |z| \leq 2$. We now define the following kernels for $j \geq 0$,

$$\Theta_j \triangleq \sum_{l\geq 0} b^2(l/2^j) P_l = \sum_{2^{j-1}<l<2^{j+1}} b^2(l/2^j) P_l$$
$$\Psi_j \triangleq \sum_{l\geq 0} b(l/2^j) P_l = \sum_{2^{j-1}<l<2^{j+1}} b(l/2^j) P_l$$

For any $\xi, \tau \in \mathbb{S}^d$, we write

$$\{\Psi_j * f\}(\xi) \triangleq \int_{\mathbb{S}^d} \Psi_j(\xi \cdot x) f(x) \mathfrak{M}(dx),$$
$$\{\Psi_j * \Psi_k\}(\xi \cdot \tau) \triangleq \int_{\mathbb{S}^d} \Psi_j(\xi \cdot x) \Psi_k(x \cdot \tau) \mathfrak{M}(dx)$$

It appears as a direct consequence of eq. (6.2) that $\Theta_j \triangleq \Psi_j * \Psi_j$ for $j \geq 0$. As detailed in [39, Theorem 2.2], these new kernels are in fact nearly exponentially localized in the sense that, for any $k > 0$, there exists a constant $c_k > 0$ such that, for any $\xi, \eta \in \mathbb{S}^d$,

$$|\Theta_j(\xi \cdot \eta)|, |\Psi_j(\xi \cdot \eta)| \leq \frac{c_k 2^{jd}}{\{1 + 2^j dist(\xi, \eta)\}^k}$$

where *dist* stands for the geodesic distance on the sphere. As proved in [40, Theorem 3.1], we have the following result

Proposition 6.2.1. *For every $f \in \mathbb{L}^p(\mathbb{S}^d)$ and $1 \leq p < \infty$, or if $p = \infty$ and f is continuous, the following identity holds in $\mathbb{L}^p$,*

$$f = P_0 * f + \lim_{J\to\infty} \sum_{j=0}^{J} \Theta_j * f$$

6.2.3 Quadrature formula and needlets. The needlets arise as by-products of kernel Ψ by means of a quadrature formula ([39, Corollary 2.9]). For all $l \in \mathbb{N}$, there indeed exists a finite subset $\mathcal{X}_l \subset \mathbb{S}^d$ and positive real numbers $\lambda_\eta > 0$, indexed by the elements $\eta \in \mathcal{X}_l$, such that for all $f \in \mathscr{P}_l$

$$\int_{\mathbb{S}^d} f(x) \mathfrak{M}(dx) = \sum_{\eta \in \mathcal{X}_l} \lambda_\eta f(\eta)$$

In particular, it is obvious from the above definition of the operator Ψ_j that $x \mapsto \Psi_j(\xi, x) \in \mathscr{P}_{[2^{j+1}]}$, so that $x \mapsto \Psi_j(\xi, x)\Psi_j(x, \tau) \in \mathscr{P}_{[2^{j+2}]}$. Thus we can apply the quadrature formula to write

$$\Theta_j(\xi \cdot \tau) = \int_{\mathbb{S}^d} \Psi_j(\xi \cdot x)\Psi_j(x \cdot \tau)\mathfrak{M}(dx) = \sum_{\eta \in \mathcal{X}_{[2^{j+2}]}} \lambda_\eta \Psi_j(\xi \cdot \eta)\Psi_j(\eta \cdot \tau) \tag{6.3}$$

Now, write $\mathcal{X}_{[2^{j+2}]} = \mathcal{Z}_j$ and define the needlet of center $\eta \in \mathcal{Z}_j$ and level j by

$$\psi_{j,\eta}(\xi) \triangleq \sqrt{\lambda_\eta}\Psi_j(\xi \cdot \eta)$$

With these notations, eq. (6.3) leads to

$$\Theta_j * f(\xi) = \sum_{\eta \in \mathcal{X}_{[2^{j+2}]}} \sqrt{\lambda_\eta}\Psi_j(\xi \cdot \eta)\{\sqrt{\lambda_\eta}\Psi_j * f(\eta)\} = \sum_{\eta \in \mathcal{Z}_j} (\psi_{j,\eta}, f)\psi_{j,\eta}(\xi)$$

As described in [39, Corollary 2.9], the choice of the sets of cubature points $\mathcal{Z}_j$ is not unique, but one can impose the conditions $\#\mathcal{Z}_j \approx 2^{jd}$ and $\lambda_\eta \approx 2^{-jd}$. These last results together with Proposition 6.2.1 lead to the following equality in $\mathbb{L}^p$, $p \geq 1$,

$$f = P_0 * f + \sum_{j \geq 0} \sum_{\eta \in \mathcal{Z}_j} (f, \psi_{j,\eta})\psi_{j,\eta} \tag{6.4}$$

The $\psi_{j,\eta}$'s appear therefore as building blocks on the sphere. They obviously inherit the fine localization properties of the Ψ_j's, which prompted Narcowich, Petrushev and Ward to call them *needlets*. Besides, they are more and more localized around their center as j increases and therefore capture sample phenomena occurring at finer and finer scales. These last features turn them into a very handy tool to tackle statistical problems on the sphere. From this localization property it follows that for $0 < p \leq \infty$,

$$c_p 2^{jd\{\frac{1}{2}-\frac{1}{p}\}} \leq \|\psi_{j,\eta}\|_p \leq C_p 2^{jd\{\frac{1}{2}-\frac{1}{p}\}} \tag{6.5}$$

Moreover, as shown in [119, Lemma 2], we have the following useful lemma

Lemma 6.2.1. *For any $j \geq 0$, we have,*

1) For every $0 < p \leq \infty$

$$\| \sum_{\eta \in \mathcal{Z}_j} \lambda_\eta \psi_{j,\eta} \|_p \leq c 2^{jd\{\frac{1}{2}-\frac{1}{p}\}} \left(\sum_{\eta \in \mathcal{Z}_j} |\lambda_\eta|^p \right)^{\frac{1}{p}} \tag{6.6}$$

2) For every $1 \leq p \leq +\infty$

$$\left(\sum_{\eta \in \mathcal{Z}_j} |(f, \psi_{j,\eta})|^p \right)^{\frac{1}{p}} 2^{jd\{\frac{1}{2}-\frac{1}{p}\}} \leq c\|f\|_p \tag{6.7}$$

We refer the reader to the above-mentioned article for a detailed proof. Let's now turn to the case where f belongs to a Besov space on the sphere and describe how these latter spaces relate to needlets.

6.3 Besov spaces on the sphere and needlets. In this section we summarize the main properties of Besov spaces on the sphere following the presentations given in [39, 119, Section 5]. Besov spaces on the sphere can be defined as follows

Definition 6.3.1. *The Besov space $B^s_{rq} \triangleq B^s_{rq}(\mathbb{S}^d)$, where $s \in \mathbb{R}$, $0 < r, q \leq \infty$, is the set of all measurable functions on $\mathbb{S}^d$ such that*

$$\|f\|_{B^s_{rq}} \triangleq \left(\sum_{j=0}^{\infty} \{2^{js} \|\Theta_j * f\|_r\}^q \right)^{\frac{1}{q}} < \infty$$

where the ℓ^q-norm is replaced by the ℓ^∞-norm when $q = \infty$. It is in fact possible to show that this definition is independent of the choice of φ used to build kernels Θ_j.

Besides, the following noteworthy theorem ([39, Theorem 5.5]) sheds some light on the tight intertwining between Besov spaces and needlet coefficients.

Theorem 6.3.1. *Let be given s, r, q such that $1 \leq r \leq +\infty$, $s > 0$, $0 \leq q \leq +\infty$. For any sequence $\{g_{j,\eta}, \eta \in \mathcal{Z}_j, j \geq 0\}$, we write*

$$\|g\|_{\boldsymbol{b}^s_{rq}} = \| \left\{ 2^{j\{s+\frac{d}{2}-\frac{d}{r}\}} \|\{g_{j,\eta}\}_{\eta \in \mathcal{Z}_j}\|_{\ell^r} \right\}_{j \geq 0} \|_{\ell^q}$$

In addition, for any measurable function f, we define $\beta_{j,\eta} \triangleq (f, \psi_{j,\eta})$ provided it makes sense, and we consider the sequence $\{\beta_{j,\eta}, \eta \in \mathcal{Z}_j, j \geq 0\}$. Then we have $\|\beta\|_{\boldsymbol{b}^s_{rq}} \approx \|f\|_{B^s_{rq}}$ and, thus, $f \in B^s_{r,q}$ if and only if

$$\|\beta\|_{\boldsymbol{b}^s_{rq}} < \infty \tag{6.8}$$

In the sequel we shall write $\|f\|_{B^s_{rq}}$ in place of $\|\beta\|_{\boldsymbol{b}^s_{rq}}$. Furthermore we will denote by $B^s_{r,q}(M)$ the ball of radius M of the Besov space $B^s_{r,q}$. Let's now recall the Besov embedding theorem on the sphere. We refer the reader to [119, Theorem 5] for a detailed proof.

Theorem 6.3.2. *(The Besov embedding)*

$$\begin{aligned} &B^s_{r,q} \subseteq B^s_{p,q}, && \text{if } p \leq r \leq \infty \\ &B^s_{r,q} \subseteq B^{s+\frac{d}{p}-\frac{d}{r}}_{p,q}, && \text{if } s > \frac{d}{r} - \frac{d}{p} \text{ and } r \leq p \leq \infty \end{aligned}$$

6.4 Setting and notations. In this section, we describe the model and introduce notations that will be used throughout the paper. We start with a few notations. For $d \geq 1$, $s > \frac{d}{r}$, $0 < r \leq \infty$, we set

$$\vartheta \triangleq \vartheta^p_r \triangleq \frac{s + \frac{d}{p} - \frac{d}{r}}{2(s + \frac{d}{2} - \frac{d}{r})}, \qquad \varsigma \triangleq \frac{s}{2s+d}, \qquad \vartheta^\infty \triangleq \vartheta^\infty_r \triangleq \frac{s - \frac{d}{r}}{2(s + \frac{d}{2} - \frac{d}{r})}$$

We will write $X \sim \mathbb{P}$ to mean that the random variable X follows law $\mathbb{P}$, $X \sim Y$ to mean that X and Y have the same law and denote the standard Gaussian law by $\mathcal{N}(0,1)$. In the sequel C and c stand for absolute constants, which may vary from line to line or even inside a same equation. And in order to lighten the notations, we sometimes write $A \equiv \widetilde{A}$ to mean

that A is a lighter typographical way to refer to $\widetilde{A}$. We write $(\Omega, \mathcal{F}, \mathbb{P})$ a probability space on which Y, T and V are defined according to $Y = f(T) + V$, where T is uniformly distributed on $\mathbb{S}^d$, V is normal with mean zero and standard deviation σ and $f \in B^s_{rq}(M)$. In particular, we can take $(\Omega, \mathcal{F}, \mathbb{P})$ to be the canonical probability space associated to the vector (V, T), that is, $\Omega \equiv \mathbb{R} \times \mathbb{S}^d$, $\mathcal{F} = \mathscr{B}(\mathbb{R} \times \mathbb{S}^d)$, for all $w = (v, t) \in \mathbb{R} \times \mathbb{S}^d$, $(V, T)\{w\} = (V(v), T(t)) = (v, t) = w$ and $\mathbb{P} \equiv \mathbb{P}^{V,T} = \mathbb{P}^V \otimes \mathbb{P}^T$. Obviously, $\mathbb{P}^V(dv) = \varphi_\sigma(v)\lambda(dv)$, where $\varphi_\sigma(v)$ is the normal density with mean zero and standard deviation σ and λ the Lebesgue measure on $(\mathbb{R}, \mathscr{B}(\mathbb{R}))$; and $\mathbb{P}^T$ is the uniform law on the sphere $\mathbb{S}^d$, that is $\mathbb{P}^T(dt) = \mathfrak{M}(dt)/\omega_d$ where $\mathfrak{M}$ stands for the spherical surface measure introduced earlier. We write as well $\mathbb{P}_f \triangleq \mathbb{P}^{Y,T}$ the law of the vector (Y, T) and $\mathbb{E}_f$ the expectation with respect to $\mathbb{P}_f$. When there is no ambiguity, we denote $\mathbb{P} \equiv \mathbb{P}_f$ and $\mathbb{E} \equiv \mathbb{E}_f$. Alternatively and when appropriate, we will write the model $Y = f(T) + \sigma V$ with corresponding modifications.

6.5 Needlet estimation of f on the sphere. Given the set of n iid observations (Y_i, T_i), $i = 1, \ldots, n$, we can compute

$$\frac{1}{n}\sum_{i\le n} Y_i \psi_{j,\eta}(T_i) = \frac{1}{n}\sum_{i\le n} f(T_i)\psi_{j,\eta}(T_i) + \frac{1}{n}\sum_{i\le n} \sigma V_i \psi_{j,\eta}(T_i)$$

In the sequel, we will adopt the following notations

$$\begin{aligned} y^*_{j,\eta} &\triangleq \omega_d \sum_{i\le n} Y_i \psi_{j,\eta}(T_i)/n, \\ \zeta^*_{j,\eta} &\triangleq \omega_d \sum_{i\le n} f(T_i) \psi_{j,\eta}(T_i)/n, \\ \gamma^*_{j,\eta} &\triangleq \omega_d \sum_{i\le n} \sigma V_i \psi_{j,\eta}(T_i)/n. \end{aligned}$$

In addition we write

$$\begin{aligned} \varrho^2_{j,\eta} &\triangleq \sum_{i\le n} \psi_{j,\eta}(T_i)^2/n, \\ \xi_{j,\eta} &= \sqrt{n}\gamma^*_{j,\eta}/(\sigma\omega_d \varrho_{j,\eta}). \end{aligned}$$

Since the V_i's are iid standard normal and independent from the T_i's, we know that

$$\mathbb{V}\mathrm{ar}(\gamma^*_{j,\eta} | T_1, \ldots T_n) = \sigma^2 \omega_d^2 \varrho^2_{j,\eta}/n.$$

Thus $\xi_{j,\eta} \sim \mathcal{N}(0,1)$ conditionally on the T_i's. We therefore observe the sequence $\{y^*_{j,\eta}, j \ge 0, \eta \in \mathcal{Z}_j\}$, such that $y^*_{j,\eta} = \zeta^*_{j,\eta} + \{\sigma\omega_d \varrho_{j,\eta}/\sqrt{n}\}\xi_{j,\eta}$, for all $j \ge 0$ and all $\eta \in \mathcal{Z}_j$.
Eq. (6.4) shows that the estimation of f by $f^\diamond \equiv f^\diamond(Y_i, T_i; i = 1, \ldots n)$ reduces to the estimation of its needlet coefficients $\beta_{j,\eta}$ and $P_0 * f$. It is easily proved that $\hat{\beta}_{j,\eta} \triangleq y^*_{j,\eta}$ and $\hat{P}_0 \triangleq \sum Y_i/n$ are respectively strongly consistent and unbiased estimator of $\beta_{j,\eta}$ and $P_0 * f$. We further want the estimator $f^\diamond$ to be adaptive to inhomogeneous smoothness. In that perspective we use a hard thresholding method, which aims at canceling out coefficient estimates $\hat{\beta}_{j,\eta}$ that result mainly from noise. In the sequel we study two estimators $f^\circledast$ and $f^\bigstar$ built respectively upon a

stochastic and a deterministic thresholding method. We denote by $\beta^{\circledast}_{j,\eta}$ the needlet coefficients of $f^{\circledast}$ and set $\beta^{\circledast}_{j,\eta} \triangleq \hat{\beta}_{j,\eta}\mathbb{1}_{\{|\hat{\beta}_{j,\eta}|\geq\kappa_{j,\eta}t(n)\}}$, where $\kappa_{j,\eta} = \varpi\varrho_{j,\eta}$, ϖ is a constant and $t(n) = \sqrt{\log n/n}$. Similarly, we denote by $\beta^{\bigstar}_{j,\eta}$ the needlet coefficients of $f^{\bigstar}$ and set $\beta^{\bigstar}_{j,\eta} \triangleq \hat{\beta}_{j,\eta}\mathbb{1}_{\{|\hat{\beta}_{j,\eta}|\geq\kappa t(n)\}}$, where κ is a constant. In the sequel, we will write $f^{\diamond}$, $\beta^{\diamond}_{j,\eta}$ and $\varkappa$ to refer indifferently to $f^{\circledast}$, $\beta^{\circledast}_{j,\eta}$ and ϖ, or $f^{\bigstar}$, $\beta^{\bigstar}_{j,\eta}$ and κ.

Finally, we cut the series expansion of $f^{\diamond}$ at level J such that $2^{Jd} = n/\{C_0\log n\}$. With these notations, the needlet estimator of f can be written as

$$f^{\diamond}_J = \hat{P}_0 + \sum_{j=0}^{J}\sum_{\eta\in\mathcal{Z}_j}\beta^{\diamond}_{j,\eta}\psi_{j,\eta} \tag{6.9}$$

Before we move on to the study of the minimax rates for the estimator $f^{\diamond}$, notice that in the above construction of $f^{\diamond}$, we remain free to choose the values of $\varkappa$ and C_0. We will see later that C_0 is in fact very much related to $\varkappa$ so that we are truly left with one tuning parameter $\varkappa$. We will give some hints on ways of evaluating it in Section 6.7.

6.6 Minimax rates for $\mathbb{L}^p$ norms and Besov spaces on the sphere. In the sequel, we will denote by $\mathfrak{C}^{\circledast}_z$ the set of conditions

$$\mathfrak{C}^{\circledast}_z \quad \begin{cases} \varpi \geq 4\max\left(4e^2\omega_d^2\|f\|_\infty^2, \omega_d^2\sigma^2, z+1\right), \\ C_0 \geq \varpi\max\left(\dfrac{2C_\infty^2}{c_2^2e^2}, \dfrac{2}{m^-}\right), \\ 2^{Jd} = \dfrac{n}{C_0\log n} \end{cases}$$

and $\mathfrak{C}^{\bigstar}_z$ the set of conditions

$$\mathfrak{C}^{\bigstar}_z \quad \begin{cases} \kappa \geq 4\max\left(2\omega_d C_2\max(4\|f\|_\infty^2, 3\sigma^2), z+1\right), \\ C_0 > \max(6\omega_d\|f\|_\infty C_\infty, \kappa/\{2m^-\}), \\ 2^{Jd} = \dfrac{n}{C_0\log n} \end{cases}$$

where the constants C_∞, c_2 are defined in Proposition 6.8.2 and m^- is defined in Lemma 6.10.1. Once again, the couple $f^{\diamond}, \mathfrak{C}^{\diamond}_z$ will denote indifferently $f^{\circledast}, \mathfrak{C}^{\circledast}_z$ or $f^{\bigstar}, \mathfrak{C}^{\bigstar}_z$. We now present two theorems that describe the asymptotic properties of the estimator $f^{\diamond}$ of f. In a first theorem, we compute an upper-bound on the loss of our estimator over Besov balls and $\mathbb{L}^p$-norms. Its proof can be found in Section 6.8.

Theorem 6.6.1. *Let be given $f \in \mathbb{L}^\infty$. Consider the estimator $f^{\diamond}$ (see eq. (6.9)) of f built upon n iid observations (Y_i, T_i) drawn from the model stated in eq. (6.1). Then, for $d \geq 1$, $s > \frac{d}{r}$, $0 < r \leq \infty$, we have*

a) For any $z > 1$, there exists some constant c_∞ such that, as soon as the conditions $\mathfrak{C}^{\diamond}_z$ are verified,

$$\sup_{f\in B^s_{r,q}(M)}\mathbb{E}\|f^{\diamond} - f\|_\infty^z \leq c_\infty(\log n)^{2z}\left(\frac{n}{\log n}\right)^{-z\vartheta^\infty} \tag{6.10}$$

b) For any $1 \leq p < \infty$, there exists a constant c_p such that, as soon as the conditions $\mathfrak{C}_p^\diamond$ are verified,

$$\sup_{f \in B^s_{r,q}(M)} \mathbb{E}\|f^\diamond - f\|_p^p \leq c_p \{\log n\}^p \left(\frac{n}{\log n}\right)^{-p\vartheta}, \qquad \text{if } r \leq \frac{dp}{2s+d} \text{ and } p \geq 2 \tag{6.11}$$

$$\sup_{f \in B^s_{r,q}(M)} \mathbb{E}\|f^\diamond - f\|_p^p \leq c_p \{\log n\}^p \left(\frac{n}{\log n}\right)^{-p\varsigma}, \qquad \text{if } r > \frac{dp}{2s+d} \tag{6.12}$$

Notice that the above result places $f^\diamond$ within a larger $\log n$ factor of the $n/\log n$ term than in [119, Theorem 8]. The proof we present here is marginally simpler than theirs and eventually more systematic since it introduces a function of a floating parameter l as an upper-bound and optimizes with respect to l. To be more specific, in contrary to [119, Proposition 15], Proposition 6.8.2 does not use the fact that there exists an index $J_1(s)$ beyond which $|\beta_{j,\eta}| \leq t(n)$, which makes our demonstration simpler albeit less precise.
In a second theorem, we compute a lower bound on the loss of f estimators over Besov balls and $\mathbb{L}^p$-norms. Its proof follows similar lines as the proof of the lower bound detailed in [119]. It is therefore not reported here but made available at `https://sites.google.com/site/jrmonnier/publications/test`.

Theorem 6.6.2. *(Lower bound) We write $\inf_\theta$ the lower-bound over all estimators θ of f, that is all measurable functions of the $Y_i, T_i, i = 1 \ldots, n$. Then, for $d \geq 1$, $s > \frac{d}{r}$, $0 < r \leq \infty$, we have*

a) If $1 \leq p \leq 2$,

$$\inf_\theta \sup_{f \in B^s_{rq}(M)} \mathbb{E}_f \|\theta - f\|_p^p \geq c n^{-p\varsigma}$$

b) If $2 < p \leq +\infty$

$$\inf_\theta \sup_{f \in B^s_{rq}(M)} \mathbb{E}_f \|\theta - f\|_p^p \geq \begin{cases} cn^{-p\varsigma}, & \text{if } r > \frac{dp}{2s+d} \\ cn^{-p\vartheta}, & \text{if } r \leq \frac{dp}{2s+d} \end{cases}$$

These two theorems demonstrate that our estimator $f^\diamond$ is in fact nearly-optimal in all the above settings. Although these minimaxity results hold for a " big enough" sample size n, the estimator $f^\diamond$ fares well in practice over finite samples too, as will be shown through simulations in the next section.

6.7 Simulations. For the sake of brevity, we only report here the main results of our simulations. The interested reader is referred to the addendum at `https://sites.google.com/site/jrmonnier/publications/test` for a thorough discussion.
Remark we expect the stochastic thresholding to outperform the deterministic one, since it adjusts the constant thresholding parameter ϖ by the sample noise standard deviation $\varrho_{j,\eta}$ at sample coefficient $\hat{\beta}_{j,\eta}$. The comparison between $f^\bigstar$ and $f^\circledast$ on simulated data shows that the two estimators perform similarly at needlet levels $0 \leq j \leq 3$, due to the fact that $\varrho_{j,\eta}$ remains almost constant across cubature points η at these resolution levels. However, $\varrho_{j,\eta}$ varies more widely from one cubature point to another at higher needlet levels causing $f^\circledast$ to adjust more efficiently to the noise than $f^\bigstar$ and outperform it.

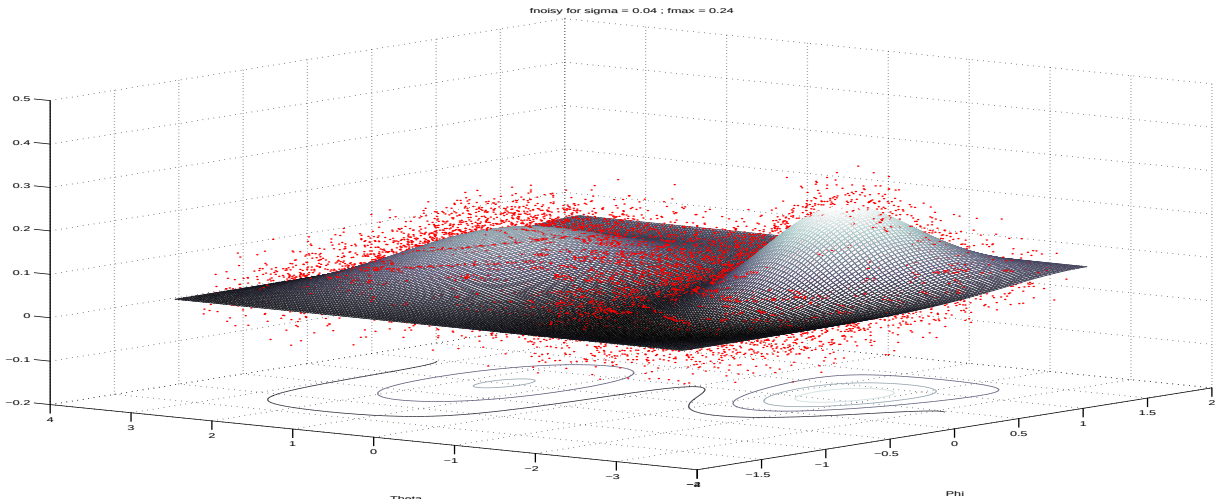

Figure 6.2: Display of the function $f : x \in \mathbb{S}^2 \mapsto 0.65\exp(-k_1\|x - x_1\|_2)/b_1 + 0.35\exp(-k_2\|x - x_2\|_2)/b_2$ *on a grid of points of the unit sphere of* $\mathbb{R}^3$ *parametrized by their spherical coordinates colatitude* φ *and longitude* θ. *We choose* $x_1 = (0, 1, 0)$, $x_2 = (0, -0.8, 0.6)$, $k_1 = 0.7$, $k_2 = 2$ *and* $b_i = \int_{\mathbb{S}^2} \exp(k_i\|x - x_i\|_2)\mathfrak{M}(dx)$, $i = 1, 2$. *We set* $\sigma = 0.04$ *and represent* $N = 10,000$ *noisy observations* Y_i *at locations* T_i *simulated using the transformation* $\theta = 2\pi(\text{rand}() - .5)$ *and* $\varphi = \sin^{-1}(2\text{rand}() - 1)$

We therefore run simulations with $f^{\circledast}$. Notice that the condition on ϖ depends on $\|f\|_\infty$, which is unknown in practice. However, if we have any prior insight into f, we can replace $\|f\|_\infty$ by any real constant that overshoots it, which gives us more flexibility. We compute conditions $\mathfrak{C}_z^{\circledast}$ numerically. With our test function f (see Figure 6.2), such that $\|f\|_\infty = 0.24$, we obtain $C_0 \geq \varpi 5 \cdot 10^5$. It thus appears that our proof of the near-optimality of $f^{\circledast}$ imposes drastic conditions on the parameter C_0. From a theoretical standpoint, $f_J^{\circledast}$ is the near optimal estimator of f as soon as $N/\log N$ is of order $C_0 2^{2J}$, which means that we would have to gather unrealistically large data samples in order to build an estimator $f_J^{\circledast}$ of f that would contain information up to degree of resolution J for large C_0. However, numerical simulations tend to demonstrate that our procedure fares well under much less drastic conditions.
The most obvious way of fixing the free thresholding parameter ϖ is to monitor the proportion of coefficients that are zeroed out at each resolution level as a function of ϖ. It is clear that the more coefficients thresholded at high levels, the smoother the estimator. The ultimate choice of ϖ should therefore be related to an *a priori* knowledge of the smoothness of f. Numerical simulations show that $f^{\circledast}$ recovers the overall shape of f, even for values of σ that are large in front of $\|f\|_\infty$. Without over-fitting the data, we obtain an estimation error $\|f_2^{\circledast} - f\|_\infty = 0.046$ for $\sigma = 0.04$ (see Figure 6.3) and $\|f_2^{\circledast} - f\|_\infty = 0.062$ for $\sigma = 0.5$.
Finally, notice that, despite the "curse of dimensionality" on minimax rates, conditions $\mathfrak{C}_z^{\diamond}$ are loosened as d increases while the upper-bound constants that appear in Theorem 6.6.1 become smaller.

6.8 Proof of the minimax rate. Let us now move on to the proofs of the theorems presented in Section 6.6. We first introduce two propositions that we will need later on in the proof.

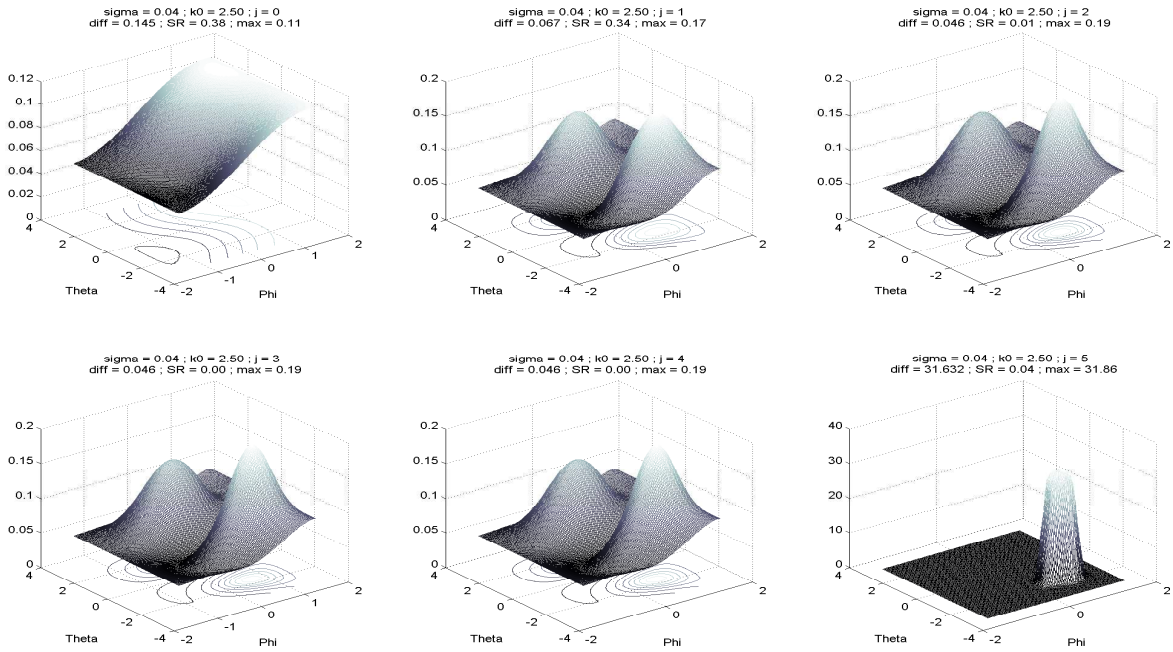

Figure 6.3: Computation of $f^{\circledast}$ from the observation of $20,000$ vectors (Y_i, T_i). To clearly picture the contribution of each level j to the value of the estimator at each point, we graph $f_J^{\circledast}$ for $J = 0, 1, 2, 3$ on the grid. In the title of each sub-figure we indicate the value of σ, ϖ (constant multiple of k_0), J (corresponds to j), diff (which stands for the value of $\|f^{\circledast} - f\|_\infty$ on the grid), SR (which stands for "survival rate" and displays the percentage of coefficients that survives thresholding at level J), and max *(which gives the maximum value of the estimator $f^{\circledast}$ on the grid)*

Proposition 6.8.1. *For all $z > 0$, we have*

$$\mathbb{E}|\hat{P}_0 - P_0 * f|^z \leq Cn^{-\frac{z}{2}}$$

In the sequel, we denote by $\mathfrak{D}^{\circledast}(\gamma, z)$ the set of conditions

$$\begin{aligned} \varpi &\geq \max\left(16e^2\omega_d^2\|f\|_\infty^2, 4\omega_d^2\sigma^2, z, 4\left\{\frac{2\gamma}{d}+1\right\}\right), \\ C_0 &\geq \max\left(\frac{1}{m^-}\max\left(\frac{z}{2}, \frac{\gamma}{d}\right), \varpi\max\left(\frac{2C_\infty^2}{c_2^2e^2}, \frac{2}{m^-}\right)\right), \qquad \mathfrak{D}^{\circledast}(\gamma, z) \\ 2^{Jd} &= \frac{n}{C_0\log n} \end{aligned}$$

and $\mathfrak{D}^{\bigstar}(\gamma, z)$ the set of conditions

$$\begin{aligned} \kappa &\geq \max\left(8\omega_d C_2\max(4\|f\|_\infty^2, 3\sigma^2), \max\left(z, 8(\frac{\gamma}{d}+\frac{1}{2})\right)\right), \\ C_0 &> \max(6\omega_d\|f\|_\infty C_\infty, \kappa/\{2m^-\}), \qquad \mathfrak{D}^{\bigstar}(\gamma, z) \\ 2^{Jd} &= \frac{n}{C_0\log n} \end{aligned}$$

As usual, the couple $f^\diamond, \mathfrak{D}^\diamond(\gamma, z)$ will denote indifferently $f^{\circledast}, \mathfrak{D}^{\circledast}(\gamma, z)$ or $f^\bigstar, \mathfrak{D}^\bigstar(\gamma, z)$.

Proposition 6.8.2. *Consider the constant m^- defined in Lemma 6.10.1, and c_2 and C_∞ such that, for all $j \geq 0, \eta \in \mathcal{Z}_j$, $c_2 \leq \|\psi_{j,\eta}\|_2$ and $\|\psi_{j,\eta}\|_\infty \leq C_\infty 2^{jd/2}$. For any $f \in \mathbb{L}^\infty$, $\gamma > 0$, $z > 1$, $l \in [0, z]$, and under the set of conditions $\mathfrak{D}^\diamond(\gamma, z)$ on $\varkappa$, C_0 and J, the following two inequalities hold true,*

$$\sum_{j=0}^{J} 2^{j\gamma} \mathbb{E} \sup_{\eta \in \mathcal{Z}_j} |\beta^\diamond_{j,\eta} - \beta_{j,\eta}|^z \leq C \left\{ t(n)^{z-l} (J+1)^z \sum_{j=0}^{J} 2^{j\gamma} \sup_{\eta \in \mathcal{Z}_j} |\beta_{j,\eta}|^l + n^{-\frac{z}{2}} \right\} \tag{6.13}$$

$$\sum_{j=0}^{J} 2^{j(\gamma-d)} \mathbb{E} \sum_{\eta} |\beta^\diamond_{j,\eta} - \beta_{j,\eta}|^z \leq C \left\{ t(n)^{z-l} \sum_{j=0}^{J} 2^{j(\gamma-d)} \left(\sum_{\eta \in \mathcal{Z}_j} |\beta_{j,\eta}|^l \right) + n^{-\frac{z}{2}} \right\} \tag{6.14}$$

We delay their proofs to Section 6.9 and Section 6.10. The proof of Proposition 6.8.2 in the deterministic thresholding case follows very similar lines as with stochastic thresholding. For the sake of brevity, we therefore only detail the proof in the stochastic thresholding case. The interested reader is referred to `https://sites.google.com/site/jrmonnier/publications/test` for a full proof. Let us now prove that Proposition 6.8.1 and Proposition 6.8.2 yield the statements of Theorem 6.6.1.

6.8.1 Minimax rate for the $\mathbb{L}^\infty$-norm. We begin with eq. (6.10). Let's first assume that $r = q = \infty$, that is $f \in B^s_{\infty,\infty}(M)$. It is clear that

$$\begin{aligned} \mathbb{E}\|f^\diamond - f\|^z_\infty \leq C \Big\{ & \mathbb{E}\| \sum_{j=0}^{J} \sum_{\eta \in \mathcal{Z}_j} (\beta^\diamond_{j,\eta} - \beta_{j,\eta}) \psi_{j,\eta} \|^z_\infty \\ & + \| \sum_{j>J} \sum_{\eta \in \mathcal{Z}_j} \beta_{j,\eta} \psi_{j,\eta} \|^z_\infty + \mathbb{E}|\hat{P}_0 - P_0 * f|^z \Big\} \triangleq I + II + III \end{aligned} \tag{6.15}$$

Let's now prove that each of the terms I, II and III are at most $\mathcal{O}(\{\log n\}^{2z} \{n/\log n\}^{-zs/(2s+d)})$. We indeed see immediately that III is of the good order thanks to Proposition 6.8.1 and $\frac{z}{2} \geq \frac{zs}{2s+d}$. For II we have

$$\begin{aligned} II^{\frac{1}{z}} & \leq C \sum_{j>J} \| \sum_{\eta \in \mathcal{Z}_j} \beta_{j,\eta} \psi_{j,\eta} \|_\infty \leq \sum_{j>J} \sup_{\eta \in \mathcal{Z}_j} |\beta_{j,\eta}| \|\psi_{j,\eta}\|_\infty \\ & \leq C \sum_{j>J} 2^{-j(s+\frac{d}{2})} C_\infty 2^{\frac{jd}{2}} \leq C 2^{-Js} \leq C \left\{ \frac{\log n}{n} \right\}^{\frac{s}{d}} \end{aligned}$$

where the second inequality is a direct result from Lemma 6.2.1, eq. (6.6); and the third inequality comes from Theorem 6.3.1, eq. (6.8) together with eq. (6.5) and the fact that $f \in B^s_{\infty,\infty}(M)$. It is now enough to notice that $z\frac{s}{d} \geq \frac{zs}{2s+d}$ to conclude that II is of the good order.
For I, we apply successively the triangular inequality and Hölder with the pair of conjugate exponents z and $z/(z-1)$, $z > 1$,

$$\mathbb{E}\| \sum_{j=0}^{J} \sum_{\eta \in \mathcal{Z}_j} (\beta^\diamond_{j,\eta} - \beta_{j,\eta}) \psi_{j,\eta} \|^z_\infty = (J+1)^{z-1} \mathbb{E} \sum_{j=0}^{J} \| \sum_{\eta \in \mathcal{Z}_j} (\beta^\diamond_{j,\eta} - \beta_{j,\eta}) \psi_{j,\eta} \|^z_\infty$$

And finally, we apply Lemma 6.2.1, eq. (6.6) to get

$$I \leq C(J+1)^{z-1} \sum_{j=0}^{J} 2^{jd\frac{z}{2}} \mathbb{E} \sup_{\eta \in \mathcal{Z}_j} |\beta_{j,\eta}^{\diamond} - \beta_{j,\eta}|^z$$

Then we apply Proposition 6.8.2, eq. (6.13) with $\gamma = d\frac{z}{2}$ and thus under conditions $\mathfrak{D}^{\diamond}(dz/2, z)$. Notice in particular that this latter set of conditions is equivalent to $\mathfrak{C}_z^{\diamond}$. This leads us to,

$$\sum_{j=0}^{J} 2^{jd\frac{z}{2}} \mathbb{E} \sup_{\eta \in \mathcal{Z}_j} |\beta_{j,\eta}^{\diamond} - \beta_{j,\eta}|^z \leq C \left\{ t(n)^{z-l}(J+1)^z \sum_{j=0}^{J} 2^{jd\frac{z}{2}} \sup_{\eta \in \mathcal{Z}_j} |\beta_{j\eta}|^l + n^{-\frac{z}{2}} \right\}$$

where $l \in [0, z]$. We denote A, B the two terms in-between braces on the right-hand-side above. Notice first that the last term B is of the right order as $\frac{z}{2} > \frac{zs}{2s+d}$. Moreover, since $f \in B^s_{\infty\infty}(M)$, we have $\sup_{\eta \in \mathcal{Z}_j} |\beta_{j\eta}|^l \leq M^l 2^{-jl(s+\frac{d}{2})}$. The first term A can therefore be bounded by

$$A \leq Ct(n)^{z-l}(J+1)^z \sum_{j \leq J} 2^{jd\frac{z}{2}} 2^{-jl(s+\frac{d}{2})} = Ct(n)^{z-l}(J+1)^z \sum_{j \leq J} 2^{j\alpha(l)}$$

where we have written $\alpha(l) \triangleq \frac{2s+d}{2}(l^* - l)$ and $l^* = \frac{dz}{2s+d}$. Obviously $\alpha(l)$ is a decreasing function of l. Moreover we have $z > l^*$. We can thus explore all the following cases,

i) $\boxed{l = l^*}$ implies $A \leq C(\log n)^{z+1} t(n)^{z-l^*} = C(\log n)^{z+1}[t(n)^2]^{\frac{sz}{2s+d}}$, as $z - l^* = 2\frac{sz}{2s+d}$, which is of the right order.

ii) $\boxed{l > l^*}$ implies $\alpha(l) < 0$ and $A \leq C(\log n)^z t(n)^{z-l}$. However $\frac{z-l}{2} \geq \frac{sz}{2s+d}$ is impossible as $\frac{z-l}{2} < \frac{z-l^*}{2} = \frac{sz}{2s+d}$.

iii) $\boxed{l < l^*}$ implies $\alpha(l) > 0$ and $A \leq C(\log n)^z t(n)^{z-l-\frac{2\alpha(l)}{d}}$. Notice that $z - l - \frac{2\alpha(l)}{d} = 2\frac{ls}{d}$ and $\frac{1}{2}(2\frac{ls}{d}) \geq \frac{zs}{2s+d}$ leads to $l \geq l^*$, which is impossible.

Therefore, we have $I \leq C(\log n)^{2z} \{\log n/n\}^{\frac{sz}{2s+d}}$, which finishes to prove eq. (6.10) of Theorem 6.6.1 in the case where $r = q = \infty$. The Besov embedding $B^s_{rq}(M) \subset B^{s-\frac{d}{r}}_{\infty\infty}(M)$ allows for a direct transposition of this result to the general case where r and q are chosen arbitrarily. Thus it appears that, in the general case, each of the terms I, II and III are at most $\mathcal{O}(\{\log n\}^{2z}\{n/\log n\}^{-z\vartheta^{\infty}})$. Which finishes the proof of eq. (6.10).

6.8.2 Minimax rate for the $\mathbb{L}^p$-norm in the regular case, $r > \frac{dp}{2s+d}$. Let's prove eq. (6.12), that is the regular case. Since $B^s_{r,q}(M) \subset B^s_{p,q}(M)$ for $r \geq p$, this case will be assimilated to the case $p = r$, and from now on, we only consider $r \leq p$. We have

$$\begin{aligned} \mathbb{E}\|f^{\diamond} - f\|_p^p \leq C\Big\{ & \mathbb{E}\|\sum_{j=0}^{J} \sum_{\eta \in \mathcal{Z}_j} (\beta_{j,\eta}^{\diamond} - \beta_{j,\eta})\psi_{j,\eta}\|_p^p \\ & + \|\sum_{j>J} \sum_{\eta \in \mathcal{Z}_j} \beta_{j,\eta}\psi_{j,\eta}\|_p^p + \mathbb{E}|\hat{P}_0 - P_0 * f|^p \Big\} \triangleq I + II + III \end{aligned} \tag{6.16}$$

Let's now prove that each of the terms I, II and III are at most $\mathcal{O}(\{\log n\}^p \{n/\log n\}^{-p\varsigma})$. We indeed see immediately that III is of the good order thanks to Proposition 6.8.1 and $\frac{p}{2} \geq \frac{sp}{2s+d}$. For II we have

$$\begin{aligned} II^{\frac{1}{p}} &\leq C \sum_{j>J} \| \sum_{\eta \in \mathcal{Z}_j} \beta_{j,\eta} \psi_{j,\eta} \|_p \leq C \sum_{j>J} 2^{-j(s-\frac{d}{r}+\frac{d}{p})} \\ &\leq C 2^{-J(s-\frac{d}{r}+\frac{d}{p})} = C \left\{ \frac{\log n}{n} \right\}^{\frac{s}{d}-\frac{1}{r}+\frac{1}{p}} \end{aligned}$$

where the second inequality comes from Theorem 6.3.1, eq. (6.8), and uses the embedding $B^s_{r,q}(M) \subset B^{s-\frac{d}{r}+\frac{d}{p}}_{p,q}(M)$ for $r \leq p$. Thus, we have to find the conditions which lead to $\frac{s}{d}-\frac{1}{r}+\frac{1}{p} \geq \frac{s}{2s+d}$. Since we are in the regular case, we have $r > \frac{dp}{2s+d}$, that is $\frac{s}{2s+d} \leq \frac{rs}{dp}$. Thus, as $r \leq p$ and $s > \frac{d}{r}$, we have

$$0 \leq \frac{r}{d}\left(\frac{1}{r}-\frac{1}{p}\right)\left(s-\frac{d}{r}\right) = \left(\frac{s}{d}-\frac{1}{r}+\frac{1}{p}\right) - \frac{rs}{dp} \leq \left(\frac{s}{d}-\frac{1}{r}+\frac{1}{p}\right) - \frac{s}{2s+d}$$

which shows that II is of the good order.
For I, we use the triangular inequality together with Hölder inequality to get

$$\mathbb{E}\| \sum_{j=0}^{J} \sum_{\eta \in \mathcal{Z}_j} (\beta^{\diamond}_{j,\eta} - \beta_{j,\eta}) \psi_{j,\eta} \|^p_p \leq C(J+1)^{p-1} \sum_{j=0}^{J} 2^{jd(\frac{p}{2}-1)} \sum_{\eta \in \mathcal{Z}_j} \mathbb{E}|\beta^{\diamond}_{j,\eta} - \beta_{j,\eta}|^p.$$

Then we apply Proposition 6.8.2, eq. (6.14) with $\gamma = d\frac{p}{2}, z = p$ and thus under conditions $\mathfrak{D}^{\diamond}(dp/2, p)$. This leads us to,

$$\sum_{j=0}^{J} 2^{jd(\frac{p}{2}-1)} \mathbb{E} \sum_{\eta} |\beta^{\diamond}_{j,\eta} - \beta_{j,\eta}|^p \leq C \left\{ t(n)^{p-l} \sum_{j=0}^{J} 2^{jd(\frac{p}{2}-1)} \left(\sum_{\eta \in \mathcal{Z}_j} |\beta_{j,\eta}|^l \right) + n^{-\frac{p}{2}} \right\}$$

where $l \in [0,p]$. We denote A, B the two terms in-between braces on the right-hand-side above. Notice first that the last term B is of the right order as $\frac{p}{2} > \frac{sp}{2s+d}$. Now choose $l \in [0,r]$. The embedding $B^s_{rq}(M) \subset B^s_{lq}(M)$ ensures that $\sum_{\eta \in \mathcal{Z}_j} |\beta_{j,\eta}|^l \leq M^l 2^{-jl\{s+\frac{d}{2}-\frac{d}{l}\}}$. The first term A can therefore be bounded by

$$A \leq C t(n)^{p-l} \sum_{j \leq J} 2^{jd(\frac{p}{2}-1)} 2^{-jl\{s+\frac{d}{2}-\frac{d}{l}\}} = C t(n)^{p-l} \sum_{j \leq J} 2^{j\alpha(l)}$$

where we have written $\alpha(l) \triangleq \frac{2s+d}{2}(l^*-l)$ and $l^* = \frac{dp}{2s+d}$. Obviously $\alpha(l)$ is a decreasing function of l. Moreover, as we are in the regular case, we have $r > l^*$. We can thus explore all cases,

i) $\boxed{l = l^*}$ implies $A \leq C(\log n) t(n)^{p-l^*} = C \log n [t(n)^2]^{\frac{sp}{2s+d}}$, as $p - l^* = 2\frac{sp}{2s+d}$, which is of the right order.

ii) $\boxed{l > l^*}$ implies $\alpha(l) < 0$ and $A \leq C t(n)^{p-l}$. However $\frac{p-l}{2} \geq \frac{sp}{2s+d}$ is impossible as $\frac{p-l}{2} < \frac{p-l^*}{2} = \frac{sp}{2s+d}$.

iii) $\boxed{l < l^*}$ implies $\alpha(l) > 0$ and $A \leq Ct(n)^{p-l-\frac{2\alpha(l)}{d}}$. Notice that $p - l - \frac{2\alpha(l)}{d} = 2\frac{ls}{d}$ and $\frac{1}{2}(2\frac{ls}{d}) \geq \frac{ps}{2s+d}$ leads to $l \geq l^*$, which is impossible.

Thus, we have $I \leq C(\log n)^p \left\{\frac{\log n}{n}\right\}^{\frac{sp}{2s+d}}$, which finishes to prove eq. (6.12).

6.8.3 Minimax rate for the $\mathbb{L}^p$-norm in the sparse case, $r \leq \frac{dp}{2s+d}$. Let's now turn to the proof of eq. (6.11). We proceed as above and observe first that in order to have $s > 0$ as well as $r \leq \frac{pd}{2s+d} \Leftrightarrow s \leq \frac{pd}{2}(\frac{1}{r} - \frac{1}{p})$, it is necessary that $p \geq r$. As above, we have

$$\begin{aligned}\mathbb{E}\|f^\diamond - f\|_p^p \leq C\Big\{&\mathbb{E}\|\sum_{j=0}^{J}\sum_{\eta\in\mathcal{Z}_j}(\beta_{j,\eta}^\diamond - \beta_{j,\eta})\psi_{j,\eta}\|_p^p \\ &+ \|\sum_{j>J}\sum_{\eta\in\mathcal{Z}_j}\beta_{j,\eta}\psi_{j,\eta}\|_p^p + \mathbb{E}|\hat{P}_0 - P_0 * f|^p\Big\} \triangleq I + II + III\end{aligned} \tag{6.17}$$

Let's prove that each of the terms I, II and III are at most $\mathcal{O}(\{\log n\}^p \{n/\log n\}^{-p\vartheta})$. For $p \geq 2$, III is of the right order. For II, using again the embedding $B_{r,q}^s(M) \subset B_{p,q}^{s-\frac{d}{r}+\frac{d}{p}}(M)$ for $r \leq p$ and Theorem 6.3.1, we have

$$II^{\frac{1}{p}} \leq C\Big\|\sum_{j>J}\sum_{\eta\in\mathcal{Z}_j}\beta_{j,\eta}\psi_{j,\eta}\Big\|_p \leq C2^{-J(s-\frac{d}{r}+\frac{d}{p})} \leq C\left\{\frac{\log n}{n}\right\}^{\frac{s}{d}-\frac{1}{r}+\frac{1}{p}}$$

And the constraint $p(\frac{s}{d} - \frac{1}{r} + \frac{1}{p}) \geq \frac{p}{2}\frac{s+\frac{d}{p}-\frac{d}{r}}{s+\frac{d}{2}-\frac{d}{r}}$ holds true since $s > \frac{d}{r}$.
For I, we use again the triangular inequality together with Hölder inequality to get

$$\mathbb{E}\|\sum_{j=0}^{J}\sum_{\eta\in\mathcal{Z}_j}(\beta_{j,\eta}^\diamond - \beta_{j,\eta})\psi_{j,\eta}\|_p^p \leq C(J+1)^{p-1}\sum_{j=0}^{J}2^{jd(\frac{p}{2}-1)}\sum_{\eta\in\mathcal{Z}_j}\mathbb{E}|\beta_{j,\eta}^\diamond - \beta_{j,\eta}|^p.$$

Then we apply Proposition 6.8.2, eq. (6.14) with $\gamma = d\frac{p}{2}, z = p$ and thus under conditions $\mathfrak{D}^\diamond(dp/2, p)$. This leads us to,

$$\sum_{j=0}^{J}2^{jd(\frac{p}{2}-1)}\mathbb{E}\sum_{\eta}|\beta_{j,\eta}^\diamond - \beta_{j,\eta}|^p \leq C\left\{t(n)^{p-l}\sum_{j=0}^{J}2^{jd(\frac{p}{2}-1)}\left(\sum_{\eta\in\mathcal{Z}_j}|\beta_{j,\eta}|^l\right) + n^{-\frac{p}{2}}\right\}$$

where $l \in [0, p]$. We denote A, B the two terms in-between braces on the right-hand-side above. Notice first that, similarly with III above, the last term B is of the right order. Now choose $l \in [r, p]$. The embedding $B_{rq}^s(M) \subset B_{lq}^{s-\frac{d}{r}+\frac{d}{l}}(M)$ ensures that $\sum_{\eta\in\mathcal{Z}_j}|\beta_{j,\eta}|^l \leq M^l 2^{-jl\{s+\frac{d}{2}-\frac{d}{r}\}}$. The first term A can therefore be bounded by

$$A \leq Ct(n)^{p-l}\sum_{j\leq J}2^{jd(\frac{p}{2}-1)}2^{-jl\{s+\frac{d}{2}-\frac{d}{r}\}} = Ct(n)^{p-l}\sum_{j\leq J}2^{j\alpha(l)}$$

where we have written $\alpha(l) \triangleq (s + \frac{d}{2} - \frac{d}{r})(l^* - l)$ and

$$l^* = \frac{d(\frac{p}{2} - 1)}{s + \frac{d}{2} - \frac{d}{r}}$$

As $s > \frac{d}{r}$, $\alpha(l)$ is a decreasing function of l. Moreover

$$l^* - \frac{dp}{2s+d} = \frac{d}{r(s + \frac{d}{2} - \frac{d}{r})} \left\{ \frac{dp}{2s+d} - r \right\}$$

Since we are in the sparse case, that is $r \leq \frac{dp}{2s+d}$, and $s > d/r$, we have $r \leq \frac{dp}{2s+d} \leq l^*$. Notice now that $l^* < p$ since $l^* < p \Leftrightarrow 0 < p(s - \frac{d}{r}) + d$. Thus we can choose $l \in [r, p]$ with $r \leq \frac{dp}{2s+d} \leq l^* < p$. We again optimize with respect to l,

i) $\boxed{l = l^*}$ implies $A \leq C(\log n)t(n)^{p-l^*}$ and $\frac{p-l^*}{2} = p\vartheta$, which is of the right order.

ii) $\boxed{l > l^*}$ leads to $A \leq Ct(n)^{p-l}$ and $\frac{p-l}{2} < \frac{p-l^*}{2} = p\vartheta$, which makes it impossible to have $\frac{p-l}{2} \geq p\vartheta$.

iii) $\boxed{l < l^*}$ leads to $A \leq Ct(n)^{p-l-\frac{2\alpha(l)}{d}}$ and $\frac{1}{2}(p - l - \frac{2\alpha(l)}{d}) \geq p\vartheta$ leads to $l \geq l^*$, which is impossible.

Thus, we have $I \leq C(\log n)^p \left\{ \frac{\log n}{n} \right\}^{p\vartheta}$, which finishes to prove eq. (6.11). □

6.9 Proof of Proposition 6.8.1. First notice that

$$\mathbb{E}\left(|\hat{P}_0 - P_0 * f|^z \right) \leq C \left\{ \mathbb{E}|\frac{1}{n}\sum_{i \leq n} \{f(T_i) - \mathbb{E}f(T)\}|^z + \mathbb{E}|\frac{1}{n}\sum_{i \leq n} V_i|^z \right\}$$

We write $X_i = f(T_i) - \mathbb{E}f(T)$. We have $|X_i| \leq 2\|f\|_\infty$, $\mathbb{E}X_i = 0$. And we define $t^2 \triangleq \mathbb{E}X_i^2$ and $s(z) \triangleq \mathbb{E}|X_i|^z < \infty$. We can thus apply Rosenthal inequality (see [121, p. 54]) to obtain, for $z \geq 2$, $\mathbb{E}|\sum X_i/n|^z \leq C\{n^{-z+1}s(z) + n^{-\frac{z}{2}}t^z\} \leq Cn^{-\frac{z}{2}}$. For $0 < z \leq 2$, the well-known ordering of the $\mathbb{L}^p$ norms $\|.\|_{\mathbb{L}^1} \leq \|.\|_{\mathbb{L}^2}$ on probability spaces and the fact that the X_i's are mutually independent and centered lead to $\mathbb{E}|\sum X_i/n|^z \leq \left(\mathbb{E}|X_i|^2\right)^{\frac{z}{2}} n^{-\frac{z}{2}} \leq t^z n^{-\frac{z}{2}}$. Moreover notice that, since the V_i's are iid standard normal, $\sum V_i/n \sim n^{-\frac{1}{2}}\sigma Z$, where Z is standard normal. And thus $\mathbb{E}|\sum V_i/n|^z = n^{-\frac{z}{2}}\sigma^z \mathbb{E}|Z|^z \leq Cn^{-\frac{z}{2}}$, which concludes the proof. □

6.10 Proof of Proposition 6.8.2. In what follows, we will write $\|.\|_p$ to denote the usual norm of $\mathbb{L}^p(\mathbb{S}^d, \mathfrak{M}/\omega_d)$. This will make the transition between expectations over functions of uniform random variables and $\mathbb{L}^p$-norms easier. Besides, with this notation, eq. (6.5) transforms into

$$c_p/(\omega_d^{1/p}) \leq \|\psi_{j,\eta}\|_p 2^{-jd\{\frac{1}{2} - \frac{1}{p}\}} \leq C_p/(\omega_d^{1/p}) \tag{6.18}$$

6.10.1 Two useful Lemmas. In this paragraph we introduce two lemmas that will prove very helpful in the demonstration of Proposition 6.8.2. The first one is concerned with finding an upper-bound to the probability of the events $\{\varrho_{j,\eta}^2 \leq s\}$ and $\{\varrho_{j,\eta}^2 \geq t\}$. It goes as follows

Lemma 6.10.1. *For any $s \in (0, \|\psi_{j,\eta}\|_2^2)$ and any $t \in (\|\psi_{j,\eta}\|_2^2, +\infty)$, we have*

$$\mathbb{P}(\varrho_{j,\eta}^2 < s) \leq n^{-\nu_0(C_0,s)}, \qquad \mathbb{P}(\varrho_{j,\eta}^2 > t) \leq n^{-\nu_*(C_0,t)}$$

where we have written

$$\nu_0(C_0, s) \triangleq \frac{C_0(\|\psi_{j,\eta}\|_2^2 - s)^2}{(2C_4^4/\omega_d) + \frac{4}{3}C_\infty^2\{\|\psi_{j,\eta}\|_2^2 - s\}},$$
$$\nu_*(C_0, t) \triangleq \frac{C_0(t - \|\psi_{j,\eta}\|_2^2)^2}{(2C_4^4/\omega_d) + \frac{4}{3}C_\infty^2\{t - \|\psi_{j,\eta}\|_2^2\}}$$

Remember for later use that

$$m_{j,\eta} \triangleq \nu_0(1, \frac{\|\psi_{j,\eta}\|_2^2}{2}) = \nu_*(1, \frac{3\|\psi_{j,\eta}\|_2^2}{2}) = \frac{\|\psi_{j,\eta}\|_2^4}{(8C_4^4/\omega_d) + \frac{8}{3}C_\infty^2\|\psi_{j,\eta}\|_2^2}$$

Besides, since the map $g : x \in \mathbb{R}^+ \mapsto \frac{x^2}{8C_4^4 + \frac{8}{3}C_\infty^2 x}$ is non-decreasing and, given eq. (6.18), we have, for all $j \geq 0$, $\eta \in \mathcal{Z}_j$,

$$m^- \triangleq g(c_2^2/\omega_d) \leq m_{j,\eta} \leq m^+ \triangleq g(C_2^2/\omega_d)$$

Proof. This is in fact a direct application of Bernstein inequality. Let's start with the term $\mathbb{P}(\varrho_{j,\eta}^2 > t)$. Notice that

$$\begin{aligned}\mathbb{P}(\varrho_{j,\eta}^2 > t) &= \mathbb{P}\left(\frac{1}{n}\sum_{i=1}^n \psi_{j,\eta}(T_i)^2 > t\right) \\ &= \mathbb{P}\left(\frac{1}{n}\sum_{i=1}^n \{\psi_{j,\eta}(T_i)^2 - \|\psi_{j,\eta}\|_2^2\} > t - \|\psi_{j,\eta}\|_2^2\right)\end{aligned}$$

We write $X_i \triangleq \psi_{j,\eta}(T_i)^2 - \|\psi_{j,\eta}\|_2^2$. Now, given that $\mathbb{E}X_i = 0$, $\|X_i\|_\infty \leq 2\|\psi_{j,\eta}(.)^2\|_\infty \leq 2C_\infty^2 2^{jd} \leq 2C_\infty^2 2^{Jd}$ and $\mathbb{E}X_i^2 \leq \|\psi_{j,\eta}\|_4^4 \leq C_4^4\{2^{jd(\frac{1}{2}-\frac{1}{4})}\}^4/\omega_d \leq C_4^4 2^{Jd}/\omega_d$ and $2^{Jd} \leq n/\{C_0 \log n\}$, we can apply Bernstein inequality. For $t - \|\psi_{j,\eta}\|_2^2 > 0$, we get

$$\begin{aligned}\mathbb{P}(\varrho_{j,\eta}^2 > t) &\leq \exp\left(-\frac{n(t - \|\psi_{j,\eta}\|_2^2)^2}{2\mathbb{E}\{\psi_{j,\eta}(T_i)^2 - \|\psi_{j,\eta}\|_2^2\}^2 + \frac{2}{3}t\|\psi_{j,\eta}(.)^2 - \|\psi_{j,\eta}\|_2^2\|_\infty}\right) \\ &\leq \exp\left(-\frac{n(t - \|\psi_{j,\eta}\|_2^2)^2}{2^{Jd}(2C_4^4/\omega_d + \frac{4}{3}C_\infty^2\{t - \|\psi_{j,\eta}\|_2^2\})}\right) \\ &\leq \exp\left(-\frac{C_0(t - \|\psi_{j,\eta}\|_2^2)^2}{2C_4^4/\omega_d + \frac{4}{3}C_\infty^2\{t - \|\psi_{j,\eta}\|_2^2\}}\log n\right) \\ &= \exp\left(-\nu_*(C_0, t)\log n\right)\end{aligned}$$

As regards the term $\mathbb{P}(\varrho_{j,\eta}^2 < s)$, write

$$\mathbb{P}(\varrho_{j,\eta}^2 < s) = \mathbb{P}\left(\frac{1}{n}\sum_{i=1}^n \psi_{j,\eta}(T_i)^2 < s\right)$$

$$= \mathbb{P}\left(\frac{1}{n}\sum_{i=1}^{n}\{\psi_{j,\eta}(T_i)^2 - \|\psi_{j,\eta}\|_2^2\} < -(\|\psi_{j,\eta}\|_2^2 - s)\right)$$
$$= \mathbb{P}\left(\frac{1}{n}\sum_{i=1}^{n}(-X_i) > \|\psi_{j,\eta}\|_2^2 - s\right)$$

Besides $(-X_i)$ verifies the same hypotheses as X_i above. Thus for $s \in (0, \|\psi_{j,\eta}\|_2^2)$, we have $\|\psi_{j,\eta}\|_2^2 - s > 0$ and we are brought back to the preceding case. Which concludes the proof. □
□

The second Lemma focuses on finding an upper bound on the probability that $\kappa_{j,\eta}t(n)$ be beyond or under a given constant value $g_{j,\eta}$.

Lemma 6.10.2. *Let $z > 0$ be given. Let $g_{j,\eta}$ be a strictly positive constant that eventually depends on j and η. For any $l \in [0, z]$, any $s \in (0, \|\psi_{j,\eta}\|_2^2)$ and any $t \in (\|\psi_{j,\eta}\|_2^2, +\infty)$, we have*

$$\mathbb{P}(g_{j,\eta} \geq \frac{\kappa_{j,\eta}}{2}t(n)) \leq C g_{j,\eta}^{2l} t(n)^{-2l} + n^{-\nu_0(C_0,s)} \tag{6.19}$$
$$\mathbb{P}(g_{j,\eta} < 2\kappa_{j,\eta}t(n)) \leq C g_{j,\eta}^{l-z} t(n)^{z-l} + n^{-\nu_*(C_0,t)} \tag{6.20}$$

In particular eq. (6.19) together with the obvious fact that, for any $x, y \geq 0$, $\sqrt{x+y} \leq \sqrt{x} + \sqrt{y}$, lead to

$$\mathbb{P}(g_{j,\eta} \geq \frac{\kappa_{j,\eta}}{2}t(n))^{\frac{1}{2}} \leq C g_{j,\eta}^{l} t(n)^{-l} + n^{-\frac{\nu_0(C_0,s)}{2}} \tag{6.21}$$

Besides, if $g_{j,\eta} \leq C2^{-j\frac{d}{2}}$, we have obviously that

$$g_{j,\eta}^{z} \leq C g_{j,\eta}^{l} \tag{6.22}$$

Notice in particular that Lemma 6.2.1, eq. (6.7) and the fact that $f \in \mathbb{L}^\infty$ lead to $|\beta_{j,\eta}| \leq C2^{-j\frac{d}{2}}$, which in turn implies that both $|\beta_{j,\eta}|$ and $\sup_{\eta \in \mathcal{Z}_j} |\beta_{j,\eta}|$ verify eq. (6.22).

Proof. Let's start with the proof of eq. (6.19). For any $s \in (0, \|\psi_{j,\eta}\|_2^2)$, we have

$$\mathbb{E}\mathbb{1}_{\{g_{j,\eta} \geq \frac{\kappa_{j,\eta}}{2}t(n)\}} = \mathbb{E}\mathbb{1}_{\{g_{j,\eta} \geq \frac{\kappa_{j,\eta}}{2}t(n)\}}(\mathbb{1}_{\{\varrho_{j,\eta}^2 \geq s\}} + \mathbb{1}_{\{\varrho_{j,\eta}^2 \leq s\}})$$

For any $l \geq 0$, the left term can be bounded as follows

$$\begin{aligned}\mathbb{E}\mathbb{1}_{\{g_{j,\eta} \geq \frac{\kappa_{j,\eta}}{2}t(n)\}}\mathbb{1}_{\{\varrho_{j,\eta}^2 \geq s\}} &\leq \mathbb{E}\mathbb{1}_{\{g_{j,\eta} \geq \frac{\varpi\sqrt{s}}{2}t(n)\}} \\ &\leq \mathbb{1}_{\{g_{j,\eta} \geq \frac{\varpi\sqrt{s}}{2}t(n)\}} g_{j,\eta}^{2l}\left\{\frac{\varpi\sqrt{s}}{2}t(n)\right\}^{-2l} \\ &\leq C g_{j,\eta}^{2l} t(n)^{-2l}\end{aligned}$$

As regards the right one, we have

$$\mathbb{E}\mathbb{1}_{\{g_{j,\eta} \geq \frac{\kappa_{j,\eta}}{2}t(n)\}}\mathbb{1}_{\{\varrho_{j,\eta}^2 \leq s\}} \leq \mathbb{P}(\varrho_{j,\eta}^2 \leq s) \leq n^{-\nu_0(C_0,s)}$$

where the last inequality is a direct application of Lemma 6.10.1. This finishes to prove eq. (6.19). Let's now turn to eq. (6.20). Its proof follows the same lines. For any $t \in (\|\psi_{j,\eta}\|_2^2, +\infty)$, we have

$$\mathbb{E}\mathbb{1}_{\{g_{j,\eta}<2\kappa_{j,\eta}t(n)\}} = \mathbb{E}\mathbb{1}_{\{g_{j,\eta}<2\kappa_{j,\eta}t(n)\}}(\mathbb{1}_{\{\varrho_{j,\eta}^2\leq t\}} + \mathbb{1}_{\{\varrho_{j,\eta}^2>t\}})$$

The term on the right-hand-side can therefore be bounded by

$$\mathbb{E}\mathbb{1}_{\{g_{j,\eta}<2\kappa_{j,\eta}t(n)\}}\mathbb{1}_{\{\varrho_{j,\eta}^2>t\}} \leq \mathbb{P}(\varrho_{j,\eta}^2 > t) \leq n^{-\nu_*(C_0,t)}$$

where the second inequality is a direct application of Lemma 6.10.1. Let l be chosen such that $l \in [0, z]$, that is $z - l \geq 0$ and turn to the other term. We have

$$\begin{aligned}\mathbb{E}\mathbb{1}_{\{g_{j,\eta}<2\kappa_{j,\eta}t(n)\}}\mathbb{1}_{\{\varrho_{j,\eta}^2\leq t\}} &\leq \mathbb{E}\mathbb{1}_{\{g_{j,\eta}<2\sqrt{t}\varpi t(n)\}} \\ &\leq g_{j,\eta}^{l-z}(2\sqrt{t}\varpi t(n))^{z-l} = Cg_{j,\eta}^{l-z}t(n)^{z-l}\end{aligned}$$

which finishes to prove eq. (6.20). □ □

6.10.2 Proof of Proposition 6.8.2 in the stochastic thresholding case. The proof relies on the following Lemma, which gives upper-bounds on various measures of the deviation of $\hat{\beta}_{j,\eta}$ from the true coefficient $\beta_{j,\eta}$, the last one in eq. (6.25) being threshold-dependent.

Lemma 6.10.3. *Let's define the constant C_∞ by $\|\psi_{j,\eta}\|_\infty \leq C_\infty 2^{jd/2}$ as in eq. (6.5) and $C_0 > 0$. For any $q \geq 1$, there exist constants $C_1(q), C_2(q)$ such that, as soon as the following conditions are verified,*

$$\begin{aligned} &f \in \mathbb{L}^\infty, && \varpi \geq 4\omega_d^2 \max(4e^2\|f\|_\infty^2, \sigma^2), \\ &C_0 > \varpi \max(2C_\infty^2/\{c_2^2e^2\}, 2/m^-), && 2^J \triangleq n/\{C_0 \log n\} \end{aligned}$$

we can write,

$$\mathbb{E}|\hat{\beta}_{j,\eta} - \beta_{j,\eta}|^q \leq C_1(q)n^{-\frac{q}{2}} \tag{6.23}$$

$$\mathbb{E}\sup_{\eta\in\mathcal{Z}_j}|\hat{\beta}_{j,\eta} - \beta_{j,\eta}|^q \leq C_2(q)(j+1)^q n^{-\frac{q}{2}} \tag{6.24}$$

$$\mathbb{P}\left(|\hat{\beta}_{j,\eta} - \beta_{j,\eta}| \geq \varpi\varrho_{j,\eta}t(n)\right) \leq 2n^{-\frac{\varpi}{2}} \tag{6.25}$$

Proof. **Proof of eq. (6.25).** A triangular inequality gives $|\hat{\beta}_{j,\eta} - \beta_{j,\eta}| \leq |\zeta_{j,\eta}^* - \beta_{j,\eta}| + |\gamma_{j,\eta}^*|$. We notice in particular that, for any $u > 0$, $\{|\hat{\beta}_{j,\eta} - \beta_{j,\eta}| \geq u\} \subset \{|\zeta_{j,\eta}^* - \beta_{j,\eta}| \geq \frac{u}{2}\} \bigcup \{|\gamma_{j,\eta}^*| \geq \frac{u}{2}\}$. And therefore

$$\mathbb{P}(|\hat{\beta}_{j,\eta} - \beta_{j,\eta}| \geq u) \leq \mathbb{P}(|\zeta_{j,\eta}^* - \beta_{j,\eta}| \geq \frac{u}{2}) + \mathbb{P}(|\gamma_{j,\eta}^*| \geq \frac{u}{2}) \triangleq I(u) + II(u) \tag{6.26}$$

Obviously, this result holds true for a stochastic u as well. Therefore we can take $u = \kappa_{j,\eta}t(n)$, where we have written $\kappa_{j,\eta} = \varpi\varrho_{j,\eta}$. Thanks to eq. (6.26), we only need to bound $I(\kappa_{j,\eta}t(n)/2)$ and $II(\kappa_{j,\eta}t(n)/2)$. We first deal with this latter term.

Upper bound for $II(\kappa_{j,\eta}t(n)/2)$. Recall from Section 6.5 that $|\gamma^*_{j,\eta}| \sim \omega_d \varrho_{j,\eta}\sigma |\xi|/\sqrt{n}$, where $\xi \sim \mathcal{N}(0,1)$ conditionally on the T_i's. We can thus write

$$\begin{aligned} II(\kappa_{j,\eta}t(n)/2) &= \mathbb{P}(|\gamma^*_{j,\eta}| \geq \frac{\kappa_{j,\eta}t(n)}{2}) = \mathbb{P}(|\xi| \geq \frac{\varpi\sqrt{\log n}}{2\sigma\omega_d}) \\ &\leq \frac{4\sigma\omega_d}{\varpi\sqrt{2\pi\log n}} \exp\left(-\frac{\varpi^2 \log n}{8\sigma^2\omega_d^2}\right) \leq n^{-\varpi^2/8\sigma^2\omega_d^2} \end{aligned}$$

where the before last inequality results from a conditioning with respect to the T_i's and a regular Gaussian tail-inequality and the last inequality holds true for n big enough. So in order to get eq. (6.25), we just need to pick ϖ such that $\varpi \geq 4\sigma^2\omega_d^2$. We now turn to the other term.

Upper bound for $I(\kappa_{j,\eta}t(n)/2)$. We write $X_i \triangleq \omega_d f(T_i)\psi_{j,\eta}(T_i) - \beta_{j,\eta}$. Obviously $\zeta^*_{j,\eta} - \beta_{j,\eta} = \sum X_i/n$, where the sum is over all the X_i's, $i = 1, \ldots, n$. Since $\kappa_{j,\eta} = \varpi\varrho_{j,\eta}$, the problem reduces to finding an upper bound to $I(\varrho_{j,\eta}\delta)$ where δ is a given constant. We will subsequently obtain an upper bound for $I(\kappa_{j,\eta}t(n)/2)$ by choosing $\delta \equiv \varpi t(n)/2$. With these notations, we have $I(\varrho_{j,\eta}\delta) = \mathbb{P}(|\sum X_i| \geq n\varrho_{j,\eta}\delta)$. In a first step, we remove the absolute values and focus on finding an upper bound to $\mathbb{P}(\sum X_i \geq n\varrho_{j,\eta}\delta)$. Let h be a strictly positive non-decreasing function. We can write

$$h(\sum X_i) \geq h(\sum X_i)\mathbb{1}_{\{\sum X_i \geq n\varrho_{j,\eta}\delta\}} \geq h(n\varrho_{j,\eta}\delta)\mathbb{1}_{\{\sum X_i \geq n\varrho_{j,\eta}\delta\}}$$

Taking the expectation leads to

$$\mathbb{E}h(\sum X_i) \geq \mathbb{E}h(n\varrho_{j,\eta}\delta)\mathbb{1}_{\{\sum X_i \geq \varrho_{j,\eta}\delta\}} \tag{6.27}$$

Since h is a strictly positive function, we can apply a reverse Hölder inequality to the right-hand-side ([89, Theorem 2.12]). That is, with $p = 1/2$ and $q = -1$ as conjugate exponents

$$\mathbb{E}h(n\varrho_{j,\eta}\delta)\mathbb{1}_{\{\sum X_i \geq n\varrho_{j,\eta}\delta\}} \geq \mathbb{P}(\sum X_i \geq n\varrho_{j,\eta}\delta)^2 \left(\mathbb{E}\frac{1}{h(n\varrho_{j,\eta}\delta)}\right)^{-1} \tag{6.28}$$

Let's choose $h(x) \triangleq e^{\lambda x}$, where $\lambda > 0$. Combining eq. (6.27) and eq. (6.28), we get

$$\mathbb{P}(\sum X_i \geq n\varrho_{j,\eta}n\delta)^2 \leq \mathbb{E}e^{-\lambda n\varrho_{j,\eta}\delta}\mathbb{E}e^{\lambda\sum X_i}$$

This together with the independence of the T_i's and thus of the X_i's leads to

$$\mathbb{P}(\sum X_i \geq n\varrho_{j,\eta}\delta)^2 \leq \mathbb{E}e^{-\lambda n\varrho_{j,\eta}\delta}\left(\mathbb{E}e^{\lambda X_i}\right)^n \tag{6.29}$$

Let's first look for an upper bound to $(\mathbb{E}e^{\lambda X_i})^n = \exp(n\log\mathbb{E}e^{\lambda X_i})$. Obviously

$$e^{\lambda X_i} = 1 + \lambda X_i + (e^{\lambda X_i} - 1 - \lambda X_i) = 1 + \lambda X_i + \lambda^2 X_i^2\theta(\lambda X_i) \tag{6.30}$$

where we have written $\theta(x) = (e^x - 1 - x)/(x^2)\mathbb{1}_{\{x\neq 0\}} + (1/2)\mathbb{1}_{\{x=0\}}$. As is easily verified, θ is a positive non-decreasing function. Moreover, notice that $\mathbb{E}X_i = 0$, $\mathbb{E}X_i^2 \leq \omega_d^2\|f\|_\infty^2\|\psi_{j,\eta}\|_2^2$ and $\|X_i\|_\infty \leq 2\omega_d\|f\|_\infty\|\psi_{j,\eta}\|_\infty$ and $\|\psi_{j,\eta}\|_\infty \leq C_\infty 2^{Jd/2}$. Therefore, taking the expectation in eq. (6.30) leads to

$$\mathbb{E}e^{\lambda X_i} \leq 1 + \lambda^2\omega_d^2\|f\|_\infty^2\|\psi_{j,\eta}\|_2^2\theta(2\lambda\omega_d\|f\|_\infty C_\infty 2^{Jd/2})$$

Notice finally that $\log(1+u) \leq u$ for all $u \geq 0$, so that

$$\begin{aligned}(\mathbb{E}e^{\lambda X_i})^n &\leq \exp\{n\log(1+\lambda^2\omega_d^2\|f\|_\infty^2\|\psi_{j,\eta}\|_2^2\theta(\lambda\omega_d\|f\|_\infty C_\infty 2^{Jd/2}))\} \\ &\leq \exp\{n\lambda^2\omega_d^2\|f\|_\infty^2\|\psi_{j,\eta}\|_2^2\theta(2\lambda\omega_d\|f\|_\infty C_\infty 2^{Jd/2})\} \end{aligned} \tag{6.31}$$

We now turn to the problem of bounding $\mathbb{E}e^{-\lambda n\varrho_{j,\eta}\delta}$. Notice that

$$\mathbb{E}e^{-\lambda n\varrho_{j,\eta}\delta} \leq \mathbb{E}e^{-\lambda n\varrho_{j,\eta}\delta}\mathbb{1}_{\{\varrho_{j,\eta}^2\leq t\}} + \mathbb{E}e^{-\lambda n\sqrt{t}\delta}\mathbb{1}_{\{\varrho_{j,\eta}^2>t\}} \triangleq A_0 + B_0 \tag{6.32}$$

We have obviously $B_0 \leq e^{-\lambda n\sqrt{t}\delta}$. As regards A_0, notice that for any $t \in (0, \|\psi_{j,\eta}\|_2^2)$, we have $A_0 \leq \mathbb{P}(\varrho_{j,\eta}^2 \leq t) \leq n^{-\nu_0(C_0,t)}$ where the last inequality is a direct application of Lemma 6.10.1. Combining the upper bounds on A_0 and B_0 together with eq. (6.32), eq. (6.31) and eq. (6.29), we obtain

$$\begin{aligned}\mathbb{P}(\sum X_i \geq n\varrho_{j,\eta}\delta)^2 &\leq (e^{-\lambda n\sqrt{t}\delta} + e^{-\nu_0(C_0,t)\log n})e^{n\lambda^2\omega_d^2\|f\|_\infty^2\|\psi_{j,\eta}\|_2^2\theta(2\lambda\omega_d\|f\|_\infty C_\infty 2^{Jd/2})} \\ &\triangleq e^{-\nu_1(t,C_0,\delta,\lambda)\log n} + e^{-\nu_2(t,C_0,\delta,\lambda)\log n}\end{aligned}$$

where

$$\begin{aligned}\nu_1(t,C_0,\delta,\lambda) &\triangleq \frac{n}{\log n}\sqrt{t}\lambda\delta - \frac{n}{\log nC_\infty^2 2^{Jd}}\frac{\|\psi_{j,\eta}\|_2^2}{4}\theta_1(2\lambda\omega_d\|f\|_\infty C_\infty 2^{Jd/2}) \\ \nu_2(t,C_0,\delta,\lambda) &\triangleq \nu_0(C_0,t) - \frac{n}{\log nC_\infty^2 2^{Jd}}\frac{\|\psi_{j,\eta}\|_2^2}{4}\theta_1(2\lambda\omega_d\|f\|_\infty C_\infty 2^{Jd/2})\end{aligned}$$

and $\theta_1(x) = x^2\theta(x)$. Recall that $2^{Jd} = n/\{C_0\log n\}$, that is $2^{-Jd/2} = \sqrt{C_0}t(n)$. As $C_\infty 2^{Jd/2}$ explodes, it is clear that we have to take $\lambda = \lambda_0 \triangleq a2^{-Jd/2} = a\sqrt{C_0}t(n),\ a>0$ for $\nu_i,\ i=1,2$ to have a lower bound. Besides we take $\delta = \delta_0 \triangleq \varpi t(n)/2$. With these parameters values, we have $\theta_1(2\lambda_0\omega_d\|f\|_\infty C_\infty 2^{Jd/2}) = \theta_1(2\omega_d\|f\|_\infty C_\infty a) \leq 2\omega_d^2\|f\|_\infty^2 C_\infty^2 a^2 e^{2\omega_d\|f\|_\infty C_\infty a}$, where the last inequality follows from the mean value theorem. Hence, if we choose $C_0 \triangleq b^2\varpi,\ b>0$, we obtain

$$\nu_1(t,b^2\varpi,\delta_0,\lambda_0) \geq \varpi\left(\sqrt{t}ab\frac{\sqrt{\varpi}}{2} - \frac{(ab)^2}{2}\omega_d^2\|f\|_\infty^2\|\psi_{j,\eta}\|_2^2 e^{2\omega_d\|f\|_\infty C_\infty a}\right) \tag{6.33}$$

$$\nu_2(t,b^2\varpi,\delta_0,\lambda_0) \geq \varpi\left(b^2\nu_0(1,t) - \frac{(ab)^2}{2}\omega_d^2\|f\|_\infty^2\|\psi_{j,\eta}\|_2^2 e^{2\omega_d\|f\|_\infty C_\infty a}\right) \tag{6.34}$$

In order to verify eq. (6.25), we just need to pick $t \in (0, \|\psi_{j,\eta}\|_2^2)$, $a>0$ and $b>0$ such that $\nu_i(t,b^2\varpi,\delta_0,\lambda_0) \geq \varpi,\ i=1,2$. Given eq. (6.33) and eq. (6.34), it leads to the following three constraints on the parameters ϖ, a, b, t

$$\begin{aligned}\sqrt{\varpi} &\geq \frac{2}{ab\sqrt{t}}\left(1 + \frac{(ab)^2}{2}\omega_d^2\|f\|_\infty^2\|\psi_{j,\eta}\|_2^2 e^{2\omega_d\|f\|_\infty C_\infty a}\right) \\ \nu_0(1,t) &\geq \frac{1}{b^2} + \frac{a^2}{2}\|f\|_\infty^2\omega_d^2\|\psi_{j,\eta}\|_2^2 e^{2\omega_d\|f\|_\infty C_\infty a} \\ t &\in (0, \|\psi_{j,\eta}\|_2^2)\end{aligned}$$

which are obviously always feasible. In particular, we can take $t = t_0 \triangleq \|\psi_{j,\eta}\|_2^2/2$, $a = c_b\sqrt{2}/(b\omega_d\|f\|_\infty)$, $c_b = 1/(e\|\psi_{j,\eta}\|_2)$, $b \geq \max(C_\infty\sqrt{2}/(c_2 e), \sqrt{2/m^-})$, where c_2 and m^- have been defined in Lemma 6.10.1 and $\varpi \geq \{4\omega_d\|f\|_\infty/(\sqrt{2}c_b\sqrt{t_0})\}^2 = 16e^2\omega_d^2\|f\|_\infty^2$. Under these conditions, we have thus proved that $\mathbb{P}(\sum X_i \geq n\varrho_{j,\eta}\varpi t(n)) \leq n^{-\varpi/2}$. Besides, it is clear that $\mathbb{P}(\sum X_i \leq -n\varrho_{j,\eta}\varpi t(n)) = \mathbb{P}(\sum(-X_i) \geq n\varrho_{j,\eta}\varpi t(n))$. And the $(-X_i)$'s verify the same properties as the X_i's, which prompts us to apply the same reasoning as above. This leads straightforwardly to $\mathbb{P}(|\sum X_i| \geq n\varrho_{j,\eta}\varpi t(n)) \leq 2n^{-\varpi/2}$ and finishes the proof of eq. (6.25).

Proof of eq. (6.24). First notice that with $\#\mathcal{Z}_j = 2^{jd}$ and for $q \geq 1$ we have

$$\begin{aligned}\mathbb{E}\sup_{\eta\in\mathcal{Z}_j}|\hat{\beta}_{j,\eta}-\beta_{j,\eta}|^q &= \int_{\mathbb{R}^+} qu^{q-1}\mathbb{P}(\sup_{\eta\in\mathcal{Z}_j}|\hat{\beta}_{j,\eta}-\beta_{j,\eta}|\geq u)du \\ &\leq \int_{\mathbb{R}^+} qu^{q-1}\left\{1\wedge 2^{jd}\mathbb{P}(|\hat{\beta}_{j,\eta}-\beta_{j,\eta}|\geq u)\right\}du \qquad (6.35)\end{aligned}$$

In order to prove eq. (6.24), we need to find an upper bound to right-hand-side of eq. (6.35). However we have shown earlier in eq. (6.26) that

$$\mathbb{P}(|\hat{\beta}_{j,\eta}-\beta_{j,\eta}|\geq u) \leq I(u) + II(u)$$

Upper bound for $II(u)$. Recall from Section 6.5 that $|\gamma^*_{j,\eta}| \sim \omega_d\sigma\varrho_{j,\eta}|\xi|/\sqrt{n}$, where $\xi \sim \mathcal{N}(0,1)$ conditionally on the T_i's. Therefore we can write, for any $t > 0$,

$$\begin{aligned}\mathbb{P}(|\gamma^*_{j,\eta}|\geq\frac{u}{2}) &= \mathbb{P}(\omega_d\sigma\varrho_{j,\eta}|\xi|\geq\frac{u}{2}\sqrt{n};\varrho^2_{j,\eta}>t)+\mathbb{P}(\omega_d\sigma\varrho_{j,\eta}|\xi|\geq\frac{u}{2}\sqrt{n};\varrho^2_{j,\eta}\leq t)\\ &\triangleq A_1(u)+A_2(u)\end{aligned}$$

We use a regular Gaussian tail-inequality to bound $A_2(u)$,

$$\begin{aligned}A_2(u) &= \mathbb{E}\mathbb{1}_{\{\omega_d\sigma\varrho_{j,\eta}|\xi|\geq\frac{u}{2}\sqrt{n}\}}\mathbb{1}_{\{\varrho^2_{j,\eta}\leq t\}} = \mathbb{E}\mathbb{1}_{\{\varrho^2_{j,\eta}\leq t\}}\mathbb{E}[\mathbb{1}_{\{\omega_d\sigma\varrho_{j,\eta}|\xi|\geq\frac{u}{2}\sqrt{n}\}}|T_1,\ldots,T_n]\\ &\leq \mathbb{E}\mathbb{1}_{\{\varrho^2_{j,\eta}\leq t\}}\left\{1\wedge\frac{4\sigma\omega_d\varrho_{j,\eta}}{u\sqrt{2\pi n}}\exp\left(-\frac{u^2n}{8\omega_d^2\sigma^2\varrho^2_{j,\eta}}\right)\right\}\\ &\leq \frac{4\omega_d\sigma\sqrt{t}}{u\sqrt{2\pi n}}\exp\left(-\frac{u^2n}{8\omega_d^2\sigma^2t}\right)\end{aligned}$$

In order to find an upper bound for $A_1(u)$, we use the independence of the T_i's from the V_i's together with the fact that $\|\psi_{j,\eta}\|_\infty \leq C_\infty 2^{jd/2}$, and thus $\varrho_{j,\eta} \leq C_\infty 2^{jd/2}$. We write indeed

$$\begin{aligned}A_1(u) &= \mathbb{P}(\omega_d\sigma\varrho_{j,\eta}|\xi|\geq\frac{u}{2}\sqrt{n};\varrho^2_{j,\eta}>t) = \mathbb{E}\mathbb{E}\left[\mathbb{1}_{\{\omega_d\sigma\varrho_{j,\eta}|\xi|\geq\frac{u}{2}\sqrt{n}\}}|T_1,\ldots,T_n\right]\mathbb{1}_{\{\varrho^2_{j,\eta}>t\}}\\ &\leq \mathbb{E}\mathbb{E}\left[\mathbb{1}_{\{|\xi|\geq\frac{u}{2\omega_d\sigma C_\infty}\sqrt{n}2^{-jd/2}\}}|T_1,\ldots,T_n\right]\mathbb{1}_{\{\varrho^2_{j,\eta}>t\}}\\ &\leq \mathbb{E}\left\{1\wedge\frac{4C_\infty\omega_d\sigma2^{jd/2}}{u\sqrt{2\pi n}}\exp\left(-\frac{u^2}{8\omega_d^2\sigma^2C_\infty^2}n2^{-jd}\right)\right\}\mathbb{1}_{\{\varrho^2_{j,\eta}>t\}}\\ &\leq \left\{1\wedge\frac{4C_\infty\omega_d\sigma2^{Jd/2}}{u\sqrt{2\pi n}}\exp\left(-\frac{u^2}{8\omega_d^2\sigma^2C_\infty^2}n2^{-Jd}\right)\right\}\mathbb{P}(\varrho^2_{j,\eta}>t)\end{aligned}$$

$$\leq \left\{1 \wedge \frac{4C_\infty \omega_d \sigma}{u\sqrt{2\pi C_0}} \exp\left(-\frac{u^2 C_0}{8\omega_d^2 \sigma^2 C_\infty^2}\right)\right\} \exp\left(-\nu_*(C_0,t)\log n\right) \tag{6.36}$$

where the last inequality is a direct application of Lemma 6.10.1 with $t \in (\|\psi_{j,\eta}\|_2^2, \infty)$.
Upper bound for $I(u)$. We can write

$$\zeta_{j,\eta}^* - \beta_{j,\eta} = \frac{\omega_d}{n} \sum_{i \leq n} \{f(T_i)\psi_{j,\eta}(T_i) - \mathbb{E}f(T_i)\psi_{j,\eta}(T_i)\}$$

Since $\|\psi_{j,\eta}\|_\infty \leq C_\infty 2^{\frac{jd}{2}}$, we have $\|f(.)\psi_{j,\eta}(.) - \mathbb{E}f(T_i)\psi_{j,\eta}(T_i)\|_\infty \leq 2\|f\|_\infty C_\infty 2^{\frac{jd}{2}} \leq 2\|f\|_\infty C_\infty 2^{\frac{Jd}{2}}$. Moreover we have $w^2 \triangleq \mathbb{E}\{f(T_i)\psi_{j,\eta}(T_i) - \mathbb{E}f(T_i)\psi_{j,\eta}(T_i)\}^2 \leq \|f\|_\infty^2 \|\psi_{j,\eta}\|_2^2$. We can thus apply a Bernstein-type inequality to find

$$\begin{aligned}\mathbb{P}\left(|\zeta_{j,\eta}^* - \beta_{j,\eta}| \geq \frac{u}{2}\right) &= \mathbb{P}\left(\frac{\omega_d}{n}\Big|\sum_{i\leq n}\{f(T_i)\psi_{j,\eta}(T_i) - \mathbb{E}f(T_i)\psi_{j,\eta}(T_i)\}\Big| \geq \frac{u}{2}\right) \\ &\leq 2\exp\left(-\frac{nu^2}{8\omega_d^2 w^2 + \frac{8}{3}\omega_d \|f\|_\infty C_\infty 2^{\frac{Jd}{2}} u}\right)\end{aligned}$$

And, using the convexity of the exponential map, we get,

$$\begin{aligned}\exp\left(-\frac{nu^2}{8\omega_d^2 w^2 + (8/3)\omega_d\|f\|_\infty C_\infty 2^{Jd/2} u}\right) &\leq \exp\left(-\frac{nu^2}{16\omega_d^2 w^2}\right) \\ &\quad + \exp\left(-\frac{nu}{(16/3)\omega_d \|f\|_\infty C_\infty 2^{Jd/2}}\right)\end{aligned}$$

Upper bound to $\mathbb{E}\sup_{\eta\in\mathcal{Z}_j} |\hat{\beta}_{j,\eta} - \beta_{j,\eta}|^q$. We have shown above that we can write $\mathbb{P}(|\hat{\beta}_{j,\eta} - \beta_{j,\eta}| \geq u) \leq I(u) + II(u) \leq I(u) + \{A_1(u) + A_2(u)\}$ and we have computed upper bounds to the three terms on the right-hand-side. Let's now use these results to actually prove eq. (6.24). Notice that for $x, y \in \mathbb{R}^+$ we have $1 \wedge (x+y) \leq 1 \wedge x + 1 \wedge y$. As the three terms $A_1(u), A_2(u)$ and $I(u)$ are positive, we deduce from eq. (6.35) that

$$\begin{aligned}\mathbb{E}\sup_{\eta\in\mathcal{Z}_j} |\hat{\beta}_{j,\eta} - \beta_{j,\eta}|^q &\leq \int_{\mathbb{R}^+} qu^{q-1}\{1 \wedge 2^{jd} I(u)\}du \\ &+ \int_{\mathbb{R}^+} qu^{q-1}\{1 \wedge 2^{jd} A_1(u)\}du + \int_{\mathbb{R}^+} qu^{q-1}\{1 \wedge 2^{jd} A_2(u)\}du\end{aligned} \tag{6.37}$$

We proceed to bound the three integrals that appear on the right-hand-side of eq. (6.37). Notice first that, since $2^{Jd} \leq n/C_0$,

$$\begin{aligned}&\int_{\mathbb{R}^+} qu^{q-1}\{1 \wedge 2^{jd} A_1(u)\}du \\ &\qquad \leq \int_{\mathbb{R}^+} qu^{q-1} 2^{Jd} A_1(u)du \\ &\qquad \leq ne^{-\nu_*(C_0,t)\log n} \int_{\mathbb{R}^+} \frac{q}{C_0} u^{q-1} \left\{1 \wedge \frac{4\omega_d \sigma C_\infty}{u\sqrt{2\pi C_0}} \exp\left(-\frac{u^2 C_0}{8\omega_d^2\sigma^2 C_\infty^2}\right)\right\} du \\ &\qquad = C(q) n^{-\nu_*(C_0,t)+1}\end{aligned}$$

where we have denoted the integral on the right-hand-side of the before-last line by $C(q)$. Therefore, in order to get eq. (6.24), it is enough to choose t such that $\nu_*(C_0,t)-1 \geq q/2$, which is always possible since $\nu_*(C_0,t)$ is a positive, strictly increasing and unbounded function of t for $t > \|\psi_{j,\eta}\|_2^2$. Thus we can pick any $t \geq t_q$, where $t_q \triangleq [\nu_*^{-1}(C_0,.)](1+q/2)$, with obvious notations. Let's now fix $t > t_q$ and turn to the integral of $A_2(u)$. Notice first that for $u^2 \geq 4^2 jd\omega_d^2\sigma^2 t/n$, that is $u \geq u^* \triangleq 4\sqrt{jd\omega_d^2\sigma^2 t/n}$, we have

$$2^{jd}\exp\left(-\frac{u^2 n}{8\omega_d^2\sigma^2 t}\right) \leq \exp\left(-\frac{u^2 n}{16\omega_d^2\sigma^2 t}-\frac{u^2 n}{16\omega_d^2\sigma^2 t}+jd\right) \leq \exp\left(-\frac{u^2 n}{16\omega_d^2\sigma^2 t}\right)$$

Thus we can write

$$\begin{aligned}
&\int_{\mathbb{R}^+} qu^{q-1}\{1\wedge 2^{jd}A_2(u)\}du \\
&\leq \int_{0\leq u\leq u^*} qu^{q-1}du + \int_{u\geq u^*} qu^{q-1}\left\{1\wedge 2^{jd}A_2(u)\right\}du \\
&\leq (4\sqrt{dt})^q j^{\frac{q}{2}} n^{-\frac{q}{2}} + \int_{u\geq u^*} qu^{q-1}\left\{1\wedge \frac{4\omega_d\sigma\sqrt{t}}{u\sqrt{2\pi n}}2^{jd}\exp\left(-\frac{u^2 n}{8\omega_d^2\sigma^2 t}\right)\right\}du \\
&\leq (4\sqrt{dt})^q j^{\frac{q}{2}} n^{-\frac{q}{2}} + \int_{u\geq u^*} qu^{q-1}\left\{1\wedge \frac{4\omega_d\sigma\sqrt{t}}{u\sqrt{2\pi n}}\exp\left(-\frac{u^2 n}{16\omega_d^2\sigma^2 t}\right)\right\}du \\
&\leq (4\sqrt{dt})^q j^{\frac{q}{2}} n^{-\frac{q}{2}} + n^{-\frac{q}{2}}\int_{v\geq 4\sqrt{jd\omega_d^2\sigma^2 t}} qv^{q-1}\left\{1\wedge \frac{4\omega_d\sigma\sqrt{t}}{v\sqrt{2\pi}}\exp\left(-\frac{v^2}{16\omega_d^2\sigma^2 t}\right)\right\}dv \\
&\leq C'(q)(j+1)^{\frac{q}{2}} n^{-\frac{q}{2}}
\end{aligned}$$

where the before last inequation results from the change of variable $v = u\sqrt{n}$ and the last inequation from the fact that, for $j \geq 0$, the integral on the domain $v \geq 4\sqrt{jd\omega_d^2\sigma^2 t}$ is smaller than the integral on $v \in \mathbb{R}^+$. Finally, we deal with the integral of $I(u)$ in eq. (6.37). It can be bounded using the same technique as for the integral of $A_2(u)$. We have indeed, for $u \geq u^* \triangleq (j\omega_d/\sqrt{n})\max(4w\sqrt{2d}, 32d\|f\|_\infty C_\infty/3)$,

$$\begin{aligned}
&2^{jd}\left\{\exp\left(-\frac{nu^2}{16\omega_d^2 w^2}\right)+\exp\left(-\frac{u\sqrt{n}}{(16/3)\omega_d\|f\|_\infty C_\infty}\right)\right\} \\
&\qquad \leq \exp\left(-\frac{nu^2}{32\omega_d^2 w^2}\right)+\exp\left(-\frac{u\sqrt{n}}{(32/3)\omega_d\|f\|_\infty C_\infty}\right)
\end{aligned}$$

Thus we can write

$$\begin{aligned}
&\int_{\mathbb{R}^+} qu^{q-1}\{1\wedge 2^{jd}I(u)\}du \\
&\leq \int_{0\leq u\leq u^*} qu^{q-1}du + \int_{u\geq u^*} qu^{q-1}\left\{1\wedge 2^{jd}I(u)\right\}du \\
&\leq a^q j^q n^{-\frac{q}{2}} + \int_{u\geq u^*} qu^{q-1}1\wedge\left\{\exp\left(-\frac{nu^2}{32\omega_d^2 w^2}\right)+\exp\left(-\frac{u\sqrt{n}}{\frac{32}{3}\omega_d\|f\|_\infty C_\infty}\right)\right\}du \\
&\leq C''(q)(j+1)^q n^{-\frac{q}{2}}
\end{aligned}$$

where in the last equation we have made the change of variable $v = u\sqrt{n}$ and used the fact that for $j \geq 0$ the resulting integral is bounded by a constant, since $\omega_d^2 w^2 \leq 2\omega_d \|f\|_\infty^2 C_2^2$. Which concludes the proof of eq. (6.24).

Proof of eq. (6.23). We could prove eq. (6.23) using the same arguments as for eq. (6.24). However, we can also see eq. (6.23) as a direct consequence of Rosenthal inequality (see [121, p. 54]). We have indeed, for $q > 0$,

$$\mathbb{E}|\hat{\beta}_{j,\eta} - \beta_{j,\eta}|^q \leq C(q)(\mathbb{E}|\zeta^*_{j,\eta} - \beta_{j,\eta}|^q + \mathbb{E}|\gamma^*_{j,\eta}|^q)$$

Recall that we have $\gamma^*_{j,\eta} = \omega_d \sum V_i \psi_{j,\eta}(T_i)/n$. The $\{\omega_d V_i \psi_{j,\eta}(T_i)\}_{i\leq n}$ are iid with $\mathbb{E}\omega_d V_i \psi_{j,\eta}(T_i) = 0$ and $\mathbb{E}\{\omega_d V_i \psi_{j,\eta}(T_i)\}^2 = \omega_d^2 \sigma^2 \|\psi_{j,\eta}\|_2^2 \leq C\omega_d \sigma^2$ and, for $q \geq 2$, $\mathbb{E}|\omega_d V_i \psi_{j,\eta}(T_i)|^q = \omega_d^q \mathbb{E}|V_i|^q \|\psi_{j,\eta}\|_q^q \leq C 2^{jd(\frac{q}{2}-1)} \omega_d^{q-1} \leq C\omega_d^{q-1} 2^{Jd(\frac{q}{2}-1)}$. Thus, for $q \geq 2$, we have

$$\begin{aligned}
\mathbb{E}|\gamma^*_{j,\eta}|^q &= \mathbb{E}|\sum \omega_d V_i \psi_{j,\eta}(T_i)/n|^q \\
&\leq C\left\{ n^{1-q}\mathbb{E}|\omega_d V \psi_{j,\eta}(T)|^q + n^{-\frac{q}{2}} \left(\mathbb{E}\{\omega_d V \psi_{j,\eta}(T)\}^2\right)^{\frac{q}{2}} \right\} \\
&\leq C\left\{ n^{1-q} C\omega_d^{q-1} 2^{Jd(\frac{q}{2}-1)} + n^{-\frac{q}{2}} \omega_d^{q/2} \sigma^q \right\} \leq C\omega_d^{q-1} n^{-\frac{q}{2}}
\end{aligned}$$

where the last inequality comes from the fact that $2^{Jd} \leq n/C_0$. And for $0 < q \leq 2$,

$$\begin{aligned}
\mathbb{E}|\gamma^*_{j,\eta}|^q = \mathbb{E}|n^{-1}\sum \omega_d V_i \psi_{j,\eta}(T_i)|^q &\leq \left\{ \mathbb{E}|n^{-1}\sum \omega_d V_i \psi_{j,\eta}(T_i)|^2 \right\}^{\frac{q}{2}} \\
&= \left\{ \sum \mathbb{E}|n^{-1}\omega_d V_i \psi_{j,\eta}(T_i)|^2 \right\}^{\frac{q}{2}} \leq C\omega_d^{q/2} \sigma^q n^{-\frac{q}{2}}
\end{aligned}$$

In the same way, for $q \geq 2$, denote $X_i = \omega_d f(T_i)\psi_{j,\eta}(T_i) - \mathbb{E}\omega_d f(T_i)\psi_{j,\eta}(T_i)$. Notice that we have $\mathbb{E}X_i = 0$ and,

$$\begin{aligned}
\mathbb{E}X_i^2 &\leq \omega_d^2 \mathbb{E} f(T)^2 \psi_{j,\eta}(T)^2 \leq \|f\|_\infty^2 C_2^2 \omega_d, \\
\mathbb{E}|X_i|^q &\leq C\omega_d^q \mathbb{E} f(T)^q \psi_{j,\eta}(T)^q \leq C\omega_d^{q-1} \|f\|_\infty^q C_q^q 2^{Jd(\frac{q}{2}-1)}
\end{aligned}$$

So that

$$\begin{aligned}
\mathbb{E}|\zeta^*_{j,\eta} - \beta_{j,\eta}|^q &= \mathbb{E}|n^{-1}\omega_d \sum \{f(T_i)\psi_{j,\eta}(T_i) - \mathbb{E}f(T_i)\psi_{j,\eta}(T_i)\}|^q \\
&\leq C(n^{1-q}\omega_d^{q-1}\|f\|_\infty^q n^{\frac{q}{2}-1} + n^{-\frac{q}{2}}\omega_d^{q/2}\|f\|_\infty^{q/2}) \leq C\omega_d^{q-1} n^{-\frac{q}{2}}
\end{aligned}$$

And for $0 < q \leq 2$, $\mathbb{E}|\zeta^*_{j,\eta} - \beta_{j,\eta}|^q \leq C\|f\|_\infty^q \omega_d^{q/2} n^{-\frac{q}{2}}$, which finishes to prove eq. (6.23). □ □

Let's turn to the proof of Proposition 6.8.2 in the stochastic thresholding case.

We start with the proof of eq. (6.13). We break down the problem into four cases,

$$\begin{aligned}
&\sum_{j=0}^{J} 2^{j\gamma} \mathbb{E} \sup_{\eta\in\mathcal{Z}_j} |\beta^{\circledast}_{j,\eta} - \beta_{j,\eta}|^z \\
&\leq \sum_{j=0}^{J} 2^{j\gamma} \mathbb{E} \sup_{\eta\in\mathcal{Z}_j} |\hat{\beta}_{j,\eta} - \beta_{j,\eta}|^z \mathbb{1}_{\{|\hat{\beta}_{j,\eta}| \geq \kappa_{j,\eta} t(n)\}} \mathbb{1}_{\{\sup_{\eta\in\mathcal{Z}_j} |\beta_{j,\eta}| \geq \frac{\kappa_{j,\eta}}{2} t(n)\}}
\end{aligned}$$

$$
\begin{aligned}
&+\sum_{j=0}^{J} 2^{j\gamma}\mathbb{E}\sup_{\eta\in\mathcal{Z}_j}|\hat{\beta}_{j,\eta}-\beta_{j,\eta}|^z\mathbb{1}_{\{|\hat{\beta}_{j,\eta}|\geq\kappa_{j,\eta}t(n)\}}\mathbb{1}_{\{\sup_{\eta\in\mathcal{Z}_j}|\beta_{j,\eta}|<\frac{\kappa_{j,\eta}}{2}t(n)\}}\\
&+\sum_{j=0}^{J} 2^{j\gamma}\mathbb{E}\sup_{\eta\in\mathcal{Z}_j}|\beta_{j,\eta}|^z\mathbb{1}_{\{|\hat{\beta}_{j,\eta}|<\kappa_{j,\eta}t(n)\}}\mathbb{1}_{\{\sup_{\eta\in\mathcal{Z}_j}|\beta_{j,\eta}|\geq 2\kappa_{j,\eta}t(n)\}}\\
&+\sum_{j=0}^{J} 2^{j\gamma}\mathbb{E}\sup_{\eta\in\mathcal{Z}_j}|\beta_{j,\eta}|^z\mathbb{1}_{\{|\hat{\beta}_{j,\eta}|<\kappa_{j,\eta}t(n)\}}\mathbb{1}_{\{\sup_{\eta\in\mathcal{Z}_j}|\beta_{j,\eta}|<2\kappa_{j,\eta}t(n)\}}\\
&\triangleq Bb+Bs+Sb+Ss
\end{aligned}
$$

We then bound separately each of the four terms Bb, Ss, Sb, Bs. Let's start with Bb,

$$
\begin{aligned}
Bb &\leq \sum_{j=0}^{J} 2^{j\gamma}\mathbb{E}\sup_{\eta\in\mathcal{Z}_j}|\hat{\beta}_{j,\eta}-\beta_{j,\eta}|^z\mathbb{1}_{\{\sup_{\eta\in\mathcal{Z}_j}|\beta_{j,\eta}|\geq\frac{\kappa_{j,\eta}}{2}t(n)\}}\\
&\leq C\sum_{j=0}^{J} 2^{j\gamma}(j+1)^z n^{-\frac{z}{2}}\left(\mathbb{E}\mathbb{1}_{\{\sup_{\eta\in\mathcal{Z}_j}|\beta_{j,\eta}|\geq\frac{\kappa_{j,\eta}}{2}t(n)\}}\right)^{\frac{1}{2}}
\end{aligned}
$$

where the last inequality comes as a direct application of Cauchy-Schwarz inequality and eq. (6.24). We can now apply Lemma 6.10.2, eq. (6.21) to the term on the right-hand-side with $g_{j,\eta}=\sup_{\eta\in\mathcal{Z}_j}|\beta_{j,\eta}|$ and $s=s_0\triangleq\|\psi_{j,\eta}\|_2^2/2$ to get

$$
\begin{aligned}
Bb &\leq C\sum_{j=0}^{J} 2^{j\gamma}(j+1)^z n^{-\frac{z}{2}}\sup_{\eta\in\mathcal{Z}_j}|\beta_{j,\eta}|^l t(n)^{-l}+C\sum_{j=0}^{J} 2^{j\gamma}(j+1)^z n^{-\frac{z}{2}}n^{-\frac{\nu_0(C_0,s_0)}{2}}\\
&\leq Cn^{-\frac{z}{2}}t(n)^{-l}(J+1)^z\sum_{j=0}^{J} 2^{j\gamma}\sup_{\eta\in\mathcal{Z}_j}|\beta_{j,\eta}|^l+Cn^{-\frac{z}{2}}(J+1)^z 2^{J\gamma}n^{-C_0\frac{m^-}{2}}\\
&\leq Ct(n)^{z-l}(J+1)^z\sum_{j=0}^{J} 2^{j\gamma}\sup_{\eta\in\mathcal{Z}_j}|\beta_{j,\eta}|^l+Cn^{-\frac{z}{2}}(J+1)^z n^{\frac{\gamma}{d}-\frac{C_0m^-}{2}}
\end{aligned}
$$

where m^- has been defined in Lemma 6.10.1 and the last inequality uses the fact that $2^{Jd}\leq n/C_0$. The term on the far right is of the good order as soon as $\gamma/d-C_0m^-/2<0$ since in that case $(J+1)^z n^{\gamma/d-C_0m^-/2}\to 0$ as $n\to\infty$. Hence the term on the far right is of the good order as soon as $C_0>2\gamma/dm^-$.
Let's now turn to Ss. We can apply Lemma 6.10.2, eq. (6.20) with $g_{j,\eta}=\sup_{\eta\in\mathcal{Z}_j}|\beta_{j,\eta}|$ and $t=t_*=3\|\psi_{j,\eta}\|_2^2/2$. This leads to

$$
\begin{aligned}
Ss &\leq \sum_{j=0}^{J} 2^{j\gamma}\sup_{\eta\in\mathcal{Z}_j}|\beta_{j,\eta}|^z\left(C\sup_{\eta\in\mathcal{Z}_j}|\beta_{j,\eta}|^{l-z}t(n)^{z-l}+n^{-\nu_*(C_0,t_*)}\right)\\
&\leq C\left(t(n)^{z-l}+n^{-C_0m^-}\right)\sum_{j=0}^{J} 2^{j\gamma}\sup_{\eta\in\mathcal{Z}_j}|\beta_{j,\eta}|^l\leq Ct(n)^{z-l}\sum_{j=0}^{J} 2^{j\gamma}\sup_{\eta\in\mathcal{Z}_j}|\beta_{j,\eta}|^l
\end{aligned}
$$

where the before last inequality uses Lemma 6.10.2, eq. (6.22) and the last inequality is valid as soon as $C_0 m^- \geq (z-l)/2$. In particular, it is enough to take $C_0 \geq z/2m^-$. Let's now turn to Bs. We have, using eq. (6.24), eq. (6.25) and Cauchy-Schwarz inequality,

$$\begin{aligned}
Bs &\leq \sum_{j=0}^{J} 2^{j\gamma} \mathbb{E} \sup_{\eta\in\mathcal{Z}_j} |\hat{\beta}_{j,\eta} - \beta_{j,\eta}|^z \mathbb{1}_{\{\sup_{\eta\in\mathcal{Z}_j} |\hat{\beta}_{j,\eta}-\beta_{j,\eta}| \geq \frac{\kappa_{j,\eta}}{2} t(n)\}} \mathbb{1}_{\{\sup_{\eta\in\mathcal{Z}_j} |\beta_{j,\eta}| < 2\kappa_{j,\eta} t(n)\}} \\
&\leq \sum_{j=0}^{J} 2^{j\gamma} \left\{ \mathbb{E} \sup_{\eta\in\mathcal{Z}_j} |\hat{\beta}_{j,\eta} - \beta_{j,\eta}|^{2z} \right\}^{\frac{1}{2}} \left\{ 2^{jd} \mathbb{P}\left(|\hat{\beta}_{j,\eta} - \beta_{j,\eta}| \geq \frac{\kappa_{j,\eta}}{2} t(n) \right) \right\}^{\frac{1}{2}} \\
&\leq \sum_{j=0}^{J} 2^{j\gamma} \left\{ C(j+1)^{2z} n^{-z} \right\}^{\frac{1}{2}} \left\{ 2^{jd} 2n^{-\frac{\varpi}{4}} \right\}^{\frac{1}{2}} \leq C 2^{J\{\gamma+\frac{d}{2}\}} (J+1)^z n^{-\frac{z}{2}} n^{-\frac{\varpi}{8}} \\
&\leq C(J+1)^z n^{\frac{\gamma}{d}+\frac{1}{2}-\frac{\varpi}{8}} n^{-\frac{z}{2}} \leq C n^{-\frac{z}{2}}
\end{aligned}$$

since $2^{Jd} \leq n/C_0$ and for $\varpi > 4(\frac{2\gamma}{d}+1)$, $(J+1)^z n^{\frac{\gamma}{d}+\frac{1}{2}-\frac{\varpi}{8}} \to 0$ as $n \to \infty$. Finally, notice that Lemma 6.2.1, eq. (6.7) and the fact that $f \in \mathbb{L}^\infty$ lead to $|\beta_{j,\eta}| \leq C 2^{-j\frac{d}{2}}$. And this together with eq. (6.25) allows us to write

$$\begin{aligned}
Sb &\leq \sum_{j=0}^{J} 2^{j\gamma} \mathbb{E} \sup_{\eta\in\mathcal{Z}_j} |\beta_{j,\eta}|^z \mathbb{1}_{\{\sup_{\eta\in\mathcal{Z}_j} |\beta_{j,\eta}-\hat{\beta}_{j,\eta}| \geq \kappa_{j,\eta} t(n)\}} \mathbb{1}_{\{\sup_{\eta\in\mathcal{Z}_j} |\beta_{j,\eta}| \geq 2\kappa_{j,\eta} t(n)\}} \\
&\leq \sum_{j=0}^{J} 2^{j\gamma} C 2^{-jz\frac{d}{2}} 2^{jd} \mathbb{P}\{|\beta_{j,\eta} - \hat{\beta}_{j,\eta}| \geq \kappa_{j,\eta} t(n)\} \leq C n^{-\frac{\varpi}{2}} \sum_{j=0}^{J} 2^{j\{\gamma+d-d\frac{z}{2}\}}
\end{aligned}$$

Here two cases arise. On the one hand, if $\gamma + d - d\frac{z}{2} \leq 0$, that is $z \geq 2(\frac{\gamma}{d}+1)$, we have asymptotically $Sb \leq C n^{-\frac{\varpi}{2}} \log n \leq C n^{-\frac{z}{2}}$ for $\varpi > z$. On the other hand, if $\gamma + d - d\frac{z}{2} > 0$, that is $z < 2(\frac{\gamma}{d}+1)$, we have $Sb \leq C n^{-\frac{\varpi}{2}} 2^{J\{\gamma+d-d\frac{z}{2}\}} \leq C n^{-\frac{\varpi}{2}+\frac{\gamma}{d}+1-\frac{z}{2}} \leq C n^{-\frac{z}{2}}$ for $\varpi \geq 2(\frac{\gamma}{d}+1)$. Therefore, it is enough to pick $\varpi > \max(z, 2\{\frac{\gamma}{d}+1\})$ in order to get $Sb \leq C n^{-z/2}$.

Let's now turn to the proof of eq. (6.14). We proceed in exactly the same way as in the previous paragraph. We start by breaking down the problem into four cases,

$$\begin{aligned}
&\sum_{j=0}^{J} 2^{j(\gamma-d)} \mathbb{E} \sum_{\eta\in\mathcal{Z}_j} |\beta^{\circledast}_{j,\eta} - \beta_{j,\eta}|^z \\
&\leq \sum_{j=0}^{J} 2^{j(\gamma-d)} \mathbb{E} \sum_{\eta\in\mathcal{Z}_j} |\hat{\beta}_{j,\eta} - \beta_{j,\eta}|^z \mathbb{1}_{\{|\hat{\beta}_{j,\eta}| \geq \kappa_{j,\eta} t(n)\}} \mathbb{1}_{\{|\beta_{j,\eta}| \geq \frac{\kappa_{j,\eta}}{2} t(n)\}} \\
&+ \sum_{j=0}^{J} 2^{j(\gamma-d)} \mathbb{E} \sum_{\eta\in\mathcal{Z}_j} |\hat{\beta}_{j,\eta} - \beta_{j,\eta}|^z \mathbb{1}_{\{|\hat{\beta}_{j,\eta}| \geq \kappa_{j,\eta} t(n)\}} \mathbb{1}_{\{|\beta_{j,\eta}| < \frac{\kappa_{j,\eta}}{2} t(n)\}} \\
&+ \sum_{j=0}^{J} 2^{j(\gamma-d)} \mathbb{E} \sum_{\eta\in\mathcal{Z}_j} |\beta_{j,\eta}|^z \mathbb{1}_{\{|\hat{\beta}_{j,\eta}| < \kappa_{j,\eta} t(n)\}} \mathbb{1}_{\{|\beta_{j,\eta}| \geq 2\kappa_{j,\eta} t(n)\}}
\end{aligned}$$

$$
\begin{aligned}
&+ \sum_{j=0}^{J} 2^{j(\gamma-d)} \mathbb{E} \sum_{\eta \in \mathcal{Z}_j} |\beta_{j,\eta}|^z \mathbb{1}_{\{|\hat{\beta}_{j,\eta}| < \kappa_{j,\eta} t(n)\}} \mathbb{1}_{\{|\beta_{j,\eta}| < 2\kappa_{j,\eta} t(n)\}} \\
&\triangleq Bb + Bs + Sb + Ss \ .
\end{aligned}
$$

We then bound separately each of the four terms Bb, Ss, Sb, Bs. Using eq. (6.23), we get, for any $l \geq 0$,

$$
\begin{aligned}
Bb &\leq \sum_{j=0}^{J} \sum_{\eta \in \mathcal{Z}_j} 2^{j(\gamma-d)} \mathbb{E} |\hat{\beta}_{j,\eta} - \beta_{j,\eta}|^z \mathbb{1}_{\{|\beta_{j,\eta}| \geq \frac{\kappa_{j,\eta}}{2} t(n)\}} \\
&\leq \sum_{j=0}^{J} \sum_{\eta \in \mathcal{Z}_j} 2^{j(\gamma-d)} \left\{ \mathbb{E} |\hat{\beta}_{j,\eta} - \beta_{j,\eta}|^{2z} \right\}^{\frac{1}{2}} \left\{ \mathbb{E} \mathbb{1}_{\{|\beta_{j,\eta}| \geq \frac{\kappa_{j,\eta}}{2} t(n)\}} \right\}^{\frac{1}{2}}
\end{aligned}
$$

We can now apply Lemma 6.10.3, eq. (6.23) to the left expectation and Lemma 6.10.2, eq. (6.21) to the right expectation with $g_{j,\eta} = |\beta_{j,\eta}|$ and $s = s_0$ to get

$$
\begin{aligned}
Bb &\leq C n^{-\frac{z}{2}} t(n)^{-l} \sum_{j=0}^{J} 2^{j(\gamma-d)} \left(\sum_{\eta \in \mathcal{Z}_j} |\beta_{j,\eta}|^l \right) + C \sum_{j=0}^{J} \sum_{\eta \in \mathcal{Z}_j} 2^{j(\gamma-d)} n^{-\frac{z}{2} - \frac{C_0 m^-}{2}} \\
&\leq C t(n)^{z-l} \sum_{j=0}^{J} 2^{j(\gamma-d)} \left(\sum_{\eta \in \mathcal{Z}_j} |\beta_{j,\eta}|^l \right) + C n^{-\frac{z}{2} + \frac{\gamma}{d} - \frac{C_0 m^-}{2}}
\end{aligned}
$$

where the last inequality uses the fact that $\# \mathcal{Z}_j \approx 2^{jd}$ and $2^{Jd} \leq n/C_0$. In particular, the far right term is of the good order as soon as $C_0 \geq 2\gamma/dm^-$. Let's now take $l \in [0, z]$ and turn to Ss. If we apply Lemma 6.10.2, eq. (6.20) with $g_{j,\eta} = |\beta_{j,\eta}|$ and $t = t_*$, we get

$$
\begin{aligned}
Ss &\leq \sum_{j=0}^{J} 2^{j(\gamma-d)} \sum_{\eta \in \mathcal{Z}_j} |\beta_{j,\eta}|^z \mathbb{E} \mathbb{1}_{\{|\beta_{j,\eta}| < 2\kappa_{j,\eta} t(n)\}} \\
&\leq C t(n)^{z-l} \sum_{j=0}^{J} 2^{j(\gamma-d)} \left(\sum_{\eta \in \mathcal{Z}_j} |\beta_{j,\eta}|^l \right) + n^{-C_0 m^-} \sum_{j=0}^{J} 2^{j(\gamma-d)} \left(\sum_{\eta \in \mathcal{Z}_j} |\beta_{j,\eta}|^z \right) \\
&\leq C \left(t(n)^{z-l} + n^{-C_0 m^-} \right) \sum_{j=0}^{J} 2^{j(\gamma-d)} \left(\sum_{\eta \in \mathcal{Z}_j} |\beta_{j,\eta}|^l \right) \\
&\leq C t(n)^{z-l} \sum_{j=0}^{J} 2^{j(\gamma-d)} \left(\sum_{\eta \in \mathcal{Z}_j} |\beta_{j,\eta}|^l \right)
\end{aligned}
$$

where the before last equation uses Lemma 6.10.2, eq. (6.22) with $g_{j,\eta} = |\beta_{j,\eta}|$ and the last equation is valid as soon as $C_0 m^- \geq \frac{z-l}{2}$, so that it is enough to take $C_0 \geq z/2m^-$. Let's now turn to Bs. We use Lemma 6.10.3, eq. (6.23) and eq. (6.25), and the fact that $\# \mathcal{Z}_j \approx 2^{jd}$ to

show that

$$\begin{aligned} Bs &\leq \sum_{j=0}^{J} 2^{j(\gamma-d)} \mathbb{E} \sum_{\eta\in\mathcal{Z}_j} |\hat{\beta}_{j,\eta} - \beta_{j,\eta}|^z \mathbb{1}_{\{|\hat{\beta}_{j,\eta}-\beta_{j,\eta}|\geq \frac{\kappa_{j,\eta}}{2} t(n)\}} \\ &\leq \sum_{j=0}^{J} 2^{j(\gamma-d)} \sum_{\eta\in\mathcal{Z}_j} \left(\mathbb{E}|\hat{\beta}_{j,\eta} - \beta_{j,\eta}|^{2z}\right)^{\frac{1}{2}} \mathbb{P}\left\{|\hat{\beta}_{j,\eta} - \beta_{j,\eta}| \geq \frac{\kappa_{j,\eta}}{2} t(n)\right\}^{\frac{1}{2}} \\ &\leq C \sum_{j=0}^{J} 2^{j\gamma} n^{-\frac{z}{2}} n^{-\frac{\varpi}{4}} \leq C n^{-\frac{z}{2}+\frac{\gamma}{d}-\frac{\varpi}{4}} \leq C n^{-\frac{z}{2}} \end{aligned}$$

where, as usual, the before last inequality uses the fact that $2^{Jd} \leq n/C_0$ and the last inequality is valid as soon as $\varpi \geq 4\frac{\gamma}{d}$. Let's now turn to Sb. Notice again that f bounded implies that $|\beta_{j,\eta}| \leq C 2^{-\frac{jd}{2}}$. This together with eq. (6.25) and $\#Z_j \approx 2^{jd}$ leads us to

$$\begin{aligned} Sb &\leq \sum_{j=0}^{J} 2^{j(\gamma-d)} \mathbb{E} \sum_{\eta\in\mathcal{Z}_j} |\beta_{j,\eta}|^z \mathbb{1}_{\{|\beta_{j,\eta}-\hat{\beta}_{j,\eta}|\geq \kappa_{j,\eta} t(n)\}} \\ &\leq C \sum_{j=0}^{J} 2^{j(\gamma-d)} 2^{jd} 2^{-jd\frac{z}{2}} \mathbb{P}\{|\beta_{j,\eta} - \hat{\beta}_{j,\eta}| \geq \kappa_{j,\eta} t(n)\} \\ &\leq C \sum_{j=0}^{J} 2^{j\{-d\frac{z}{2}+\gamma\}} n^{-\frac{\varpi}{2}} \leq C n^{-\frac{\varpi}{2}} \sum_{j=0}^{J} 2^{j\{\gamma+d-d\frac{z}{2}\}} \end{aligned}$$

Here we face the same dichotomy as at the end of the previous paragraph. This concludes the proof of eq. (6.13). □

Acknowledgements. *The author would like to thank Dominique Picard for serving as his adviser and for many fruitful discussions and suggestions. He would also like to thank anonymous referees for their suggestions, which helped improving the overall presentation of the paper.*

7

Spectral analysis of restricted call and put operators and application to stable risk-neutral density recovery

Abstract. In this paper, we propose a new method for estimating the conditional risk-neutral density (RND) directly from a cross-section of put option bid-ask quotes. More precisely, we propose to view the RND recovery problem as an inverse problem. We first show that it is possible to define *restricted put and call operators* that admit a singular value decomposition (SVD), which we compute explicitly. We subsequently show that this new framework allows to devise a simple and fast quadratic programming method to recover the smoothest RND whose corresponding put prices lie inside the bid-ask quotes. This method is termed the spectral recovery method (SRM). Interestingly, the SVD of the restricted put and call operators sheds some new light on the RND recovery problem. The SRM improves on other RND recovery methods in the sense that 1) it is fast and simple to implement since it requires to solve one single quadratic program, yet being fully nonparametric; 2) it takes the bid ask quotes as sole input and does not require any sort of calibration, smoothing or preprocessing of the data; 3) it is robust to the paucity of price quotes; 4) it returns the smoothest density giving rise to prices that lie inside the bid ask quotes. The estimated RND is therefore as well-behaved as can be; 5) it returns a closed form estimate of the RND on the interval $[0, B]$ of the positive real line, where B is a positive constant that can be chosen arbitrarily. We thus obtain both the middle part of the RND together with its full left tail and part of its right tail. We confront this method to both real and simulated data and observe that it fares well in practice. The SRM is thus found to be a promising alternative to other RND recovery methods. ■

Key-Words: Risk-neutral density; Nonparametric estimation; Singular value decomposition; Spectral analysis; Quadratic programming.

Contents

7.1 Introduction.

7.1.1 The setting. Over the last four decades, the no-arbitrage assumption has proved to be a fruitful starting point that paved the way for the elaboration of a rich theoretical framework for derivatives pricing known today as *arbitrage pricing theory*. Among its numerous achievements, the arbitrage pricing theory has set forth two fundamental theorems. The *First Fundamental Theorem of Asset Pricing* (see [48, p.72]) proves that a market is arbitrage-free if and only if there exists a measure $\mathbb{Q}$ equivalent to the historical (or statistical) measure $\mathbb{P}$, which turns the underlying price process into a martingale. $\mathbb{Q}$ is therefore referred to as a *martingale measure*. The *Second Fundamental Theorem of Asset Pricing* (see [48, p.73]) proves in turn that this martingale measure is unique if and only if the market is *complete* (see [48, p.300] for terminology). Let us denote by S_τ the positive valued price of the underlying at a deterministic future date τ and by $\pi(S_\tau)$ the payoff of a contingent claim maturing at time τ. Let us moreover denote by q the marginal density of S_τ under $\mathbb{Q}$ with respect to the Lebesgue measure on the positive real line, assuming that it exists. As initially proved in [49], the arbitrage price of this derivative security writes as its discounted expected payoff under $\mathbb{Q}$, that is,

$$e^{-r\tau}\mathbb{E}_{\mathbb{Q}}\pi(S_\tau) = e^{-r\tau}\int_{x\geq 0}\pi(x)\mathbb{Q}(S_\tau \in dx) = e^{-r\tau}\int_{x\geq 0}\pi(x)q(x)dx,$$

where r stands for the continuously compounded risk-free rate. It is a widely acknowledged fact that financial markets are incomplete, shall it only be due to the presence of jumps in the underlying price process. In such a setting, and as described above, there exist eventually very many qs, and therefore, very many corresponding systems of arbitrage-free prices. Let us denote by $\mathscr{Q}$ the corresponding set of valid densities q. The elements q of $\mathscr{Q}$ are most often referred to as risk-neutral densities (RNDs) and we will stick to this terminology in the sequel.

RNDs are of crucial interest for Central Banks and, in fact, most institutions and people concerned with financial markets since they represent the market sentiment about a given underlying price process at a future point in time (see [50]). They are also of crucial interest to the financial derivatives industry since the knowledge of q allows to price new derivative securities in an arbitrage-free way with respect to traded ones. For these reasons, the literature related to risk-neutral density estimation is very extensive, the bulk of it dating back to the late 90's and early 2k's. It is not our purpose here to present an exhaustive review of this literature. Excellent and up-to-date reviews can in fact be found in [51, 52]. Older but still relevant ones can be found in [53, 50].

Among derivative securities, call and put options play a very particular role since they are actively traded in the market and thus believed to be efficiently priced. Let us recall that a call of strike ξ and maturity τ gives its holder the right to buy the underlying security at maturity time τ at price ξ. It is an insurance against a rise in the price of the underlying. Its payoff writes

$\pi(S_\tau, \xi) = \theta(S_\tau, \xi) = (S_\tau - \xi)^+$, where we have written $(x)^+ = \max(x, 0)$ for $x \in \mathbb{R}$. Conversely, a put option gives the right to sell the underlying security. It is an insurance against a fall in the underlying price and its payoff writes $\theta^*(S_\tau, \xi) = (\xi - S_\tau)^+$. Here and in what follows, we denote the strike price by ξ and not by k, which will stand for a running index in $\mathbb{N}$.

According to the celebrated Breeden-Litzenberger formula, the second derivative of put and call prices with respect to their strike price both equal the discounted RND $e^{-r\tau}q$ (see [54]). Therefore, if a continuum of put or call prices were available in the market, we would have direct access to the RND by the latter formula. However, this is not the case and only a few strike prices around the forward price are quoted and actively traded at each maturity date. Depending on the market, we overall reckon from 5 to 50 quotes at a given maturity date τ. To complicate the matter even more, quotes do not appear as a single price. Dealers quote in fact a bid price, at which they offer to buy the security, and an ask price, at which they offer to sell the security. The difference between both prices is referred to as the bid-ask spread. For an interesting insight into the nature of option quotes and sources of error in them, the reader is referred to, say, [55, p.786].

7.1.2 The problem and brief literature review. As detailed above, if traded puts and calls at a given maturity τ are arbitrage free, they must write as their expected discounted payoff with respect to a single RND q drawn from the set $\mathscr{Q}$. Given the paucity of quoted option prices at a given maturity τ and the presence of a bid-ask spread, it is clear that many RNDs could in fact be hidden behind quoted option prices. Therefore, the RND quest is not that much about estimating the true RND that is used by the market for pricing purpose, since the nature of the quotes does not allow to identify it uniquely. It is rather more about recovering a valid RND, meaning an actual density function, to be chosen according to a criterion typically related to its smoothness or information content. Historically, three main routes have been used to recover a RND from quoted option prices: parametric methods, nonparametric methods and models of the underlying price process. Each of them have their pros and cons. Parametric methods are well adapted to small data sets and always recover a density. However, they constrain the RND to belong to a given parametric family. On the other hand, models of the underlying price process have been the first great success of arbitrage pricing theory with the celebrated geometric Brownian motion (see [56, 57]). However, the limitation of the log-normal distribution is now widely acknowledged and no satisfying stochastic process has yet been proposed that both reproduce accurately the dynamics of the underlying price process and be analytically tractable. Nonparametric methods circumvent both of these problems in the sense that they do not require any stringent assumption on the process generating the data (they are model-free) and can recover all possible densities. As a main drawback, these methods are often data intensive.

Let us briefly come back on some contributions to the nonparametric literature which are relevant to the present paper. We can classify nonparametric methods as follows.

- *The expansion methods.* It includes the Edgeworth (see [58]) and cumulant expansions (see [59]), which allow to estimate a finite number of RND cumulants. It also includes orthonormal basis methods such as Hermite polynomials (see [60]), which rely on well known Hilbert space techniques and give access to the middle part of the RND.
- *The kernel regression methods.* As a recent example, [61] have introduced a shape con-

strained local polynomial estimator of the RND. Notice that it performs estimation on the average quoted prices (that is, the average of the bid-ask quotes) and requires therefore to pre-process them in order to make them arbitrage-free. Moreover, the returned RND depends on the kernel chosen and it is not clear how it relates to the other valid RNDs in term of information content or smoothness.

- *The maximum entropy method.* It is introduced in [62, 63], where the RND q is obtained via the maximization of an entropy criterion. According to [53, p.19], this method often gives bumpy (multimodals) estimates since it imposes no smoothness restriction on the estimated density. In addition, it is said in [64, p.1620], that this method presents convergence issues.
- *Other methods*, which do not belong to any of the three categories above. Among them, we can refer to the positive convolution approximation (PCA) of [65]. In practice, it fits a finite (but large) convex linear combination of normal densities to the average quoted put prices and approximates the RND by the weights of the linear combination. It thus presents similarities with [64], since it ultimately fits a discrete set of probabilities to the average quoted prices. We can also refer to the smoothed implied volatility smile method (SML) as in [51]. This method uses the Black-Scholes formula as a non-linear transform. It consists in fitting a polynomial through the implied volatilities obtained from average quoted prices, and using the continuum of option prices obtained in that way to get the RND via the Breeden-Litzenberger formula. [51] refines this method by taking the bid-ask quotes into account at the implied volatility fit stage. The SML method gives access to the middle part of the RND. [51] proposes in addition a method for appending generalized extreme value (GEV) tail distributions to it. The SML method is cumbersome and can seem a bit odd since it requires going from price space to implied volatility space, back and forth. It is claimed that it is outperformed in term of accuracy and stability by simpler parametric methods in [66].

7.1.3 Our results. In this paper, we propose to view the RND recovery problem as an inverse problem. We first show that it is possible to define *restricted put and call operators* that admit a singular value decomposition (SVD), which we compute explicitly. We subsequently show that this new framework allows to devise a simple and fast quadratic programming method to recover the smoothest RND that is consistent with market bid-ask quotes.

To be more precise, let us denote by $\mathcal{I}$ the segment $[0, B]$ of the positive real line. We define the restricted put and call operators, denoted by γ^* and γ, from $\mathbb{L}_2\mathcal{I}$ into itself (see eq. (7.1) and eq. (7.2) below) and show that they are conjugates of one another. We prove that the resulting self-adjoint operator $\gamma^*\gamma$ is compact. As a consequence of the spectral theorem (see [122]), γ^* admits a singular value decomposition with positive decreasing singular values. We prove that the corresponding singular bases are complete in $\mathbb{L}_2\mathcal{I}$ (see Theorem 7.3.1, item 3)) and compute them explicitly together with their singular values (see Figure 7.1). To fix notations, we will write $(\varphi_k)_{k\geq 0}$ and $(\psi_k)_{k\geq 0}$ the two orthonormal families of $\mathbb{L}_2\mathcal{I}$ such that $\gamma^*\gamma\varphi_k = \lambda_k^2\varphi_k$, $\gamma\gamma^*\psi_k = \lambda_k^2\psi_k$, where $(\lambda_k)_{k\geq 0}$ is a positive decreasing sequence of singular values. Precisely, we

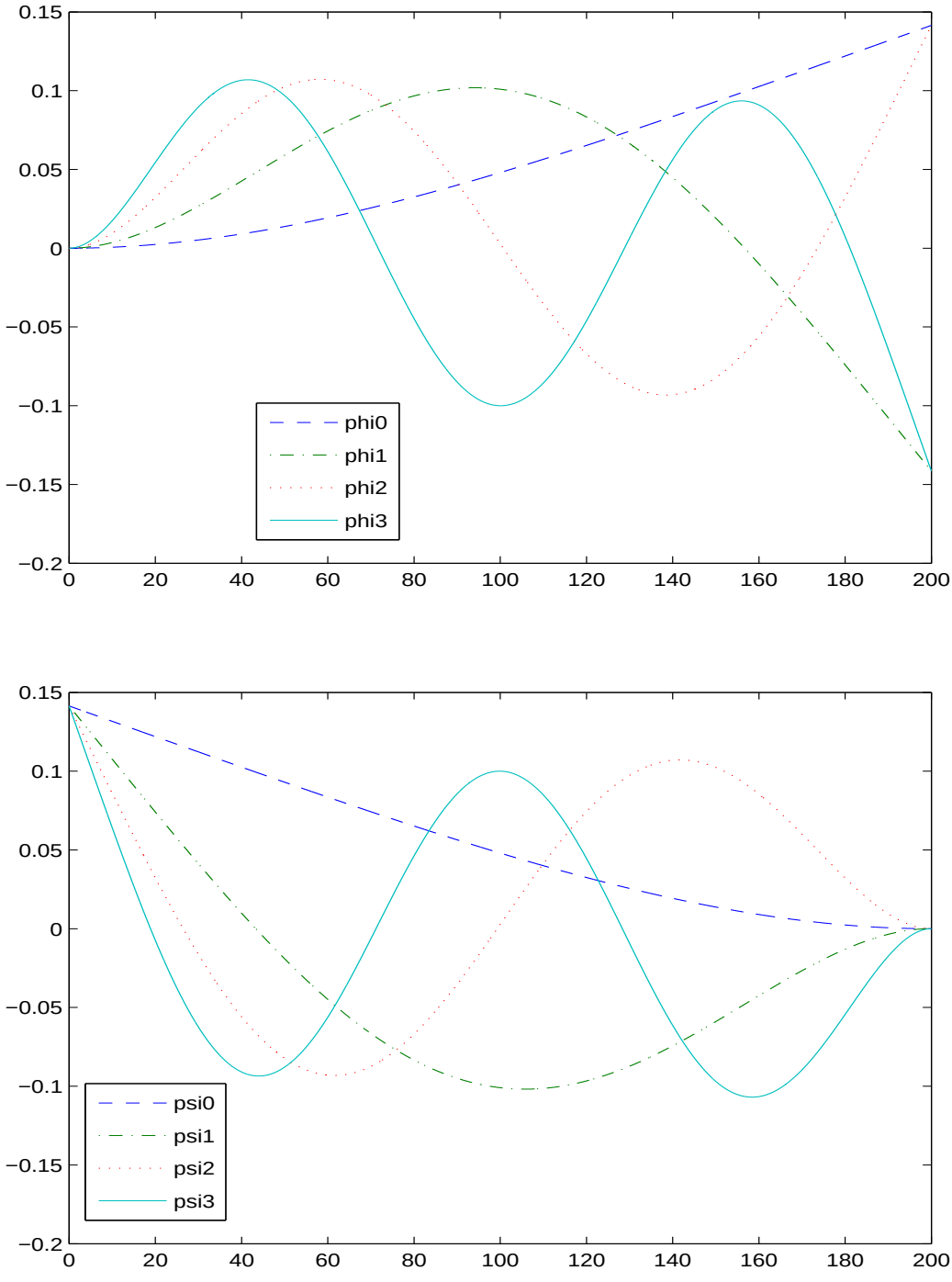

Figure 7.1: Here, we plot the first four elements of both singular bases. At the top we plot φ_k, $k = 0, \ldots, 3$. *At the bottom, we plot* ψ_k, $k = 0, \ldots, 3$.

obtain explicitly,

$$\lambda_k = \left(\frac{B}{\rho_k}\right)^2,$$

where

$$\rho_k = \frac{\pi}{2} + k\pi + (-1)^k \beta_k, \qquad k \in \mathbb{N},$$

and, for all $k \in \mathbb{N}$, β_k is the smallest positive solution of the following fixed point equation in u,

$$\exp(\pi/2 + k\pi + (-1)^k u) = \frac{1+\cos(u)}{\sin(u)}.$$

Interestingly, the positive sequence (β_k) decreases exponentially fast toward zero as detailed in Lemma 7.6.3. Therefore, the sequence of singular values $(\lambda_k)_{k\geq 0}$ tends asymptotically toward zero at a rate of order k^{-2}. The RND recovery problem is therefore said to be mildly ill-posed with a degree of ill-posedness equal to 2 (see [123, p.40]). Furthermore, for all $\xi \in \mathcal{I}$, we obtain,

$$\begin{aligned}
\varphi_k(\xi) &= \Big(a_{k,1} e^{\rho_k \xi/B} + a_{k,2} e^{-\rho_k \xi/B}\Big) + \Big(a_{k,3}\cos(\rho_k t/B) + a_{k,4}\sin(\rho_k \xi/B)\Big), \\
\psi_k(\xi) &= \Big(a_{k,1} e^{\rho_k \xi/B} + a_{k,2} e^{-\rho_k \xi/B}\Big) - \Big(a_{k,3}\cos(\rho_k t/B) + a_{k,4}\sin(\rho_k \xi/B)\Big).
\end{aligned}$$

where the coefficients $a_{k,i}, i = 1, \ldots, 4$ are such that,

$$\begin{aligned}
a_{k,1} &= \frac{1}{\sqrt{B}} \frac{(-1)^k}{e^{\rho_k} + (-1)^k}, \\
a_{k,2} &= (-1)^k e^{\rho_k} a_{k,1} = \frac{1}{\sqrt{B}} \frac{1}{1 + (-1)^k e^{-\rho_k}}, \\
a_{k,3} &= -\frac{1}{\sqrt{B}}, \\
a_{k,4} &= \frac{1}{\sqrt{B}} \frac{1 - (-1)^k e^{-\rho_k}}{1 + (-1)^k e^{-\rho_k}}.
\end{aligned}$$

Based on this new framework, we propose a spectral approach to RND recovery. It is fully nonparametric and can recover the restriction of any density to the interval $\mathcal{I}$. To that end, we notice that the singular bases functions φ_k and ψ_k are in fact oscillations $h_{k,2}$ at frequency ρ_k/B carried by the exponential trend $h_{k,1}$ (see eq. (7.7) and eq. (7.6) for notations). Conveniently, smooth densities are therefore essentially captured by low singular spaces. The idea of recovering the smoothest density among the valid ones was initially suggested in [64]. Subsequently, [53] rightfully pointed out that the smoothness criterion can be debated as it is difficult to give it an economic or even information theoretic meaning. Our spectral approach sheds some new light on this issue and makes it clear that the smoothness criterion is justified by the fact that the restricted call and put operators behave as low-pass frequency filters. It is therefore illusory to look for high frequency information about the RND in a set of quoted options prices, since this information has been drastically attenuated by the operator. The smoothness criterion arises therefore as a by-product of the spectral nature of the restricted put and call operators and

might well not be an intrinsic property of the true RND. Interestingly, smooth densities are also easier to recover by nonparametric means.

In what follows, we exploit the rich framework offered by the SVD of the restricted put and call operators to recover the smoothest RND that is compatible with market quotes. As detailed in eq. (7.24) below, the discounted restricted put operator coincides with the put price function (as a function of the strike) on $\mathcal{I}$. We therefore propose to recover the smoothest RND such that its image by the discounted restricted put operator $e^{-r\tau}\gamma^*$ lies in-between the bid-ask quotes (see eq. (7.24)). Conveniently, the singular bases present the property of being image of one another by second derivation modulo a multiplication by the corresponding singular value of γ^* (see Theorem 7.6.1). This allows us to characterize the smoothness of the estimated RND directly in term of a quadratic form of the coefficients of the estimated put price function, which depends on the singular values of the restricted put operator (see Proposition 7.7.1). This crucial feature allows to recover the smoothest RND as the solution of a simple quadratic program, which takes the bid ask quotes as sole input. Our estimation method improves on existing ones in several ways, which we sum up here.

- It is fast and simple to implement since it requires to solve one single quadratic program, yet being fully nonparametric.
- It is robust to the paucity of price quotes since the smaller the number of quotes, the less constrained the quadratic program and thus the easier to solve.
- It takes the bid ask quotes as sole input and does not require any sort of smoothing or preprocessing of the data.
- It returns the smoothest density giving rise to price quotes that lie inside the bid ask quotes. The estimated RND is therefore as well-behaved as can be.
- It returns a closed form estimate of the RND on $\mathcal{I}$. We thus obtain both the middle part of the RND together with its left tail and part of its right tail. Interestingly, the left tail contains crucial information about market sentiments relative to a potential forthcoming market crash.

It is noteworthy that the singular vectors φ_0 and ψ_0 corresponding to the largest singular value λ_0 of γ and γ^* look themselves very much like cross sections of put and call prices, respectively (see Figure 7.1). In that sense, they will be able to capture the bulk of the shape of a cross section of option prices, while the subsequent singular vectors will add corrections to this general behavior. This is a crucial feature of this SVD that leads us to think that the singular bases of the restricted pricing operators are appropriate tools to recover the RND q. Interestingly, the performance of our quadratic programming algorithm on real data is indeed quite convincing (see Section 7.8 for details).

Readers interested in appending a full right tail to this estimated RND are referred to [51], who proposes a simple method for smooth pasting of parametric GEV tail distributions to an estimated RND.

Here is the paper layout. We introduce the restricted call and put operators, γ and γ^*, and operators derived thereof in Section 7.2. We detail the properties of operators $\gamma^*\gamma$ and $\gamma\gamma^*$ on the one hand, and γ and γ^* on the other hand, in Section 7.3 and Section 7.4, respectively. Other results relative to these four operators are reported in Section 7.5. Section 7.6 gives

explicit expressions for the (λ_k), (φ_k) and (ψ_k). The SRM is detailed in Section 7.7. Finally, we run a simulation study in Section 7.8. An Appendix regroups some additional useful results.

7.2 Definitions and setting. Let us define the restricted call operator on the interval $\mathcal{I} = [0, B]$ as the operator γ from $\mathbb{L}_2\mathcal{I}$ into $\mathbb{L}_2\mathcal{I}$ such that,

$$\begin{aligned}(\gamma f)(\xi) &= \int_{\mathcal{I}} \theta(\xi, x) f(x) dx, \qquad \xi \in \mathcal{I}, f \in \mathbb{L}_2\mathcal{I}, \\ \theta(\xi, x) &= (x - \xi)^+.\end{aligned} \tag{7.1}$$

It is a trivial fact that γf belongs indeed to $\mathbb{L}_2\mathcal{I}$. Let's denote by $\langle ., . \rangle$ the usual scalar product on $\mathbb{L}_2\mathcal{I}$ and by $\|.\|_{\mathbb{L}_2\mathcal{I}}$ the associated norm. Now, it is enough to notice that for all $\xi, x \in \mathcal{I}$, $|\theta(\xi, x)| \leq B$ and apply Cauchy-Schwartz inequality to obtain,

$$\|\gamma f\|^2_{\mathbb{L}_2\mathcal{I}} \leq \int_{\mathcal{I}} d\xi \left(\int_{\mathcal{I}} dx |\theta(\xi, x)||f(x)| \right)^2 \leq B^4 \|f\|^2_{\mathbb{L}_2\mathcal{I}} < \infty.$$

The adjoint operator γ^* of γ is such that, for all $f, g \in \mathbb{L}_2\mathcal{I}$,

$$\begin{aligned}\langle \gamma^* f, g \rangle &= \langle f, \gamma g \rangle \\ &= \int_{\mathcal{I}} du f(u) \int_{\mathcal{I}} dx \theta(u, x) g(x) \\ &= \int_{\mathcal{I}} dx g(x) \int_{\mathcal{I}} du \theta(u, x) f(u).\end{aligned}$$

Hence

$$\begin{aligned}\gamma^* f(\xi) &= \int_{\mathcal{I}} \theta^*(\xi, x) f(x) dx, \qquad \xi \in \mathcal{I}, f \in \mathbb{L}_2\mathcal{I}, \\ \theta^*(\xi, x) &= \theta(x, \xi).\end{aligned} \tag{7.2}$$

So that γ^* is nothing but the restricted put operator on the interval $\mathcal{I}$. In particular, we can write

$$\gamma^*\gamma f(\xi) = \int_{\mathcal{I}} \vartheta_1(\xi, x) f(x) dx, \qquad \xi \in \mathcal{I}, f \in \mathbb{L}_2\mathcal{I}, \tag{7.3}$$

$$\gamma\gamma^* f(\xi) = \int_{\mathcal{I}} \vartheta_2(\xi, x) f(x) dx, \qquad \xi \in \mathcal{I}, f \in \mathbb{L}_2\mathcal{I}, \tag{7.4}$$

where

$$\begin{aligned}\vartheta_1(\xi, x) &= \int_{\mathcal{I}} du \theta^*(\xi, u) \theta(u, x) \\ &= \int_{\mathcal{I}} du (\xi - u)^+ (x - u)^+ = \int_0^{\xi \wedge x} du (\xi - u)(x - u) \\ &= \xi x (\xi \wedge x) - (\xi + x)(\xi \wedge x)^2/2 + (\xi \wedge x)^3/3,\end{aligned}$$

and

$$\begin{aligned}\vartheta_2(\xi,x) &= \int_{\mathcal{I}} du\theta(\xi,u)\theta^*(u,x)\\ &= \int_{\mathcal{I}} du(u-\xi)^+(u-x)^+ = \int_{\xi\vee x}^{B} du(u-\xi)(u-x)\\ &= \xi x(B-\xi\vee x) - (\xi+x)(B-\xi\vee x)^2/2 + (B-\xi\vee x)^3/3.\end{aligned}$$

Let us now turn to the detailed inspection of these operators.

7.3 Results relative to $\gamma^*\gamma$ and $\gamma\gamma^*$. Let us denote by $\mathcal{R}(\kappa)$ the range of an operator κ of $\mathbb{L}_2\mathcal{I}$ and by $\mathcal{N}(\kappa)$ its null space (see [124, p.23]). Obviously both $\gamma^*\gamma$ and $\gamma\gamma^*$ are self-adjoint. This translates into the fact that their kernels are symmetric (meaning $\vartheta_i(\xi,x) = \vartheta_i(x,\xi)$). In addition, both ϑ_1 and ϑ_2 are continuous on the bounded square $\mathcal{I}\times\mathcal{I}$. Therefore, the associated operators are compact (see [124, Ex. 4.8.4, p.172]). As such, they verify the spectral theorem (see [124, Th. 4.10.1, 4.10.2, p.187-189]).

Theorem 7.3.1. *Given the operators $\gamma^*\gamma$ and $\gamma\gamma^*$ defined in eq. (7.3) and eq. (7.4) above, we have the following results.*

1) The operators $\gamma^*\gamma$ and $\gamma\gamma^*$ are compact and self-adjoint. As such, they admit countable families of orthonormal eigenvectors (φ_k) and (ψ_k) associated to the same positive decreasing sequence of eigenvalues λ_k^2, which are complete in $\mathcal{R}(\gamma^*\gamma)$ and $\mathcal{R}(\gamma\gamma^*)$, respectively.

2) Besides, we have

$$\begin{aligned}\mathcal{R}(\gamma^*\gamma) &\subset \mathbb{L}_2\mathcal{I}\cap\mathscr{C}^4\mathcal{I},\\ \mathcal{R}(\gamma^*\gamma) &\subset \mathbb{L}_2\mathcal{I}\cap\mathscr{C}^4\mathcal{I},\end{aligned}$$

where $\mathscr{C}^4\mathcal{I}$ stands for the set of four times differentiable functions on $\mathcal{I}$.

3) Furthermore, the orthonormal families (φ_k) and (ψ_k) are complete in $\mathbb{L}_2\mathcal{I}$. In other words, they are both orthonormal bases of $\mathbb{L}_2\mathcal{I}$. In fact, we can write

$$\begin{aligned}\mathbb{L}_2\mathcal{I} &= \overline{\mathcal{R}(\gamma^*\gamma)} = Span\{\varphi_k, k\in\mathbb{N}\},\\ &= \overline{\mathcal{R}(\gamma\gamma^*)} = Span\{\psi_k, k\in\mathbb{N}\},\end{aligned}$$

where $\overline{\mathcal{R}(\gamma^*\gamma)}$ stands for the closure of $\mathcal{R}(\gamma^*\gamma)$ in $\mathbb{L}_2\mathcal{I}$ (see [124, p.16]) and $Span\{\varphi_k, k\in\mathbb{N}\}$ for the set of (potentially infinite) linear combinations of elements φ_k.

4) Therefore, $\gamma^*\gamma$ and $\gamma\gamma^*$ are both invertible and admit the fourth order differential operator ∂_ξ^4 as an inverse (see [124, p.155] for terminology). More precisely, we have got

$$\begin{aligned}\partial_\xi^4\gamma^*\gamma f &= f, &&\forall f\in\mathbb{L}_2\mathcal{I},\\ \gamma^*\gamma\partial_\xi^4 f &= f, &&\forall f\in\mathcal{R}(\gamma^*\gamma),\end{aligned}$$

and idem for $\gamma\gamma^*$.

5) Finally, we have the following spectral decompositions,

$$\begin{aligned}f &= \sum_{k\geq 0}\langle f,\varphi_k\rangle\varphi_k, &&f\in\mathbb{L}_2\mathcal{I},\\ \gamma^*\gamma f &= \sum_{k\geq 0}\lambda_k^2\langle f,\varphi_k\rangle\varphi_k, &&f\in\mathbb{L}_2\mathcal{I},\end{aligned}$$

and

$$f = \sum_{k\geq 0} \langle f, \psi_k \rangle \psi_k, \qquad f \in \mathbb{L}_2\mathcal{I},$$
$$\gamma\gamma^* f = \sum_{k\geq 0} \lambda_k^2 \langle f, \psi_k \rangle \psi_k, \qquad f \in \mathbb{L}_2\mathcal{I}.$$

Proof. As detailed above, 1) follows directly from the spectral theorem. 2) follows directly from the kernel representations in eq. (7.3) and eq. (7.4). It can also be seen from the fact that, for any $f \in \mathbb{L}_2\mathcal{I}$, both γf and $\gamma^* f$ are twice differentiable, which follows by simple inspection of eq. (7.1) and eq. (7.2). 3) follows directly from Proposition 7.5.1 below. 4) is a direct consequence of Lemma 7.8.1 below. Finally, 5) follows directly from 1) and 3). □

7.4 Results relative to γ and γ^*. The following theorem details the properties of the restricted put and call operators. It builds upon Theorem 7.3.1 above.

Theorem 7.4.1. *Given operators γ and γ^* defined in eq. (7.1) and eq. (7.2) above, we have the following results.*

1) *Consider the sequence of positive decreasing singular values λ_k and singular vectors (φ_k) and (ψ_k) defined in Theorem 7.3.1 above. The restricted put and call operators γ^* and γ are such that, for all $k \geq 0$,*

$$\gamma\varphi_k = \lambda_k \psi_k, \qquad \gamma^*\psi_k = \lambda_k \varphi_k.$$

2) *Besides, we have*

$$\mathcal{R}(\gamma^*) \subset \mathbb{L}_2\mathcal{I} \cap \mathscr{C}^2\mathcal{I},$$
$$\mathcal{R}(\gamma) \subset \mathbb{L}_2\mathcal{I} \cap \mathscr{C}^2\mathcal{I},$$

where $\mathscr{C}^2\mathcal{I}$ stands for the set of two times differentiable functions on $\mathcal{I}$.

3) *In addition, we have $\mathbb{L}_2\mathcal{I} = \overline{\mathcal{R}(\gamma^*)} = \overline{\mathcal{R}(\gamma)}$. So that both γ and γ^* are invertible and admit the second order partial differential operator ∂_ξ^2 as an inverse. In particular, we obtain*

$$\partial_\xi^2 \gamma f(\xi) = \partial_\xi^2 \gamma^* f(\xi) = f(\xi), \qquad \forall f \in \mathbb{L}_2\mathcal{I}. \tag{7.5}$$

So that the knowledge of γf or/and $\gamma^* f$ allows to recover f directly as their second derivative. This is nothing but the so-called Breeden-Litzenberger formula restricted to the interval $\mathcal{I}$.

4) *We have furthermore the following spectral decompositions,*

$$f = \sum_{k\geq 0} \langle f, \varphi_k \rangle \varphi_k, \qquad f \in \mathbb{L}_2\mathcal{I},$$
$$\gamma f = \sum_{k\geq 0} \lambda_k \langle f, \varphi_k \rangle \psi_k, \qquad f \in \mathbb{L}_2\mathcal{I},$$

and

$$f = \sum_{k\geq 0} \langle f, \psi_k\rangle \psi_k, \qquad f \in \mathbb{L}_2\mathcal{I},$$
$$\gamma^* f = \sum_{k\geq 0} \lambda_k \langle f, \psi_k\rangle \varphi_k, \qquad f \in \mathbb{L}_2\mathcal{I}.$$

5) Finally, we have a put-call parity on the interval that can be written as follows

$$(\gamma - \gamma^*)f(\xi) = \bar{m}_1(f) - \xi \bar{m}_0(f),$$

where we have defined $\bar{m}_k(f) := \int_{\mathcal{I}} x^k f(x)dx$.

Proof. The proof of 1) follows directly from [123, p.37]. 2) follows by simple inspection of eq. (7.2) and eq. (7.1). The first part of 3) follows from the facts that $\mathcal{R}(\gamma) = \mathcal{R}(\gamma\gamma^*)$ and $\mathcal{R}(\gamma^*) = \mathcal{R}(\gamma^*\gamma)$ (see 1) above) and Theorem 7.3.1, item 3). The second part of 3) follows partly from Lemma 7.8.1 below (see Appendix) and partly from the obvious fact that $f = \gamma^*\partial_\xi^2 f$ for all $f \in \mathcal{R}(\gamma^*)$ (idem for γ). 4) follows directly from 1) and 3). Finally, 5) follows immediately from the following obvious computations,

$$\begin{aligned}(\gamma - \gamma^*)f(\xi) &= \gamma f(\xi) - \gamma^* f(\xi)\\ &= \int_{\mathcal{I}} [\theta(\xi, x) - \theta^*(\xi, x)] f(x)dx\\ &= \int_{\mathcal{I}} (x - \xi) f(x)dx\\ &= \bar{m}_1(f) - \xi \bar{m}_0(f).\end{aligned}$$

□

We regroup other results relative to the above operators in the following section.

7.5 Other results relative to $\gamma^*\gamma$, $\gamma\gamma^*$, γ^* and γ. We prove here that both orthonormal families (φ_k) and (ψ_k) are complete in $\mathbb{L}_2\mathcal{I}$. Other interesting results are to be found in the Appendix. Some of them are purely technical, while some others are of more general interest.

Proposition 7.5.1. *We have got,*

$$\begin{aligned}\mathbb{L}_2\mathcal{I} &= \overline{\mathcal{R}(\gamma^*\gamma)} = \mathit{Span}\{\varphi_k, k \geq 0\},\\ &= \overline{\mathcal{R}(\gamma\gamma^*)} = \mathit{Span}\{\psi_k, k \geq 0\},\end{aligned}$$

where $\overline{\mathcal{R}(\gamma^*\gamma)}$ *stands for the closure of* $\mathcal{R}(\gamma^*\gamma)$ *in* $\mathbb{L}_2\mathcal{I}$ *(see [124, p.16]) and* $\mathit{Span}\{\varphi_k, k \in \mathbb{N}\}$ *for the set of (potentially infinite) linear combinations of elements* φ_k.

Proof. We know from [123, §2.3.] that,

$$\begin{aligned}\mathbb{L}_2\mathcal{I} &= \overline{\mathcal{R}(\gamma^*\gamma)} \oplus^\perp \mathcal{N}(\gamma^*\gamma),\\ &= \overline{\mathcal{R}(\gamma\gamma^*)} \oplus^\perp \mathcal{N}(\gamma\gamma^*).\end{aligned}$$

Therefore, it is enough to show that both null-spaces reduce to the zero element. The kernel $\mathcal{N}(\gamma^*\gamma)$ of $\gamma^*\gamma$ is constituted by the functions $f \in \mathbb{L}_2\mathcal{I}$ that are solutions of

$$0 = \gamma^*\gamma f(\xi), \qquad \forall \xi \in \mathcal{I}.$$

Deriving four times with respect to ξ and applying Lemma 7.8.1 (see Appendix) leads to $f(\xi) = 0, \xi \in \mathcal{I}$. So that $\mathcal{N}(\gamma^*\gamma) = \{0\}$. Now it is enough to notice that $\mathcal{N}(\gamma^*\gamma) = \mathcal{N}(\gamma)$. However, we know from Lemma 7.8.2 that $f \in \mathcal{N}(\gamma)$ if and only if $\breve{f} \in \mathcal{N}(\gamma^*)$ (see eq. (7.35) for notation). Therefore $\mathcal{N}(\gamma\gamma^*) = \mathcal{N}(\gamma^*) = \breve{\mathcal{N}}(\gamma) = \breve{\mathcal{N}}(\gamma^*\gamma) = \{0\}$, where by $\breve{\mathcal{N}}$, we mean $\{\breve{f}, f \in \mathcal{N}\}$. □

7.6 Explicit computation of (λ_k), (φ_k) and (ψ_k).

7.6.1 Main result. In this section, we give explicit expressions for the singular bases and singular vectors of the restricted call and put operators. The results are gathered below in Theorem 7.6.1. Let us write

$$f_{k,1}(\xi) = e^{\rho_k \xi/B}, \qquad f_{k,2}(\xi) = e^{-\rho_k \xi/B},$$
$$f_{k,3}(\xi) = \cos(\rho_k t/B), \qquad f_{k,4}(\xi) = \sin(\rho_k \xi/B),$$

where

$$\rho_k = \frac{\pi}{2} + k\pi + (-1)^k \beta_k, \qquad k \in \mathbb{N}, \tag{7.6}$$

and , for all $k \in \mathbb{N}$, β_k is the smallest positive solution of the following fixed point equation in u,

$$\exp(\pi/2 + k\pi + (-1)^k u) = \frac{1 + \cos(u)}{\sin(u)}.$$

Interestingly, the positive sequence (β_k) decreases exponentially fast toward zero as detailed in Lemma 7.6.3. In addition, we write,

$$h_{k,1} = a_{k,1} f_{k,1} + a_{k,2} f_{k,2}, \qquad h_{k,2} = a_{k,3} f_{k,3} + a_{k,4} f_{k,4}, \tag{7.7}$$

where the coefficients $a_{k,i}, i = 1, \ldots, 4$ are such that,

$$a_{k,1} = \frac{1}{\sqrt{B}} \frac{(-1)^k}{e^{\rho_k} + (-1)^k},$$
$$a_{k,2} = (-1)^k e^{\rho_k} a_{k,1} = \frac{1}{\sqrt{B}} \frac{1}{1 + (-1)^k e^{-\rho_k}},$$
$$a_{k,3} = -\frac{1}{\sqrt{B}},$$
$$a_{k,4} = \frac{1}{\sqrt{B}} \frac{1 - (-1)^k e^{-\rho_k}}{1 + (-1)^k e^{-\rho_k}}.$$

Then, we have the following theorem.

Theorem 7.6.1. *The eigenvectors (φ_k) of $\gamma^*\gamma$ and (ψ_k) of $\gamma\gamma^*$ are such that*

$$\varphi_k = h_{k,1} + h_{k,2}, \qquad \psi_k = h_{k,1} - h_{k,2}. \tag{7.8}$$

They are related by the following relationships,

$$\gamma\varphi_k = \lambda_k\psi_k, \qquad \gamma^*\psi_k = \lambda_k\varphi_k, \tag{7.9}$$

where we have written

$$\lambda_k = \left(\frac{B}{\rho_k}\right)^2, \tag{7.10}$$

and ρ_k is defined in eq. (7.6). They verify $\|\varphi_k\|_{\mathbb{L}_2\mathcal{I}} = \|\psi_k\|_{\mathbb{L}_2\mathcal{I}} = 1$. Moreover, we have

$$\psi_k(B) = \psi_k'(B) = 0, \qquad \varphi_k(0) = \varphi_k'(0) = 0, \tag{7.11}$$

together with

$$\breve{\psi}_k = (-1)^k\varphi_k, \qquad \breve{\varphi}_k = (-1)^k\psi_k, \tag{7.12}$$

where we have written $\breve{\psi}_k(\xi) = \psi_k(B-\xi)$. And finally, we obtain as a direct consequence of eq. (7.5) above that

$$\lambda_k\partial_\xi^2\psi_k = \partial_\xi^2\gamma\varphi_k = \varphi_k,$$
$$\lambda_k\partial_\xi^2\varphi_k = \partial_\xi^2\gamma^*\psi_k = \psi_k.$$

Proof. Notice readily that eq. (7.11), eq. (7.12) and the fact that both φ_k and ψ_k are unit normed are straightforward consequences of eq. (7.8). In addition, eq. (7.9) is a repetition of Theorem 7.4.1, item 1). So that we are in fact left with proving eq. (7.8) and eq. (7.10). Each eigenvector f of $\gamma^*\gamma$ associated to the eigenvalue r^4 is solution of the problem,

$$r^4 f = \gamma^*\gamma f, \tag{7.13}$$

for some $r \neq 0$ and $f \in \mathbb{L}_2\mathcal{I}$. After differentiating four times the latter equation with respect to ξ (assuming that $f \in \mathbb{L}_2\mathcal{I} \cap \mathscr{C}^4\mathcal{I}$) and applying Lemma 7.8.1, we obtain that the solutions of eq. (7.13) are also solutions of the following fourth order ordinary differential equation,

$$r^4 d_\xi^4 f - f = 0,$$

where d_ξ^4 stands for the fourth order ordinary differential operator. Its characteristic polynomial admits four roots $\pm r^{-1}$ and $\pm ir^{-1}$. Consequently, the real solutions of the above ordinary differential equation are of the form

$$f(\xi) = b_1 e^{\xi/r} + b_2 e^{-\xi/r} + b_3\cos(\xi/r) + b_4\sin(\xi/r). \tag{7.14}$$

The φ_ks are thus of this form. Plugging this generic solution back into eq. (7.13) leads in turn, after tedious but straightforward computations, to

$$Mb = 0, \tag{7.15}$$

where b is a 4×1 vector such that $b^T = \begin{bmatrix} b_1 & b_2 & b_3 & b_4 \end{bmatrix}$ and M is the 4×4 matrix defined by

$$M(r,B) = \begin{bmatrix} r^{-1}e^{B/r} & -r^{-1}e^{-B/r} & r^{-1}\sin(B/r) & -r^{-1}\cos(B/r) \\ -r^{-2}e^{B/r} & -r^{-2}e^{-B/r} & r^{-2}\cos(B/r) & r^{-2}\sin(B/r) \\ r^{-3} & -r^{-3} & 0 & r^{-3} \\ r^{-4} & r^{-4} & r^{-4} & 0 \end{bmatrix}. \tag{7.16}$$

There exists a non-trivial solution to eq. (7.15) if and only if r is such that the determinant of M cancels, that is $\mathrm{Det}(r,M) = 0$. As detailed in Proposition 7.6.1, the roots of $\mathrm{Det}(r,M) = 0$ are exactly the $r_m = B/\nu_m$ where ν_m is defined in eq. (7.21). In addition, we prove in Proposition 7.6.2 that the system $M(r_m,B)b = 0$ admits the unique solution b_m. Reading off eq. (7.14), we obtain that the eigenvector of $\gamma^*\gamma$ associated to eigenvalue r_m^4 writes as $\alpha_m = \eta_{m,1} + \eta_{m_2}$ where both $\eta_{m,1}$ and $\eta_{m,2}$ are defined in eq. (7.20). Now, it is enough to notice that, given the properties of the sequence (ν_m) detailed in Proposition 7.6.3, $r_{2k+1}^4 = r_{2k}^4$ and $r_{2k+2}^4 < r_{2k+1}^4$, $k \in \mathbb{N}$. In addition, we know from Lemma 7.6.1 that $\alpha_{2k+1} = \alpha_{2k}$. This allows us to conclude that the eigenvalues of $\gamma^*\gamma$ are, without redundancy, the λ_k^2, $k \in \mathbb{N}$, defined in eq. (7.10) and the associated eigenspaces are unit-dimensional and respectively spanned by the eigenvectors φ_k, $k \in \mathbb{N}$, defined in eq. (7.8).
Computing $\psi_k = \lambda_k^{-1}\gamma\varphi_k$ leads, after tedious but straightforward computations to $\psi_k = h_{k,1} - h_{k,2}$ and concludes the proof. □

7.6.2 Additional results. This section contains a series of results that are used throughout the proof of Theorem 7.6.1 above. In this section we make use of the map $E : \mathbb{N} \mapsto \mathbb{N}$ such that $E(2k+1) = E(2k) = k$ for all $k \in \mathbb{N}$.

Proposition 7.6.1. *Let $M(r,B)$ be the 4×4 matrix defined in eq. (7.16). The set of solutions r to the problem $DetM(r,B) = 0$ is countable. Let us denote them by $r_m, m \in \mathbb{N}$. For any $m \in \mathbb{N}$, the solution r_m can be written as*

$$r_m = \frac{B}{\nu_m},$$

where ν_m is defined in eq. (7.21). We obtain in fact that,

$$DetM(r_m,B) = 0 \qquad \Leftrightarrow \qquad e^{\nu_m} = -\frac{1 + (-1)^{E(m)}\sin(\nu_m)}{\cos(\nu_m)}.$$

Besides, the following relationships hold true

$$\cos\nu_m := -\frac{2}{e^{\nu_m} + e^{-\nu_m}} = -\frac{1}{\cosh\nu_m}, \tag{7.17}$$

$$\sin\nu_m := -(-1)^{E(m)} + (-1)^{E(m)}\frac{2}{1 + e^{-2\nu_m}}. \tag{7.18}$$

Proof. It follows from straightforward computations that,

$$\mathrm{Det}M(r,B) = 2e^{-B/r}\left(\cos(B/r)\left(e^{B/r}\right)^2 + 2e^{B/r} + \cos(B/r)\right). \tag{7.19}$$

Let us write $\nu := B/r$ and notice that if $\cos(\nu) = 0$, then $\mathrm{Det}M(r, B) = 2 \neq 0$ so that we must have $\cos\nu \neq 0$ for eq. (7.15) to admit a non-trivial solution. To be more specific $\mathrm{Det}M(r, B) = 0$ reduces to $P(e^\nu) = 0$ where $P(x) := \cos(\nu)\, x^2 + 2x + \cos(\nu)$. However the roots of P are given by

$$\delta_\pm(\nu) := \frac{-1 \pm \sin(\nu)}{\cos(\nu)}.$$

Henceforth, $r = B/\nu$ cancels $\mathrm{Det}M(r, B)$ if and only if ν is solution of anyone of the two following fixed point equations,

$$e^\nu = \frac{-1 + \sin(\nu)}{\cos(\nu)}, \qquad\qquad e^\nu = \frac{-1 - \sin(\nu)}{\cos(\nu)}.$$

The proof follows now directly from Proposition 7.6.3. □

Proposition 7.6.2. *For any r_m solution of the equation $DetM(r_m, B) = 0$ (see Proposition 7.6.1 above), the null space of $M(r_m, B)$ is of dimension 1 and is spanned by the vector*

$$b_m^T = \begin{bmatrix} b_{m,1} & b_{m,2} & b_{m,3} & b_{m_4} \end{bmatrix},$$

where we have written,

$$\begin{aligned}
b_{m,1} &= \frac{1}{\sqrt{B}} \frac{(-1)^{E(m)}}{e^{\nu_m} + (-1)^{E(m)}}, \\
b_{m,2} &= (-1)^{E(m)} e^{\nu_m} a_{m,1} = \frac{1}{\sqrt{B}} \frac{1}{1 + (-1)^{E(m)} e^{-\nu_m}}, \\
b_{m,3} &= -\frac{1}{\sqrt{B}}, \\
b_{m,4} &= \frac{1}{\sqrt{B}} \frac{1 - (-1)^{E(m)} e^{-\nu_m}}{1 + (-1)^{E(m)} e^{-\nu_m}},
\end{aligned}$$

and ν_m is defined in eq. (7.21).

Proof. It is a matter of straightforward linear algebra and thus left to the reader. Notice however, that it relies on the use of both eq. (7.17) and eq. (7.18). □

Lemma 7.6.1. *Let us write*

$$\begin{aligned}
\zeta_{m,1}(\xi) &= e^{\nu_m \xi/B}, & \zeta_{m,2}(\xi) &= e^{-\nu_m \xi/B}, \\
\zeta_{m,3}(\xi) &= \cos(\nu_m \xi/B), & \zeta_{m,4}(\xi) &= \sin(\nu_m \xi/B),
\end{aligned}$$

where ν_m is defined in eq. (7.21). In addition, we write,

$$\eta_{m,1} = b_{m,1}\zeta_{m,1} + b_{m,2}\zeta_{m,2}, \qquad \eta_{m,2} = b_{m,3}\zeta_{m,3} + b_{m,4}\zeta_{m,4}, \tag{7.20}$$

where the coefficients $b_{m,i}, i = 1, \ldots, 4$ are defined in Proposition 7.6.2. For all $k \in \mathbb{N}$, we have the following relationships

$$\eta_{2k+1,1} = \eta_{2k,1}, \qquad\qquad \eta_{2k+1,2} = \eta_{2k,2}$$

Proof. It follows from straightforward computations using the fact that $\nu_{2m+1} = -\nu_{2m}$. □

Proposition 7.6.3. *Let us define the map $E : \mathbb{N} \mapsto \mathbb{N}$ such that $E(2k) = E(2k+1) = k$ for $k \in \mathbb{N}$. Let us write*

$$g(\nu) = \frac{-1 + \sin\nu}{\cos\nu}, \qquad h(\nu) = \frac{-1 - \sin\nu}{\cos\nu},$$

and consider the fixed point equations $e^\nu = g(\nu)$ and $e^\nu = h(\nu)$. The set of corresponding solutions is exhausted by the sequence

$$\nu_m = (-1)^m \left(\frac{\pi}{2} + E(m)\pi + (-1)^{E(m)}\beta_{E(m)}\right), \qquad m \in \mathbb{N}. \tag{7.21}$$

where (β_m) is defined in Lemma 7.6.3. In particular, notice that $\nu_{2k+1} = -\nu_{2k}$ and $|\nu_{m_1}| < |\nu_{m_2}|$ for all $m_1, m_2 \in \mathbb{N}$ such that $E(m_1) < E(m_2)$. Notice in addition that, by construction, ν_m is solution of

$$e^{\nu_m} = -\frac{1 + (-1)^{E(m)}\sin\nu_m}{\cos\nu_m}.$$

This latter result, together with the fact that $DetM(B/\nu_m, B) = 0$ (see eq. (7.19)), leads straightforwardly to the following relationships,

$$\cos\nu_m := -\frac{2}{e^{\nu_m} + e^{-\nu_m}} = -\frac{1}{\cosh\nu_m},$$
$$\sin\nu_m := -(-1)^{E(m)} + (-1)^{E(m)}\frac{2}{1 + e^{-2\nu_m}}.$$

Proof. Consider the fixed point equation $g(\nu) = e^\nu$. Given the properties of g detailed in Proposition 7.6.4, two cases arise depending whether ν is positive or negative. In the case where ν is positive, the exponential map meets g at points of the form $p_m = \frac{3\pi}{2} + 2m\pi - u_m$ for $m \in \mathbb{N} = \{0, 1, 2, \ldots\}$ and some small but positive u_ms. A direct application of Lemma 7.6.2 shows that the negative solutions are exactly the $-p_m, m \in \mathbb{N}$.
The second fixed point equation $h(\nu) = e^\nu$ can be rewritten as $g(-\nu) = e^\nu$. The positive solutions are of the form $q_m = \frac{\pi}{2} + 2m\pi + v_m, m \in \mathbb{N}$. And, from Lemma 7.6.2 again, the corresponding negative solutions are the $-q_m, m \in \mathbb{N}$.
Let us write $t_m = \frac{\pi}{2} + m\pi + (-1)^m\beta_m, m \in \mathbb{N}$. It is clear that $t_{2k} = q_k$ and $t_{2k+1} = p_k$ for $k \in \mathbb{N}$. In particular, t_m is solution of

$$e^{t_m} = -\frac{1 + (-1)^m \sin t_m}{\cos t_m} \tag{7.22}$$

Let us define the map $E : \mathbb{N} \mapsto \mathbb{N}$ such that $E(2k+1) = E(2k) = k$ for all $k \in \mathbb{N}$. We define $\nu_m, m \in \mathbb{N}$ such that $\nu_m = (-1)^m t_{E(m)}$, that is $\nu_{2k} = t_k$ and $\nu_{2k+1} = -t_k$, $k \in \mathbb{N}$. By construction, ν_m exhausts the set of solutions of both fixed point equations $e^\nu = g(\nu)$ and $e^\nu = h(\nu)$. In fact, ν_m is solution of

$$e^{\nu_m} = -\frac{1 + (-1)^{E(m)}\sin\nu_m}{\cos\nu_m}$$

□

Proposition 7.6.4. *Notice readily that $h(\nu) = g(-\nu)$, so that it is enough to study the properties of g alone. We have the following results,*

1. *g is defined on the domain $\mathcal{D}_g = \mathbb{R}\backslash\{\frac{3\pi}{2} + 2m\pi, m \in \mathbb{Z}\}$;*
2. *g is 2π periodic and such that, for all $\nu \in \mathcal{S}_g = (-\frac{\pi}{2}, \frac{3\pi}{2})$, $g(\nu + 2m\pi) = g(\nu)$;*
3. *Finally, g is strictly increasing on $\mathcal{S}_g$ and such that,*

$$\lim_{\nu \to_\oplus -\frac{\pi}{2}} g(\nu) = -\infty, \qquad g(\frac{\pi}{2}) = 0, \qquad \lim_{\nu \to_\ominus \frac{3\pi}{2}} g(\nu) = +\infty.$$

   where we write $\to_\oplus$ (resp. $\to_\ominus$) to mean the limit from the above (resp. below).
4. *Notice that $\mathbb{R}\backslash\mathcal{D}_g$ (resp. $\mathbb{R}\backslash\mathcal{D}_h$) corresponds exactly to the set of all the zeros of h (resp. g). Thus $\mathcal{D}_g \cap \mathcal{D}_h$ is the subset of $\mathbb{R}$ containing all the points where both g and h are well defined and different from zero.*

Proof. Let us first focus on the domain of g. It is defined on $\mathbb{R}\backslash\{\frac{\pi}{2} + m\pi, m \in \mathbb{Z}\}$. However, g can be extended by continuity to be worth zero at points $\frac{\pi}{2} + 2m\pi, m \in \mathbb{Z}$. Notice indeed that for any small positive u and $\ell \in \mathbb{N}$, one has got

$$\begin{aligned} g(\frac{\pi}{2} + (-1)^\ell u) &= \frac{-1 + \cos u}{-(-1)^\ell \sin u} \\ &= \frac{-\frac{u^2}{2} + O(u^4)}{-(-1)^\ell u + O(u^3)} = (-1)^\ell \frac{u}{2} + O(u^3). \end{aligned}$$

With a slight abuse of notations, we denote the latter extension by g. So that g is actually defined on $\mathbb{R}\backslash\{\frac{3\pi}{2} + 2m\pi, m \in \mathbb{Z}\}$. The other properties are straightforward. □

Lemma 7.6.2. *Recall that $\mathcal{D}_g$ and $\mathcal{D}_h$ are defined in Proposition 7.6.4. Notice first that $\mathcal{D}_g \cap \mathcal{D}_h$ is symmetric, meaning that if $\nu \in \mathcal{D}_g \cap \mathcal{D}_h$, then $-\nu \in \mathcal{D}_g \cap \mathcal{D}_h$. For any $\nu \in \mathcal{D}_g \cap \mathcal{D}_h$, we have the following results,*

1. *If ν is solution of the fixed point equation $e^\nu = g(\nu)$, then $-\nu$ is also a solution.*
2. *If ν is solution of the fixed point equation $e^\nu = h(\nu)$, then $-\nu$ is also a solution.*

Proof. Notice first that we have the identity $h(\nu)g(\nu) = 1$ for any $\nu \in \mathcal{D}_g \cap \mathcal{D}_h$. Its proof is immediate. And therefore, for any $\nu \in \mathcal{D}_g \cap \mathcal{D}_h$ solution of $e^\nu = g(\nu)$, we obtain $g(-\nu) = h(\nu) = g(\nu)^{-1} = e^{-\nu}$. And idem for the solutions of $e^\nu = h(\nu)$. □

Lemma 7.6.3. *The sequence (β_k) is such that, for all $k \in \mathbb{N}$, β_k is the smallest positive solution of the following fixed point equation in u,*

$$\exp(\pi/2 + k\pi + (-1)^k u) = \frac{1 + \cos(u)}{\sin(u)}.$$

In addition, the approximation $\beta_k \approx 2e^{-\frac{\pi}{2} - k\pi}$ holds true with a large degree of accuracy from $k = 1$ onward.

Proof. Let us write $t_k = \frac{\pi}{2} + k\pi + (-1)^k u$, for some small but positive u such that t_k is solution of eq. (7.22). Notice that

$$\begin{aligned}
\cos\left(\frac{\pi}{2} + k\pi + (-1)^k u\right) &= -\sin(u) = -u + O(u^3),\\
\sin\left(\frac{\pi}{2} + k\pi + (-1)^k u\right) &= (-1)^k \cos(u) = (-1)^k + O(u^2),\\
\exp\left(\frac{\pi}{2} + k\pi + (-1)^k u\right) &= e^{\frac{\pi}{2}+k\pi}(1 + (-1)^k u + O(u^2)).
\end{aligned}$$

So that eq. (7.22) reduces to

$$\exp(\pi/2 + k\pi + (-1)^k u) = \frac{1+\cos(u)}{\sin(u)}.$$

Plugging-in the Taylor expansions above, we obtain

$$e^{\frac{\pi}{2}+k\pi}(1 + (-1)^k u + O(u^2)) = \frac{2 + O(u^2)}{u + O(u^3)} = \frac{1}{u}(2 + O(u^2)),$$

which can be rewritten as

$$u = e^{-\frac{\pi}{2}-k\pi}(2 + O(u)). \tag{7.23}$$

It can be verified numerically that $2e^{-\frac{\pi}{2}-k\pi}$ is a very good approximation of β_k as soon as $k \geq 1$ in the sense that eq. (7.22) holds true with a very large degree of accuracy. □

7.7 The spectral recovery method (SRM). In this Section, we first describe how γ and γ^* relate to the bid-ask quotes. We then show that the SVD of the restricted pricing operators described above can be used to design a simple quadratic program that recovers the smoothest RND compatible with market quotes.

7.7.1 From γ and γ^* to call and put prices. Let us denote by $P(\xi)$ and $C(\xi)$ the put and call prices at strike ξ and by q the corresponding risk neutral density. Let us furthermore write $\bar{\mathcal{I}} = \mathbb{R}^+ \backslash \mathcal{I} = (B, \infty)$. We assume that the restriction $q_{|\mathcal{I}}$ to the interval $\mathcal{I}$ of q is in $\mathbb{L}_2\mathcal{I}$. For all $\xi \in \mathcal{I}$, the following relationships are immediate.

$$e^{r\tau} P(\xi) = \gamma^* q(\xi), \tag{7.24}$$

$$\begin{aligned}
e^{r\tau} C(\xi) &= \gamma q(\xi) + \int_B^\infty (x-\xi) q(x) dx\\
&= \gamma q(\xi) + m_1(q) - \xi m_0(q),
\end{aligned} \tag{7.25}$$

where we have defined,

$$m_k(f) = \int_{\bar{\mathcal{I}}} x^k f(x) dx.$$

Notice in particular that

$$m_0(q) = \mathbb{Q}(S_\tau \geq B) = 1 - \bar{m}_0(q),$$
$$m_1(q) = \mathbb{E}_\mathbb{Q}(S_\tau | S_\tau \geq B)\mathbb{Q}(S_\tau \geq B) = \mathbb{E}_\mathbb{Q} S_\tau - \bar{m}_1(q).$$

Eq. (7.24) shows that put prices directly relate to the restricted put operator. From an estimation perspective, this is a crucial feature that will allow us to recover the RND directly from market put quotes. Unfortunately, the situation is slightly different for call prices. As shown from eq. (7.25), call prices relate to the restricted call operator via $m_1(q)$ and $m_0(q)$, which are both unknown. Although, they could be estimated and give rise to an estimator of the RND based on quoted call prices, we wont pursue this route here, but rather focus on the simpler relation given by eq. (7.24).

7.7.2 A refresher on no-arbitrage constraints. For a detailed review of model-free no-arbitrage constraints, the reader is referred to [48, p.32, § 1.8] and [125]. Let us denote by S_0 the price today of the underlying stock. Let us moreover assume that it pays a continuous dividend yield δ. Let us denote by r the continuously compounded short rate and by τ the time to maturity. Let us recall first that, by no-arbitrage, put and call prices are related by the put-call parity.

$$C(\xi) - P(\xi) = S_0 e^{-\delta\tau} - \xi e^{-r\tau}. \tag{7.26}$$

Besides $C(0) = S_0$ and $P(0) = 0$. Let us now focus on put prices. We have,

$$\max(0, \xi e^{-r\tau} - S_0 e^{-\delta\tau}) \leq P(\xi) \leq \xi e^{-r\tau}, \tag{7.27}$$
$$0 \leq \partial_\xi P(\xi) \leq e^{-r\tau}, \tag{7.28}$$
$$0 \leq \partial^2_\xi P(\xi). \tag{7.29}$$

Assume we are given an increasing sequence of n strikes $\xi_1 < \xi_2 < ... < \xi_n$ and a set of corresponding put prices $m_1, \ldots, m_n$. As described in [61], the above no-arbitrage relationships translate into a finite set of affine constraints on the latter put prices. These constraints can in fact be written in matrix form as $Am \leq b_p$, where A stands for a $2n \times n$ matrix, m is the $n \times 1$ vector such that $m^T = \begin{bmatrix} m_1 & \ldots & m_n \end{bmatrix}$ and b_p is a $2n \times 1$ vector. More precisely, eq. (7.29) translates into $n-2$ constraints as,

$$[Am]_i := \frac{m_{i+1} - m_i}{\xi_{i+1} - \xi_i} - \frac{m_{i+2} - m_{i+1}}{\xi_{i+2} - \xi_{i+1}} \leq 0 := [b_p]_i, \qquad i = 1, 2, \ldots, n-2$$

Moreover, the left-hand-side of eq. (7.27) is fully captured in-sample by adding the following additional n constraints,

$$[Am]_{i+n-2} := -m_i \leq -\max(0, \xi_i e^{-r\tau} - S_0 e^{-\delta\tau}) := [b_p]_{i+n-2}, \qquad i = 1, \ldots, n \tag{7.30}$$

The right-hand-side of eq. (7.27) need not be taken into account at this stage. It is indeed less stringent than the upper-bound constraints we will impose in the next section. Finally, given the first $n-2$ constraints, eq. (7.28) reduces to two additional constraints,

$$[Am]_{2n-1} := \frac{m_n - m_{n-1}}{\xi_n - \xi_{n-1}} \leq e^{-rT} := [b_p]_{2n-1},$$
$$[Am]_{2n} := m_1 - m_2 \leq 0 := [b_p]_{2n}.$$

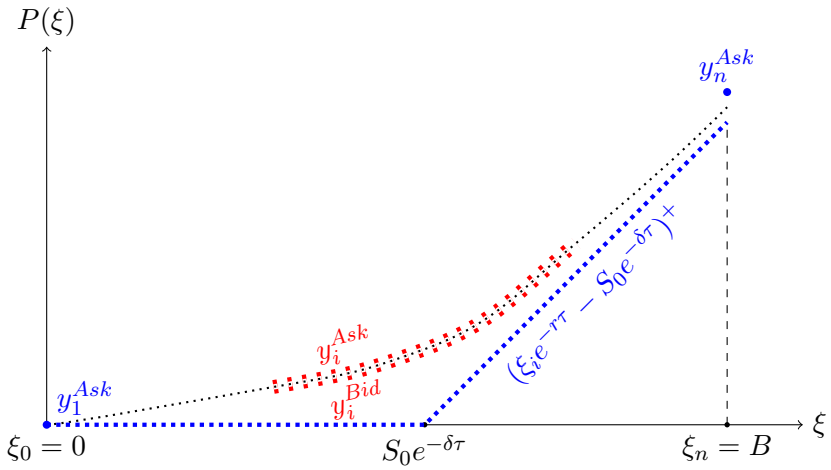

Figure 7.2: This graph sums up the set of constraints verified by estimated put prices, which are solutions of the quadratic optimization problem described in eq. (P1). Estimated put prices $m_1, \dots, m_n$ on the "dense" grid $\xi_1, \dots, \xi_n$ are displayed as black dots. They must lie in-between the bid-ask quotes, which are represented by thick red dots ranging over quoted strikes $\xi_{i_1}, \dots, \xi_{i_s}$, which correspond to a sparse subset of the underlying dense grid $\xi_1, \dots, \xi_n$. In addition, extreme put prices m_1 and m_n are bounded above by $y_1^{Ask} = 0$ and y_n^{Ask}, respectively, where the value of y_n^{Ask} is given in Section 7.7.3. Both y_1^{Ask} and y_n^{Ask} appear as thick blue dots at strikes $\xi_1 = 0$ and $\xi_n = B$, respectively. $m_1, \dots, m_n$ must also verify the in-sample constraints described by the lhs of eq. (7.27). In particular, the lhs of eq. (7.27) ensures that the m_is are lower-bounded by the $(\xi_i e^{-r\tau} - S_0 e^{-\delta\tau})^+$s, which appear as thick blue dots. Since this lower-bound is worth 0 for $i = 1$, this, together with the upper-bound $y_1^{Ask} = 0$ actually impose $m_1 = 0$. Finally, $m_1, \dots, m_n$ verify both eq. (7.28) and eq. (7.29) above. The latter constraint imposes in-sample convexity.

Finally, let us recall that if the forward price F_0 of the underlying stock is observable today, then, by no-arbitrage, it must be equal to $S_0 e^{(r-\delta)\tau}$.

7.7.3 Bid-ask spread constraints. Let us assume that the market provides us with an increasing sequence of strike prices $\xi_1 < \xi_2 < \dots < \xi_s$, where s is small. Typically s ranges from 5 to 50 depending on the underlying. In addition, the market provides us with a corresponding sequence of bid ask quotes for put options. Let us denote them by $y_1^{Ask}, \dots, y_s^{Ask}$ and $y_1^{Bid}, \dots, y_s^{Bid}$. We want the corresponding fitted put prices (m_i) to lie inside the bid ask quotes. This corresponds to the following $2s$ affine constraints,

$$m_i \leq y_i^{Ask}, \qquad -m_i \leq -y_i^{Bid}, \qquad i = 1, \dots s. \tag{7.31}$$

The quoted strikes might eventually span a very small portion of the segment $\mathcal{I}$ on which we want to recover the RND. In order to improve the quality of our estimator, we can constrain it to verify the above no-arbitrage constraints on a denser set of strikes than the quoted ones. Let us denote by $\xi_1 < \xi_2 < \dots < \xi_n$ this new set of strike prices, such that $\xi_1 = 0$, $\xi_n = B$ and including the initial quoted strikes. For later reference, we denote by $I = \{i_1, \dots, i_s\}$ the subset of $\{1, \dots, n\}$ corresponding to the indexes of the initial quoted strikes. We know that,

in any case, we must have $0 = P(0) = m_1$, so that we can define $y_1^{Ask} = 0$. Furthermore, we know from eq. (7.28) that $P(\xi)$ cannot grow at a rate faster than $e^{-r\tau}$, so that we can define y_n^{Ask} to be the corresponding linear extrapolation of the right-most market quote $y_{i_s}^{Ask}$, meaning $y_n^{Ask} = y_{i_s}^{Ask} + e^{-r\tau}(\xi_n - \xi_{i_s})$. In summary, the requirement that the m_is fall in-between the bid-ask quotes translates into $2s+2$ additional constraints, which we can write as follows

$$m_i \leq y_i^{Ask}, \qquad i \in I \cup \{1, n\}, \tag{7.32}$$

$$-m_i \leq -y_i^{Bid}, \qquad i \in I. \tag{7.33}$$

All previously mentioned constraints are summarized in Figure 7.2.

7.7.4 The quadratic program. Fix $N \in \mathbb{N}$. The choice of N will be discussed in the next Section. Let us denote by P_N the estimator of the put price P on $\mathcal{I}$ built upon the φ_k's up to level N and by $e^{-r\tau}q_N$ the corresponding inverse image by γ^*. We have explicitly, from eq. (7.24) and Theorem 7.4.1, item 4),

$$\begin{aligned} P_N &= \gamma^* e^{-r\tau} q_N, \\ P_N &= \sum_{k=0}^{N} \omega_k \varphi_k, \\ q_N &= e^{r\tau} \sum_{k=0}^{N} \lambda_k^{-1} \omega_k \psi_k, \end{aligned}$$

for some $\omega^T = \begin{bmatrix} \omega_0 & \dots & \omega_N \end{bmatrix} \in \mathbb{R}^{N+1}$. Furthermore for a given matrix M, we will denote by $[M]_{I,J}$ the sub-matrix obtained by extracting the rows of M at indexes in I and the columns of M at indexes in J. When extracting all the columns, we will write $[M]_{I,\bullet}$, and similarly for the rows. And we will naturally write $[M]_I$ in the case where M is a vector. The SRM estimator $\omega^\bigstar$ is obtained as a solution of a quadratic program. It corresponds (modulo rescaling by the λ_ks and the discount factor) to the coefficients of the smoothest density that verifies the no-arbitrage and bid-ask constraints above. To that end, notice that the $\mathbb{L}_2\mathcal{I}$-norm of the second derivative of q_N, namely $S_N = \|\partial_\xi^2 q_N\|^2_{\mathbb{L}_2\mathcal{I}}$, quantifies its smoothness. S_N is often used as a smoothness penalty and has been widely used in the context of smooth RND recovery. Obviously, the smoother q_N, the smaller S_N. As detailed in Proposition 7.7.1, S_N can be directly expressed as a quadratic form of ω involving the $N+1$ first eigenvalues of the restricted put operator γ^*. As a consequence, $\omega^\bigstar$ is solution of,

$$\arg \min_{\omega \in \mathbb{R}^{N+1}} \|\partial_\xi^2 q_N\|^2_{\mathbb{L}_2} \qquad \text{subject to} \begin{cases} [P_N]_{I\cup\{1,n\}} & \leq y^{Ask}_{I\cup\{1,n\}}, \\ -[P_N]_I & \leq -y_I^{Bid}, \\ AP_N & \leq b_p, \\ q_N(0) & = 0. \end{cases} \tag{P1'}$$

where, with a slight abuse of notations, we have written $P_N^T = \begin{bmatrix} P_N(\xi_1) & \dots & P_N(\xi_n) \end{bmatrix}$, y_I^{Bid} stands for the vector of initial put bid quotes and $y^{Ask}_{I\cap\{1,n\}}$ stands for the vector of initial put ask quotes augmented with the no arbitrage bounds $y_1^{Ask} = 0$ and $y_n^{Ask} = y_{i_s}^{Ask} + e^{-r\tau}(\xi_n - \xi_{i_s})$. Notice that we have added the constraint $q_N(0) = 0$, which does not arise as a natural property

of the ψ_ks.
Denote by $\varphi_{0,N}(\xi)^T = \begin{bmatrix}\varphi_0(\xi) & \dots & \varphi_N(\xi)\end{bmatrix}$ and, similarly, write $\psi_{0,N}(\xi)^T$. Then we have $[P_N]_i = \varphi_{0,N}(\xi_i)^T\omega$ and $q_N(\xi) = \psi_{0,N}(\xi)^T\Omega_N\omega$, where Ω_N is defined below in Proposition 7.7.1. Let us finally denote by Φ the matrix whose rows are constituted by the $\varphi_{0,N}(\xi_i)^T$, $i = 1,\dots,n$ and write $\Phi_I = [\Phi]_{I,\bullet}$. With these notations, eq. (P1') can be rewritten in canonical form as

$$\arg\min_{\omega\in\mathbb{R}^{N+1}} \frac{1}{2}\omega^T\Omega_N^4\omega \qquad \text{subject to } \begin{cases}\Phi_{I\cup\{1,n\}}\omega & \leq y^{Ask}_{I\cup\{1,n\}},\\ -\Phi_I\omega & \leq -y_I^{Bid},\\ A\Phi\omega & \leq b_p,\\ \psi_{0,N}(0)^T\Omega_N\omega & = 0.\end{cases} \tag{P1}$$

which is nothing but a quadratic program in ω. This result is due to the following Proposition.

Proposition 7.7.1. *Let us write* $f_N = \sum_{k=0}^N \lambda_k^{-1}\omega_k\psi_k$ *and*

$$\Omega_N = Diag(\lambda_0^{-1},\dots,\lambda_N^{-1}), \tag{7.34}$$

which stands for the $(N+1)\times(N+1)$ *diagonal matrix whose diagonal entries are the* λ_k^{-1} *for* $k = 0,\dots,N$. *Then*

$$\|\partial_\xi^2 f_N\|^2_{\mathbb{L}_2\mathcal{I}} = \omega^T\Omega_N^4\omega.$$

Proof. Notice indeed that $\partial_\xi^2 f_N = \omega^T\Omega_N\partial_\xi^2\psi_{0,N}$. However, as demonstrated above in Theorem 7.6.1, $\partial_\xi^2\psi_k = \lambda_k^{-1}\varphi_k$. Hence, using the property that the φ_ks constitute an orthonormal basis of $\mathbb{L}_2\mathcal{I}$, we obtain

$$\|\partial_\xi^2 f_N\|^2_{\mathbb{L}_2\mathcal{I}} = \sum_{k=0}^N \lambda_k^{-4}\omega_k^2 = \omega^T\Omega_N^4\omega.$$

□

7.7.5 Properties of eq. (P1) and choice of the spectral-cutoff N**.** A first question that arises is whether this quadratic program eventually admits a solution? In that perspective, it is straightforward to notice that eq. (P1) admits a solution if and only if $\mathrm{Span}\{\varphi_i, 0\leq i\leq N\}$ admits an element which satisfies the constraints. Let us denote by $\mathcal{D}$ the subset of $\mathbb{L}_2\mathcal{I}$ which satisfies the constraints described in eq. (P1') and assume that $\mathcal{D}\neq\emptyset$. Obviously, eq. (P1) admits a solution as soon as N is large enough, since (φ_i) is complete in $\mathbb{L}^2\mathcal{I}$ (see Proposition 7.5.1). On the other hand, it admits no solution when $\mathcal{D} = \emptyset$, that is when the constraints are incompatible. This latter situation might result from the presence of spurious data, since the presence of an arbitrage in the bid-ask quotes corresponds to a real arbitrage in the market, which would certainly be arbitraged away by practitioners.
A second natural question that arises, is how to choose the spectral cutoff N? As detailed in eq. (P1), we aim at recovering the smoothest density q_N built upon $\psi_0,\dots\psi_N$ compatible with price quotes. As described in Theorem 7.6.1, ψ_k is constituted of a periodic component $h_{k,2}$ oscillating at frequency ρ_k/B around an exponential trend $h_{k,1}$, where ρ_k grows roughly speaking like k. It is therefore natural to think that the smaller N, the smoother the singular basis

functions and thus the smoother the density q_N built upon them (although this needs not be the case, rigorously speaking). This intuitive observation, is justified through simulations (see Figure 7.3, bottom graph). In practice, we therefore suggest to choose N to be the smallest N such that eq. (P1) admits a solution. This is what we actually do in the forthcoming simulation study.
Finally, let us point out that we could have chosen to impose a positivity constraint on q_N at each point of the underlying dense grid $\xi_1, \ldots, \xi_n$, as an alternative to the in-sample convexity constraints on the (m_i)s described in eq. (P1). However, we have noticed via numerical simulations that results obtained in that way are less satisfying than with the convexity constraints on the m_is. We therefore opted for the convexity constraints.

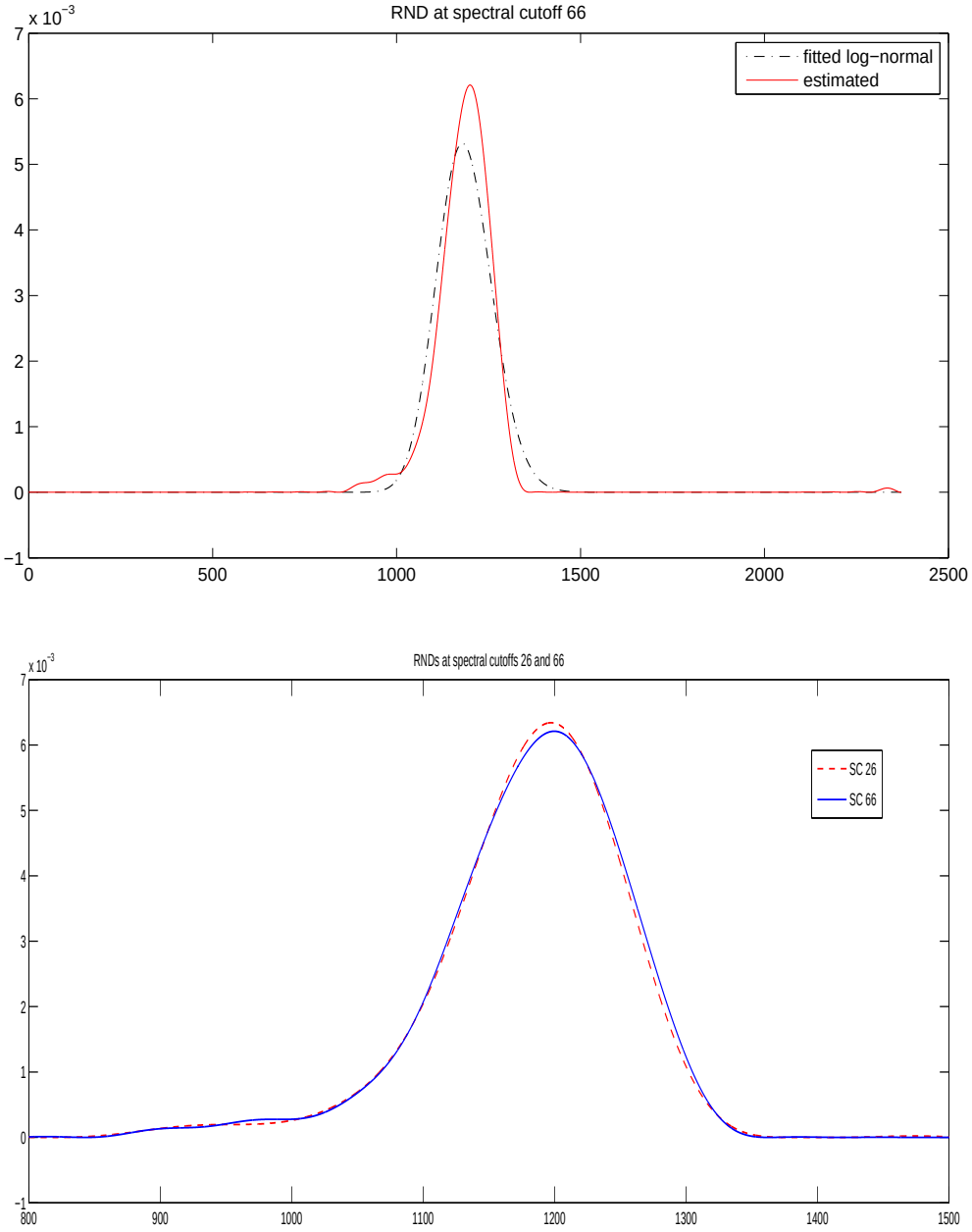

Figure 7.3: Here we plot the RND $q^{\star}_{66}$ (solid line) estimated from the real price quotes reported in Table 7.1. We choose $B = 2 * F_0 = 2 * S_0 * e^{(r-\delta)\tau} = 2372$ for that plot. In addition, we plot the best log-normal fit (in a least-square sense) to the average price quotes (dashed line). It is obtained for $\sigma_{opt} = 0.143$. At the top, we display the full left tail of the RND $q^{\star}_{66}$ and its full right tail up to B. At the bottom, we superimpose $q^{\star}_{66}$ (solid line) with $q^{\star}_{26}$ (dashed line) obtained in Figure 7.4 for an other choice of B. Notice the strong agreement between both densities, which highlights the stability of the SRM with respect to the choice of B. Interestingly, $q^{\star}_{66}$ is slightly more bumpy than $q^{\star}_{26}$ at the level of its left fat-tail. This reinforces our argument that smoothness goes hand in hand with low spectral cutoff.

7.8 Simulation study. We run a simulation study both on real and simulated data. The purpose of the estimation on simulated data is mostly to show that the SRM returns a valid RND estimator in extreme cases, when as little as 5 market quotes are available.
Recall from Lemma 7.6.3 that, from $k = 1$ onward, we can write $\beta_k \approx 2e^{-\frac{\pi}{2}-k\pi}$ in eq. (7.6) above. This approximation is not valid for $k = 0$. In that case, however, we can solve eq. (7.22) numerically to obtain $\rho_0 = 1.875104069$. This is the value of ρ_0 we use in the following simulation study.

Table 7.1: S&P 500 put option prices, Jan. 5, 2005. S&P 500 Index closing level $= 1183.74$*; Option expiration* $= 03/18/2005$ *(72 days);* $r = 2.69\%$*;* $\delta = 1.70\%$*.*

Strike price	500	550	600	700	750	800	825	850	900	925
Best bid	0.00	0.00	0.00	0.00	0.00	0.10	0.00	0.00	0.00	0.20
Best offer	0.05	0.05	0.05	0.10	0.15	0.20	0.25	0.50	0.50	0.70
Strike price	950	975	995	1005	1025	1050	1075	1100	1125	1150
Best bid	0.50	0.85	1.30	1.50	2.05	3.00	4.50	6.80	10.10	15.60
Best offer	1.00	1.35	1.80	2.00	2.75	3.50	5.30	7.80	11.50	17.20
Strike price	1170	1175	1180	1190	1200	1205	1210	1215	1220	1225
Best bid	21.70	23.50	25.60	30.30	35.60	38.40	41.40	44.60	47.70	51.40
Best offer	23.70	25.50	27.60	32.30	37.60	40.40	43.40	46.60	49.70	53.40
Strike price	1250	1275	1300	1325	1350					
Best bid	70.70	92.80	116.40	140.80	165.50					
Best offer	72.70	94.80	118.40	142.80	167.50					

7.8.1 Real data. We use the bid ask quotes reported in [51, Table 1] for put options on the S&P 500 Index on January 5, 2005. For completeness, we reproduce the table here in Table 7.1. We choose $B = 2 * S_0 e^{(r-\delta)\tau}$, which corresponds to two times the Forward price on the underlying stock. This choice is arbitrary and produces an interval $\mathcal{I}$, which is symmetric around the forward price. We observe from our simulation that the result is largely independent of the choice of B. However, the higher B, the higher we will need to go into the spectrum of γ^*, since the smoothest RND that fits the data will be more and more concentrated around the center of the interval $\mathcal{I}$. As regards the constraints, we choose the grid $\xi_1, \dots, \xi_n$ to be such that $\xi_k = k - 1, k = 1, \dots, \lfloor B \rfloor + 1$ and if $\lfloor B \rfloor < B$, we add $\xi_{\lfloor B \rfloor + 2} = B$. Of course, this grid contains the initial 35 quoted strike prices since they are integer valued. With the above choice of B, the quadratic program given in eq. (P1) finds a feasible solution from spectral cutoff 66 onward. We report $q^{\bigstar}_{66}$ below in Figure 7.3. For the sake of comparison, we plot on the same figure the log-normal distribution obtained by least-square fit to the put prices obtained as average of the bid-ask quotes. The only parameter of the log-normal distribution that must be fitted is σ (see Proposition 7.8.1), and we find $\sigma_{opt} = 0.143$. Interestingly, $q^{\bigstar}_{66}$ displays a small bump at the beginning of its left-tail, which does not appear in [51, Fig. 8] and could hardly be accounted for by parametric methods. Notice the small blip next to B in Figure 7.3. This boundary effect is due to the fact that all the ψ_ks and their first derivative are worth 0 in B. In order to show that the choice of B has very little impact, we compute the RND estimator for $B = 1.4 * S_0 e^{(r-\delta)\tau}$. Results are reported in Figure 7.4. As was expected, first feasible points appear at much lower spectral cutoffs, namely from spectral cutoff 26 onward. Therefore, we plot $q^{\bigstar}_{26}$. As can be seen from Figure 7.5, the put prices $P^{\bigstar}_{26}$ arising from eq. (P1) lie inside the bid ask quotes, while the

ones produced by the fitted log-normal density lie outside.

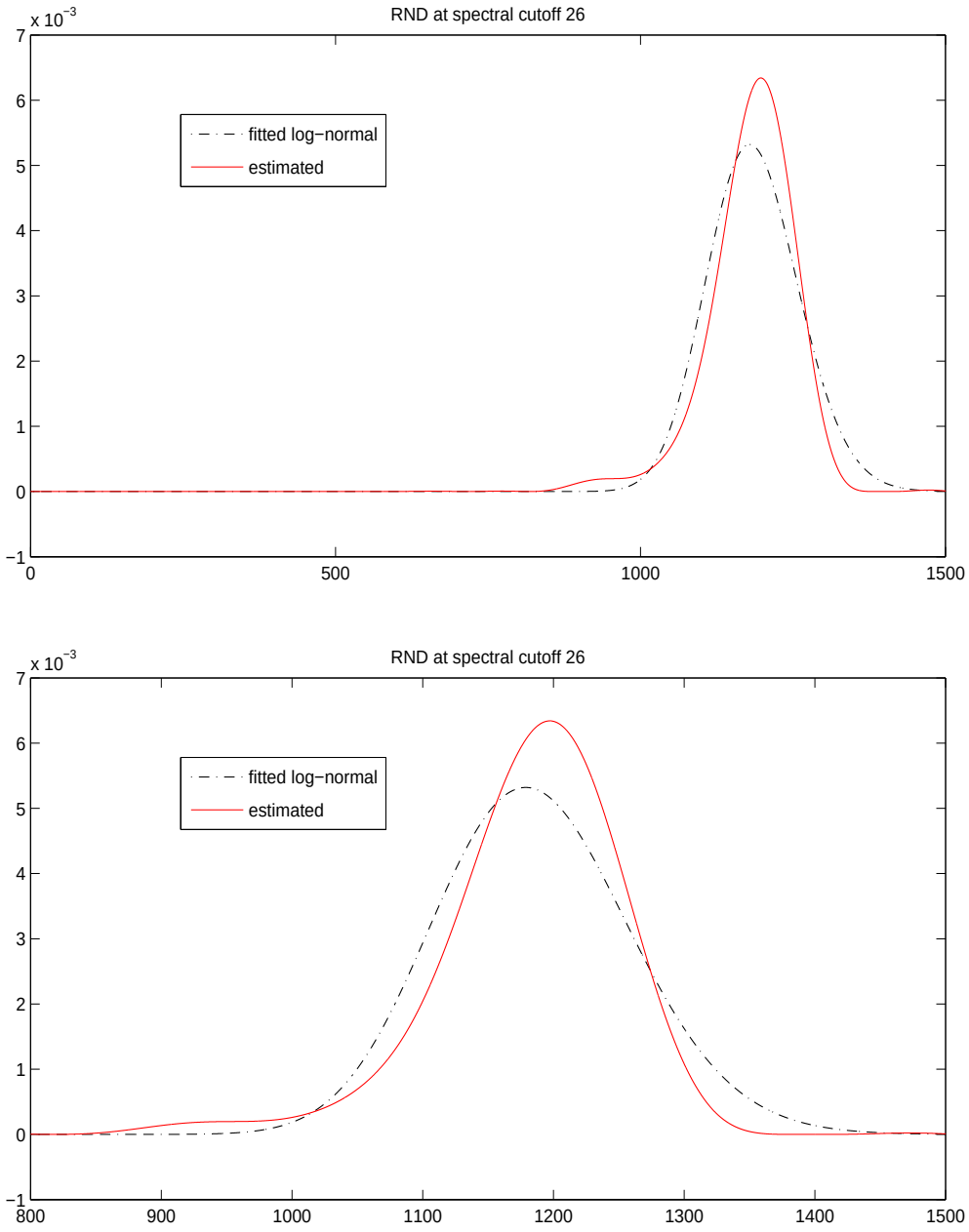

Figure 7.4: Here we plot the RND $q_{26}^{\star}$ (solid line) estimated from the real price quotes reported in Table 7.1. We choose $B = 1.4 * F_0 = 1.4 * S_0 * e^{(r-\delta)\tau} = 1660$ for that plot. In addition, we plot the best log-normal fit (in a least-square sense) to the average price quotes (dashed line). It is obtained for $\sigma_{opt} = 0.143$. At the top, we display the full left tail of the RND $q_{26}^{\star}$. At the bottom, we zoom in on the fat left tail of the estimated RND distribution.

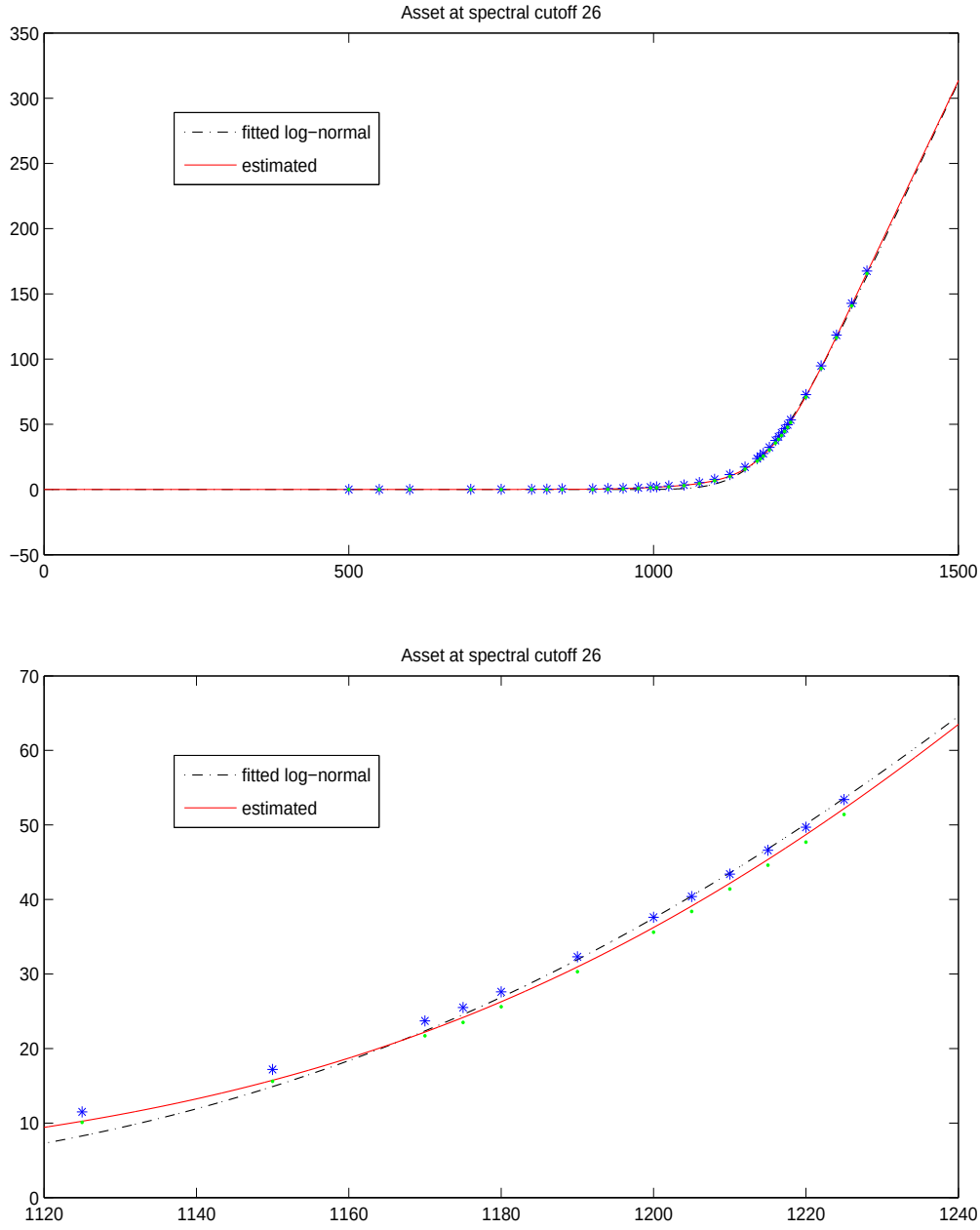

Figure 7.5: Here we plot the fitted put prices obtained from the setting described above in Figure 7.4. The solid line corresponds to the fitted prices $P_{26}^{\star}$, while the dashed line corresponds to the fitted prices obtained from a log-normal distribution. The stars and dots correspond to market ask and bid quotes, respectively. At the top, we give a large view of the fits. At the bottom we zoom in to show that $P_{26}^{\star}$ lies inside the market quotes, while the fitted log-normal prices lie outside.

7.8.2 Simulated data. As regards the simulated data, we work in the Black-Scholes setting. In that context the price of a put option admits a closed form solution and the RND is log-normal (see Proposition 7.8.1). We model the bid-ask spread as a random noise around the true price given by the Black-Scholes formula. More precisely, for a given set of quoted strikes $\xi_1 < \ldots < \xi_s$ and corresponding put prices $P(\xi_1), \ldots, P(\xi_s)$, we write $y_i^{Ask} = P(\xi_i) + z_i/2$ and $y_i^{Bid} = P(\xi_i) - z_i/2$, where $z_i = \max(1, \min(3, \varpi|\xi_i|))$, the ξ_i's are iid standard normal random variables and $\varpi = 0.1 \max_{1 \leq i \leq s} P(\xi_i)$. The bounds 1 and 3 are chosen by analogy with the real data quotes in Table 7.1. Of course, the bid-ask quotes we obtain in that way are not arbitrage free. However, they contain the true put price $P(\xi)$, which, given the nature of the quadratic program described in eq. (P1) above, is all that matters to approximate the true RND. For the sake of simplicity, we choose $r = 0$, $\delta = 0$, $\tau = 1$, $S_0 = 100$, and $\sigma = 0.3$ and $B = 2 * F_0 = 2 * S_0$. In addition we set a first strike price at $\lfloor F_0 \rfloor$ and spread the others on its left and right sides at unit length distance away from each other until we obtain s strikes. More precisely, the second strike would be $\lfloor F_0 \rfloor - 1$, the third $\lfloor F_0 \rfloor + 1$, the fourth $\lfloor F_0 \rfloor - 2$ and so on and so forth. We plot the results for the first two spectral cutoffs at which a feasible point is found below in Figure 7.6 in the case where there are as little as $s = 5$ bid ask quotes and in Figure 7.7 in the case where there are as many as $s = 50$ of them. In any case, we can see that we obtain a smooth density that resembles the log-normal density generating the initial quoted prices and that the estimate is stable from one spectral cutoff to another. Of course, the more strikes we have, the better the fit. Besides, we observe as expected from an other simulation not reported here that, the smaller the bid-ask spread, the better the fit. Notice once again that the fitted right-tail reaches zero in B, while the true one is strictly positive at that point. As before, this is due to the fact that $\psi_k(B) = 0$.

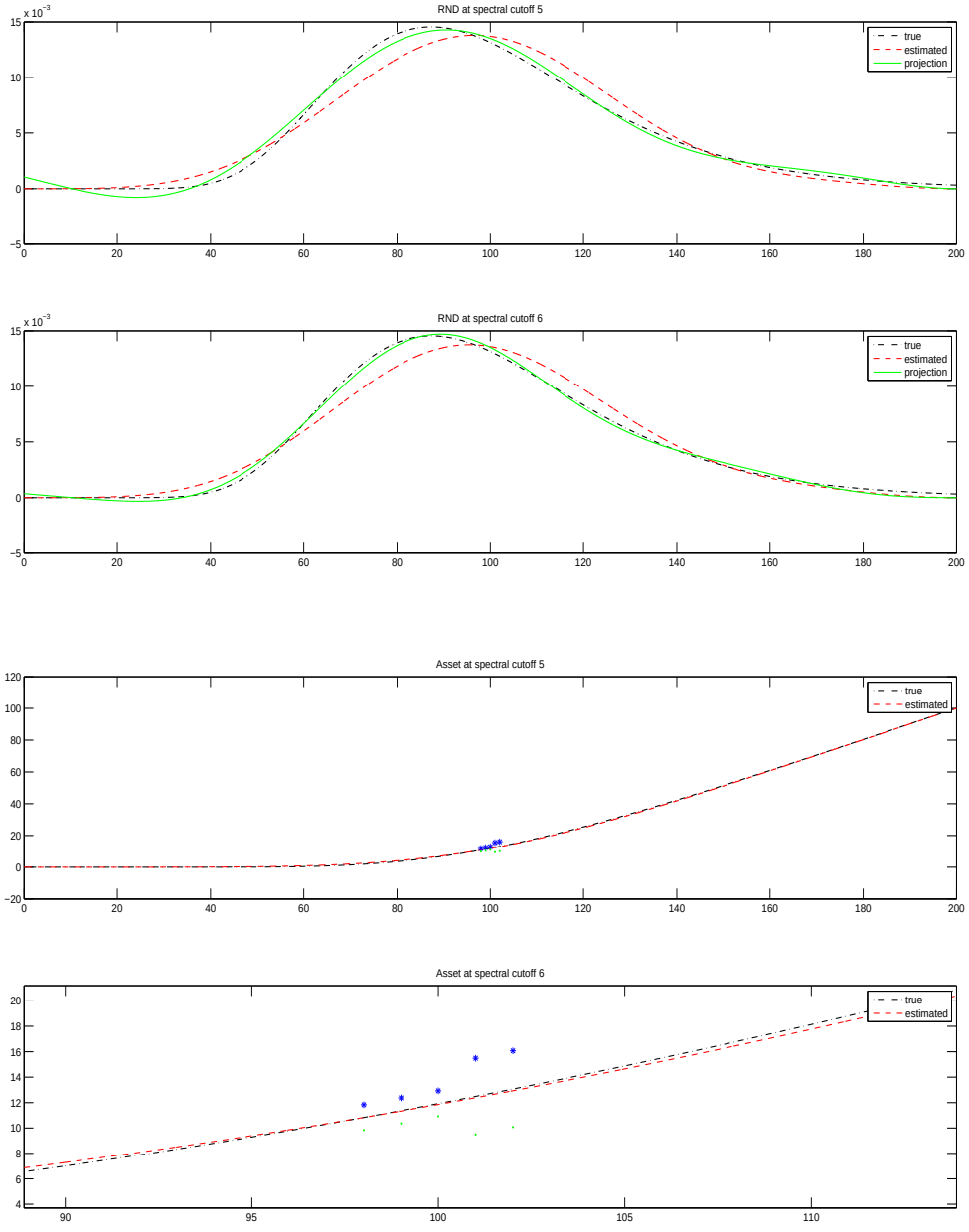

Figure 7.6: Here we are in the case of 5 *simulated bid ask quotes and with* $B = 2 * F_0 = 200$. *The first two plots display* $q_5^\star$ *and* $q_6^\star$ *(dashed line), the true log-normal RND used to generate the prices (dashed-dotted line) and the orthogonal projection of the true log-normal RND on* $\{\psi_0, \dots, \psi_N\}$ *for* $N = 5$ *and* $N = 6$ *(solid line), respectively. The last two plots display the fitted put prices, that is* $P_5^\star$ *and* $P_6^\star$ *(dashed line) together with the true prices (dashed-dotted line).*

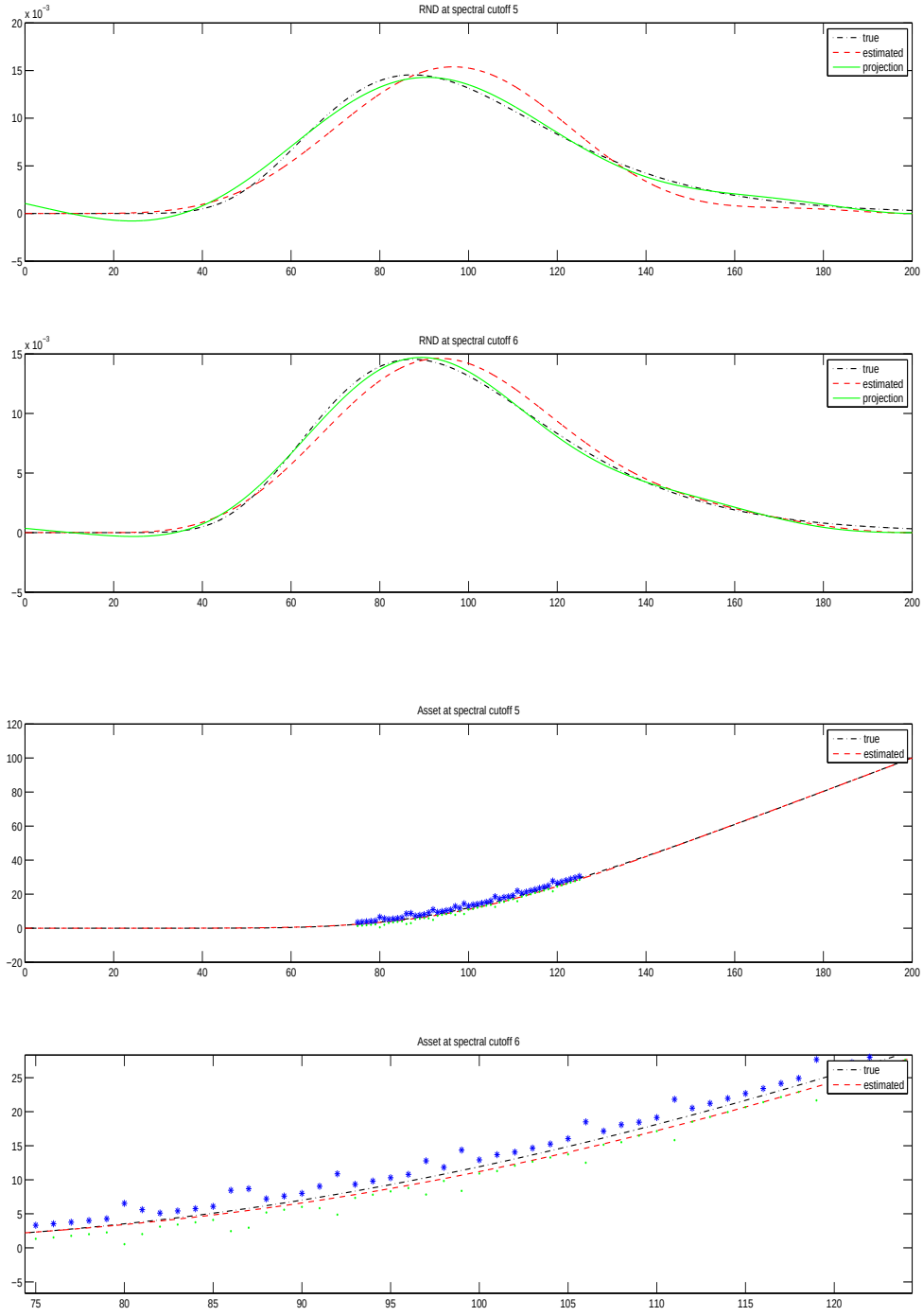

Figure 7.7: Here, we repeat the same plots as in Figure 7.7 in the case of 50 *simulated bid-ask quotes.*

Appendix.

Refresher on the Black-Scholes model. This is a well-known result of mathematical finance.

Proposition 7.8.1. *Let us denote by S_0 the price today of a stock paying dividends continuously over time at a constant rate δ and by r the continuously compounded risk-free rate. The arbitrage price today of a put option on that stock maturing at time τ is given by the following closed form formula,*

$$P(\xi) = \xi e^{-r\tau}\mathcal{N}(-d_2) - S_0 e^{-\delta\tau}\mathcal{N}(-d_1),$$

with

$$d_1 = \frac{\ln(S_0/\xi) + [(r-\delta) + \frac{1}{2}\sigma^2]\tau}{\sigma\sqrt{\tau}}, \qquad d_2 = d_1 - \sigma\sqrt{\tau},$$

where σ stands for the volatility of the stock and $\mathcal{N}$ for the standard normal cumulative distribution. In addition, the RND is log-normal and writes as

$$q(x) = \frac{1}{\sqrt{2\pi}\sigma\tau x}\exp\left(-\frac{[\ln(x/S_0) - (r-\delta)\tau + \frac{1}{2}\sigma^2\tau]^2}{2\sigma^2\tau}\right).$$

Proof. These results can be found in see [48, p.117], for example. □

Additional results relative to γ and γ^*. We now present three results relative to γ and γ^*, which are either used in the core of the paper or of interest in their own right.

Proposition 7.8.2. *The operators γ and γ^* admit no eigenvectors.*

Proof. Suppose f is an eigenvector of γ associated to eigenvalue λ, then denote by

$$\breve{f}(t) = f(B - \xi), \tag{7.35}$$

and notice that for all $\xi \in \mathcal{I}$, a direct application of Lemma 7.8.2 allows to write

$$\lambda\breve{f}(B-\xi) = \lambda f(\xi) = \gamma f(\xi) = \gamma^*\breve{f}(B-\xi).$$

Thus $\breve{f}$ must be an eigenvector of γ^*. However, it is well known that γ^* admits no eigenvalue since, for any $\lambda \neq 0$,

$$\lambda f(\xi) = \gamma^* f(\xi) = \int_0^\xi \theta^*(\xi, x) f(x)dx, \qquad \xi \in \mathcal{I},$$

defines a *homogeneous Volterra equation* in f, whose unique trivial solution is $f = 0$ (see [124, p.239, Th. 5.5.2]). □

Finally, let us point out the two following useful lemmas.

Lemma 7.8.1. *Let us denote by ∂_ξ^k the k^{th} order partial differential operator with respect to ξ. Then, for any $f \in \mathbb{L}_2\mathcal{I}$, we have the following results.*

$$f = \partial_\xi^2 \gamma f, \qquad f = \partial_\xi^2 \gamma^* f,$$
$$f = \partial_\xi^4 \gamma^* \gamma f, \qquad f = \partial_\xi^4 \gamma \gamma^* f.$$

Proof. Notice indeed that

$$\partial_\xi \gamma f(\xi) = \partial_\xi \int_\xi^B (x-\xi) f(x) dx = -\int_\xi^B f(x) dx,$$
$$\partial_\xi \gamma^* f(\xi) = \partial_\xi \int_0^\xi (\xi - x) f(x) dx = \int_0^\xi f(x) dx.$$

Therefore, we obtain immediately

$$f = \partial_\xi^2 \gamma f = \partial_\xi^2 \gamma^* f.$$

The remaining of the proof follows directly from these first results. Notice indeed that,

$$\partial_\xi^4 \gamma^* \gamma f = \partial_\xi^2 [\partial_\xi^2 \gamma^*](\gamma f) = \partial_\xi^2 \gamma f = f.$$

which concludes the proof. □

Lemma 7.8.2. *For any $f \in \mathbb{L}_2\mathcal{I}$ and $\xi \in \mathcal{I}$, we have $\gamma f(\xi) = \gamma^* \check{f}(B-\xi)$ (see eq. (7.35) for notations).*

Proof. Perform the change of variable $u = B - x$ to obtain

$$\begin{aligned}\gamma f(\xi) &= \int_\xi^B (x-\xi) f(x) dx \\ &= \int_0^{B-\xi} ([B-\xi]-u) \check{f}(u) du = \gamma^* \check{f}(B-\xi).\end{aligned}$$

□

Relation between the (φ_k)s and the (ψ_k)s. We believe that $m_0(q)$ and $m_1(q)$ could be readily estimated from the data, so that eq. (7.25) could be used to construct a second estimator of the RND based on the restricted call operator. This second estimator could eventually be combined with the one obtained from the SRM above. To that end, and for the sake of completeness, we compute the scalar products between elements of the two singular bases. Results are reported in the following proposition.

Proposition 7.8.3. *Let us write*

$$\mathfrak{p}_{k,m}(x,y) = (-x^3 + x^2 y)(-1)^{m+k} - xy^2 + y^3,$$
$$\mathfrak{q}_{k,m}(x,y) = (x^3 + x^2 y)(-1)^k + (y^3 + y^2 x)(-1)^m.$$

Then, we have the following relationships,

$$\langle \varphi_k, \psi_m \rangle = 4\frac{\mathfrak{p}_{k,m}(\rho_k,\rho_m)e^{-\rho_k-\rho_m} - \mathfrak{q}_{k,m}(\rho_k,\rho_m)e^{-\rho_k} + \mathfrak{q}_{k,m}(\rho_m,\rho_k)e^{-\rho_m} + \mathfrak{p}_{k,m}(\rho_m,\rho_k)}{(\rho_k^4-\rho_m^4)(1+(-1)^m e^{-\rho_m})(1+(-1)^k e^{-\rho_k})}, k \neq m,$$
$$\langle \varphi_k, \psi_k \rangle = \frac{-e^{-2\rho_k}(\rho_k+2) + 2\rho_k(-1)^k e^{-\rho_k} - \rho_k + 2}{(e^{-\rho_k}+(-1)^k)^2\rho_k}.$$

On the way, we obtain,

$$\langle h_{k,1}, h_{m,1} \rangle = ((-1)^k + (-1)^m)\frac{(\rho_k+\rho_m)(e^{-\rho_m}-e^{-\rho_k}) + (-1)^k(\rho_k-\rho_m)(1-e^{-(\rho_k+\rho_m)})}{(\rho_k^2-\rho_m^2)(1+(-1)^k e^{-\rho_k})(1+(-1)^m e^{-\rho_m})}, k \neq m,$$
$$\langle h_{k,1}, h_{k,1} \rangle = \frac{1-e^{-2\rho_k}+2(-1)^k\rho_k e^{-\rho_k}}{\rho_k((-1)^k+e^{-\rho_k})^2},$$
$$\langle h_{k,1}, h_{m,2} \rangle = ((-1)^k - (-1)^m)\frac{(\rho_k+\rho_m)(e^{-\rho_m}+e^{-\rho_k}) - (-1)^k(\rho_k-\rho_m)(1+e^{-(\rho_k+\rho_m)})}{(\rho_k^2+\rho_m^2)(1+(-1)^m e^{-\rho_m})(1+(-1)^k e^{-\rho_k})}, k \neq m,$$
$$\langle h_{k,1}, h_{k,2} \rangle = 0,$$
$$\langle h_{k,2}, h_{m,2} \rangle = \delta_{k,m} - \langle h_{k,1}, h_{m,1} \rangle.$$

Proof. Recall that, for all k, m, we have defined

$$h_{k,1} = a_{k,1}f_{k,1} + a_{k,2}f_{k,2}, \qquad h_{k,2} = a_{k,3}f_{k,3} + a_{k,4}f_{k,4},$$
$$\varphi_k = h_{k,1} + h_{k,2}, \qquad \psi_k = h_{k,1} - h_{k,2}.$$

Besides, we have that

$$\langle \varphi_k, \varphi_m \rangle = \delta_{k,m} = \langle h_{k,1}, h_{m,1} \rangle + \langle h_{k,2}, h_{m,2} \rangle + \langle h_{k,1}, h_{m,2} \rangle + \langle h_{k,2}, h_{m,1} \rangle,$$
$$\langle \psi_k, \psi_m \rangle = \delta_{k,m} = \langle h_{k,1}, h_{m,1} \rangle + \langle h_{k,2}, h_{m,2} \rangle - \langle h_{k,1}, h_{m,2} \rangle - \langle h_{k,2}, h_{m,1} \rangle.$$

Therefore, we obtain the following relationships,

$$\delta_{k,m} = \langle h_{k,1}, h_{m,1} \rangle + \langle h_{k,2}, h_{m,2} \rangle,$$
$$0 = \langle h_{k,1}, h_{m,2} \rangle + \langle h_{k,2}, h_{m,1} \rangle.$$

Which leads to

$$\begin{aligned}\langle \varphi_k, \psi_m \rangle &= \langle h_{k,1}, h_{m,1} \rangle - \langle h_{k,2}, h_{m,2} \rangle - \langle h_{k,1}, h_{m,2} \rangle + \langle h_{k,2}, h_{m,1} \rangle, \\ &= 2(\langle h_{k,1}, h_{m,1} \rangle - \langle h_{k,1}, h_{m,2} \rangle) - \delta_{k,m}.\end{aligned}$$

Now, it remains to compute $\langle h_{k,1}, h_{m,1} \rangle$ and $\langle h_{k,1}, h_{m,2} \rangle$. The results follow from lengthy and tedious but straightforward computations and are therefore not reported here. □

From the RND q ***of*** S_τ ***to the density of*** $\ln S_\tau$**.** Some authors have chosen to focus on the estimation of the density of $\log S_\tau$ rather than on the density of S_τ itself. Both densities relate by a simple transformation, as described in the following proposition. In our case, this transformation can be readily applied since the SRM returns an analytic expression for the estimated RND.

Proposition 7.8.4. *If X admits $f(x)$ for density on $\mathbb{R}$, then $Y = \exp(X)$ admits $\frac{1}{y} f(\ln y)$ for density on $\mathbb{R}^+$. Conversely, if Y admits $f(y)$ for density on $\mathbb{R}^+$, then $X = \ln(Y)$ admits $e^x f(e^x)$ for density on $\mathbb{R}$.*

Acknowledgements. *The author is deeply grateful to Peter Tankov for his careful reading of this manuscript and for his constructive and insightful comments, which greatly contributed to improve its clarity and content. The author is of course solely responsible for any eventual remaining error.*

Bibliography

[1] L. Devroye, L. Györfi, G. Lugosi, A probabilistic theory of pattern recognition, Springer-Verlag, 1996. 15, 17, 27, 74, 78

[2] C. J. Stone, Optimal rates of convergence for nonparametric estimators, Ann. Stat. 8 (6) (1980) 1348–1360. 16, 18, 45, 75

[3] C. J. Stone, Optimal global rates of convergence for nonparametric regression, Ann. Stat. 10 (4) (1982) 1040–1053. 16, 18, 45, 46, 75

[4] M. Kohler, Nonlinear orthogonal series estimates for random design regression, J. Stat. Plan. Infer. 115 (2003) 491–520. 17, 78

[5] M. Kohler, Multivariate orthogonal series estimates for random design regression, J. Stat. Plan. Infer. 138 (2008) 3217–3237. 17, 78

[6] V. Delouille, J. Franke, R. von Sachs, Nonparametric stochastic regression with design-adapted wavelets, The Indian Journal of Statistics 63 (2001) 328–366. 17, 78

[7] W. Sweldens, The lifting scheme: a custom-design construction of biorthogonal wavelets, Appl. Comput. Harmon. Anal. 3 (1996) 186–200. 17, 78

[8] A. Antoniadis, G. Grégoire, P. Vial, Random design wavelet curve smoothing, Statistics & Probability Letters 35 (1997) 225–232. 17, 78

[9] P. Hall, B. A. Turlach, Interpolation methods for nonlinear wavelet regression with irregularly spaced design, Ann. Stat. 25 (5) (1997) 1912–1925. 17, 78

[10] A. Kovac, B. W. Silverman, Extending the scope of wavelet regression methods by coefficient-dependent thresholding, J. Amer. Statistical Assoc. 95 (2000) 172–183. 17, 78

[11] M. H. Neumann, V. G. Spokoiny, On the efficiency of wavelet estimators under arbitrary error distributions, Math. Methods Statist. 4 (2) (1995) 137–166. 17, 78

[12] S. Sardy, D. B. Percival, A. G. Bruce, H.-Y. Gao, W. Stuetzle, Wavelet shrinkage for unequally spaced data, Satistics and Computing 9 (1999) 65–75. 17, 78

[13] A. Antoniadis, G. Grégoire, I. W. McKeague, Wavelet methods for curve estimation, J. Amer. Statistical Assoc. 89 (428) (1994) 1340–1353. 17

[14] A. Antoniadis, D. T. Pham, Wavelet regression for random or irregular design, Comput. Stat. Data An. 28 (1998) 353–369. 17, 78

[15] M. Pensky, B. Vidakovic, On non-equally spaced wavelet regression, Ann. Inst. Statist. Math. 53 (4) (2001) 681–690. 17, 78

[16] W. Greblicki, M. Pawlak, A classification procedure using the multiple fourier series, Inf. Sci. 26 (1982) 115–126. 17, 78

[17] W. Greblicki, M. Pawlak, Fourier and hermite series estimates of regression functions, Ann. Inst. Statist. Math. 37 (1985) 443–454. 17, 78

[18] E. A. Nadaraya, On estimating regression, Theory Probab. Appl. 9 (1964) 141–142. 17, 78

[19] G. S. Watson, Smooth regression analysis, The Indian Journal of Statistics 26 (4) (1964) 359–372. 17, 78

[20] T. T. Cai, L. D. Brown, Wavelet shrinkage for nonequispaced samples, Ann. Stat. 26 (5) (1998) 1783–1799. 18, 78

[21] G. Kerkyacharian, D. Picard, Regression in random design and warped wavelets, Bernoulli 10 (6) (2004) 1053–1105. 18, 78, 122

[22] Y. Baraud, Model selection for regression on a random design, ESAIM Probab. Statist. 6 (2002) 127–146. 18, 78
[23] A. Antoniadis, J. Fan, Regularization of wavelet approximations, J. Amer. Statistical Assoc. 96 (455) (2001) 939–967. 18
[24] U. Amato, A. Antoniadis, M. Pensky, Wavelet kernel penalized estimation for non-equispaced design regression, Stat. Comput. 16 (1) (2006) 37–55. 18
[25] S. Gaïffas, Sharp estimation in sup norm with random design, Statistics & Probability Letters 77 (2007) 782–794. 18, 78
[26] S. Gaïffas, On pointwise adaptive curve estimation based on inhomogeneous data, ESAIM Probab. Statist. 11 (2007) 344–364. 18, 75
[27] J. Fan, I. Gijbels, Data-driven bandwidth selection in local polynomial fitting: variable bandwidth and spatial adaptation, J. Roy. Stat. Soc. B Met. 57 (1995) 371–394. 18
[28] A. Goldenshluger, A. Nemirovski, On spatially adaptive estimation of nonparametric regression, Math. Methods Statist. 6 (1997) 135–170. 18
[29] V. G. Spokoiny, Estimation of a function with discontinuities via local polynomial fit with an adaptive window choice, Ann. Stat. 26 (1998) 1356–1378. 18
[30] G. Malgouyres, P.-G. Lemarié-Rieusset, On the support of the scaling function in a multi-resolution analysis, Comptes rendus de l'Académie des sciences 313 (6) (1991) 377–380. 26, 109
[31] D. Picard, K. Tribouley, Adaptive confidence interval for pointwise curve estimation, Ann. Stat. 28 (2000) 298–335. 27, 79
[32] J. S. Marron, Optimal rates of convergence to the Bayes risk in nonparametric discrimination, Ann. Stat. 11 (4) (1983) 1142–1155. 28, 77
[33] E. Mammen, A. B. Tsybakov, Smooth discrimination analysis, Ann. Stat. 27 (6) (1999) 1808–1829. 28, 77
[34] J.-Y. Audibert, Classification under polynomial entropy and margin assumptions and randomized estimators, Preprint, Laboratoire de Probabilités et Modèles Aléatoires, Université Paris 6 and 7. 28, 77
[35] J.-Y. Audibert, A. B. Tsybakov, Fast learning rates for plug-in classifiers, Ann. Stat. 35 (2007) 608–633. 28, 29, 45, 46, 77, 85, 88, 89, 118, 120
[36] Y. Yang, Minimax nonparametric classification. I. rates of convergence, IEEE Trans. Inf. Theory 45 (7) (1999) 2271–2284. 29, 77
[37] M. Kohler, A. Krzyzak, On the rate of convergence of local averaging plug-in classification rules under a margin condition, IEEE Trans. Inf. Theory 53 (5) (2007) 1735–1742. 29
[38] G. Kyriazis, P. Petrushev, "compactly" supported frames for spaces of distributions on the ball, preprint (2011). 29, 36
[39] F. Narcowich, P. Petrushev, J. Ward, Decomposition of Besov and Triebel-Lizorkin spaces on the sphere, J. Funct. Anal. 238 (2006) 530–564. 30, 31, 33, 122, 124, 125, 126, 127
[40] F. Narcowich, P. Petrushev, J. Ward, Localized tight frames on spheres, SIAM J. Math. Anal. 38(2) (2007) 574–594. 30, 31, 32, 122, 125
[41] W. Freeden, T. Gervens, M. Schreiner, Constructive Approximation on the Sphere (With Applications to Geomathematics), Oxford Sciences Publication. Clarendon Press, Oxford., 1998. 30, 122
[42] W. Freeden, V. Michel, Multiscale Potential Theory, with applications to Geoscience, Brikhäuser, Boston, 2004. 30, 31, 121, 122
[43] E. M. Stein, G. Weiss, Fourier Analysis on Euclidean Spaces, Princeton University Press, Princeton, N.J., 1975. 31, 124
[44] G. Faÿ, F. Guilloux, J.-F. Cardoso, J. Delabrouille, M. Le Jeune, CMB power spectrum estimation using wavelets, Phys. Rev. D 78(8). 33, 122
[45] F. Guilloux, G. Faÿ, J.-F. Cardoso, Practical wavelet design on the sphere, Appl. Comput. Harmon. Anal. 26(2) (2009) 143–160. 33, 122
[46] D. Marinucci, D. Pietrobon, A. Balbi, P. Baldi, P. Cabella, G. Kerkyacharian, P. Natoli, D. Picard, N. Vittorio, Spherical needlets for CMB data analysis, Mon. Not. R. Astron. Soc. 383(2) (2008) 539–545. 33, 122
[47] P. Baldi, G. Kerkyacharian, D. Marinucci, D. Picard, Asymptotics for spherical needlets, Ann. Stat. 37(3) (2009) 1150–1171. 33, 50, 53, 112
[48] M. Musiela, M. Rutkowski, Martingale methods in financial modeling, 2^{nd} ed., Springer-Verlag, 2008. 37, 152, 169, 181
[49] J. C. Cox, S. A. Ross, The valuation of options for alternative stochastic processes, Journal of Financial Economics 3 (1976) 145–146. 37, 152

[50] B. Bahra, Implied risk-neutral probability density functions from option prices: theory and application, Bank of England, working paper no. 1368-5562. 37, 152
[51] S. Figlewski, Estimating the implied risk neutral density for the U.S. market portfolio, in: T. Bollerslev, J. R. Russel, M. Watson (Eds.), Volatility and time series econometrics: essays in honor of Robert F. Engle, Oxford University Press, 2008. 37, 39, 152, 154, 157, 175
[52] J. C. Jackwerth, Option-implied risk neutral distributions and risk aversion, Research Foundation of AIMR (CFA Institute), 2004. 37, 152
[53] R. Cont, Beyond implied volatility: extracting information from option prices, in: J. Kertész, I. Kondor (Eds.), Econophysics: an emergent science, Dordrecht, Kluwer, 1997. 37, 39, 152, 154, 156
[54] D. T. Breeden, R. H. Litzenberger, Prices of state-contingent claims implicit in option prices, J. Bus. 51 (4) (1978) 621–651. 38, 153
[55] L. Hentschel, Errors in implied volatility estimation, J. Finan. Quant. Anal. 38 (4) (2003) 779–810. 38, 153
[56] F. Black, M. Scholes, The pricing of options and corporate liabilities, J. Polit. Econ. 81 (3) (1973) 637–654. 38, 153
[57] R. C. Merton, Theory of rational option pricing, Bell J. Econ. Manag. Sci. 4 (4) (1973) 141–183. 38, 153
[58] R. Jarrow, A. Rudd, Approximate option valuation for arbitrary stochastic processes, J. Finan. Econ. 10 (1982) 347–369. 39, 153
[59] M. Potters, R. Cont, J.-P. Bouchaud, Financial markets as adaptive systems, Europhys. Lett. 41 (3) (1998) 239–244. 39, 153
[60] P. A. Abken, D. B. Madan, S. Ramamurtie, Estimation of risk-neutral densities by Hermite polynomial approximation: with an application to eurodollar futures options, Federal Reserve Bank of Atlanta, working paper no. 96-5. 39, 153
[61] Y. Aït-Sahalia, J. Duarte, Nonparametric option pricing under shape restrictions, J. Econometrics 116 (2003) 9–47. 39, 153, 169
[62] P. W. Buchen, M. Kelly, The maximum entropy distribution of an asset inferred from option prices, J. Finan. Quant. Anal. 31 (1) (1996) 143–159. 39, 154
[63] M. Stutzer, A simple approach to derivative security valuation, J. Finance 51 (5) (1996) 1633–1652. 39, 154
[64] J. C. Jackwerth, M. Rubinstein, Recovering probability distributions from option prices, J. Finance 51 (5) (1996) 1611–1631. 39, 154, 156
[65] O. Bondarenko, Estimation of risk-neutral densities using positive convolution approximation, J. Econometrics 116 (2003) 85–112. 39, 154
[66] R. Bu, K. Hadri, Estimating option implied risk-neutral densities using spline and hypergeometric functions, Econometrics J. 10 (2007) 216–244. 40, 154
[67] C. J. Stone, Consistent nonparametric regression, Ann. Stat. 5 (4) (1977) 595–620. 45
[68] W. S. Cleveland, Robust locally weighted regression and smoothing scatterplots, J. Amer. Statistical Assoc. 74 (368) (1979) 829–836. 45
[69] V. Y. Katkovnik, Linear and nonlinear methods of nonparametric regression analysis, Soviet Automatic Control 5 (1979) 35–46. 45
[70] A. Tsybakov, Robust reconstruction of functions by a local-approximation method, Problems of Information Transmission 22 (1986) 133–146. 45
[71] H.-G. Müller, Weighted local regression and kernel methods for nonparametric curve fitting, J. Amer. Statistical Assoc. 82 (397) (1987) 231–238. 45
[72] J. Fan, Design-adaptive nonparametric regression, Journal of the American Statistical Association 87 (420) (1992) 998–1004. 45
[73] A. B. Tsybakov, Introduction to nonparametric estimation, Springer Verlag, Berlin, 2009. 50
[74] I. Johnstone, Function estimation and Gaussian sequence models, book draft (March 2011). URL http://www-stat.stanford.edu/~imj/ 50
[75] D. L. Donoho, I. M. Johnstone, G. Kerkyacharian, D. Picard, Density estimation by wavelet thresholding, Ann. Stat. 24(2) (1996) 508–539. 50, 51, 53, 78
[76] S. Mallat, Multiresolution approximations and wavelet orthonormal bases of L^2, Trans. Amer. Math. Soc. 315 (1) (1989) 69–87. 51, 60, 78
[77] Y. Meyer, Wavelets and operators, Vol. 37 of Cambridge Studies in Advanced Mathematics, Cambridge University Press, 1992. 51, 60, 61, 78
[78] G. Kerkyacharian, D. Picard, Density estimation in Besov spaces, Statistics & Probability Letters 13 (1992) 15–24. 51, 53, 78
[79] D. L. Donoho, I. M. Johnstone, Ideal spatial adaptation by wavelet shrinkage, Biometrika 81 (3) (1994)

425–455. 51, 78, 90
[80] D. L. Donoho, De-Noising by Soft-Thresholding, IEEE Trans. Inf. Theory 41(3) (1995) 613–627. 51, 78
[81] D. L. Donoho, I. M. Johnstone, G. Kerkyacharian, D. Picard, Wavelet shrinkage: Asymptotia?, J. Roy. Stat. Soc. B 57(2) (1995) 301–369. 51, 78, 123
[82] G. Kerkyacharian, D. Picard, Thresholding algorithms, maxisets and well-concentrated basis, TEST 9 (2) (2000) 283–344. 52, 64
[83] B. Delyon, A. Juditsky, On minimax wavelet estimators, Appl. Comput. Harmon. Anal. 3 (1996) 215–228. 53, 78
[84] O. V. Lepski, E. Mammen, V. G. Spokoiny, Optimal spatial adaptation to inhomogeneous smoothness: an approach based on kernel estimates with variable bandwidth selectors, Ann. Stat. 25 (3) (1997) 392–947. 55, 79, 90, 96
[85] A. Cohen, Numerical analysis of wavelet methods, Vol. 32 of Studies in mathematics and its applications, North-Holland, 2003. 57, 58, 60, 61, 62, 78, 109, 113, 114, 115, 116
[86] R. DeVore, Nonlinear approximation, Acta Numerica (1998) 51–150. 57, 58, 62, 63, 64
[87] H. Triebel, Theory of function spaces II, Brikhäuser, Boston, 2010. 57, 60
[88] R. A. DeVore, G. G. Lorentz, Constructive approximation, Grundlehren Der Mathematischen Wissenschaften, Springer-Verlag, 1993. 59, 114, 115
[89] R. A. Adams, J. Fournier, Sobolev spaces, second edition, Elsevier Science, Oxford, 2003. 60, 141
[90] I. Daubechies, Ten lectures on wavelets, CBMS-NSF regional conference series in applied mathematics, Society for Industrial and Applied Mathematics, 1992. 60, 62, 65, 78, 116
[91] S. Mallat, A wavelet tour of signal processing: the sparse way, Academic Press, 2008. 60, 65, 70, 78
[92] P. Wojtaszczyk, A Mathematical Introduction to Wavelets, Cambridge University Press, Cambridge, 1997. 60, 62
[93] C. K. Chui, An introduction to wavelets, vol.1, Wavelet Analysis and Its Applications, Academic Press, 1992. 60
[94] W. Härdle, G. Kerkyacharian, D. Picard, A. B. Tsybakov, Wavelets, approximation and statistical applications, Springer Verlag, Berlin, 1997. 60, 78, 103
[95] A. Cohen, I. Daubechies, P. Vial, Wavelets on the interval and fast wavelets transform, Appl. Comput. Harmon. Anal. 1 (1993) 54–81. 60
[96] G. G. Lorentz, M. von Golitschek, J. Makovoz, Constructive approximation: advanced problems, Springer, Berlin, 1996. 63
[97] O. Christensen, Frames and bases, an introductory course, Brikhäuser, 2008. 65, 70
[98] T. Hastie, R. Tibshirani, J. Friedman, The Elements of Statistical Learning: Data Mining, Inference and Prediction, Springer-Verlag, Berlin, 2001. 74
[99] V. N. Vapnik, Statistical learning theory, Adaptive and Learning Systems for Signal Processing, Communications, and Control, John Wiley & Sons, 1998. 74
[100] S. Gaïffas, Convergence rates for pointwise curve estimation with a degenerate design, Math. Methods Statist. 1 (2005) 1–27. 75
[101] S. Zhang, M.-Y. Wong, Z. Zheng, Wavelet threshold estimation of a regression function with random design, J. Multivariate Anal. 80 (2002) 256–284. 78
[102] R. A. Horn, C. R. Johnson, Matrix analysis, Cambridge University Press, 1990. 80
[103] L. Györfi, M. Kohler, A. Krzyzak, H. Walk, A distribution-free theory of nonparametric regression, Springer Series in Statistics, Springer, 2001. 94
[104] L. Birgé, P. Massart, Gaussian model selection, J. Eur. Math. Soc. (JEMS) 3 (2001) 203–268. 111
[105] C. Chesneau, Wavelet block thresholding for samples with random design: a minimax approach under the L^p risk, Electronic Journal of Statistics 1 (2007) 331–346. 112
[106] J.-B. Monnier, Non-parametric regression on the hyper-sphere with uniform design, TEST 20 (2) (2010) 412–446. 112
[107] A. B. Tsybakov, Optimal aggregation of classifiers in statistical learning, Ann. Stat. 32 (1) (2004) 135–166. 113
[108] M. Holschneider, A. Chambodut, M. Mandea, From global to regional analysis of the magnetic field on the sphere using wavelet frames, Phys. Earth Planet. In. 135 (2003) 107–124. 122
[109] T. Maier, Wavelet-mie-representations for solenoidal vector fields with applications to ionospheric geomagnetic data, SIAM J. Appl. Math. 65 (2005) 1888–1912. 122
[110] I. Panet, O. Jamet, M. Diament, A. Chambodut, Modelling the Earth's gravity field using wavelet frames, Springer, 2005. 122

[111] M. Fengler, Vector spherical harmonic and vector wavelet based non-linear Garlekin schemes for solving the incompressible Navier-Stokes equation on the sphere, PhD thesis, University of Kaiserslautern, Mathematics Department, Geomathematics Group. 122
[112] W. Freeden, D. Michel, V. Michel, Local multiscale approximations of geostrophic oceanic flow: theoretical background and aspects of scientific computing, Mar. Geod. 28 (2005) 313–329. 122
[113] C. Mayer, Wavelet modelling of the spherical inverse source problem with application to geomagnetism, Inverse Probl. 20 (2004) 1713–1728. 122
[114] F. J. Narcowich, J. D. Ward, Nonstationary wavelets on the m-sphere for scattered data, Appl. Comput. Harmon. Anal. 3 (1996) 324–326. 122
[115] M. Schmidt, S. Han, J. Kusche, L. Sánchez, C. Shum, Regional high-resolution spatiotemporal gravity modeling from GRACE data using spherical wavelets, Geophys. Res. Lett. 33(8). 122
[116] M. Schmidt, M. Fengler, T. Mayer-Gürr, A. Eicker, J. Kusche, L. Sánchez, S.-C. Han, Regional gravity modeling in terms of spherical base functions, J. Geodesy 81 (2007) 17–38. 122
[117] T.-H. Li, Multiscale representation and analysis of spherical data by spherical wavelets, SIAM J. Sci. Comput. 21 (1999) 924–953. 122
[118] T.-H. Li, H.-S. Oh, Estimation of global temperature fields from scattered observations by a spherical-wavelet-based spatially adaptative method, J. Roy. Stat. Soc. B 66 (2004) 221–238. 122
[119] P. Baldi, G. Kerkyacharian, D. Marinucci, D. Picard, Adaptative density estimation for directional data using needlets, Ann. Stat. 37(6) (2009) 3362–3395. 123, 124, 126, 127, 130
[120] C. Müller, Spherical Harmonics, Springer-Verlag, Berlin, 1966. 124
[121] V. V. Petrov, Limit theorems of probability theory: sequences of independent random variables, Oxford University Press, 1995. 137, 146
[122] P. R. Halmos, What does the spectral theorem say?, Am. Math. Mon. 70 (1963) 241–247. 154
[123] H. W. Engl, M. Hanke, A. Neubauer, Regularization of inverse problems, Kluwer Academic Publishers, 1996. 156, 161
[124] L. Debnath, P. Mikusiński, Introduction to Hilbert spaces with applications, Academic Press, 1990. 159, 161, 181
[125] M. H. A. Davis, D. G. Hobsony, The range of traded option prices, Math. Finance 17 (1) (2007) 1–14. 169

Résumé: On s'intéresse aux problèmes de régression, classification et à un problème inverse en finance. Nous abordons dans un premier temps le problème de régression en design aléatoire à valeurs dans un espace euclidien et dont la loi admet une densité inconnue. Nous montrons qu'il est possible d'élaborer une stratégie d'estimation optimale par projections localisées sur une analyse multi-résolution. Cette méthode originale offre un avantage calculatoire sur les méthodes d'estimation à noyau traditionnellement utilisées dans un tel contexte. On montre par la même occasion que le classifieur plug-in construit sur cette nouvelle procédure est optimal. De plus, il hérite des avantages calculatoires mentionnés plus haut, ce qui s'avère être un atout crucial dans de nombreuses applications. On se tourne ensuite vers le problème de régression en design aléatoire uniformément distribué sur l'hyper-sphère et on montre comment le tight frame de needlets permet de généraliser les méthodes traditionnelles de régression en ondelettes à ce nouveau contexte. On s'intéresse finalement au problème d'estimation de la densité risque-neutre à partir des prix d'options cotés sur les marchés. On exhibe une décomposition en valeurs singulières explicite d'opérateurs de prix restreints et on montre qu'elle permet d'élaborer une méthode d'estimation de la densité risque-neutre qui repose sur la résolution d'un simple programme quadratique.

Mots-clés: Classification binaire supervisée, Régression en design aléatoire, Analyse multi-résolution, Ondelettes, Régression sur l'hyper-sphère, Needlets, Problème inverse, Décomposition en valeurs singulières, Programmation quadratique.

Discipline: Mathématiques

Abstract: We focus on the problems of regression, classification and an inverse problem in finance. We first deal with the regression on a random design problem, with a design taking its values in a Euclidean space and whose distribution admits a density. We prove the optimality of the estimator obtained by localized projections onto a multi-resolution analysis. We then turn to the supervised binary classification problem and prove that the plug-in classifier built upon the above procedure is optimal. Interestingly enough, it is computationally more efficient than alternative plug-in classifiers, which turns out to be a crucial feature in many practical applications. We then focus on the regression on a random design problem, with a design uniformly distributed on the hyper-sphere of a Euclidean space. We show how the tight frame of needlets allows to transpose the traditional wavelet regression methods to this new setting. We finally consider the problem of recovering the risk-neutral density from quoted option prices. We show that the singular value decomposition of restricted call and put operators can be computed explicitly and used to tailor a simple quadratic program, which allows to recover a stable estimate of the risk-neutral density.

Key Words: Supervised binary classification, Regression on a random design, Multi-resolution analysis, Wavelets, Regression on the hyper-sphere, Needlets, Inverse problems, Singular value decomposition, Quadratic programming.

Laboratoire de Probabilités et Modèles Aléatoires,
CNRS-UMR, 7599, UFR de Mathématiques, case 7012
Université Paris 7, Denis Diderot
2, place Jussieu, 75251 Paris Cedex 05.